Positions available

Proteins are Molecular Machines !

Elementary steps:
Conformational motions

F-ATP Synthase

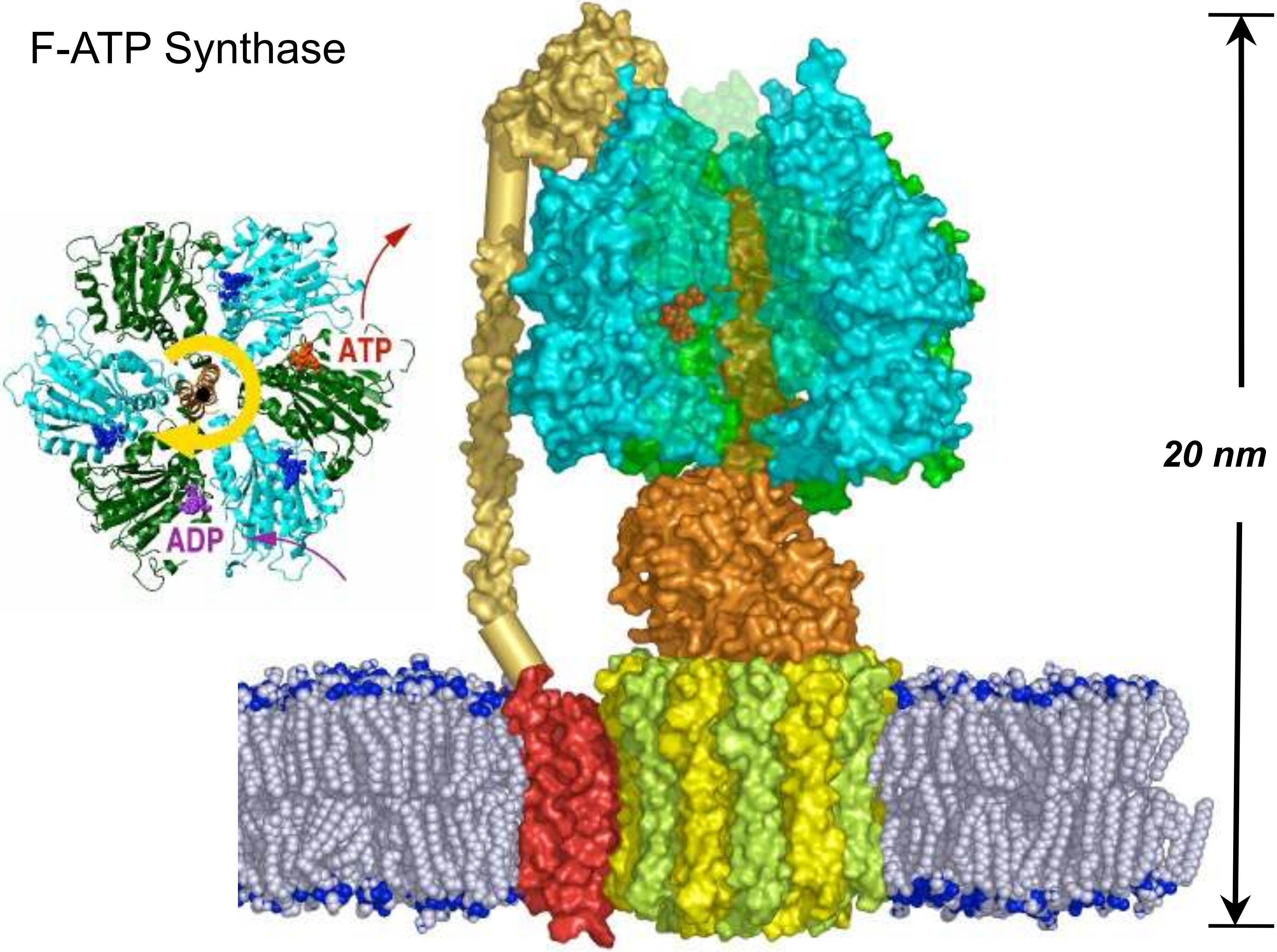

F-ATP Synthase

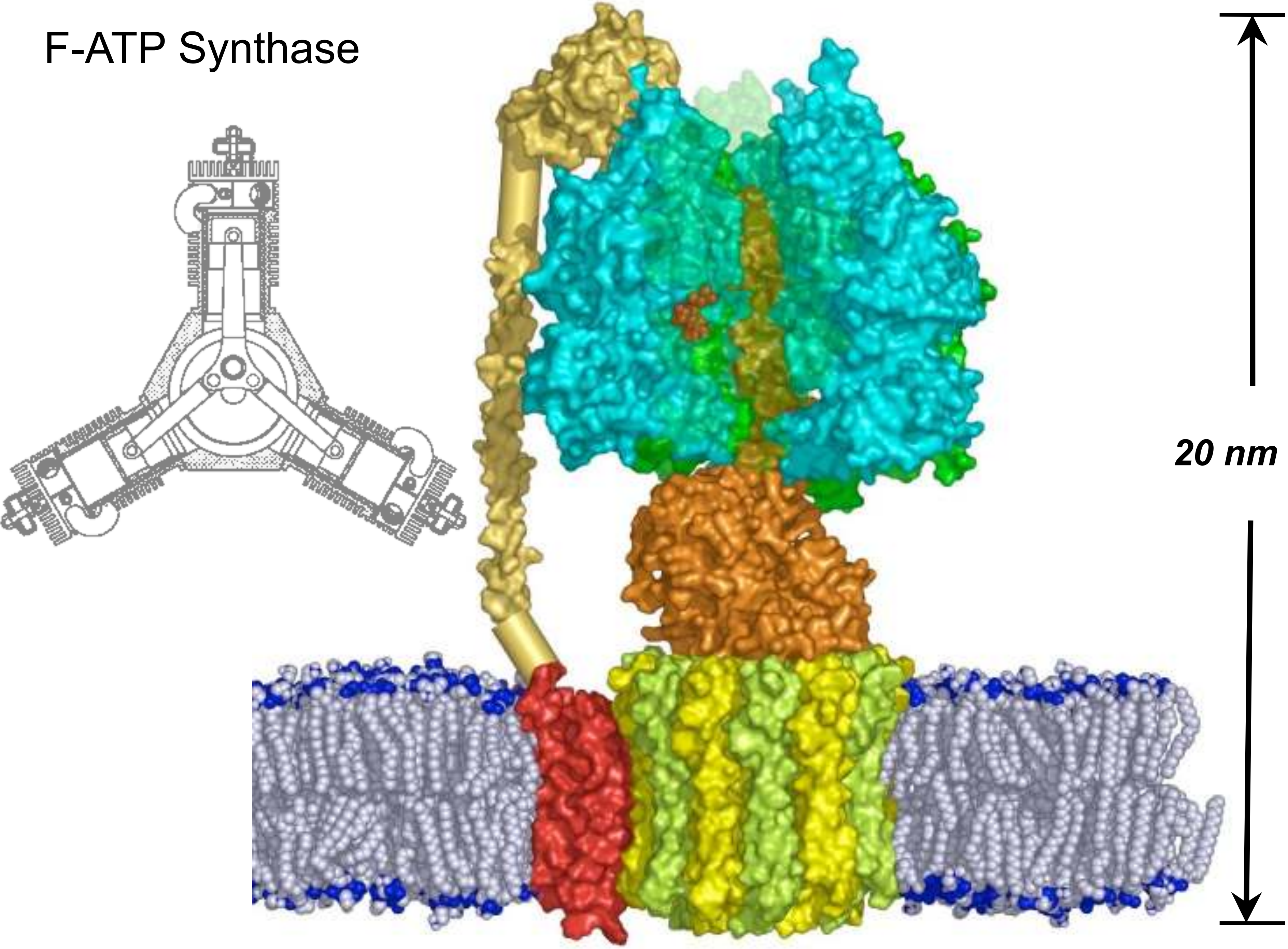

MD-Fit of
atomic xray model
to EM maps
(23 structures)

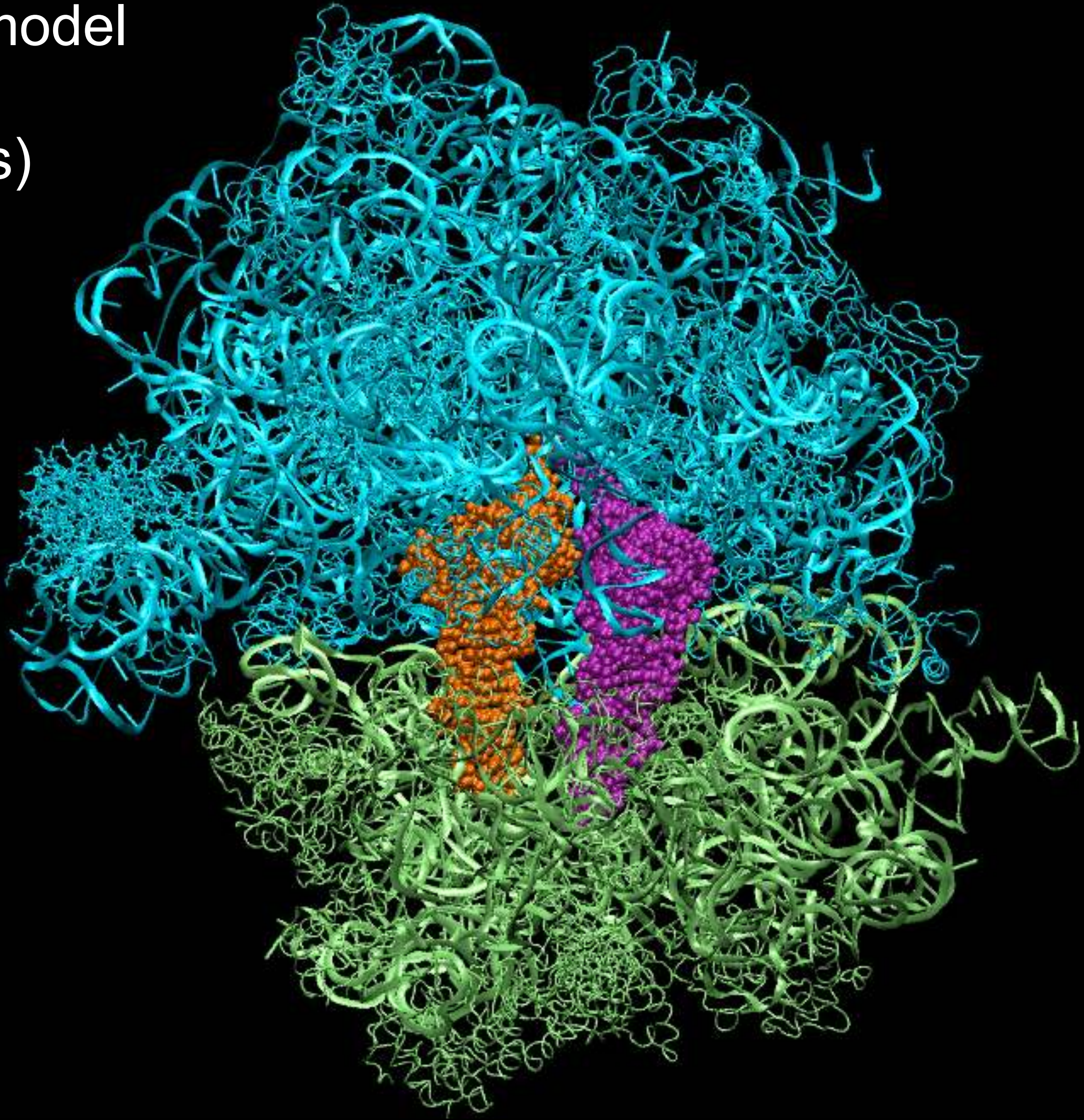

Reality

X-ray crystallography

„This is reality, not just simulations!“
Sir John Walker, European Biophysics Congress, London, 2007

Tur

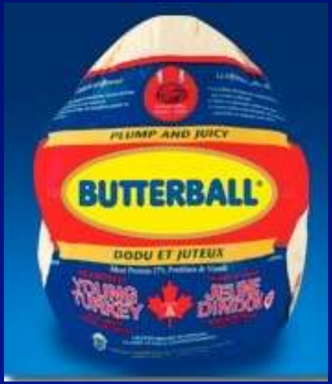

J

K

L

M

Time resolved x-ray crystallography

single particle cryo EM

(C) Stacey Burgess

AFM

Molecular dynamics simulation

Molecular dynamics simulation

Molecular dynamics simulation

Molecular dynamics simulation

MD simulations of water transport

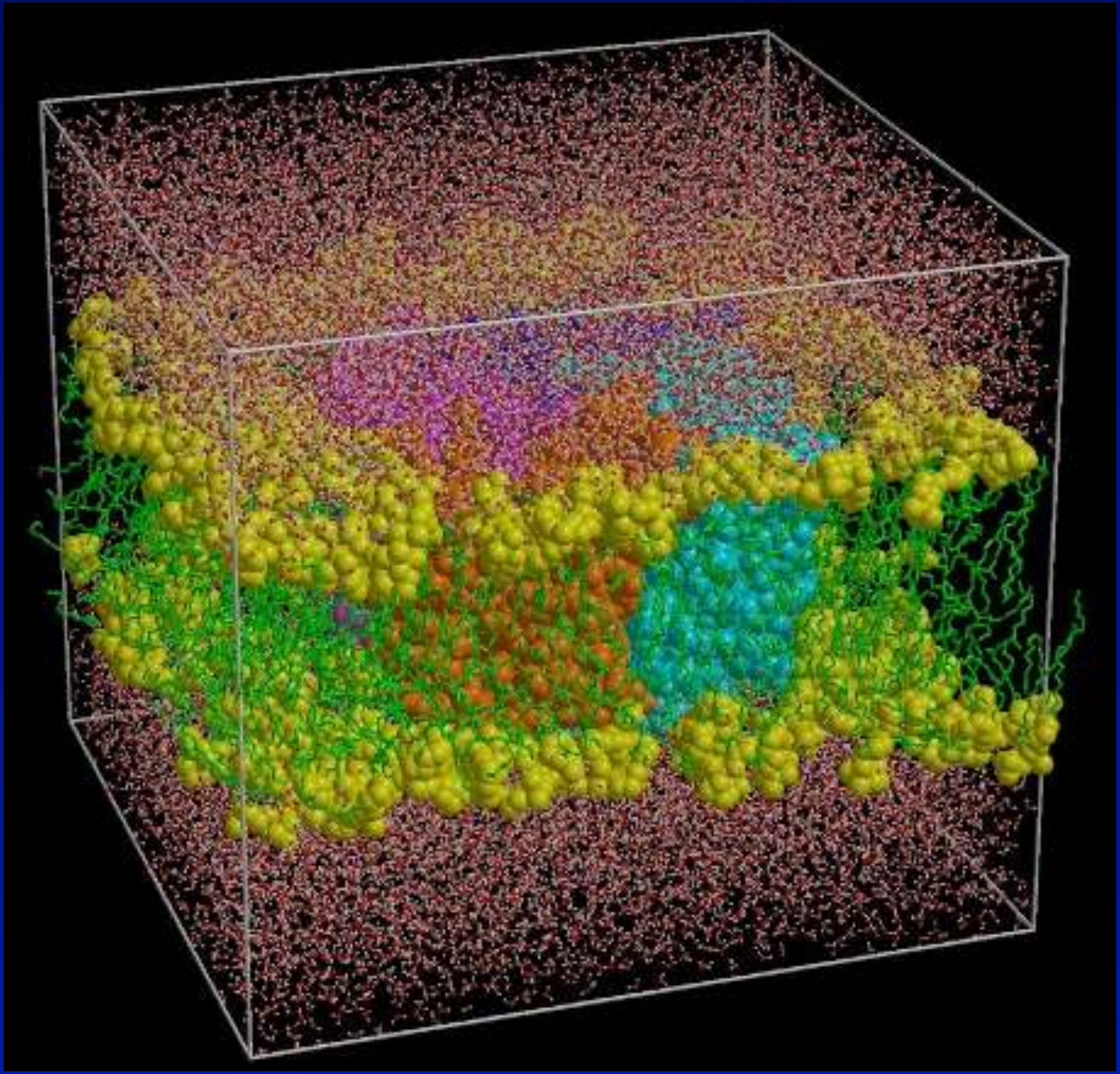

- *ca. 100 000 atoms*
- *full electrostatics, periodic boundary*
- *10 ns simulation time*

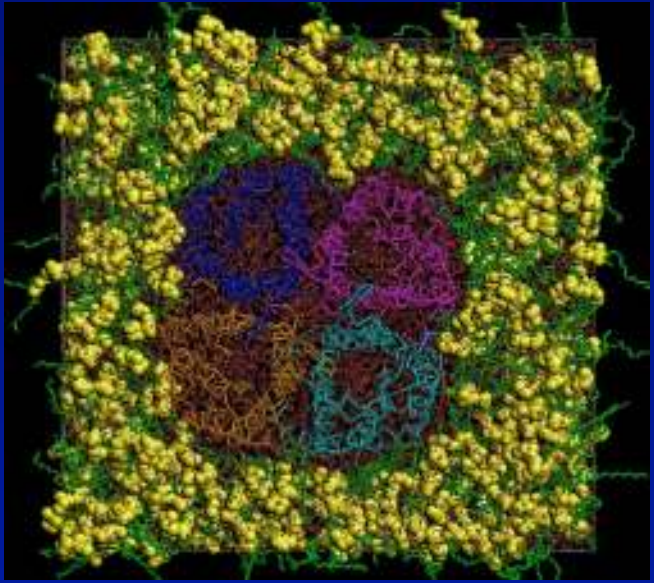

top view

B.L. de Groot, H. Grubmüller, *Science* **294**, 2353 (2001)

MD simulations of water transport

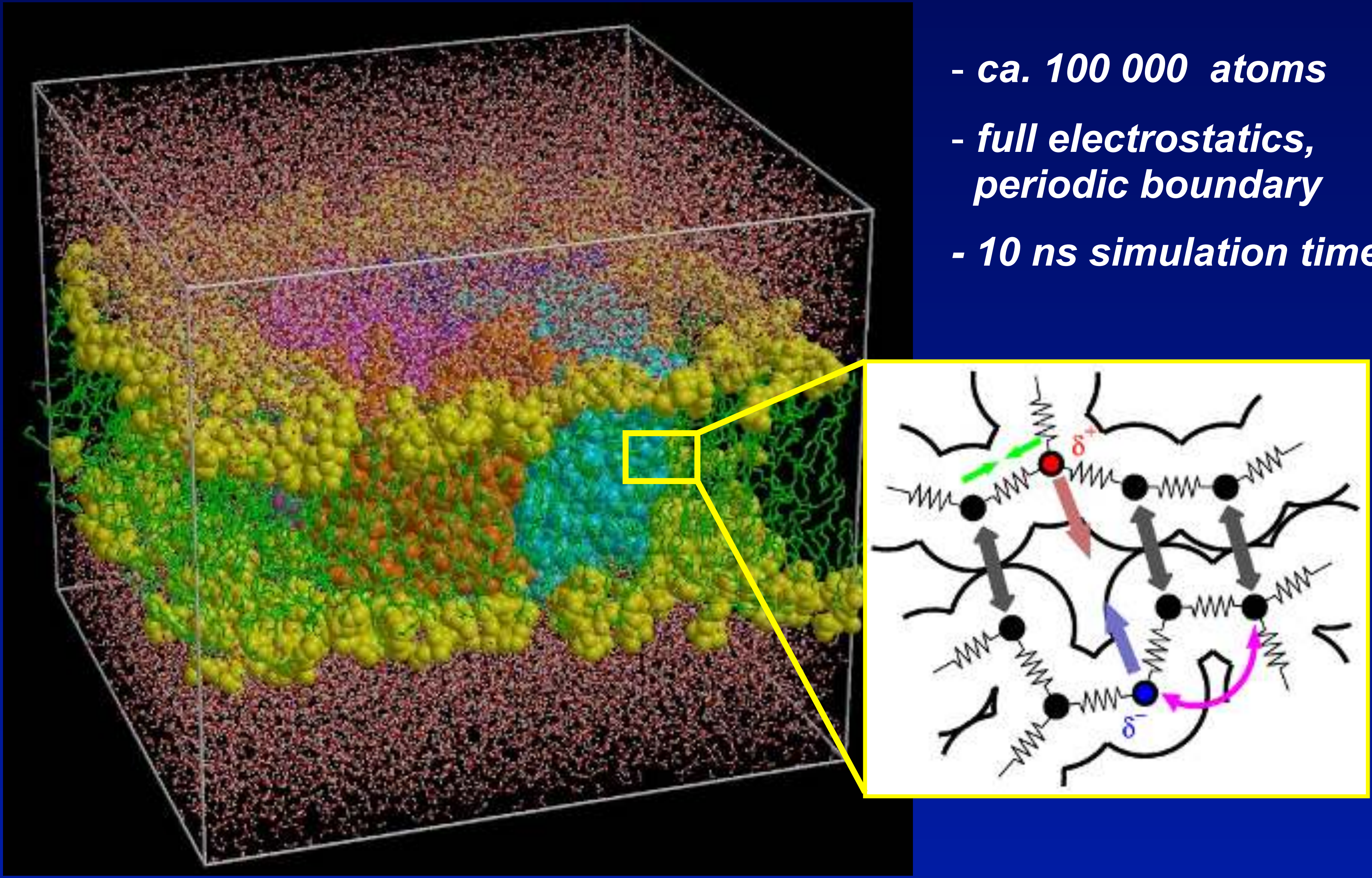

- *ca. 100 000 atoms*
- *full electrostatics, periodic boundary*
- *10 ns simulation time*

B.L. de Groot, H. Grubmüller, *Science* **294**, 2353 (2001)

Molecular Dynamics Simulations

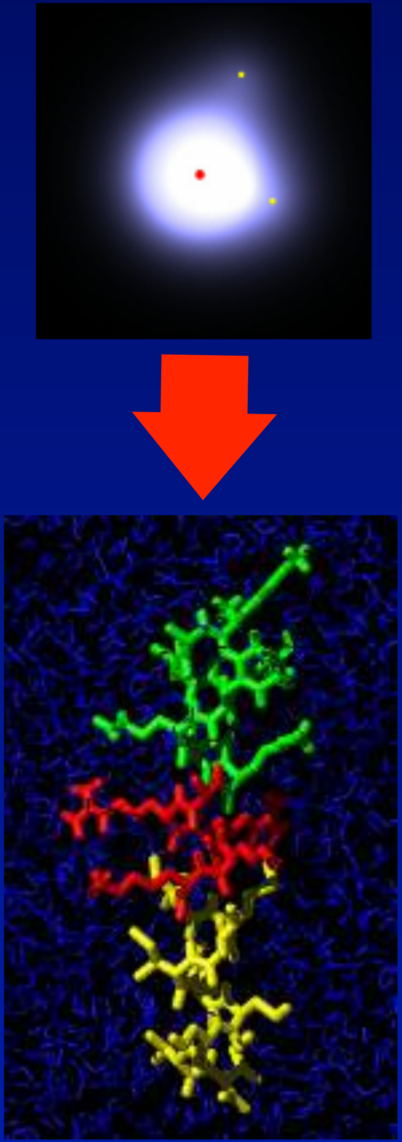

Schrödinger equation

$$i\hbar\partial_t\Psi(r,R) = H\Psi(r,R)$$

Born-Oppenheimer approximation

$$H_e\Psi_e(r;R) = E_e(R)\Psi_e(r;R)$$

Nucleic motion described classically

$$m_i\frac{d^2}{dt^2}\vec{R}_i = -\vec{\nabla}_i E(\vec{R})$$

Empirical Force field

$$E(\vec{R}) = \sum_{\text{bonded}} E_i(\vec{R}) + \sum_{\text{non-bonded}} E_i(\vec{R})$$

1955: A new field is born

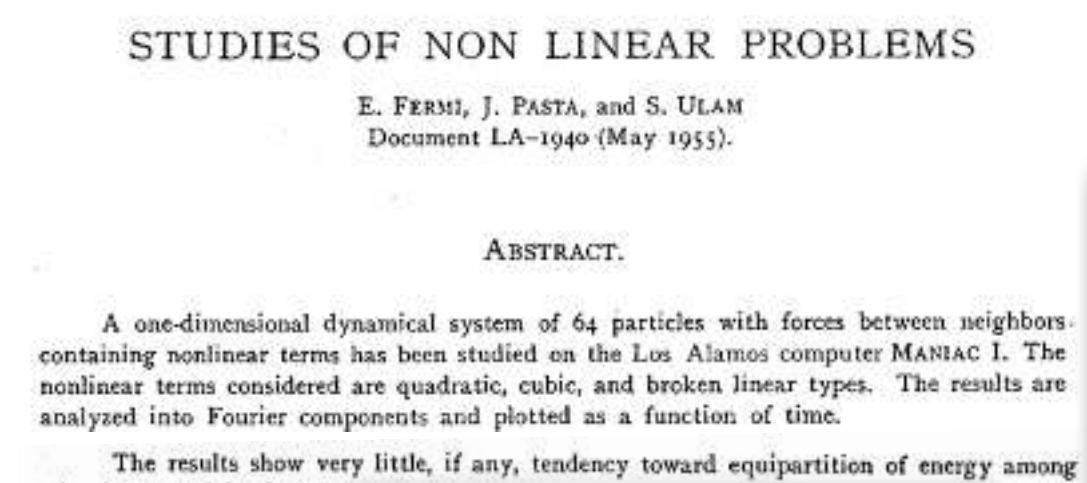

STUDIES OF NON LINEAR PROBLEMS

E. FERMI, J. PASTA, and S. ULAM
Document LA-1940 (May 1955).

ABSTRACT.

A one-dimensional dynamical system of 64 particles with forces between neighbors containing nonlinear terms has been studied on the Los Alamos computer MANIAC I. The nonlinear terms considered are quadratic, cubic, and broken linear types. The results are analyzed into Fourier components and plotted as a function of time.

The results show very little, if any, tendency toward equipartition of energy among the degrees of freedom.

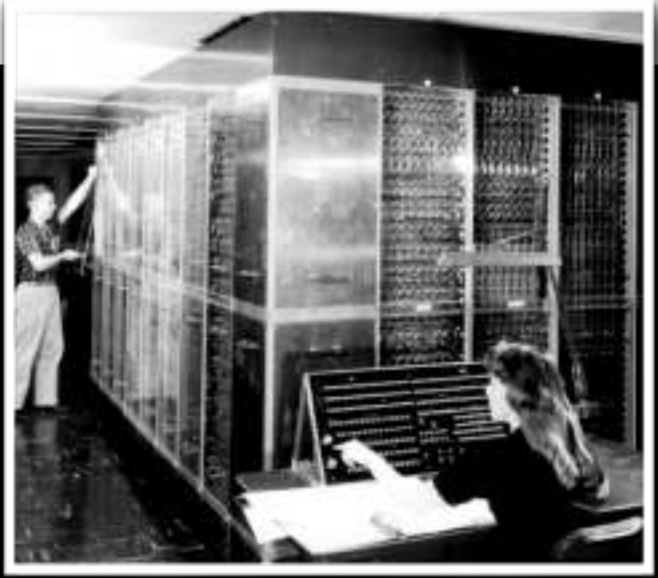

http://knuth.cs.bilgi.edu.tr/%7Ecomp149-02/projects/history_of_cnt/thedreamers/img/maniac.jpg

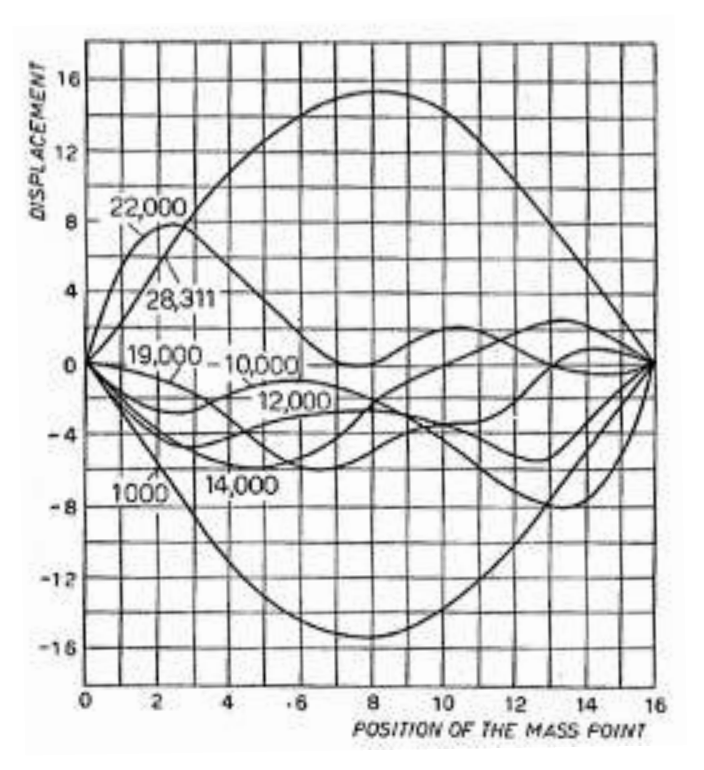

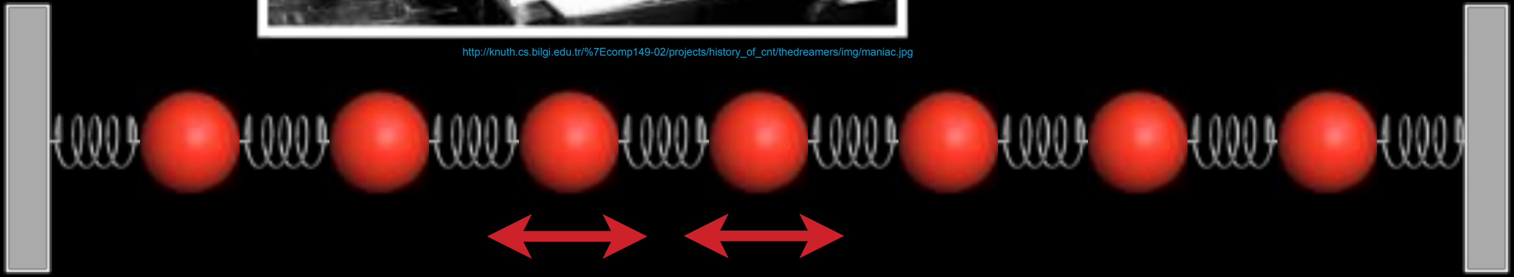

High performance parallel computing

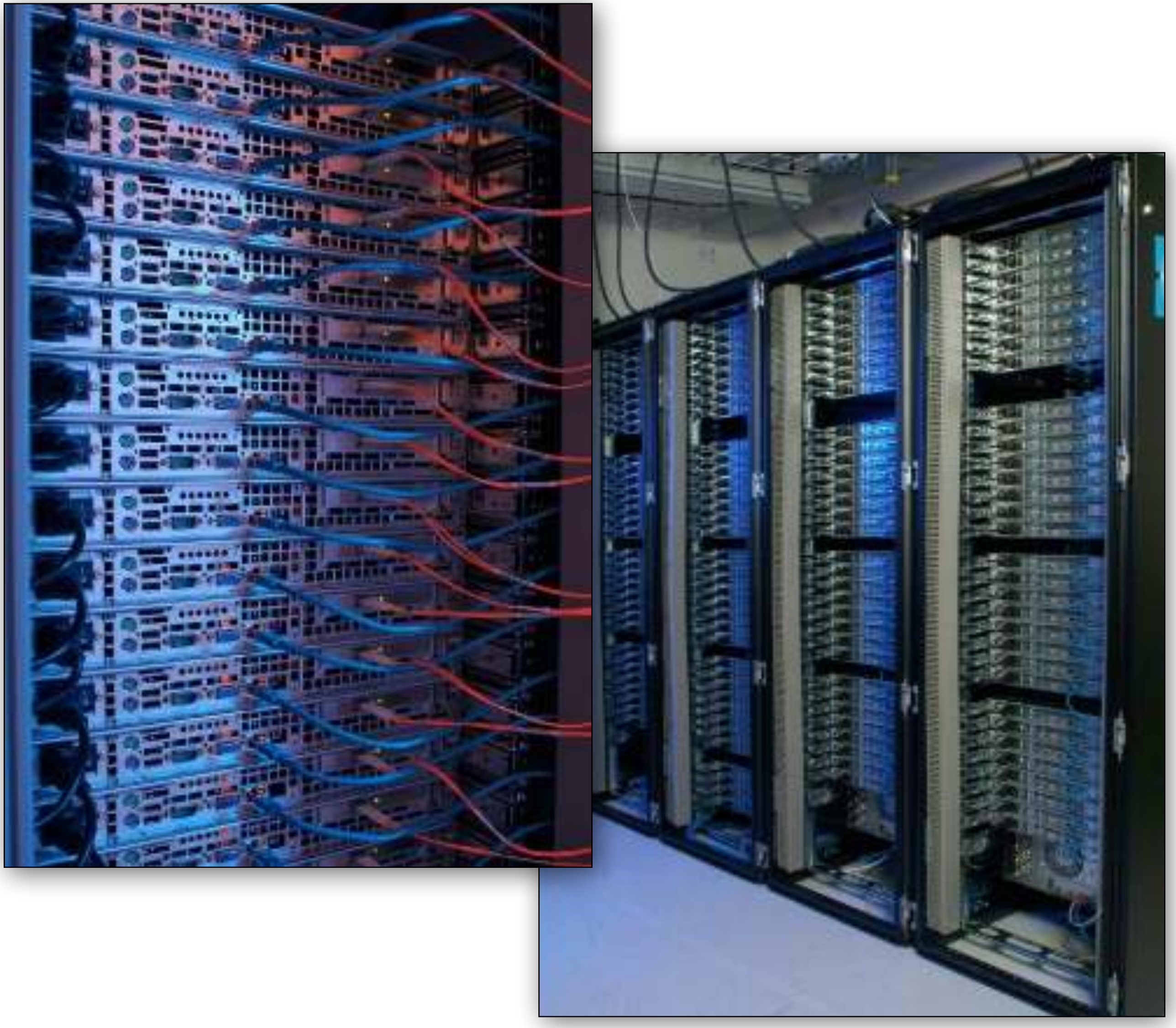

15 500 cores
150 GPUs

150 TFlop/s

12 TByte RAM
200 TByte disk

300 kW

Cassini space probe trajectory to Saturn

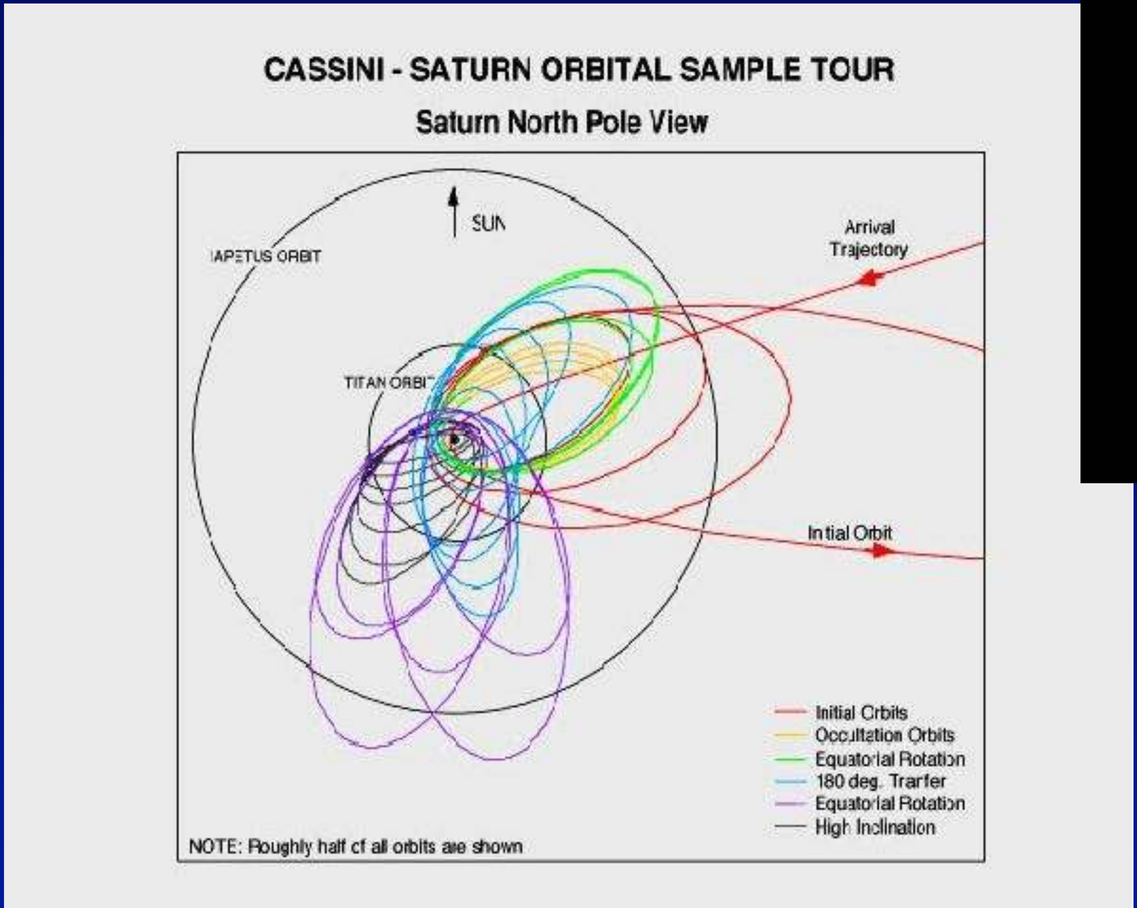

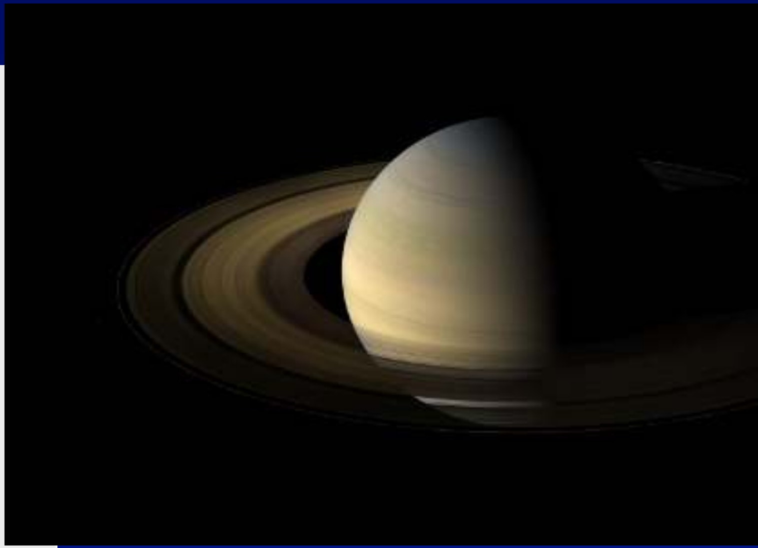

Source: MPG, Max Planck Institute for Solar System Research

MD-Experiments with Argon Gas

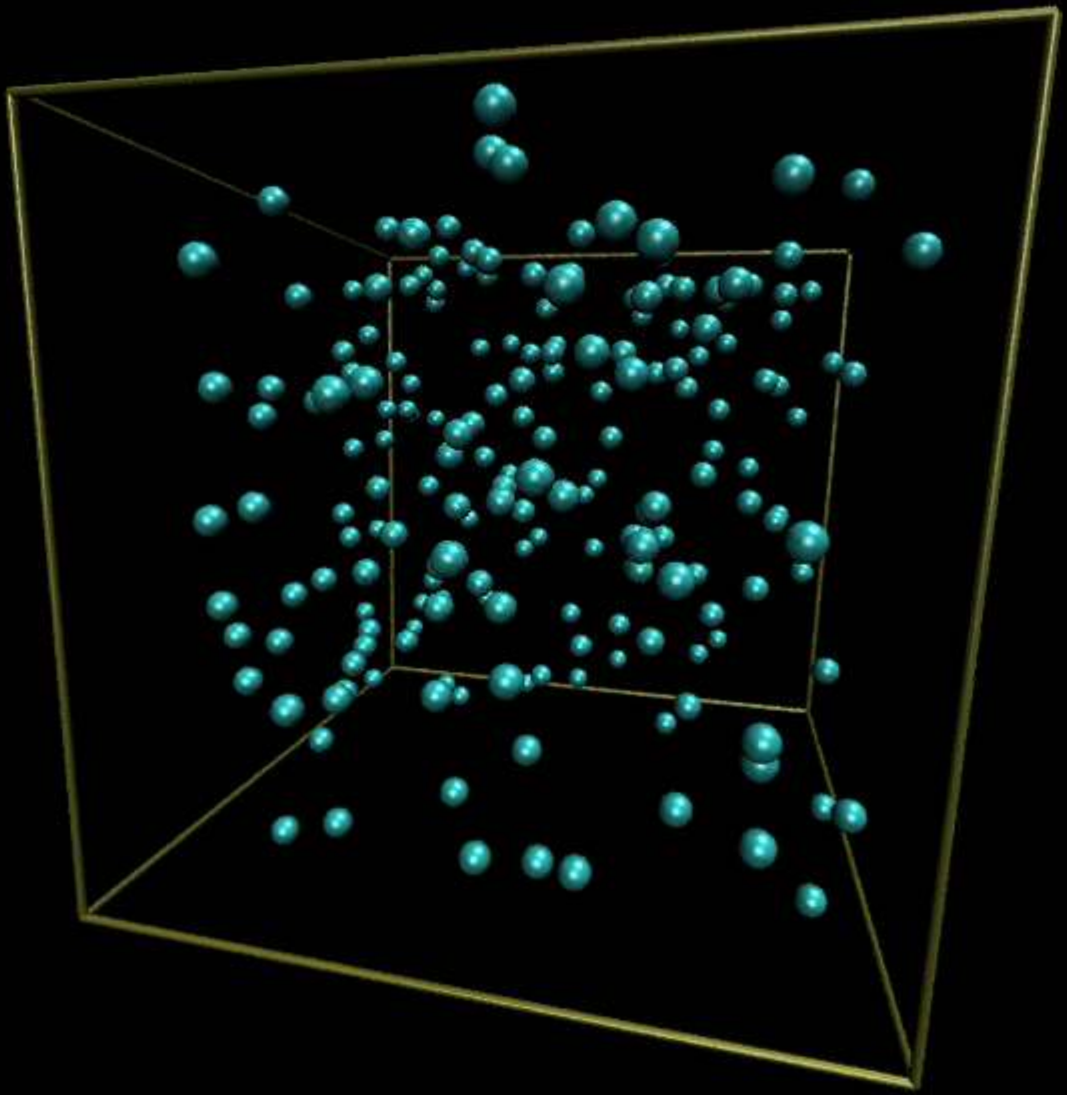

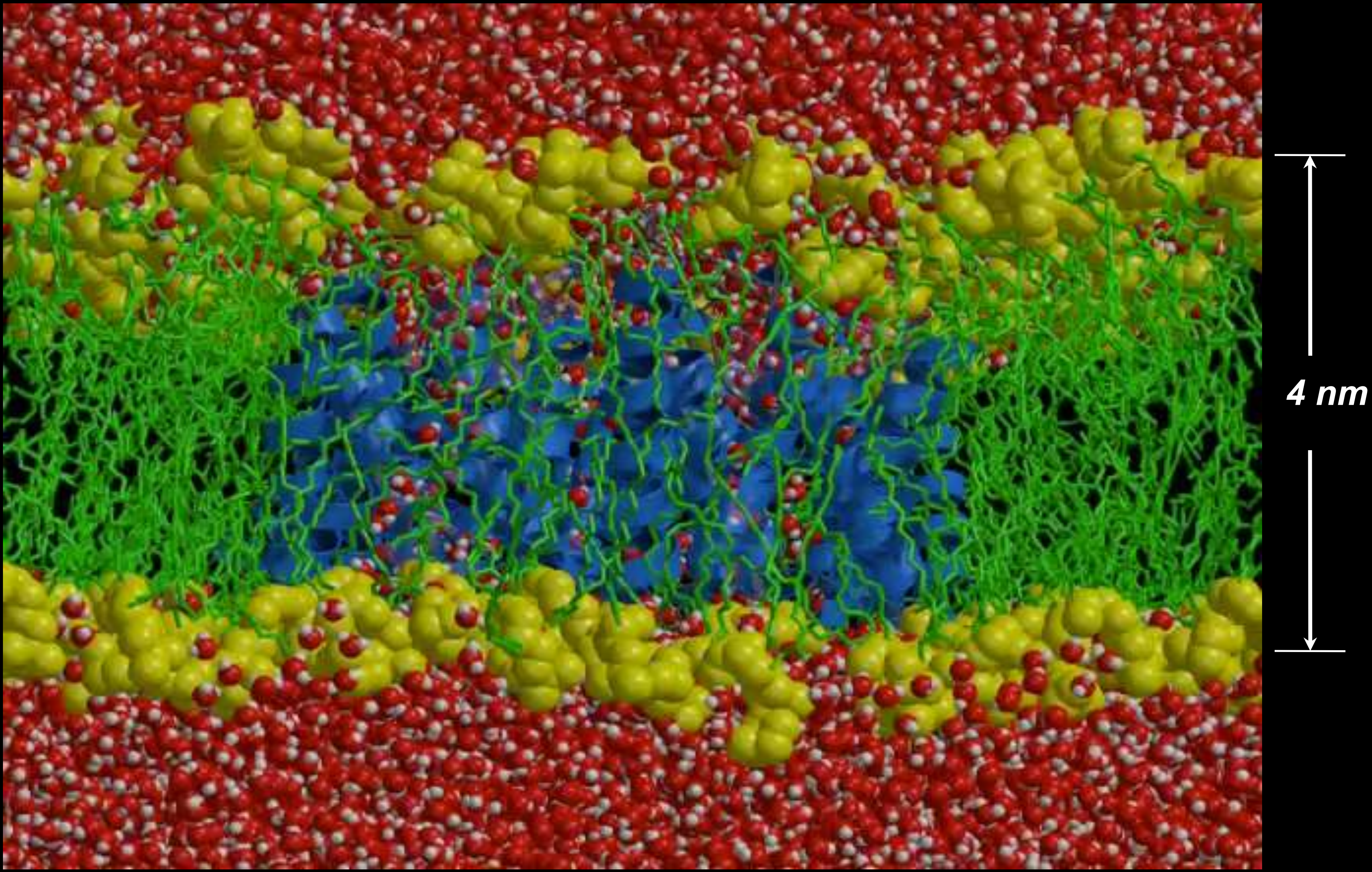

Molecular dynamics simulation, 1s $\hat{=}$ 2 ·10 $^{-11}$s

Water Permeation proceeds in steps

one out of 16 full spontaneous permeation events (2 ns)

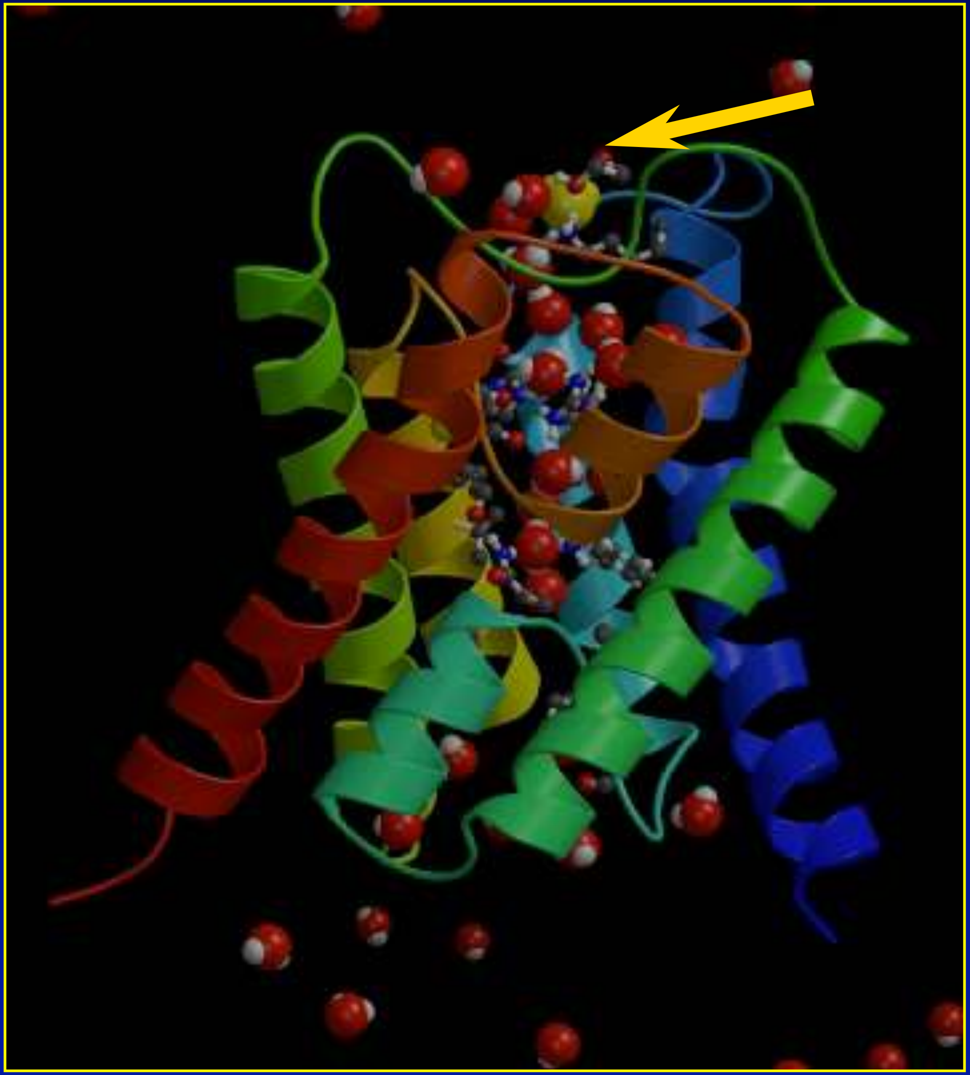

(outside the channel, only few water molecules are shown)

Timescales of protein motions

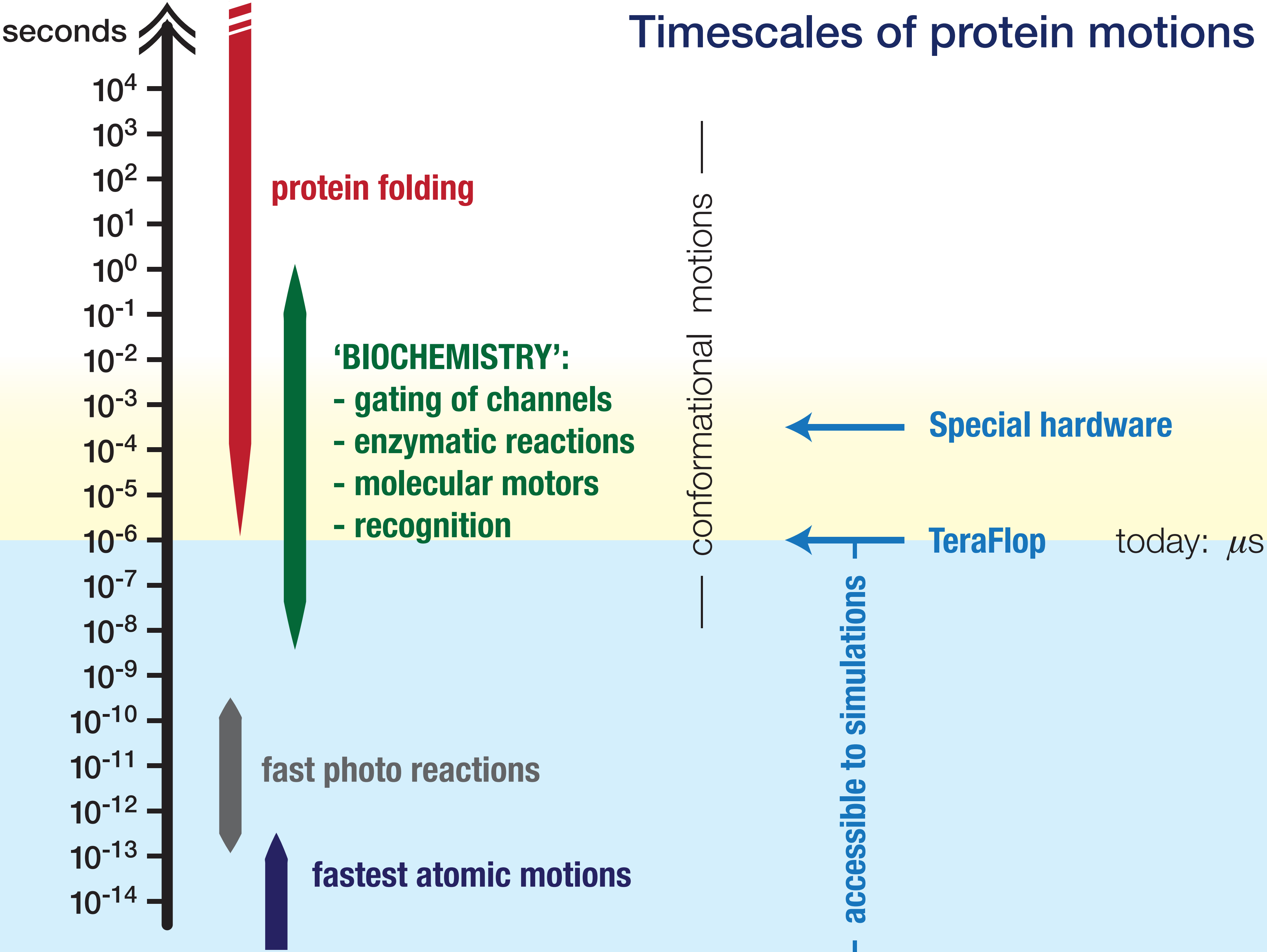

protein folding

‘BIOCHEMISTRY’:
- gating of channels
- enzymatic reactions
- molecular motors
- recognition

conformational motions

fast photo reactions

fastest atomic motions

Special hardware

TeraFlop

today: μs

accessible to simulations

Towards a mechanistic understanding of protein function

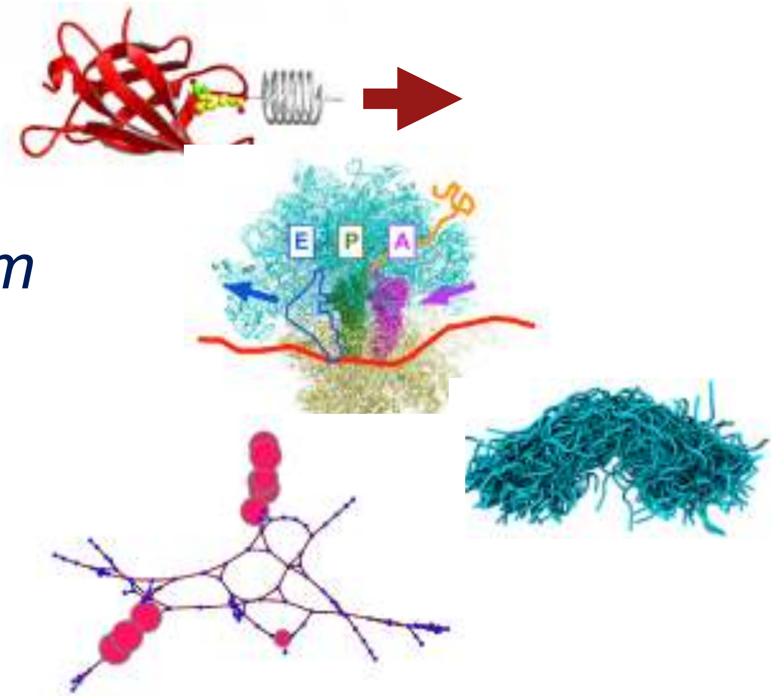

(1) Ligand unbinding revisited

(2) Ribosomal antibiotics mechanism

(3) Intrinsically Disordered Proteins

(4) The Dynasome

AFM+ X-ray + cryo EM + MD

Lars Bock, Christian Blau, Michal Kolar, Andrea Vaiana, Andreas Russek,
Sarah Rauscher, Ulf Hensen

Holger Stark, Marina Rodnina (MPI Göttingen)
Roland Beckmann, Daniel Wilson (Univ. Munich)
Simon Scheuring (Cornell Univ.)

Towards a mechanistic understanding of protein function

- *(1) Ligand unbinding revisited*
- *(2) Ribosomal antibiotics mechanism*
- *(3) Intrinsically Disordered Proteins*
- *(4) The Dynasome*

AFM+ X-ray + cryo EM + MD

Lars Bock, Christian Blau, Michal Kolar, Andrea Vaiana, Andreas Russek, Sarah Rauscher, Ulf Hensen

Holger Stark, Marina Rodnina (MPI Göttingen)
Roland Beckmann, Daniel Wilson (Univ. Munich)
Simon Scheuring (Cornell Univ.)

Single Molecule Force Spectroscopy

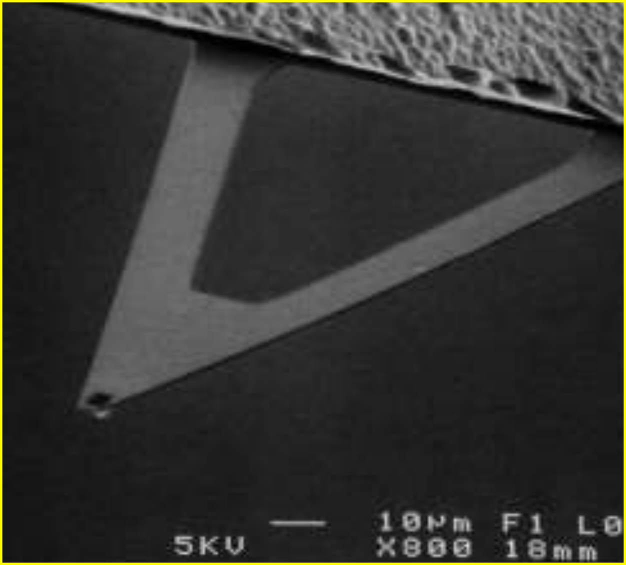

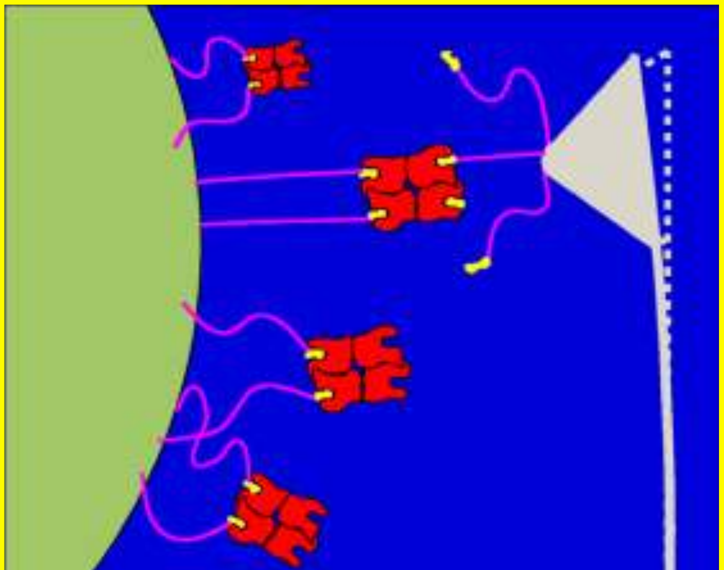

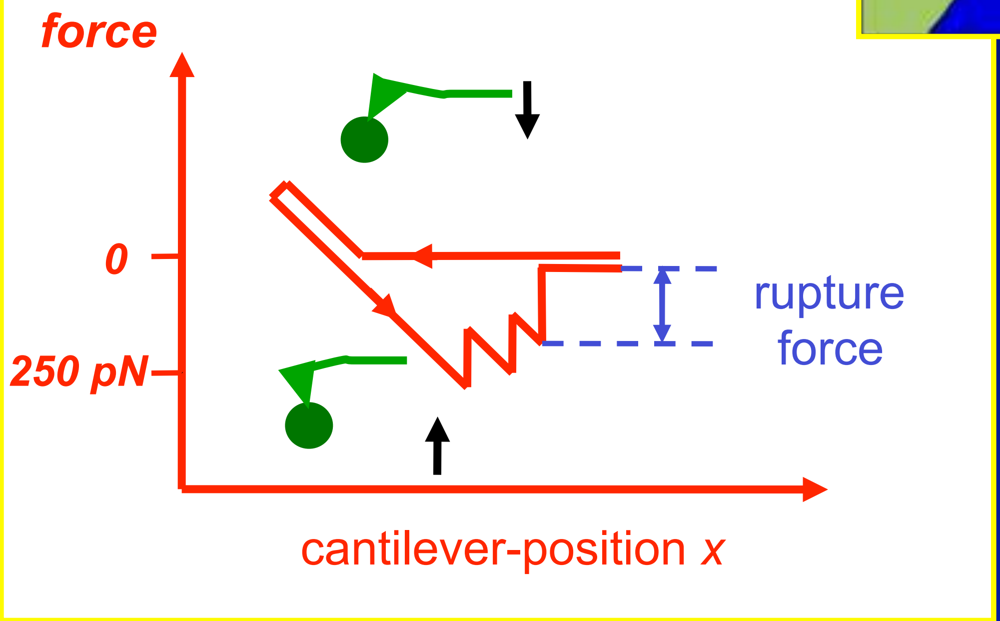

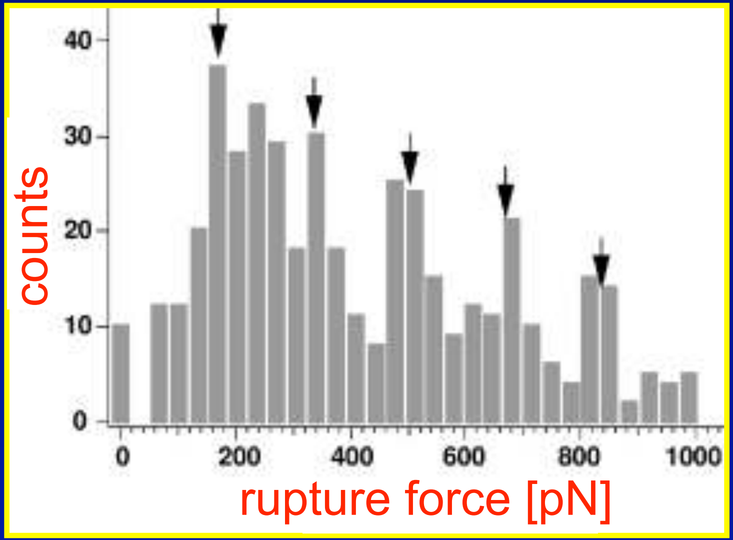

E.-L. Florin, V. T. Moy, H. E. Gaub, *Science* **264**, 415 (1994)

Force probe simulations

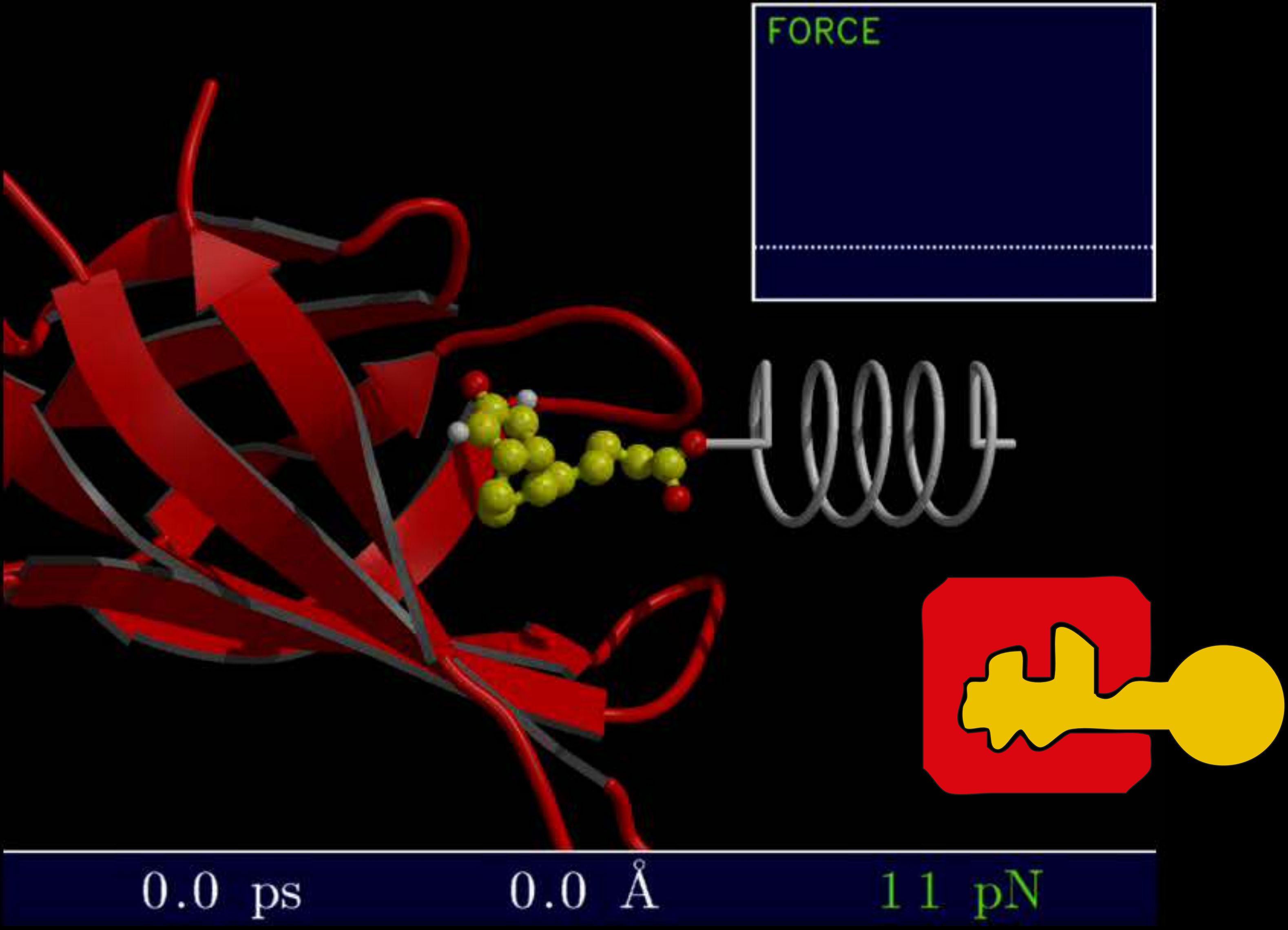

H. Grubmüller, B. Heymann, P. Tavan, Science 271, 997, 1996

AFM unbinding: Simulation vs Experiment (1996)

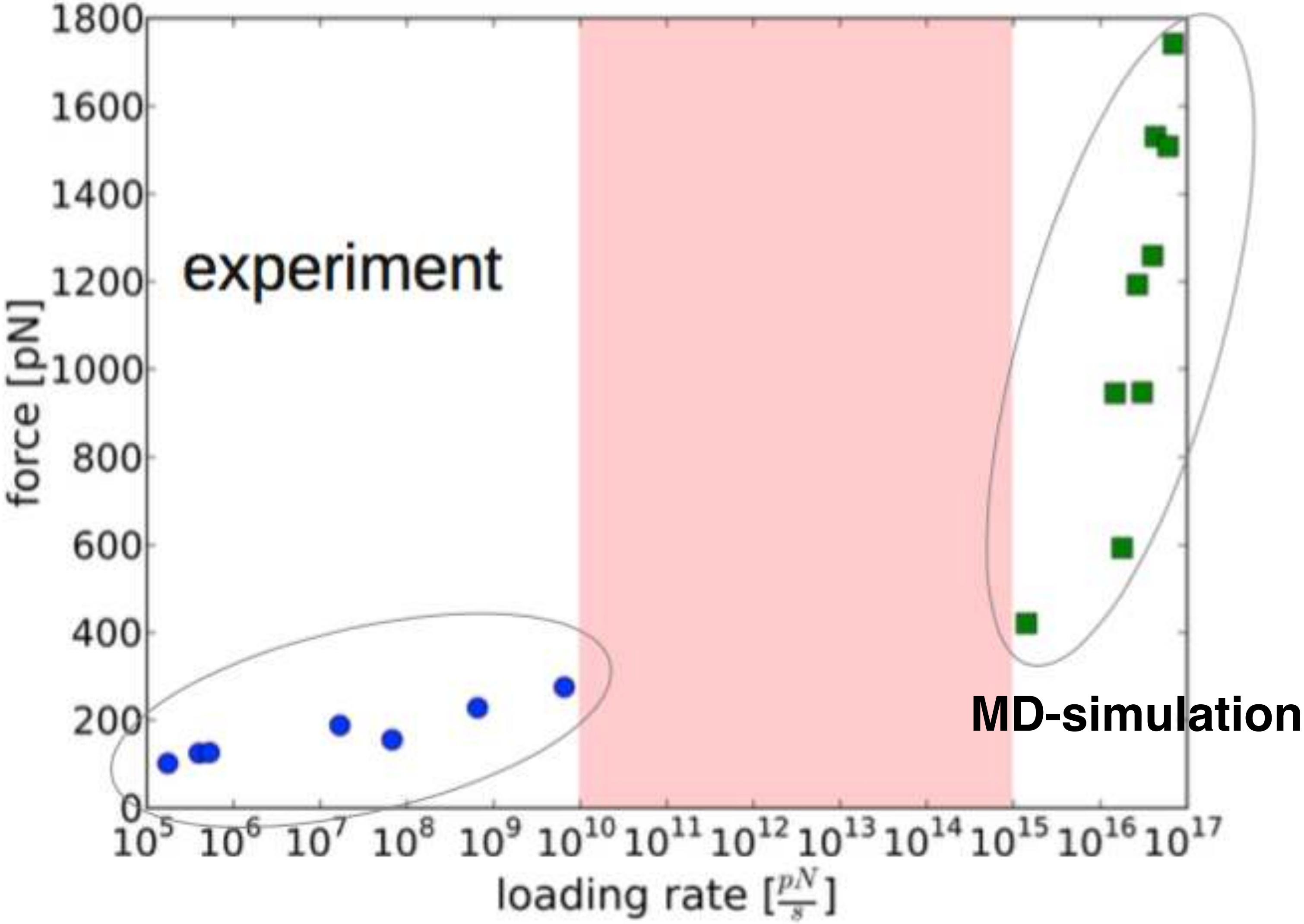

H. Grubmüller, B. Heymann, P. Tavan, Science 271, 997, 1996

Unbinding forces depend on time scale due to activated barrier crossing: soft spring

F(x):
applied force

G(x) + V(x,t)

G(x):
energy landscape
of unperturbed
system

V(x,t):
spring potential

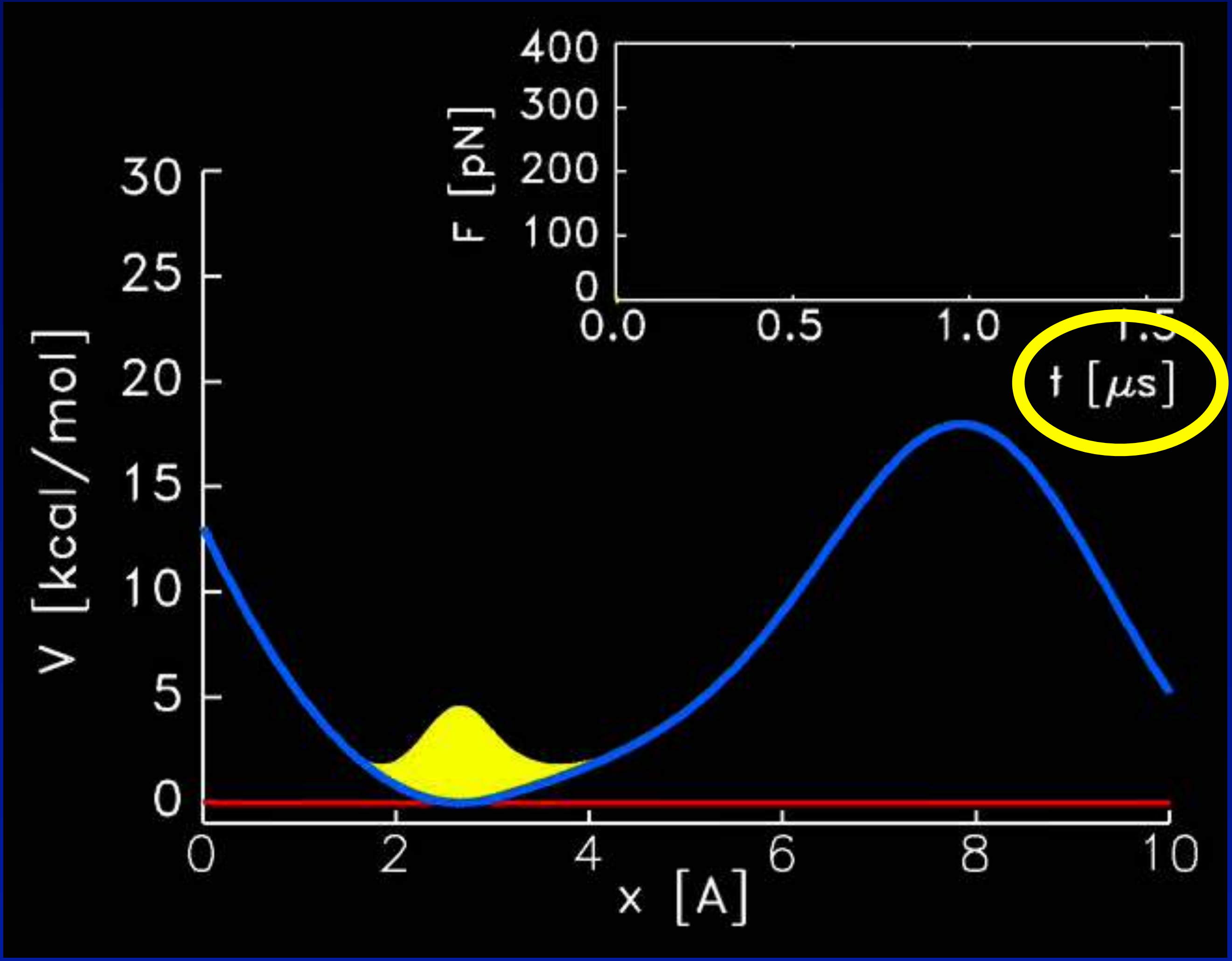

p(x): reaction coordinate probability distribution

Same process, 10^3 times slower:

F(x):
applied force

G(x) + V(x,t)

G(x):
energy landscape of unperturbed system

V(x,t):
spring potential

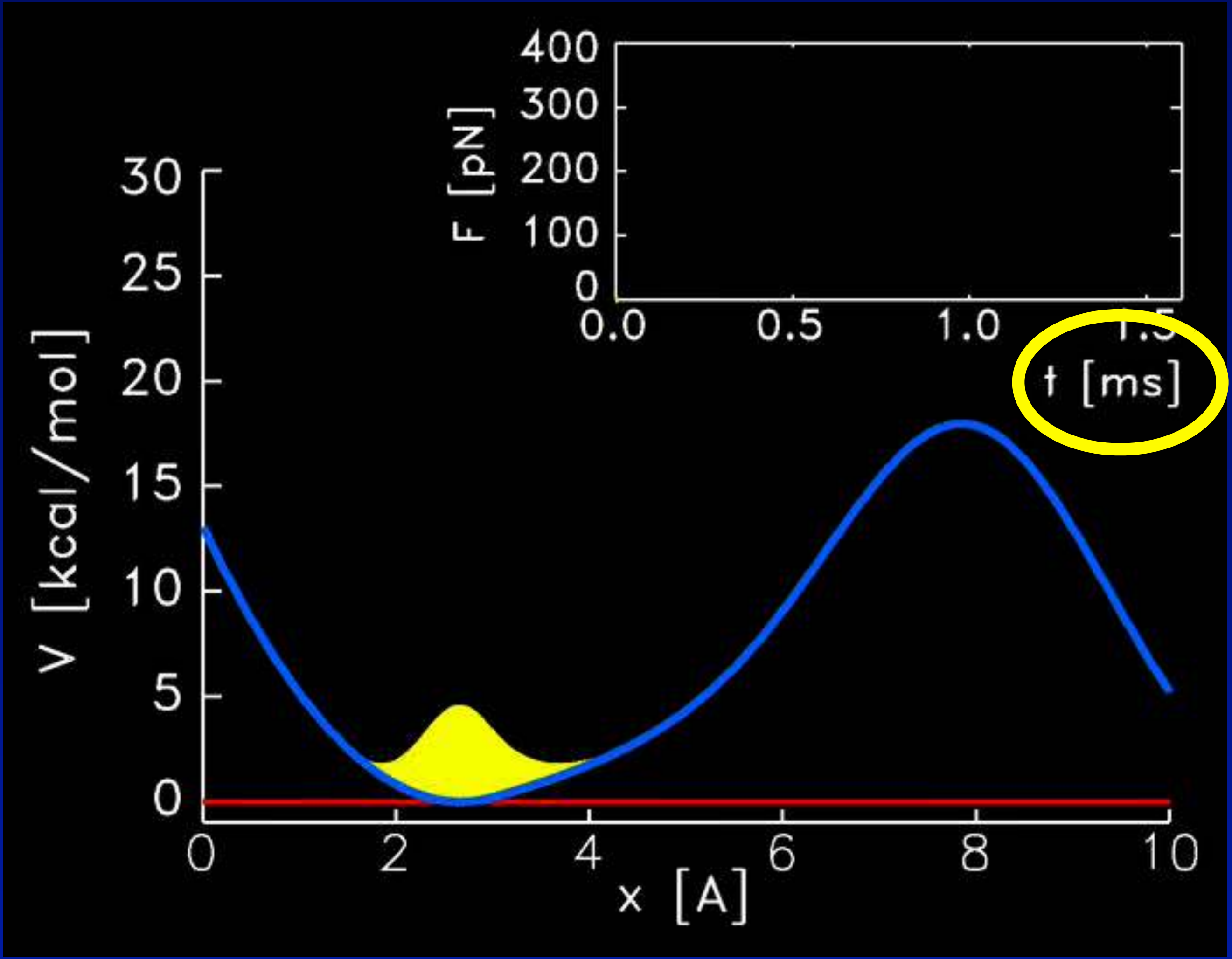

p(x): reaction coordinate probability distribution

Same process, 10^6 times slower:

F(x):
applied force

G(x) + V(x,t)

G(x):
energy landscape
of unperturbed
system

V(x,t):
spring potential

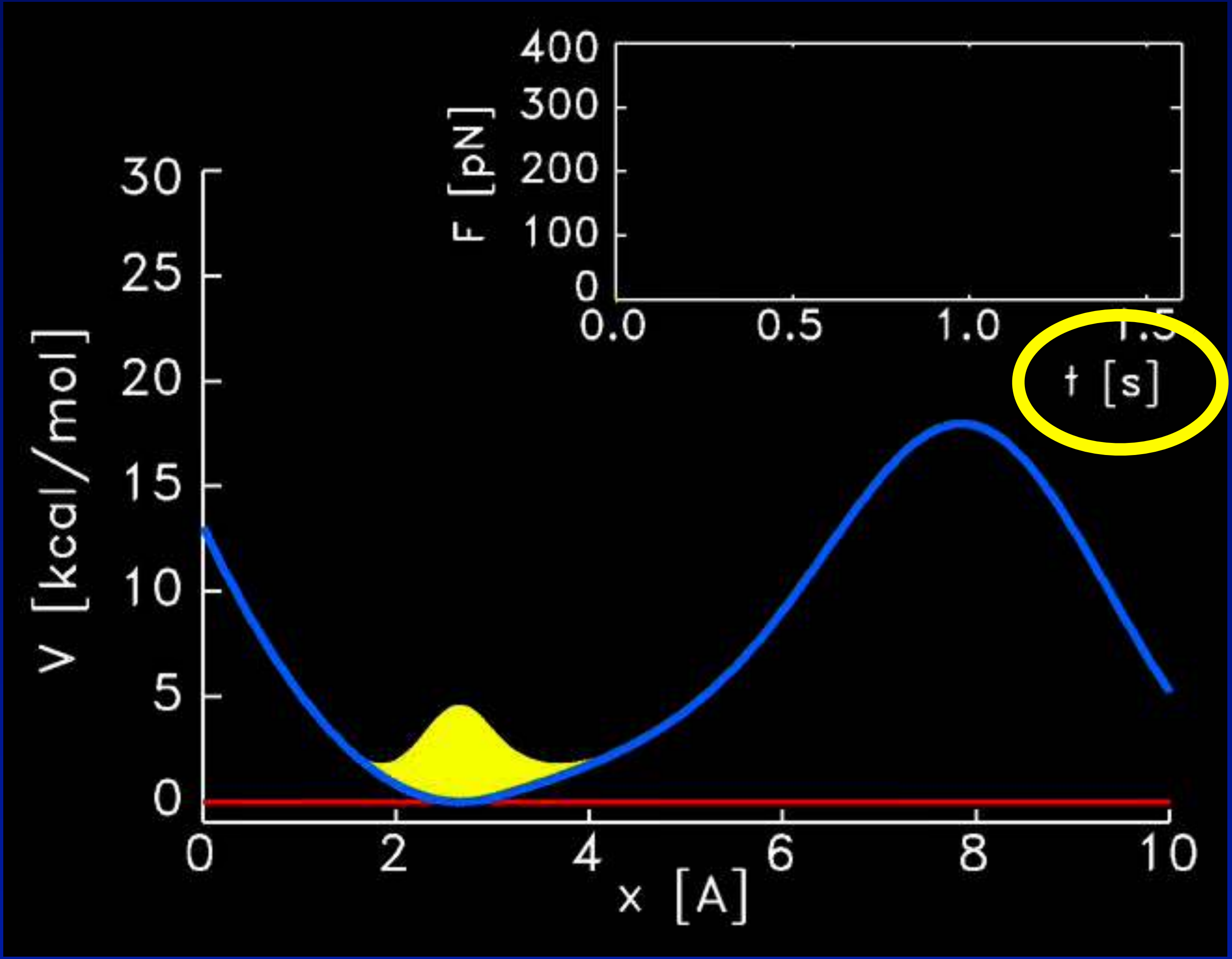

p(x): reaction coordinate probability distribution

MD Simulation Methods

- Tetramer and monomer
- Pulling spring of cantilever
- Loading rates: 10^7 ... 10^{13} pN/s
- Simulation lengths up to 8 μs
- 10...20 simulations per velocity
- WLC-Potential to mimic PEG

Exp + Sim -> Free energy landscape

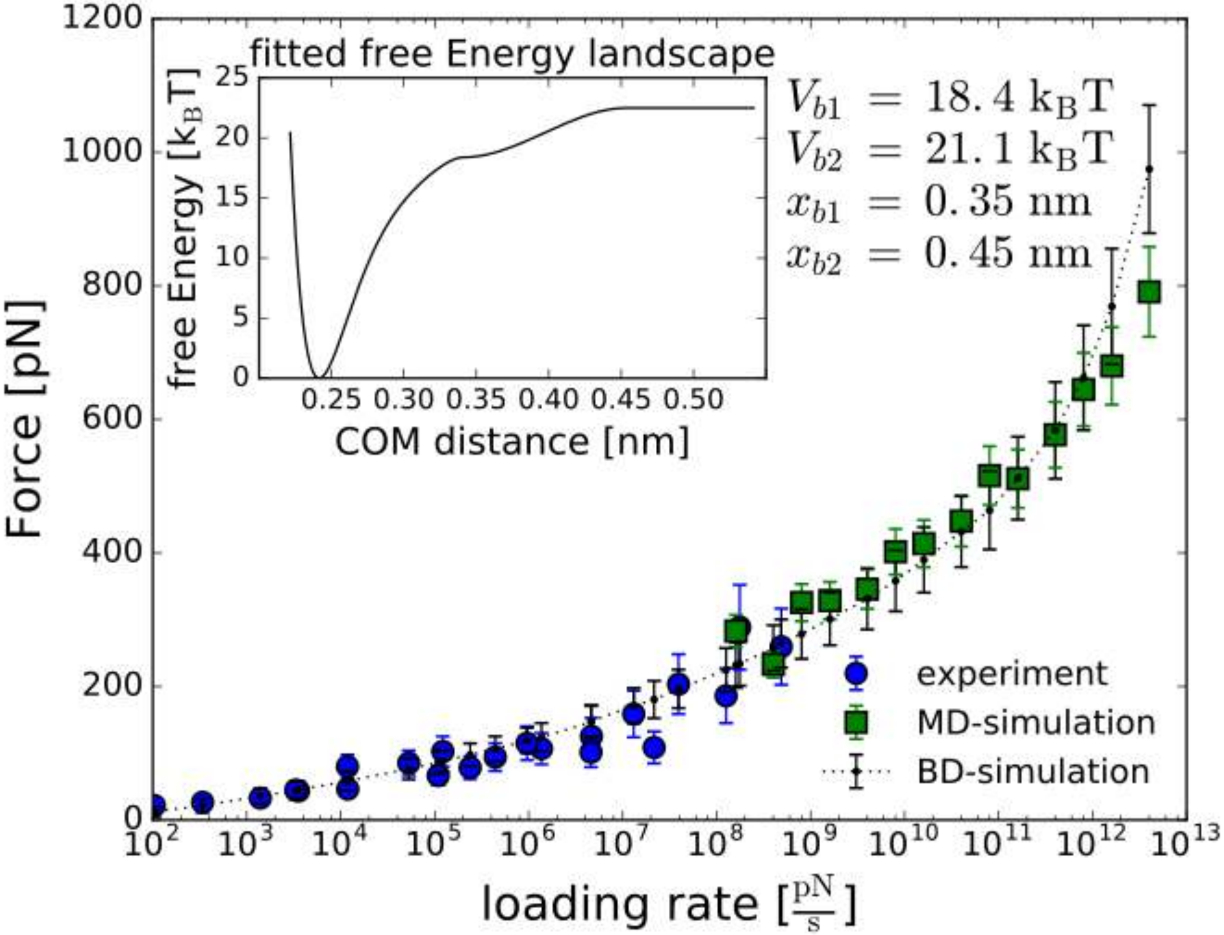

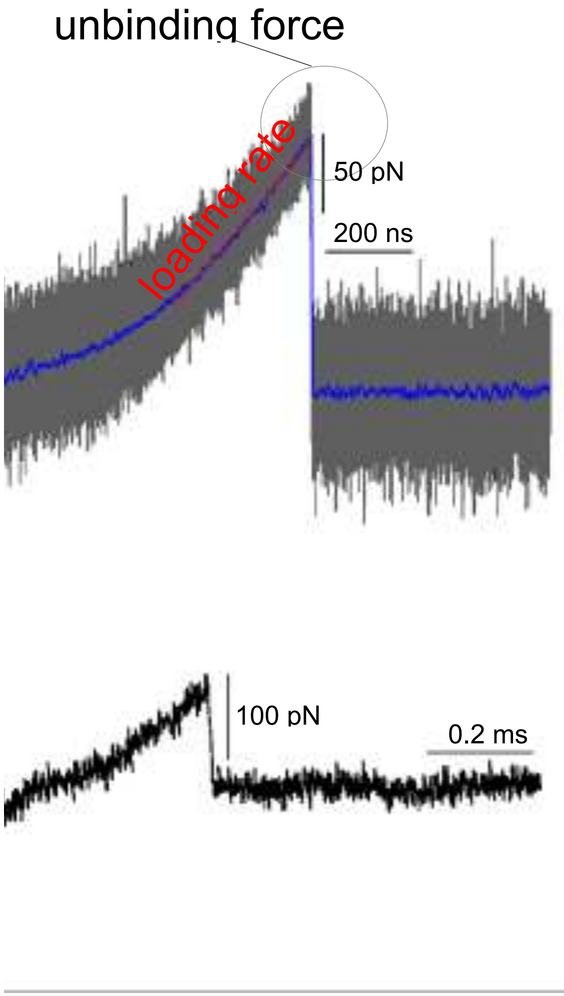

Russek, Rico, Scheuring, Grubmüller. *PNAS* (2019)

Unbinding pathways change with loading rate

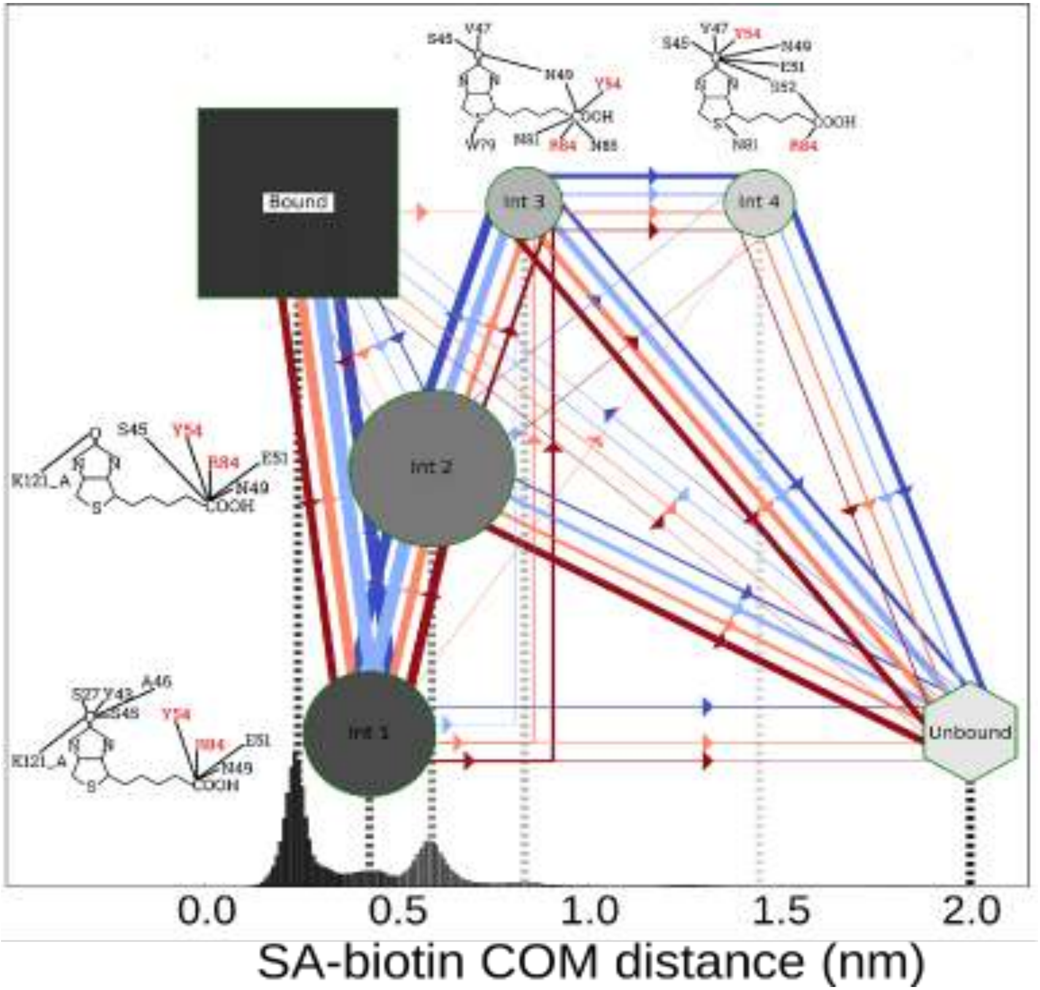

Russek, Rico, Scheuring, Grubmüller. *PNAS* (2019)

Outer Intermediate

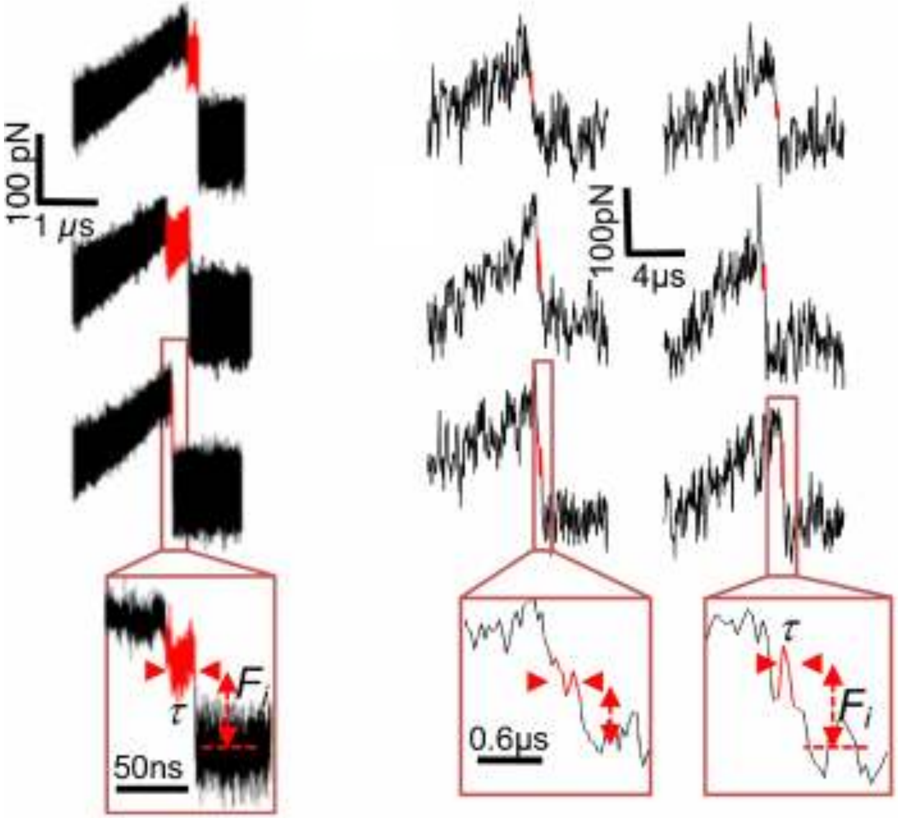

Simulation **Experiment**

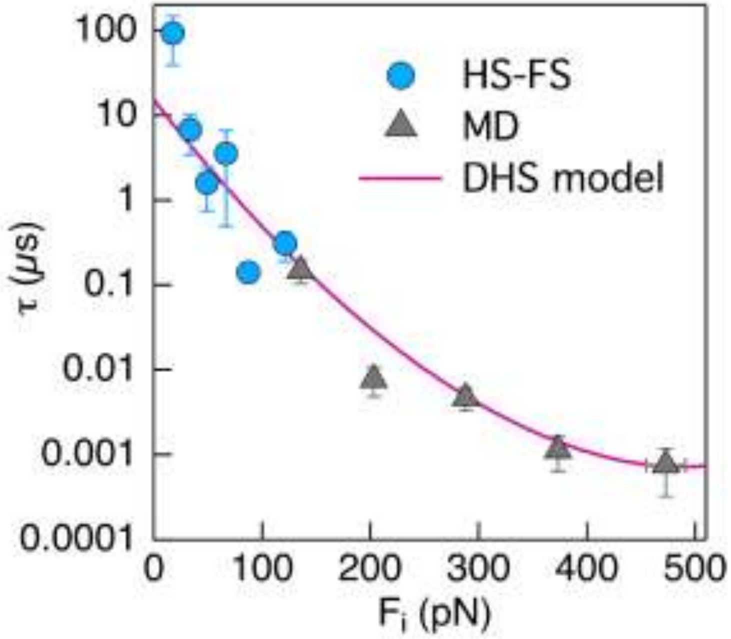

$$\tau(F)=\tau_0\left(1-\frac{\nu F x^{\ddagger}}{\Delta G^{\ddagger}}\right)^{1-1/\nu}\exp\left(-\beta\Delta G^{\ddagger}\left[1-\left(1-\frac{\nu F x^{\ddagger}}{\Delta G^{\ddagger}}\right)^{1/\nu}\right]\right)$$

$$x^{\ddagger}=0.23\,nm$$
$$\Delta G^{\ddagger}=22.5\,k_BT$$

[1] Dudko, O. K., Hummer, G. & Szabo, A. *Phys. Rev. Lett.* **96**, 108101 (2006).

Russek, Rico, Scheuring, Grubmüller. *PNAS* (2019)

Simulation of single molecule FRET experiments: FRET beyond $\kappa^2 = 2/3$

collab. U. Alexiev, C. Seidel, B. Schuler

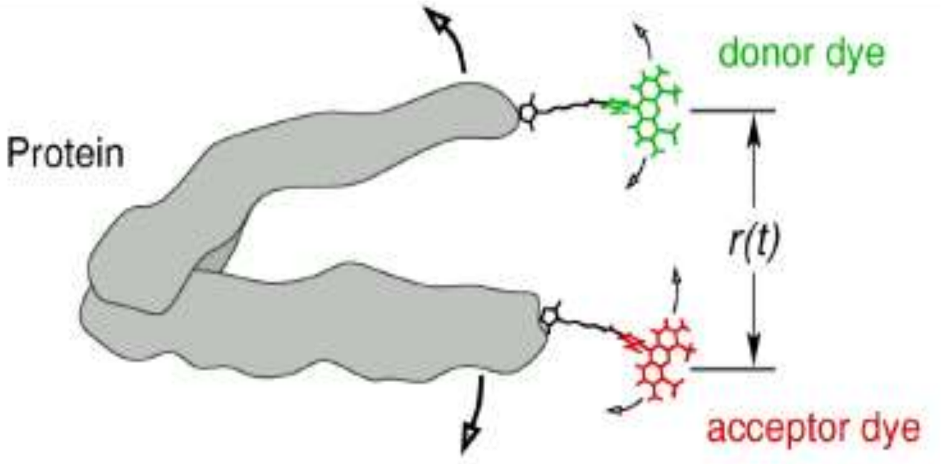

Förster Formula:

$$\frac{I_A(t)}{I_A(t) + I_D(t)} = \frac{1}{1 + \left[\frac{r(t)}{r_0}\right]^6}$$

Usual assumption ($\kappa^2 = 2/3$):
dye motion isotropic
& uncorrelated

Martin
Höfling

Nicola
Lima

Can we improve distance measurements by combining FRET and MD?

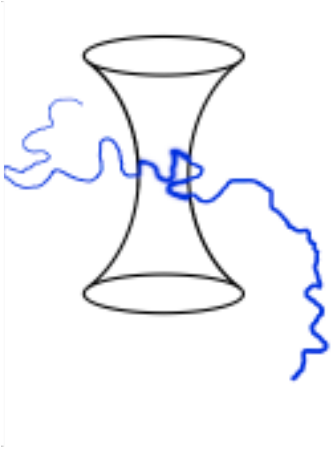

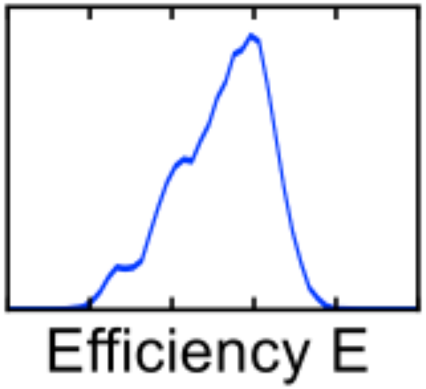

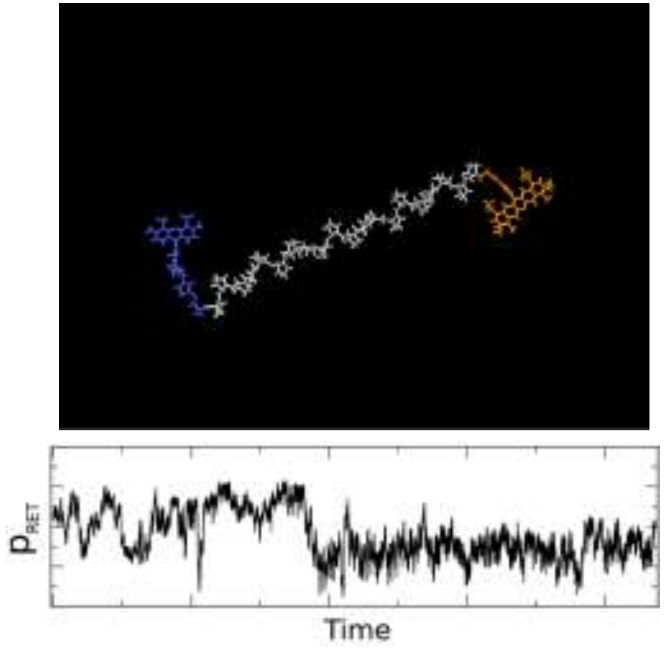

Exp.

Sim.

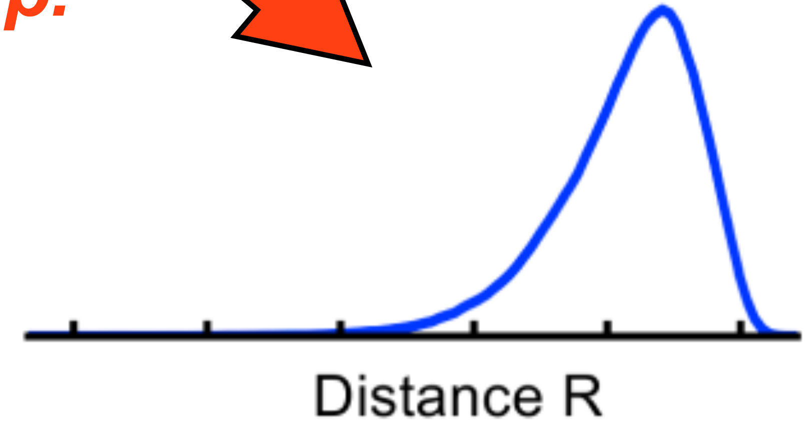

Procedure Outline

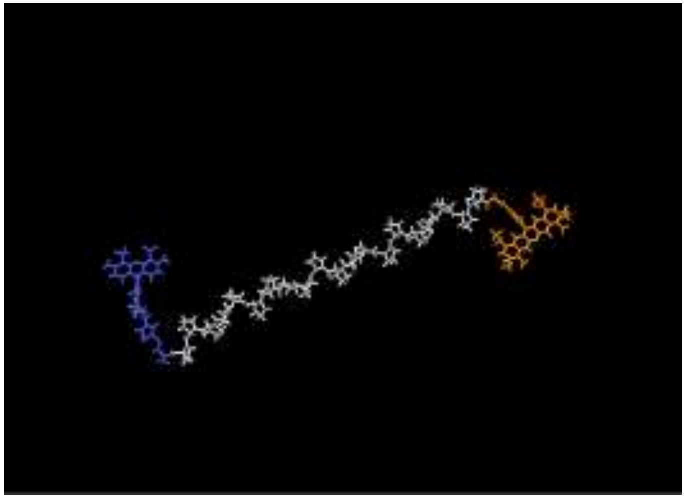

Step 1:
generate MD trajectories
--> r(t), θ(t), φ_1(t), φ_2(t)

Step 2:
generate k_{RET}(t)

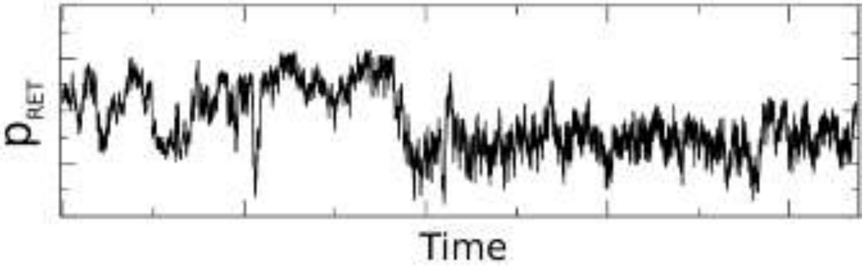

Step 3:
obtain photon statistics via MC

$$\begin{tikzcd}
 & D+A & k_T(t) & D+A \\
D+A+h\nu_E \arrow[r] & D^*+A \arrow[u, "k_{D_i}"] \arrow[rr, "k_T"] \arrow[d, "k_D"] & & D+A^* \arrow[u, "k_{A_i}"] \arrow[d, "k_A"] \\
 & D+A+h\nu_D & & D+A+h\nu_A
\end{tikzcd}$$

Step 4:
combine photon counts into bursts
from measured burst size statistics
--> efficiency histogram

$$E = \frac{n_\mathrm{A}}{n_\mathrm{A} + n_\mathrm{D}}$$

M. Höfling, N. Lima, C. A. M. Seidel, B. Schuler, H. Grubmüller (2011), PLOS One 6, e19791

Procedure Outline

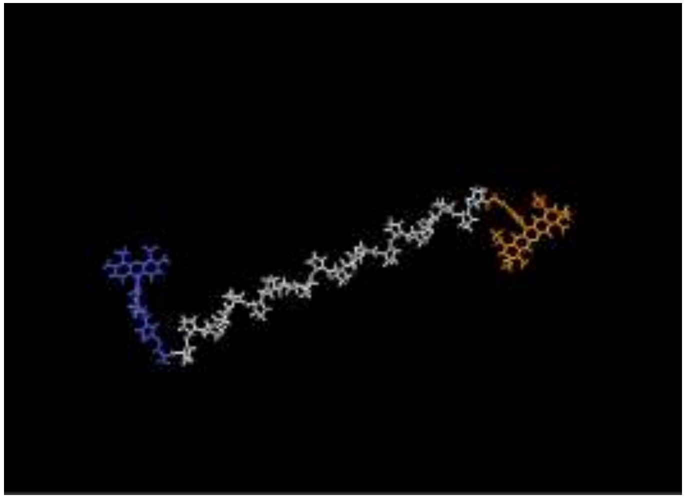

Step 1:
generate MD trajectories
--> $r(t)$, $\theta(t)$, $\varphi_1(t)$, $\varphi_2(t)$

Step 2:
generate $k_{RET}(t)$

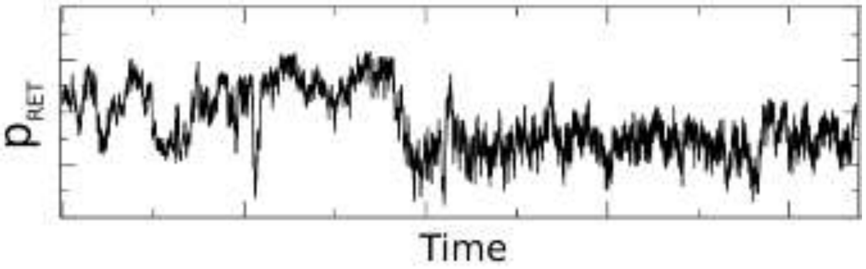

Step 3:
obtain photon statistics via MC

$$\begin{tikzcd}
 & D + A & & D + A \\
D + A + h\nu_E \arrow[r] & D^* + A \arrow[u, "k_{D_i}"'] \arrow[d, "k_D"] \arrow[rr, "k_T"', "k_T(t)"] & & D + A^* \arrow[u, "k_{A_i}"'] \arrow[d, "k_A"] \\
 & D + A + h\nu_D & & D + A + h\nu_A
\end{tikzcd}$$

Step 4:
combine photon counts into bursts
from measured burst size statistics
--> efficiency histogram

$$E = \frac{n_\mathrm{A}}{n_\mathrm{A} + n_\mathrm{D}}$$

M. Höfling, N. Lima, C. A. M. Seidel, B. Schuler, H. Grubmüller (2011), PLOS One 6, e19791

Procedure Outline

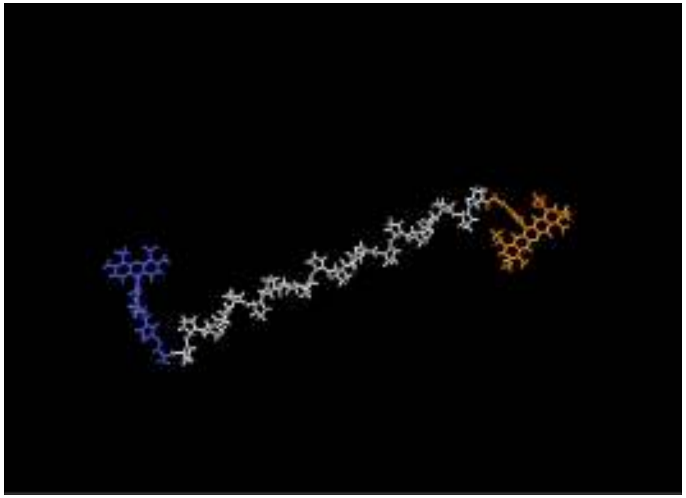

Step 1:
generate MD trajectories
--> r(t), θ(t), φ_1(t), φ_2(t)

Step 2:
generate k_{RET}(t)

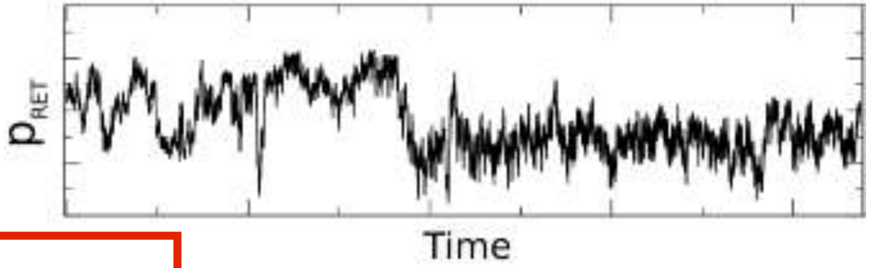

Step 3:
obtain photon statistics via MC

$$\begin{tikzcd}
 & D+A & & D+A \\
D+A+h\nu_E \arrow[r] & D^*+A \arrow[u, "k_{D_i}"'] \arrow[d, "k_D"] \arrow[rr, "k_T(t)", "k_T"'] & & D+A^* \arrow[u, "k_{A_i}"'] \arrow[d, "k_A"] \\
 & D+A+h\nu_D & & D+A+h\nu_A
\end{tikzcd}$$

Step 4:
combine photon counts into bursts
from measured burst size statistics
--> efficiency histogram

$$E = \frac{n_\mathrm{A}}{n_\mathrm{A} + n_\mathrm{D}}$$

M. Höfling, N. Lima, C. A. M. Seidel, B. Schuler, H. Grubmüller (2011), PLOS One 6, e19791

Procedure Outline

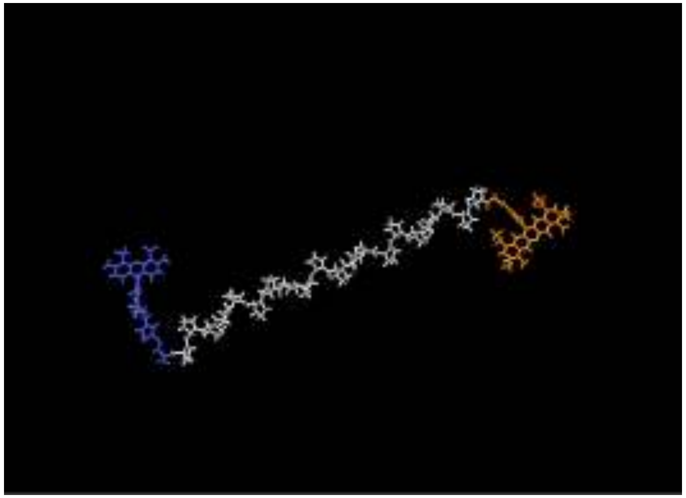

Step 1:
generate MD trajectories
--> $r(t)$, $\theta(t)$, $\varphi_1(t)$, $\varphi_2(t)$

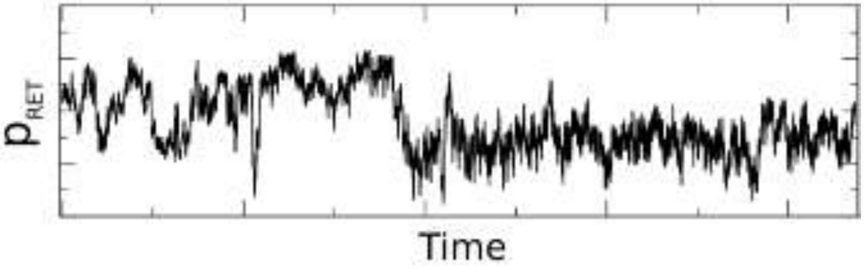

Step 2:
generate $k_{RET}(t)$

Step 3:
obtain photon statistics via MC

$$\begin{tikzcd}
 & D+A & k_T(t) & D+A \\
D+A+h\nu_E \arrow[r] & D^*+A \arrow[u, "k_{D_i}"'] \arrow[d, "k_D"'] \arrow[rr, "k_T"] & & D+A^* \arrow[u, "k_{A_i}"'] \arrow[d, "k_A"'] \\
 & D+A+h\nu_D & & D+A+h\nu_A
\end{tikzcd}$$

Step 4:
combine photon counts into bursts
from measured burst size statistics
--> efficiency histogram

$$E = \frac{n_\mathrm{A}}{n_\mathrm{A} + n_\mathrm{D}}$$

M. Höfling, N. Lima, C. A. M. Seidel, B. Schuler, H. Grubmüller (2011), PLOS One 6, e19791

Simulation vs. Experiment

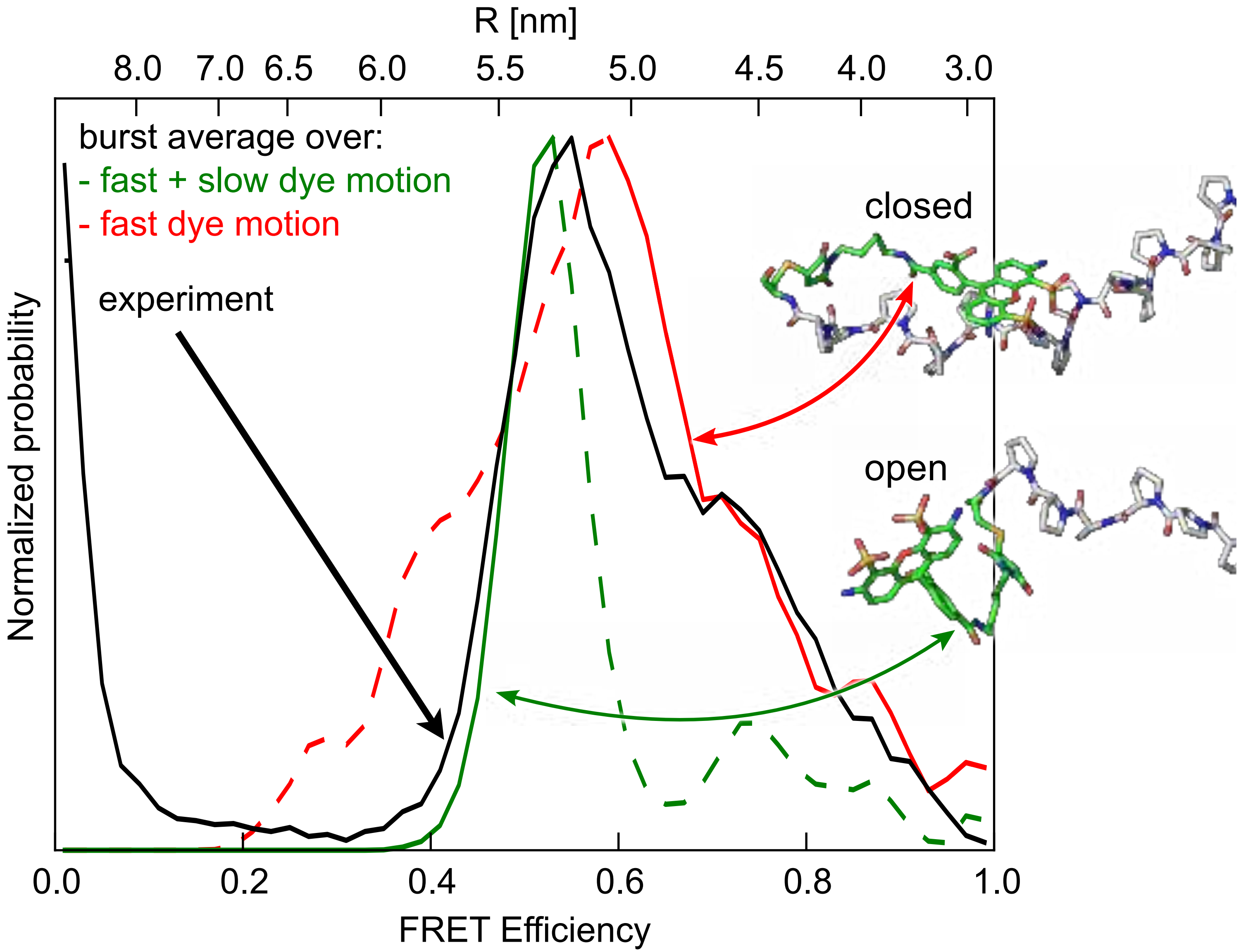

M. Höfling, N. Lima, C. A. M. Seidel, B. Schuler, H. Grubmüller (2011), PLOS One 6, e19791

Can improved distance distributions be obtained?   YES!

Example: polyproline

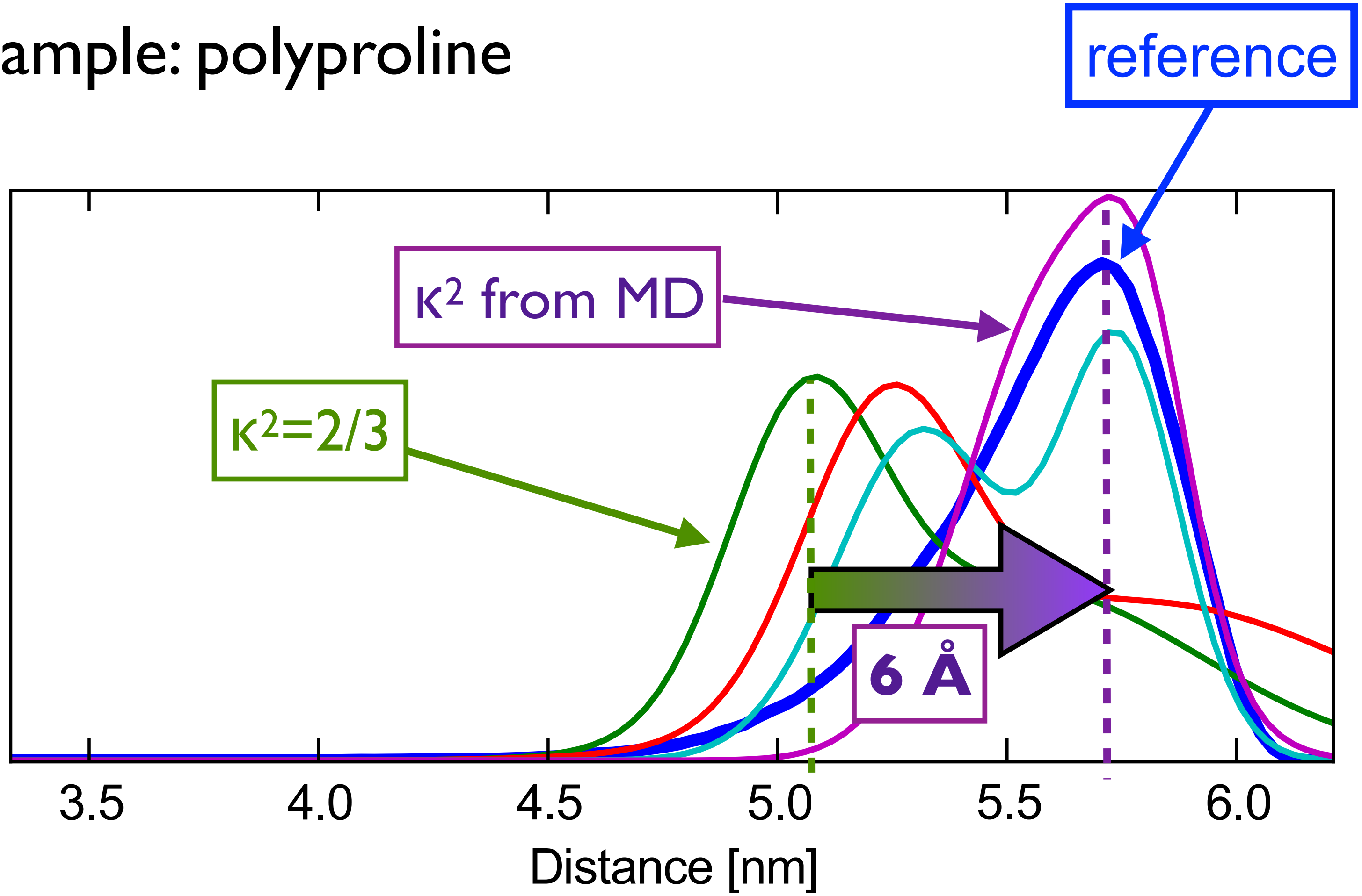

M. Höfling, N. Lima, C. A. M. Seidel, B. Schuler, H. Grubmüller (2011), PLOS One 6, e19791

F-ATP Synthase

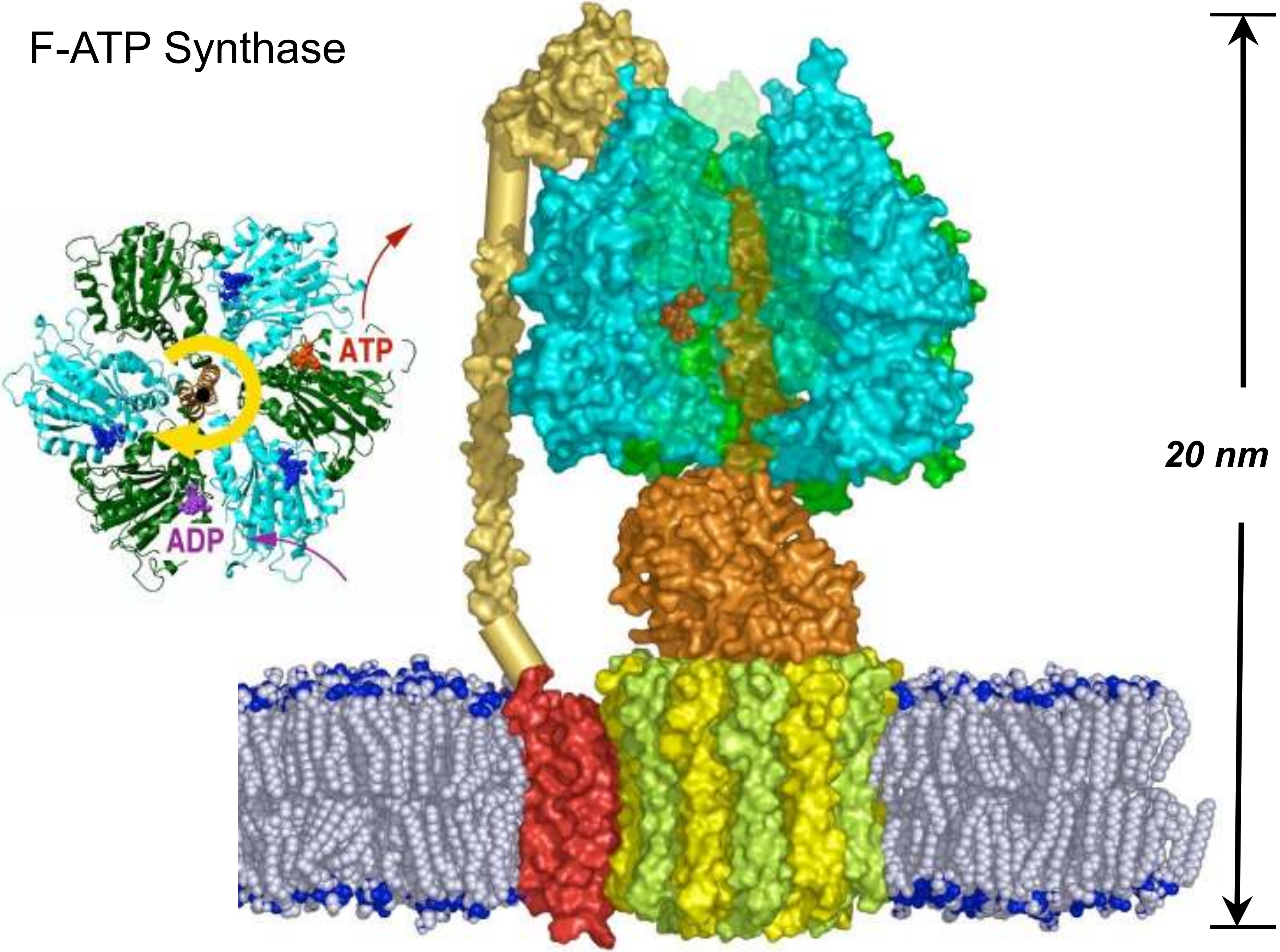

Elastic properties of the F_1-ATPase rotor – simulation setup

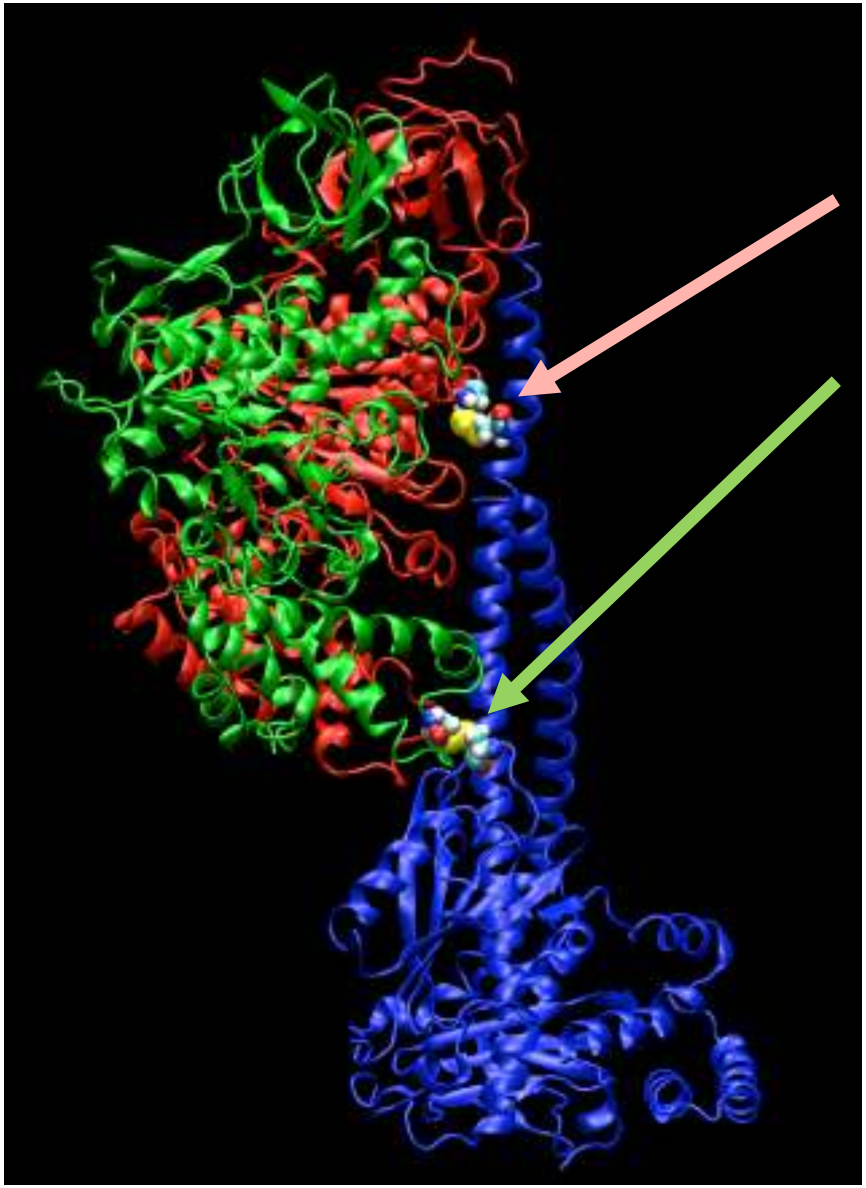

Disulfide bonds:

MIDDLE:

Cys (α_E-292) -- Cys (γ-256)

BOTTOM:

Cys (β_{TP}-395) -- Cys (γ-78)

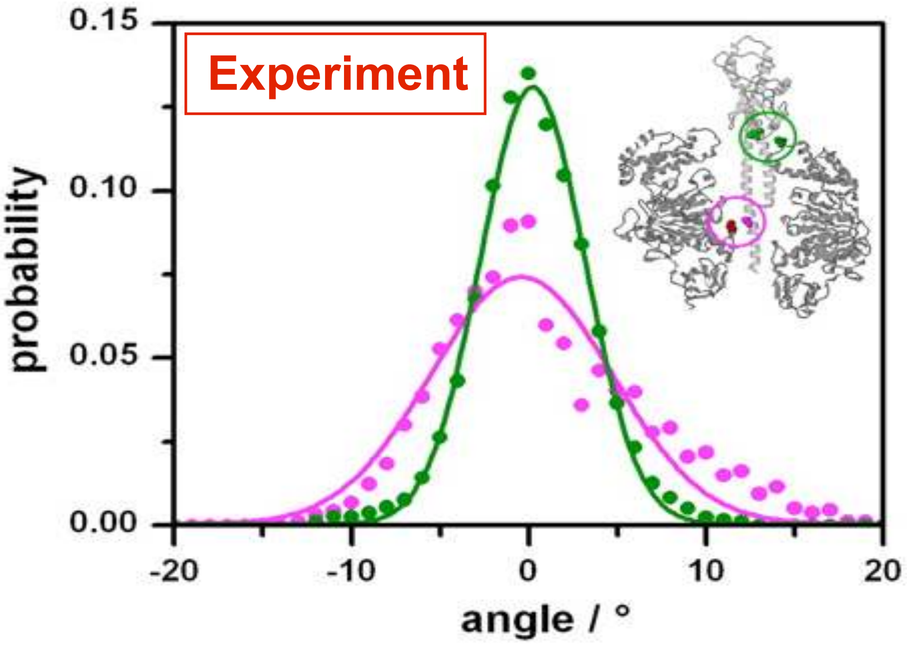

(Sielaff et al., PNAS 105:17760-17765, 2008)

Simulation of fluctuating gamma subunit within complete F1 -- 400 ns

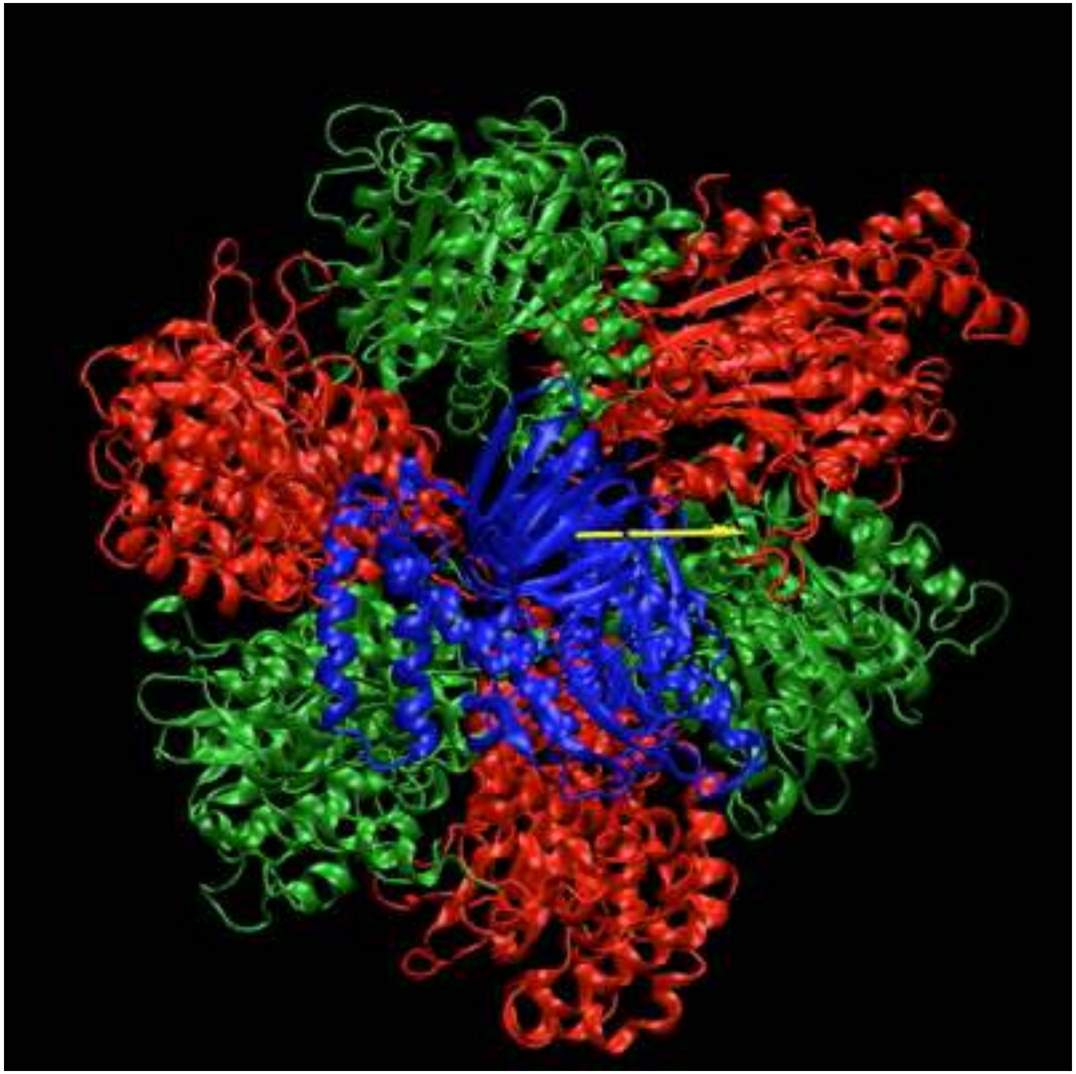

Jacek Czub
(now Gdansk)

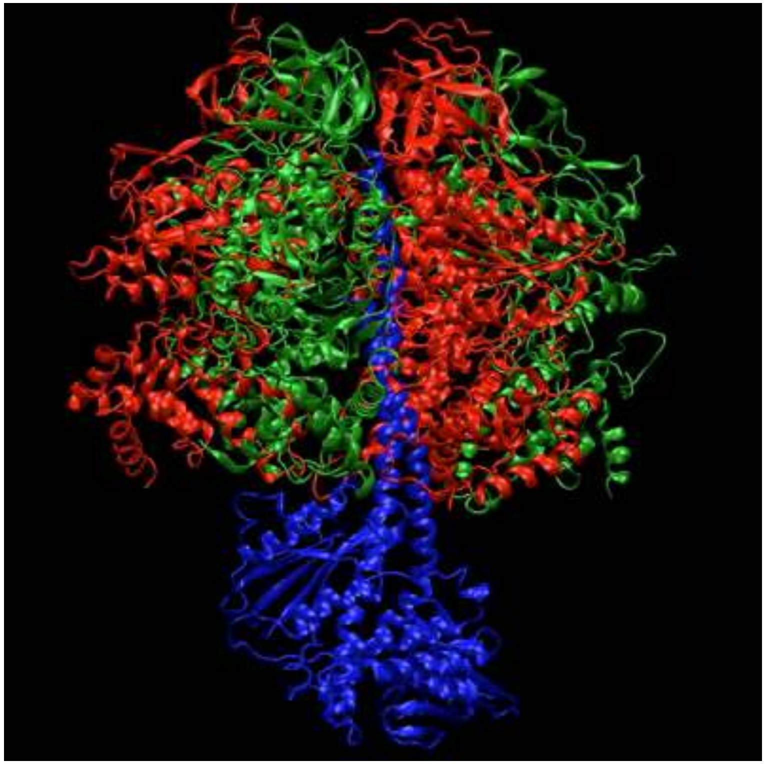

Elastic properties of the F_1-ATPase rotor – Results

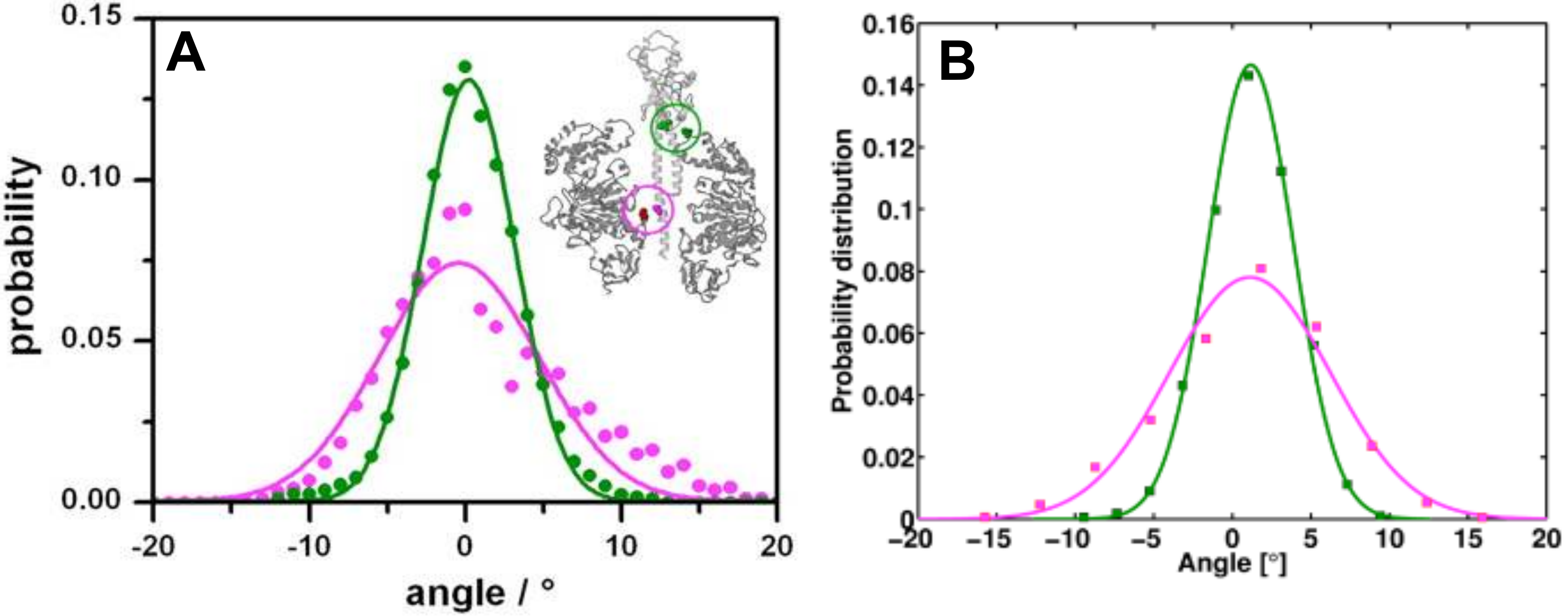

Experiment

Simulation (400 ns each)

Figure: Distributions of the rotation angle observed in the experiment (Sielaff et al. PNAS 105:17760-, 2008) (A) and obtained from molecular dynamics simulations (B).

J. Czub, H. Grubmüller, PNAS 108, 7408-7413 (2011)

Elastic properties of the F_1-ATPase rotor – Fluctuation Analysis

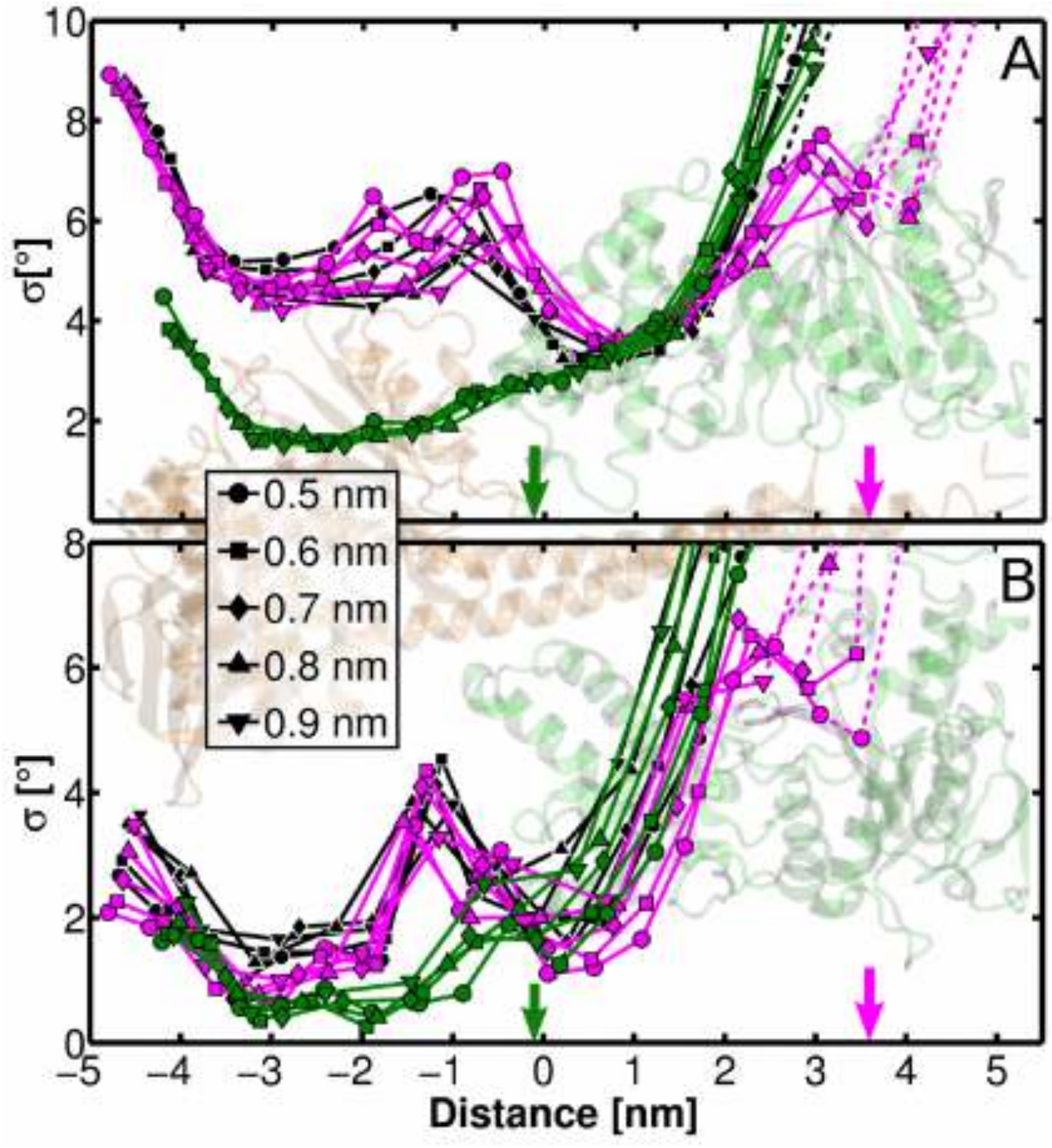

J. Czub, H. Grubmüller, PNAS 108, 7408-7413 (2011)

Elastic properties of the F_1-ATPase rotor – Fluctuation Analysis

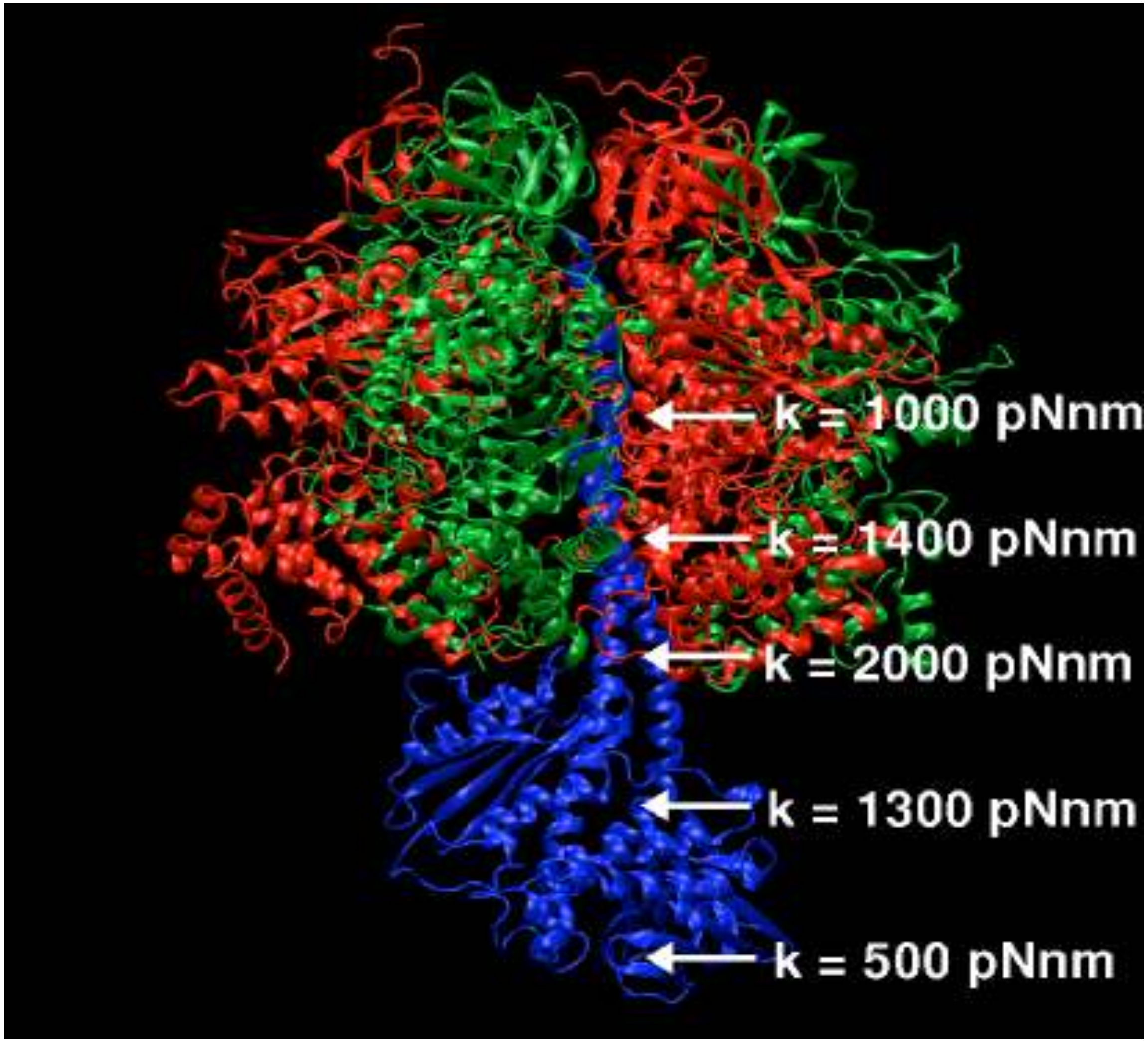

J. Czub, H. Grubmüller, PNAS 108, 7408-7413 (2011)

Elastic properties – conclusions

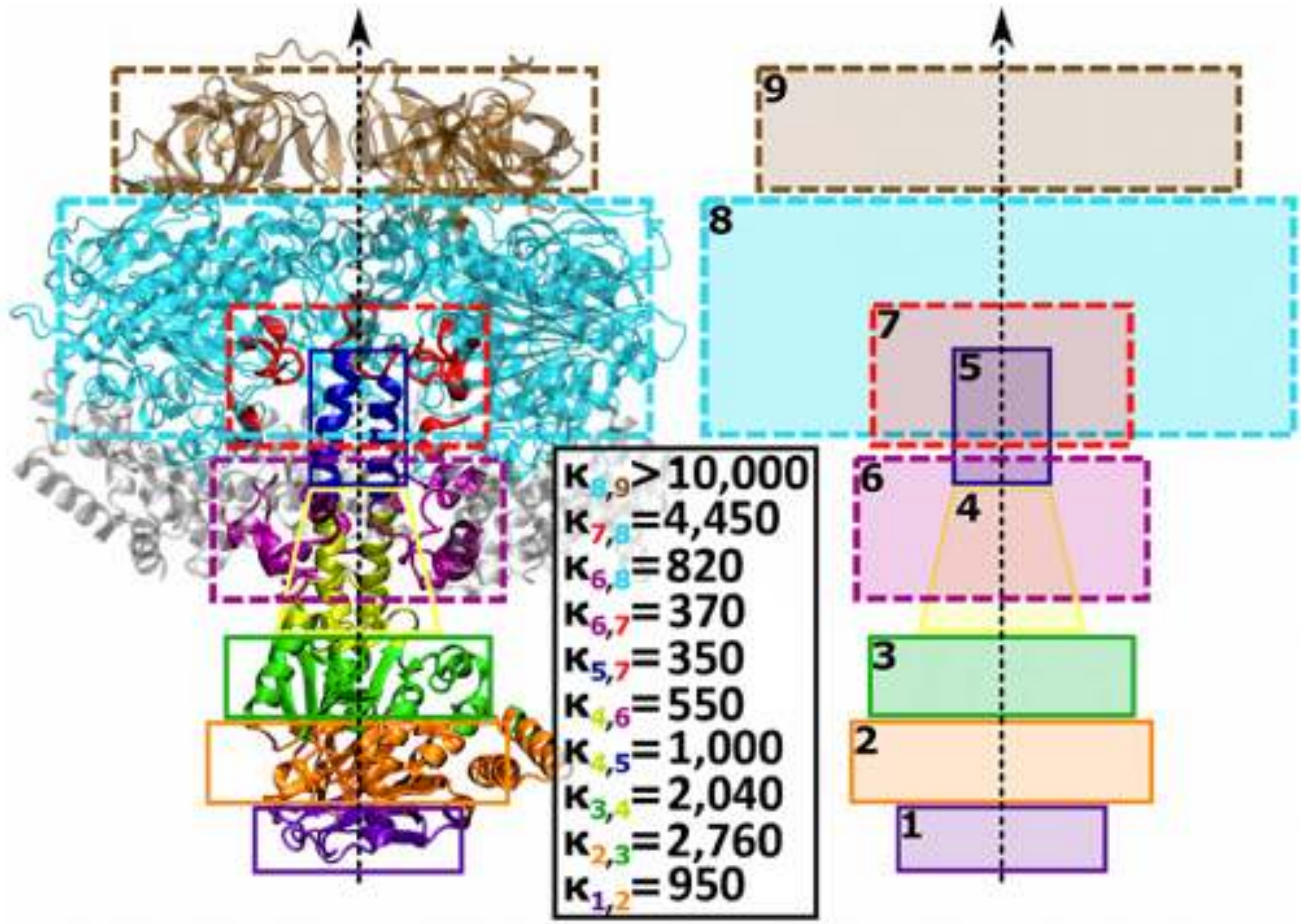

$\kappa_{8,9} > 10{,}000$
$\kappa_{7,8} = 4{,}450$
$\kappa_{6,8} = 820$
$\kappa_{6,7} = 370$
$\kappa_{5,7} = 350$
$\kappa_{4,6} = 550$
$\kappa_{4,5} = 1{,}000$
$\kappa_{3,4} = 2{,}040$
$\kappa_{2,3} = 2{,}760$
$\kappa_{1,2} = 950$

elastic moduli [pNnm]

45%: $(\alpha\beta)_3$–domain

25%: γ–stalk

30%: shaft domain

J. Czub, H. Grubmüller, PNAS 108, 7408-7413 (2011)

Driving Rotary motions with a flexible Axis

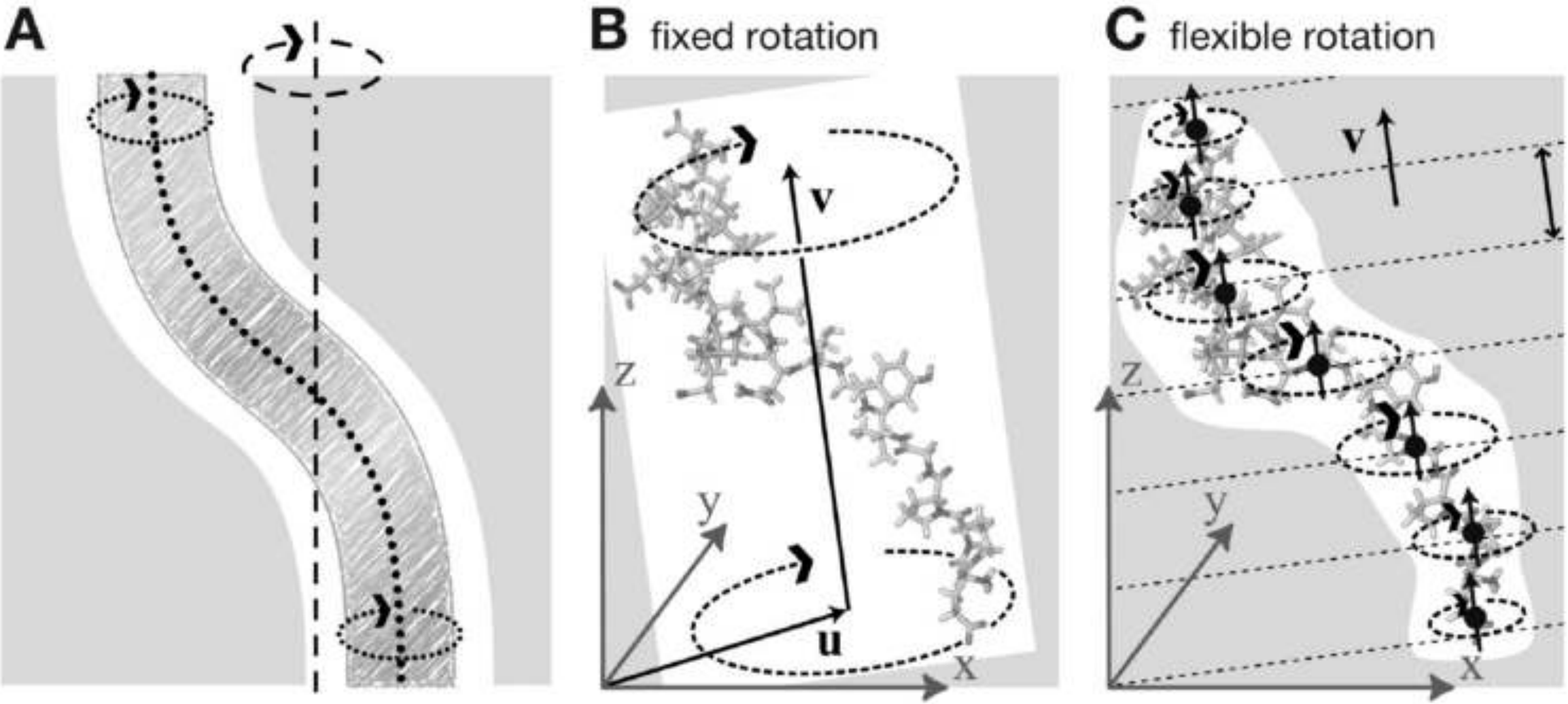

C. Kutzner, J. Czub, H. Grubmüller, JCTC 7, 1381-1393 (2011)

120^o Gamma Subunit Rotation

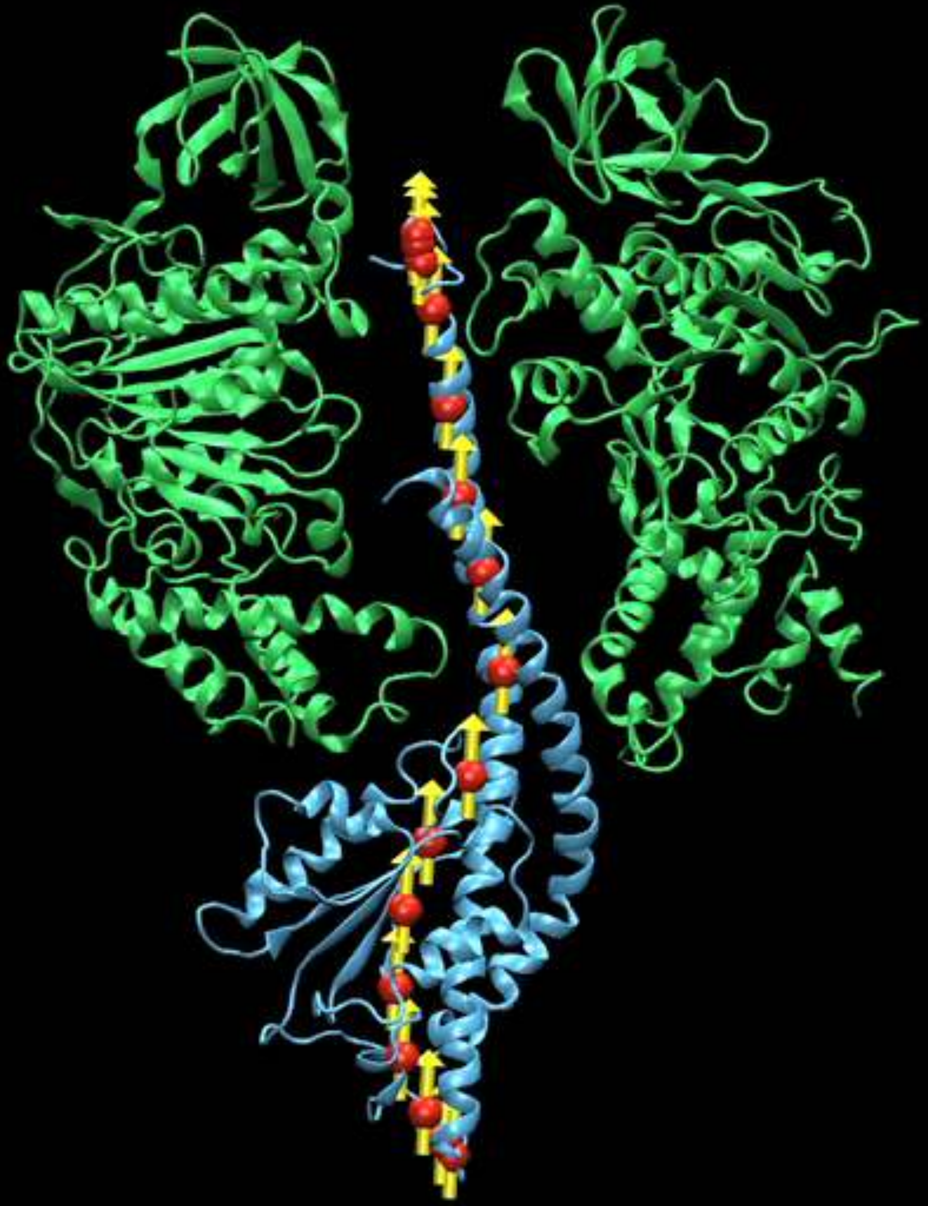

Free energy landscape of gamma subunit rotation with bound ATP --> Convergence

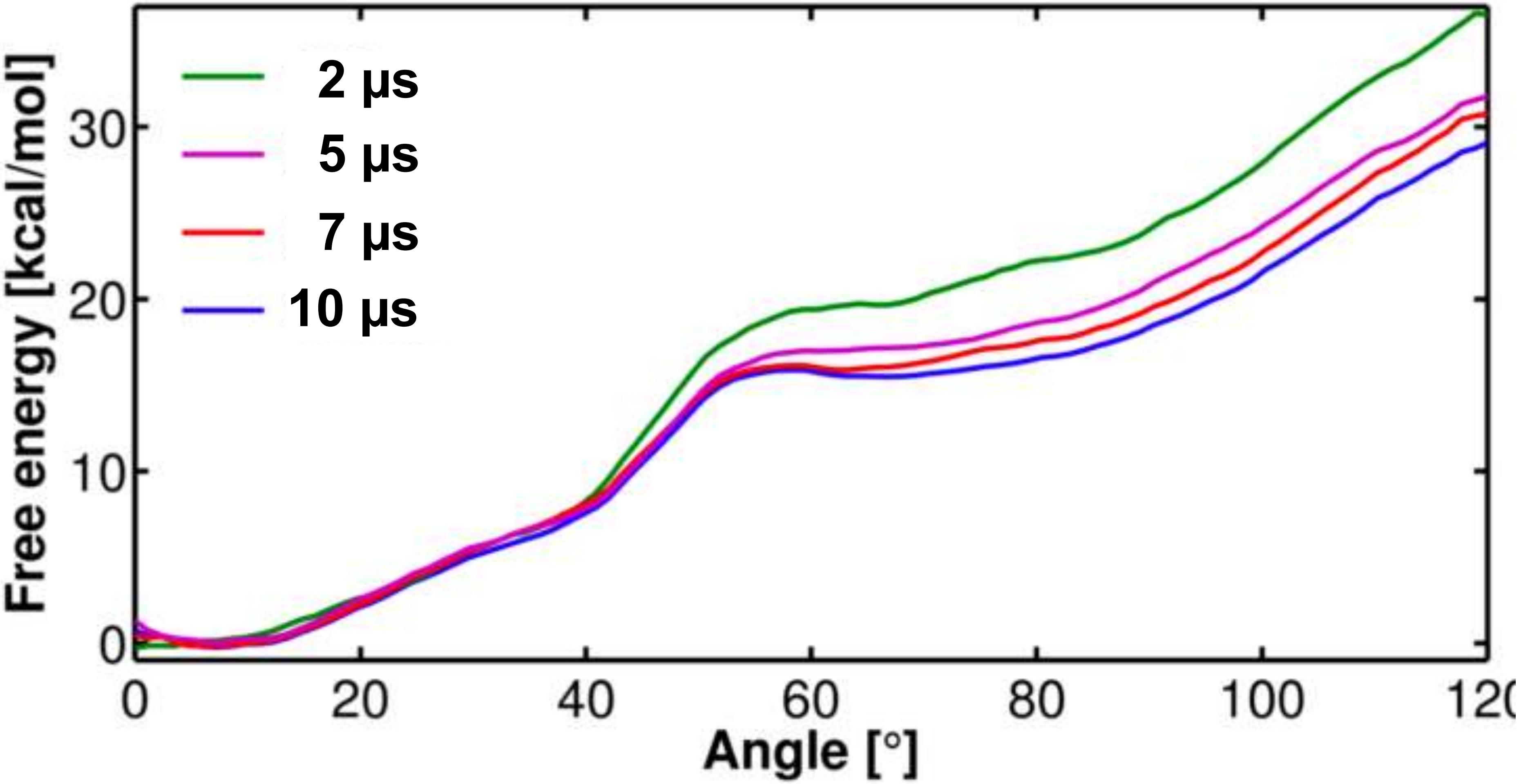

J. Czub, M. Wieczoŕ, B. Prokopowicz, H. Grubmüller, J. Am. Chem. Soc. 2017, 139, 4025–4034 (2017)

Free energy landscape of gamma subunit rotation

with bound ATP and ADP

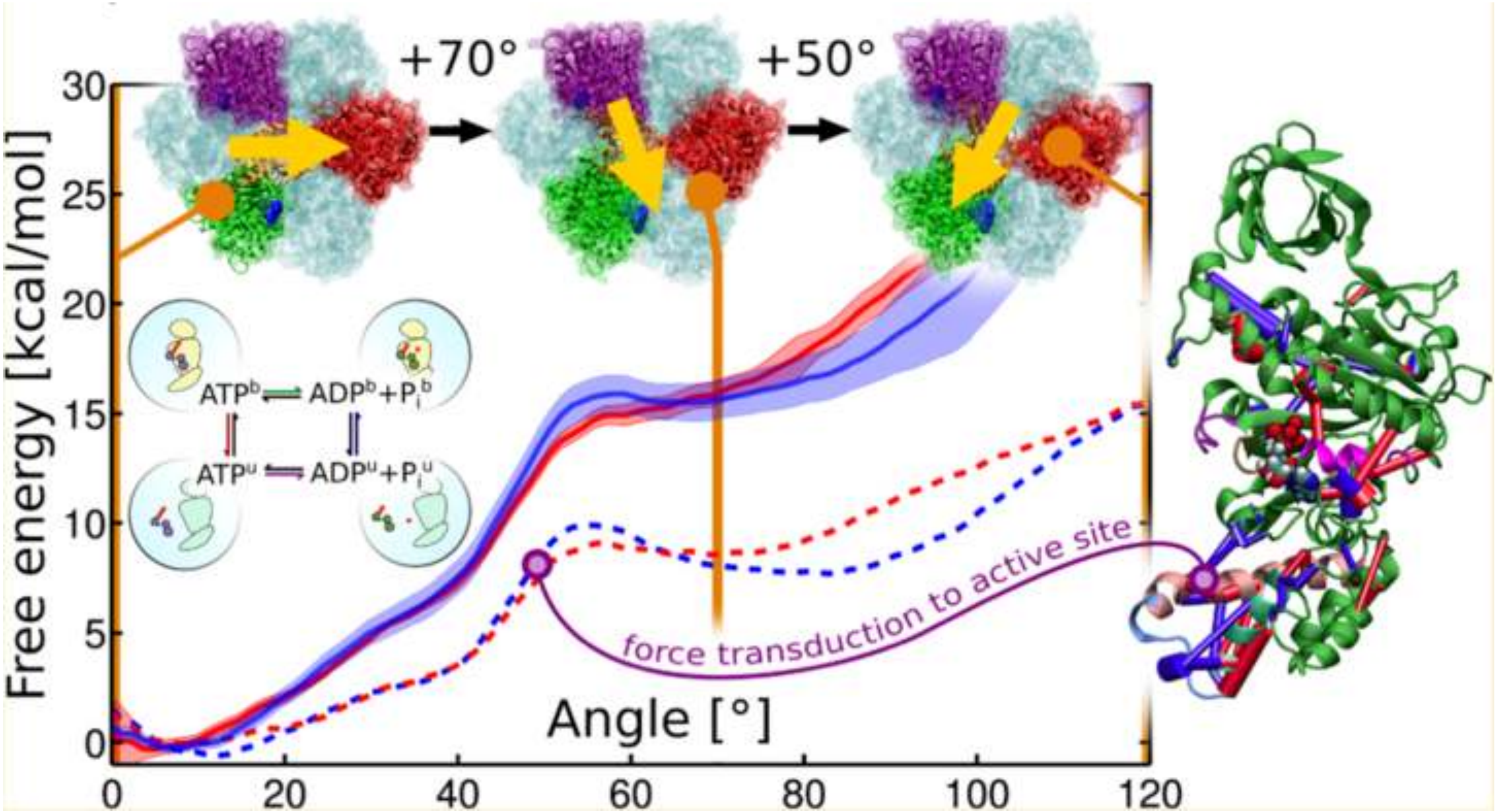

J. Czub, M. Wieczoŕ, B. Prokopowicz, H. Grubmüller, J. Am. Chem. Soc. 2017, 139, 4025–4034 (2017)

Conformational changes upon gamma subunit rotation (in synthesis direction)

70° sub-step seen as metastable free energy minimum (pre ATP release)

Major free energy input via γ-rotation before 70° sub-step

=> Fine-tuned for 13 kcal/mol total energy turnover

=> compatible with kinetics

120^o Gamma Subunit Rotation

0 ns
0°

Conformational changes upon gamma subunit rotation

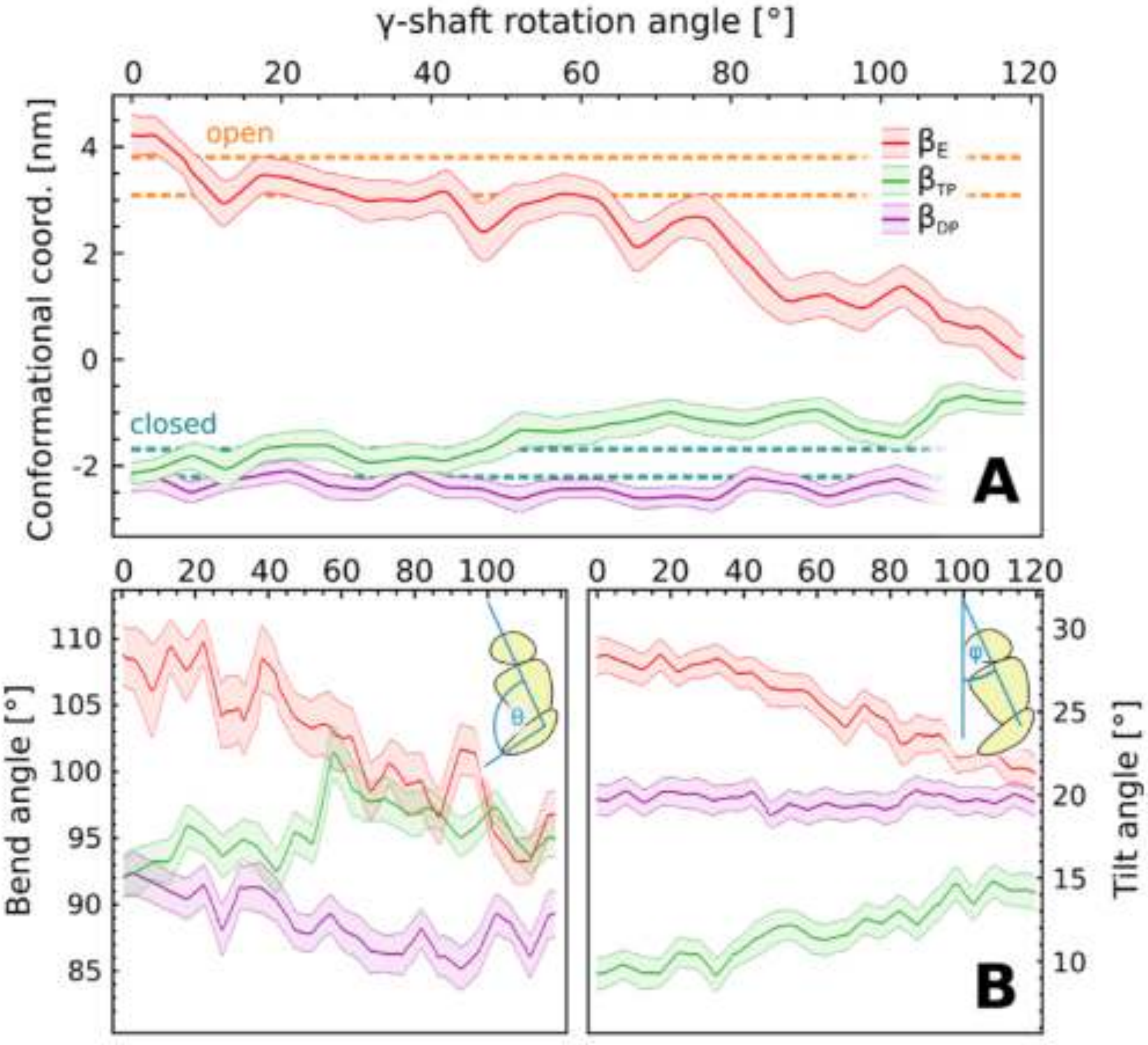

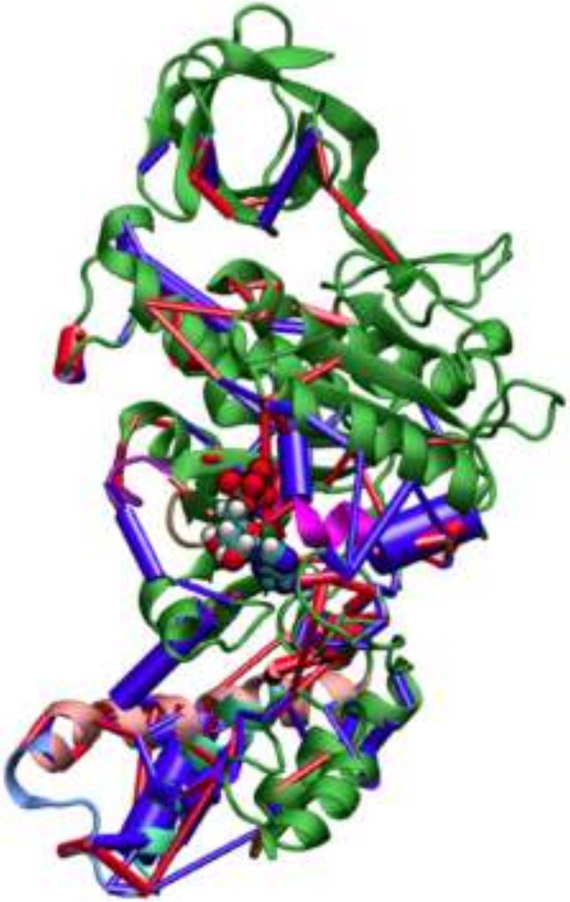

J. Czub, M. Wieczoŕ, B. Prokopowicz, H. Grubmüller, J. Am. Chem. Soc. 2017, 139, 4025–4034 (2017)

Conformational changes upon gamma subunit rotation (in synthesis direction)

β_{TP} opens only partially during γ-rotation

=> full β_{TP} opening only after ATP release

=> Helix 2 as a gate-keeper

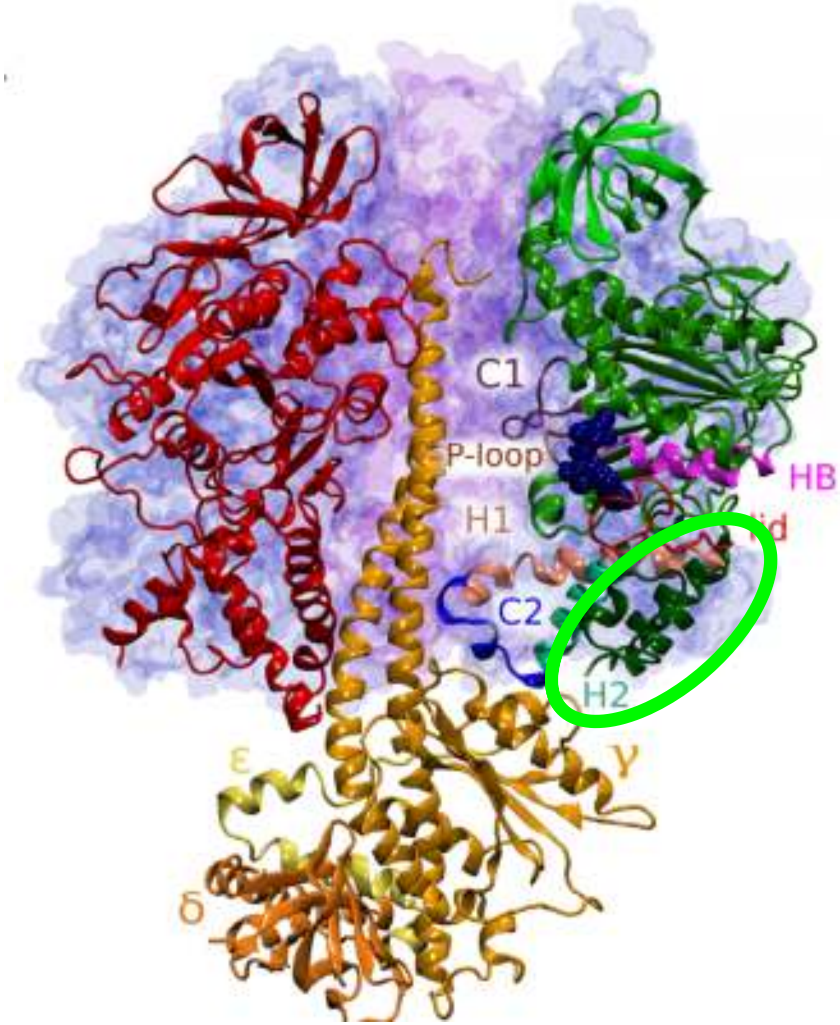

J. Czub, M. Wieczoŕ, B. Prokopowicz, H. Grubmüller, J. Am. Chem. Soc. 2017, 139, 4025–4034 (2017)

Electrostatic repulsion between H2 and gamma prevents completion of opening before ATP release

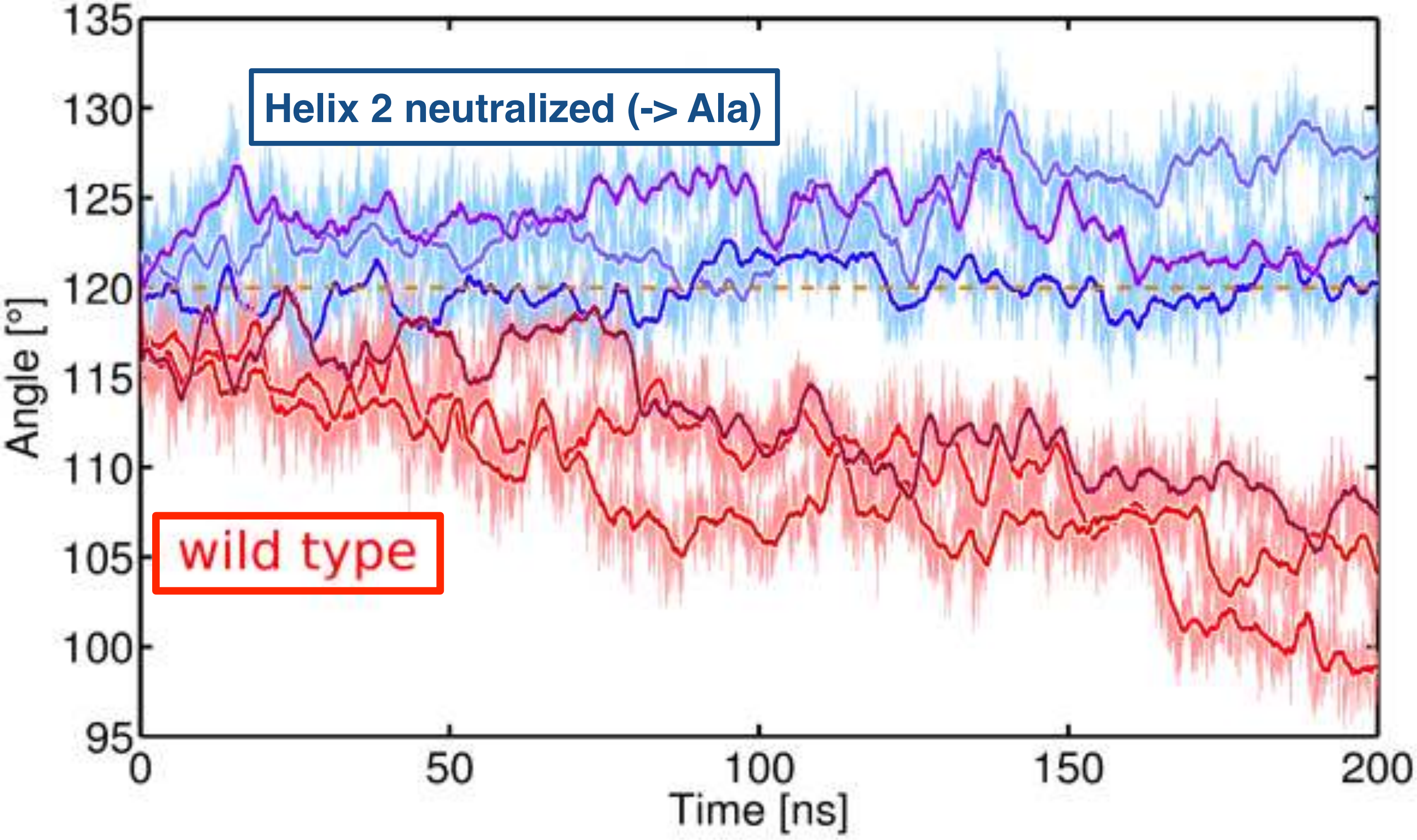

J. Czub, M. Wieczoŕ, B. Prokopowicz, H. Grubmüller, J. Am. Chem. Soc. 2017, 139, 4025–4034 (2017)

Conformational changes upon gamma subunit rotation (in synthesis direction)

β_E closes spontaneously during γ-rotation, to stable half-open state

=> not the rate-limiting step

=> subsequent ADP binding allosterically contributes to full β_{TP} opening

=> avoids 'waste' of energy through irreversible downhill ADP binding

J. Czub, M. Wieczoŕ, B. Prokopowicz, H. Grubmüller, J. Am. Chem. Soc. 2017, 139, 4025–4034 (2017)

Spontaneous closure of β_E is driven by competing interactions

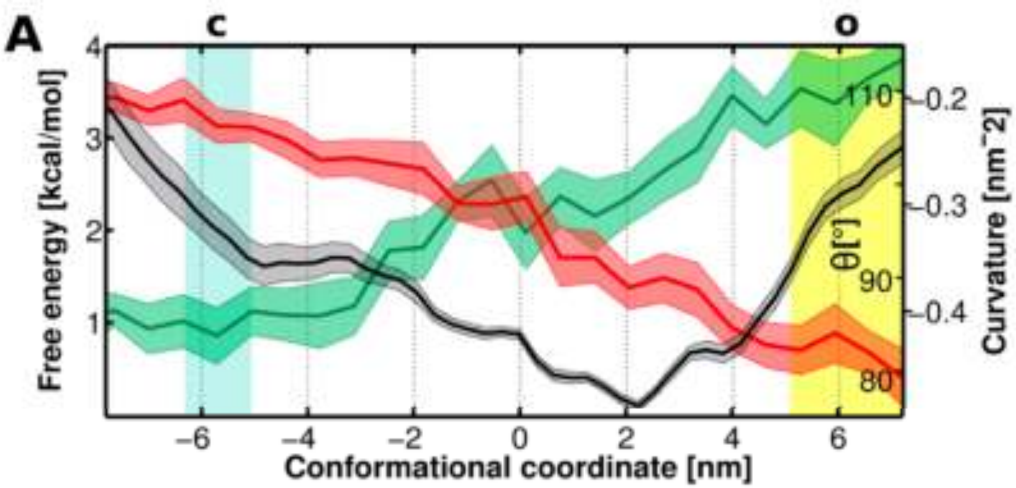

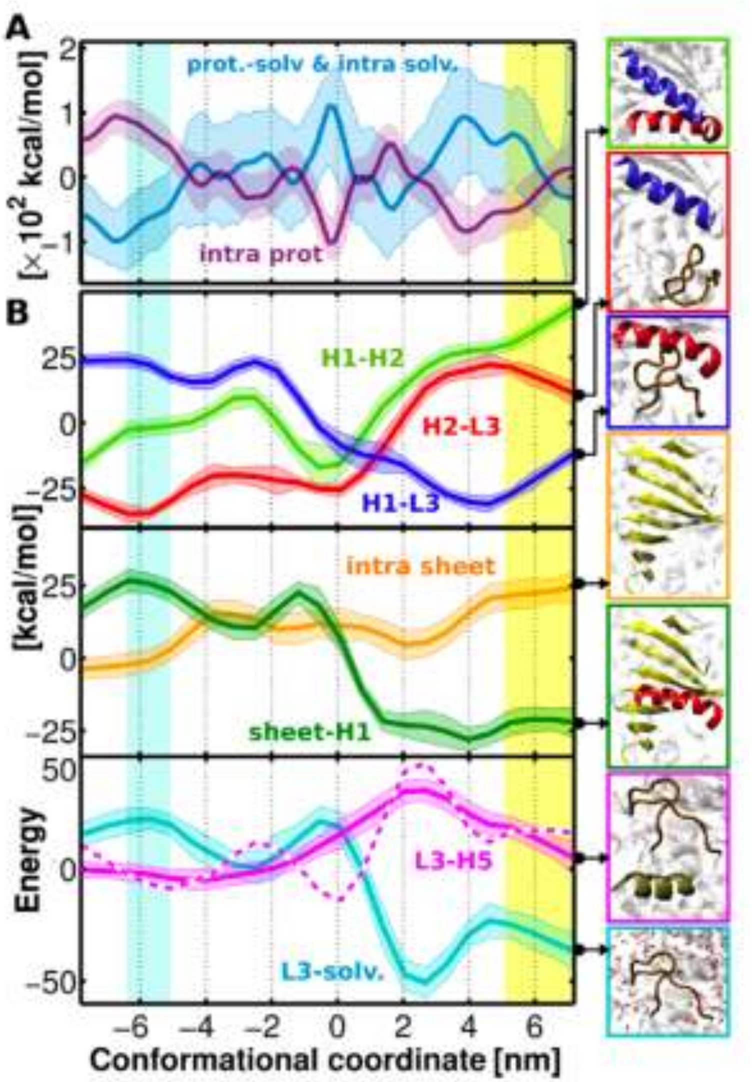

J. Czub, M. Wieczoŕ, B. Prokopowicz, H. Grubmüller, J. Am. Chem. Soc. 2014, 136, 6960–6968 (2014)

Conformational changes upon gamma subunit rotation (in synthesis direction)

Affinity reduction for bound ATP

due to electrostatic

coupling with Arg finger(s)

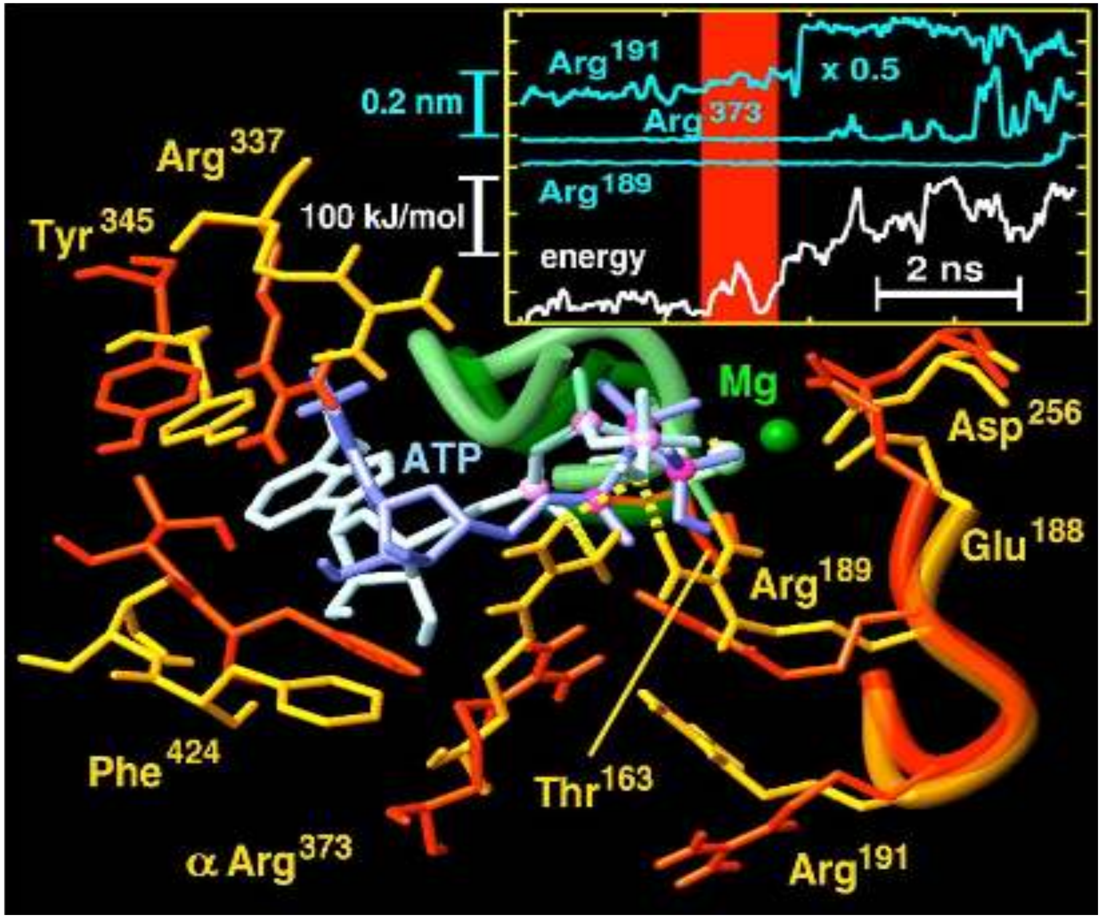

Towards a mechanistic understanding of protein function

(1) Ligand unbinding revisited

(2) Ribosomal antibiotics mechanism

(3) Intrinsically Disordered Proteins

(4) The Dynasome

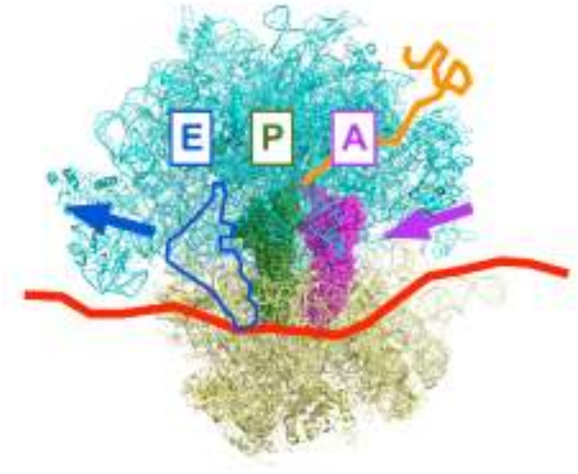

AFM+ X-ray + cryo EM + MD

Lars Bock, Christian Blau, Michal Kolar, Andrea Vaiana, Andreas Russek, Sarah Rauscher, Ulf Hensen

Holger Stark, Marina Rodnina (MPI Göttingen)
Roland Beckmann, Daniel Wilson (Univ. Munich)
Simon Scheuring (Cornell Univ.)

Ribosomal tRNA translocation and stalling: X-ray + cryoEM + MD

Lars Bock, Christian Blau, Andrea Vaiana

Collab.: Holger Stark, Marina Rodnina (MPI Göttingen)
Roland Beckmann, Daniel Wilson (Univ. Munich)

The Ribosome

2.5 MDa

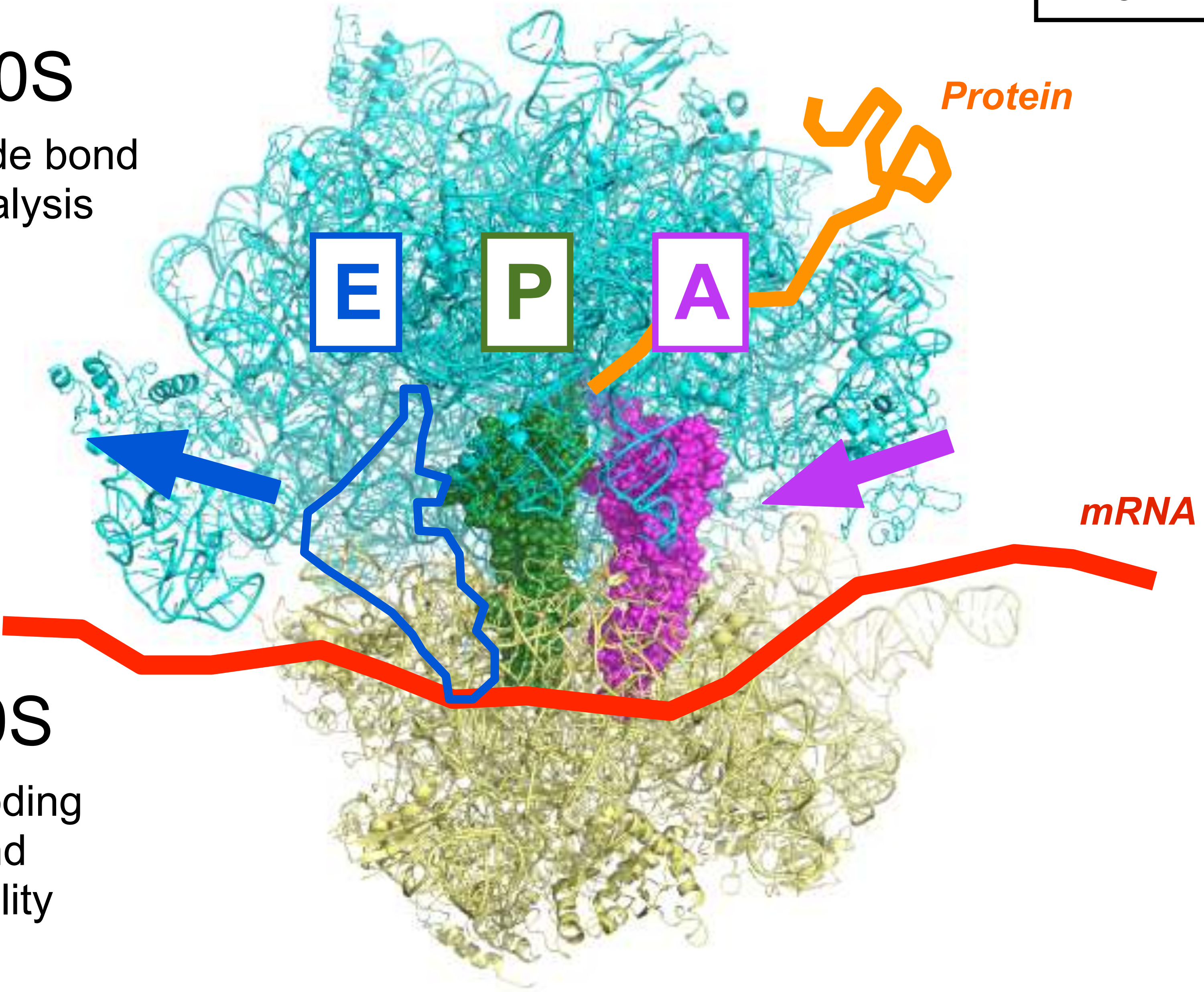

50S

Peptide bond
catalysis

30S

Decoding
and
fidelity

Refinement of x-ray structure against Cryo-EM densities

Crystal structure [1]

Refined against 13 EM-maps

by flexible fitting (DireX [2])

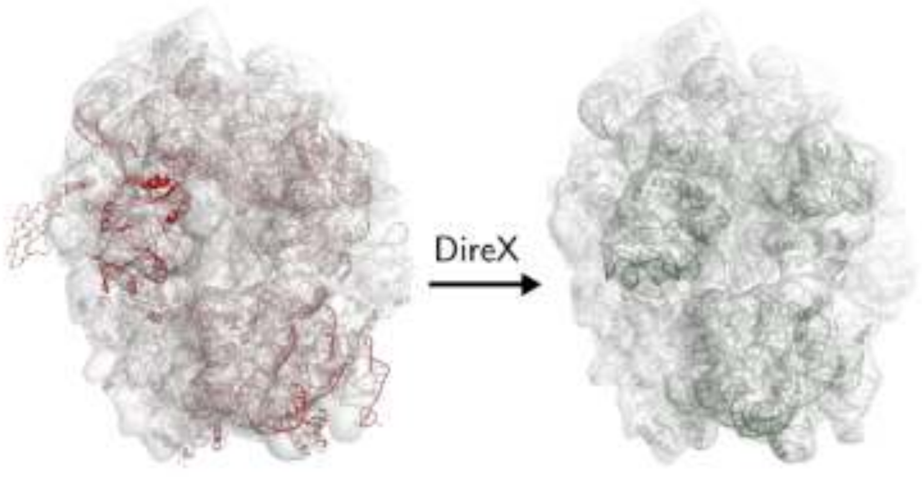

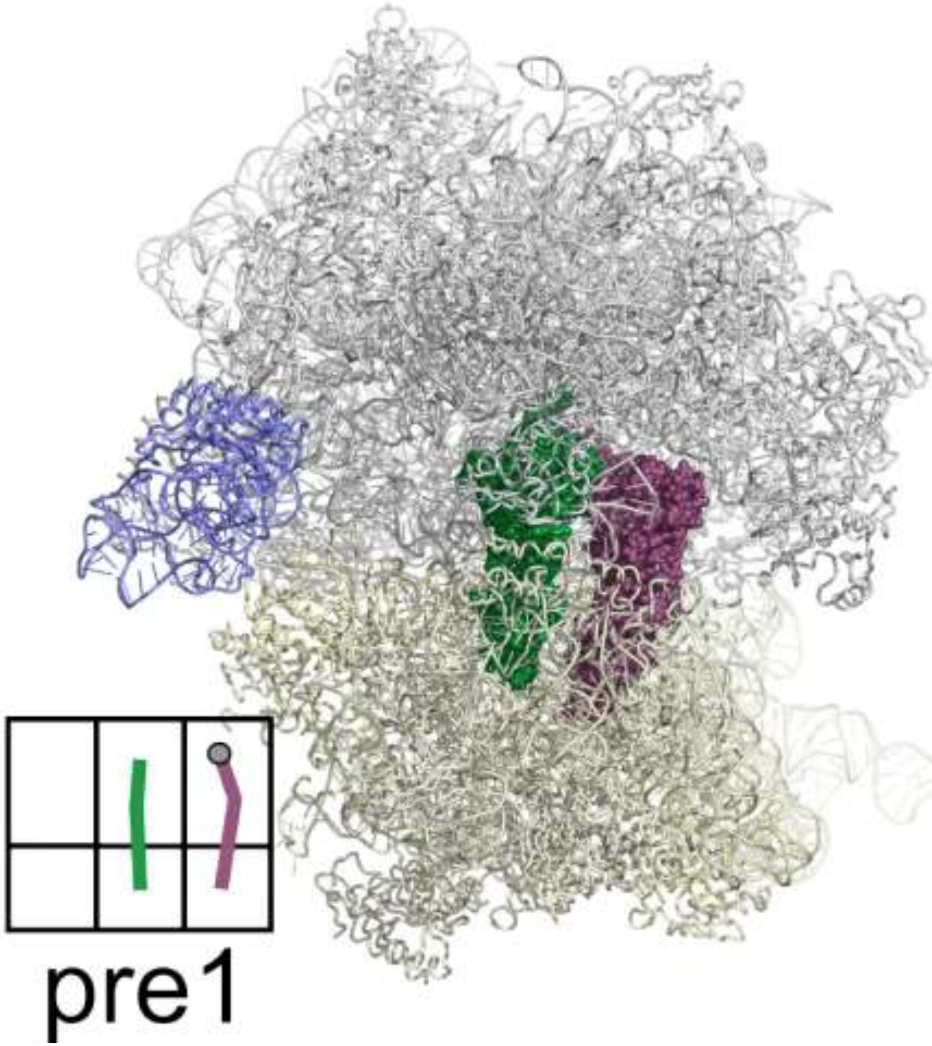

[1] Zhang et al., 2009, Science
[2] Schröder et al., 2007, Structure

Correlation does not imply causality

Multiple MD Simulations

- 13 MD simulations (min one per state)
- at least 100 ns for each state
  ~1500 ns total simulation time

ms...min

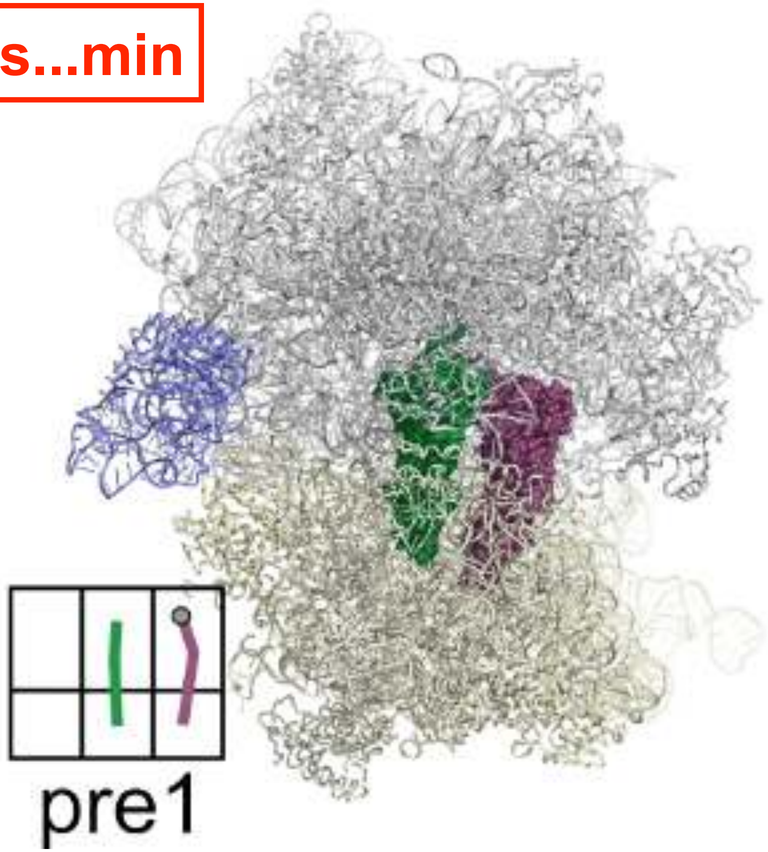

- Amber99sb force field
- GROMACS 4.0
- 150mM KCl 7mM Mg2Cl
- SPC/E water
- 2.2 M atoms
- NPT simulations

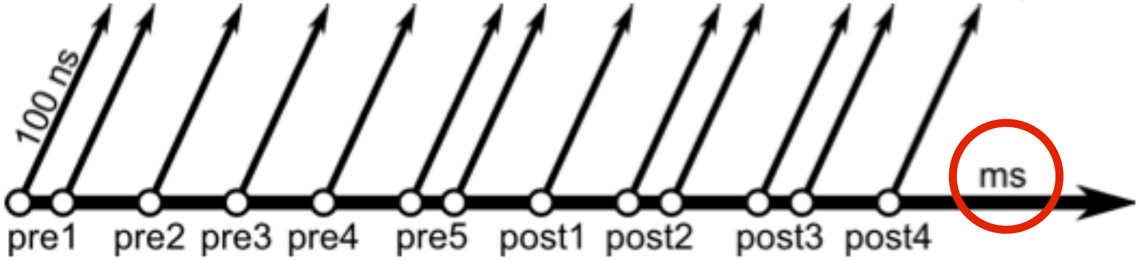

Dynamics, energetics, and driving forces from MD Simulations

ns...µs

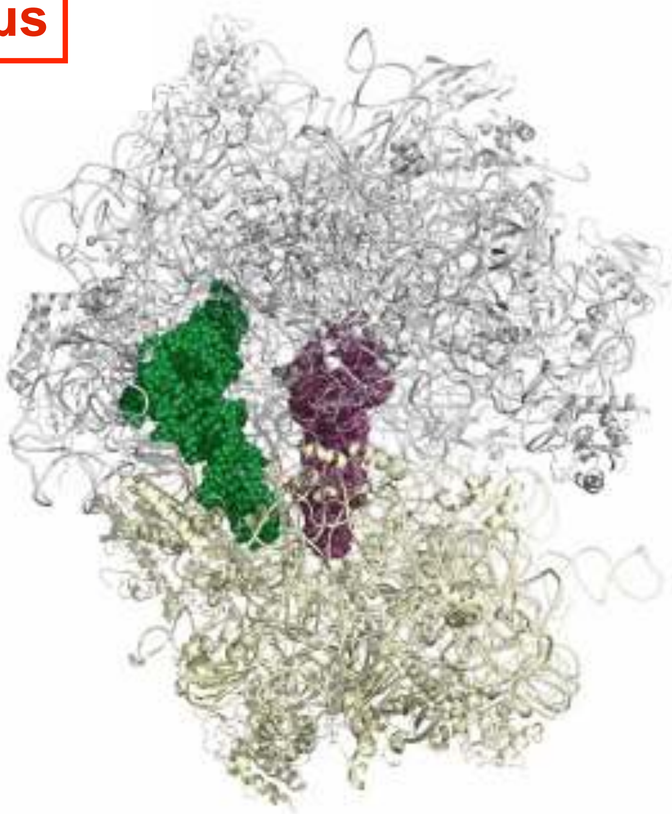

ms...min

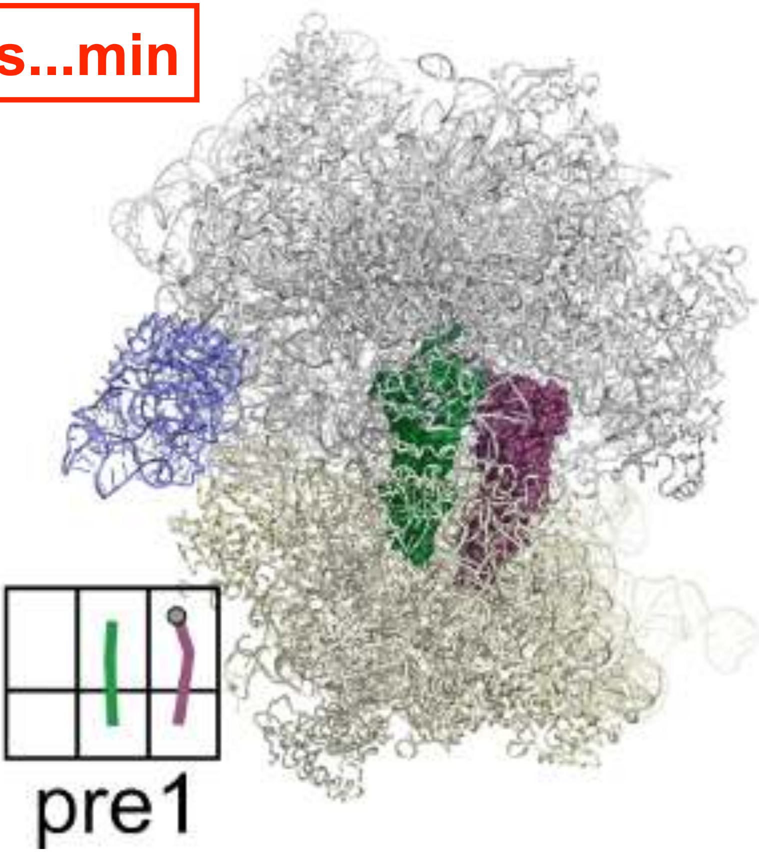

Coordinated conformational motions: L1 and tRNAs

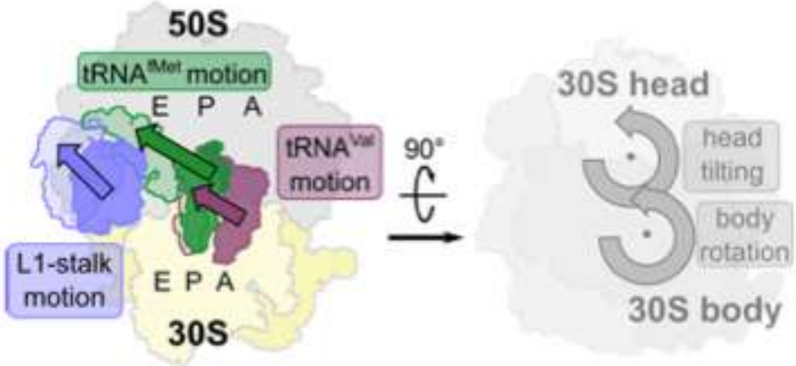

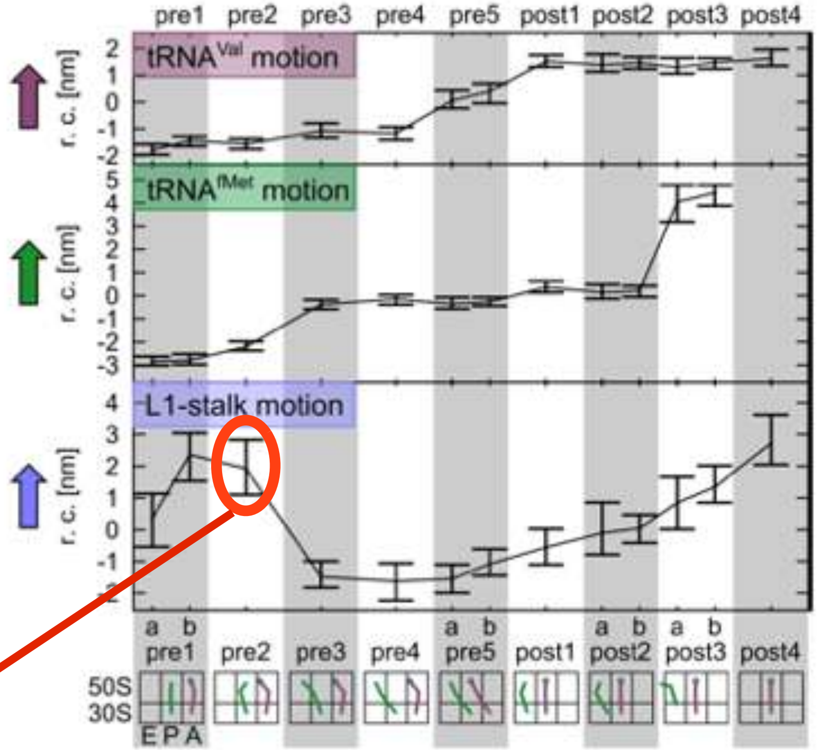

structural fluctuations @ 100 ns

Which motions limit translocational transition rates?

... and how are these overcome by the ribosome?

Transition rate estimates from MD

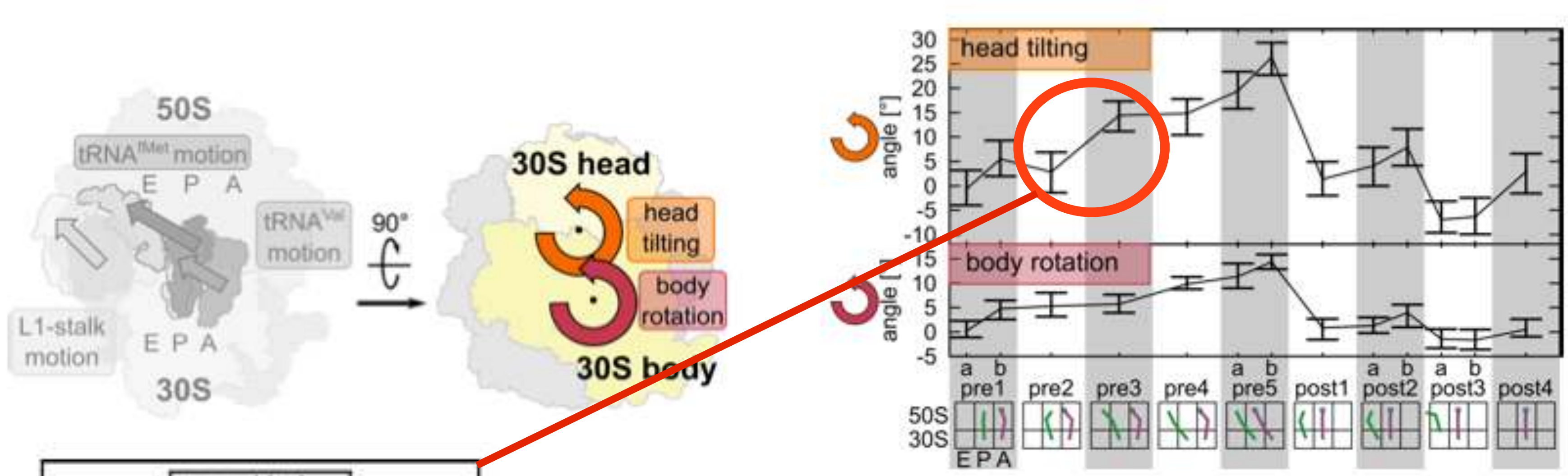

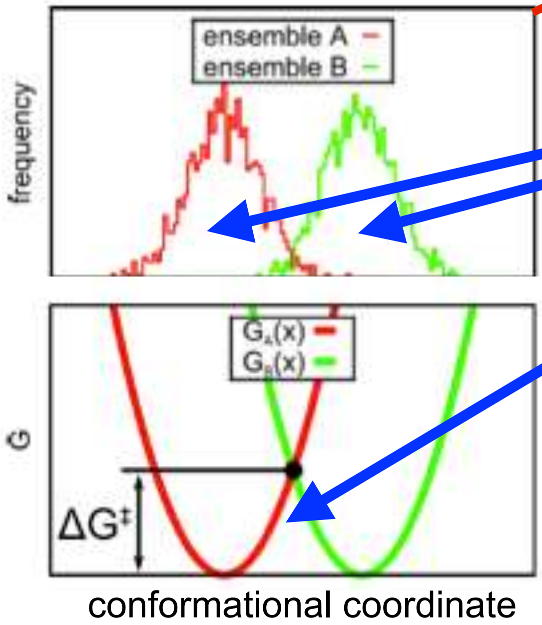

MD: fluctuations @ 100 ns

overlap -> barrier height

MD: Attempt frequency

$$k = A\exp(\Delta G^\ddagger / k_b T)$$

Rate-limiting: tRNA movement

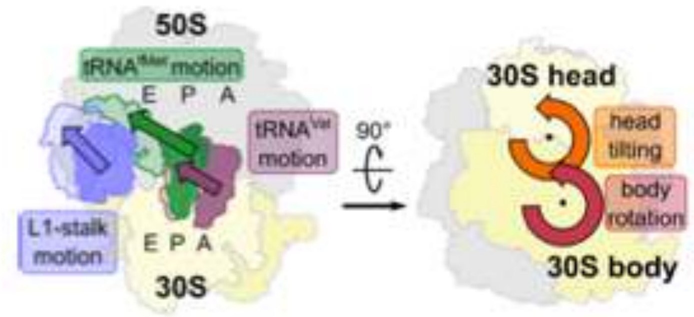

Most transition rates are determined by barriers which limit tRNA movement.

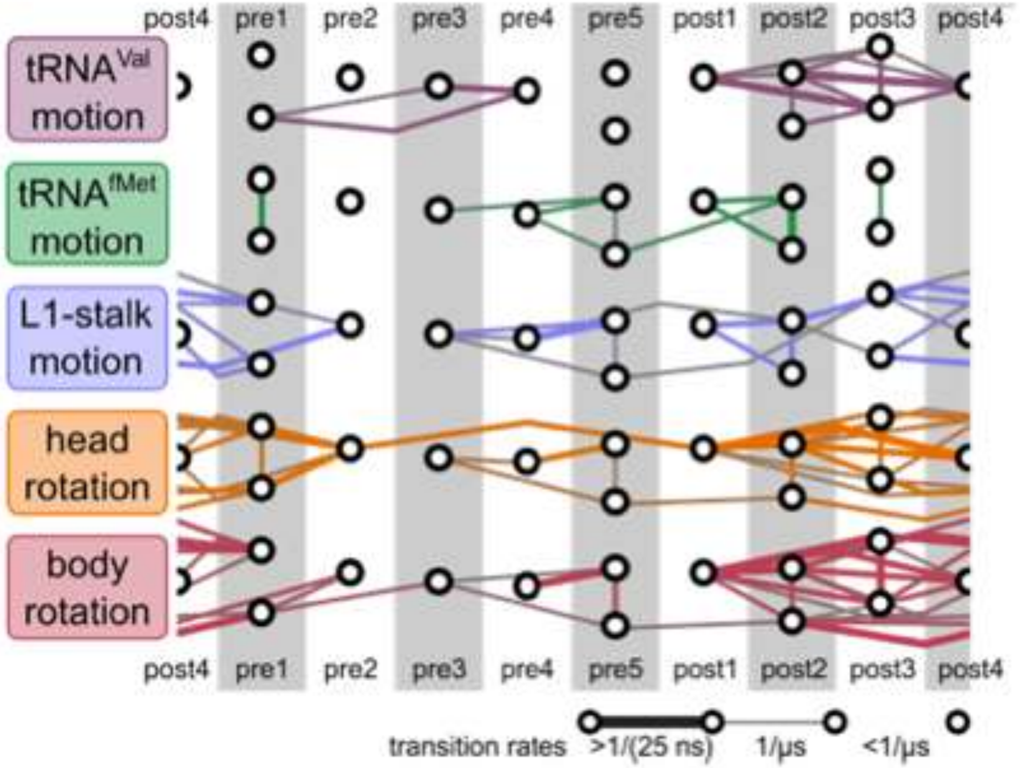

Bock LV, Blau C, Schröder GF, Davydov II, Fischer N, Stark H, Rodnina MV, Vaiana AC, Grubmüller H. **Energy barriers and driving forces in tRNA translocation through the ribosome.** *Nature Struct. Molec. Biol.*, in press

Local interactions: L1 stalk

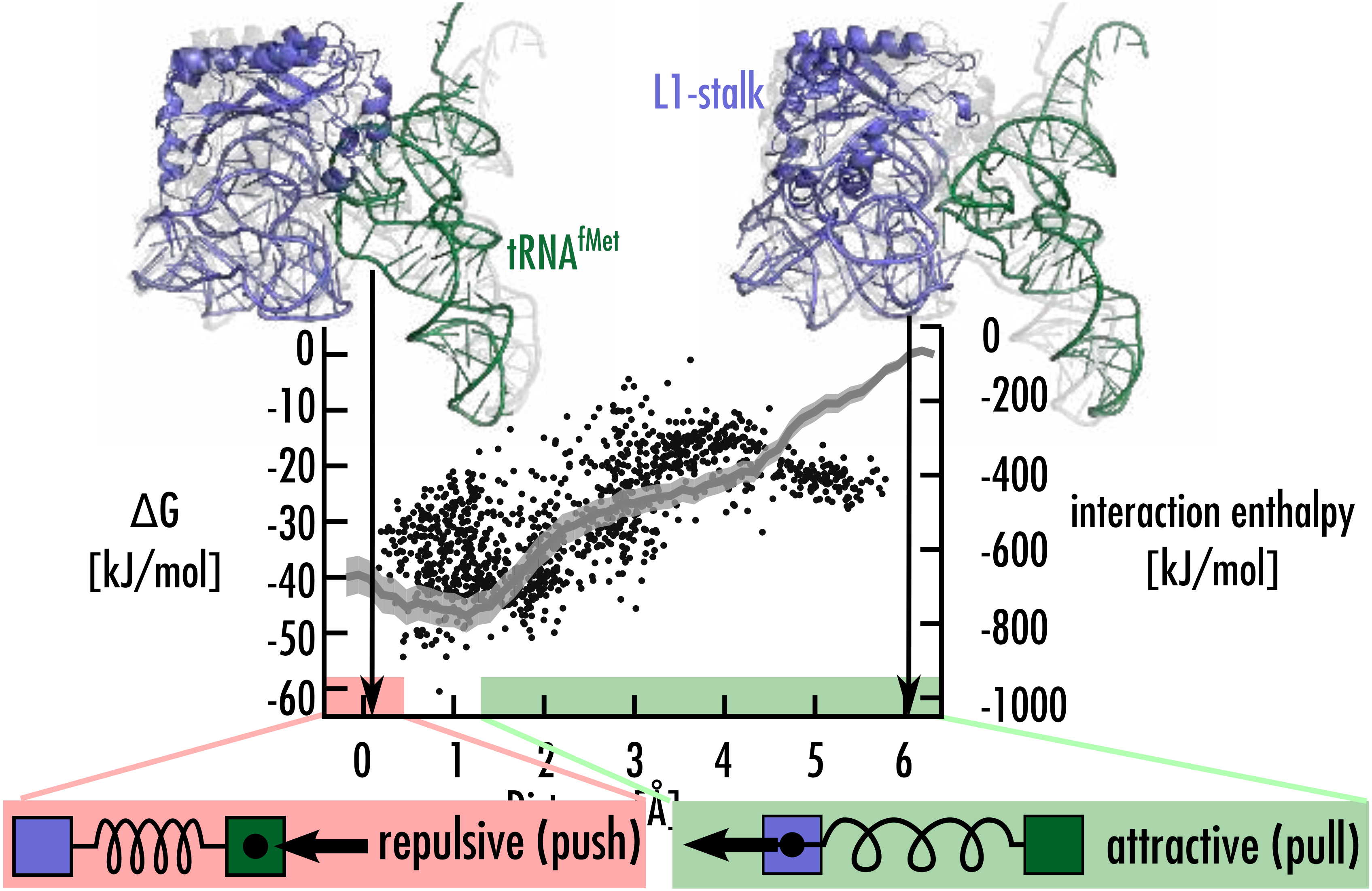

Bock LV, Blau C, Schröder GF, Davydov II, Fischer N, Stark H, Rodnina MV, Vaiana AC, Grubmüller H.
Nature Struct. Molec. Biol. 20, 1390, (2014)

Elongation dynamics of the nascent peptide in the exit tunnel

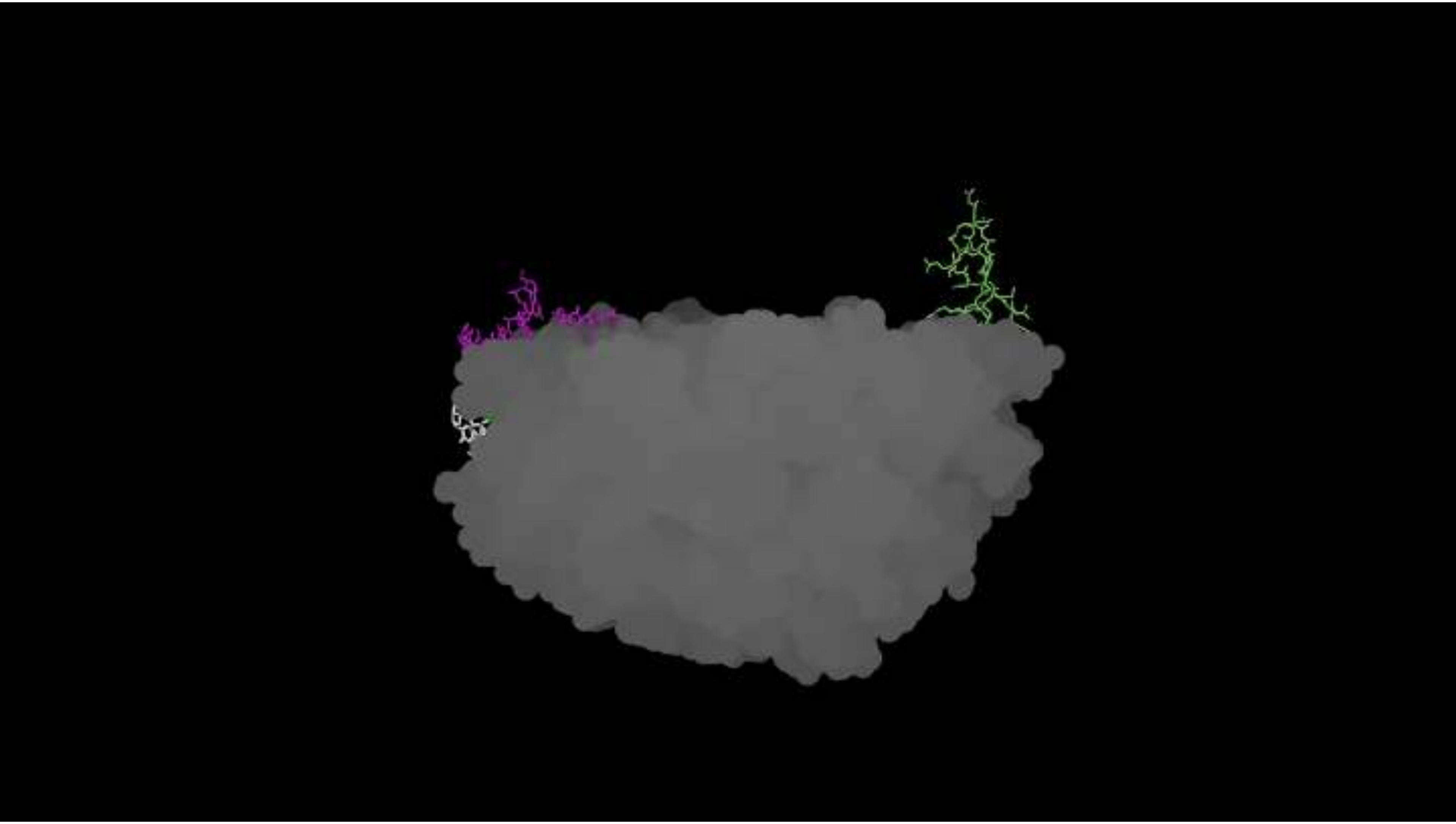

Michal Kolar, unpublished data

Elongation dynamics of the nascent peptide in the exit tunnel

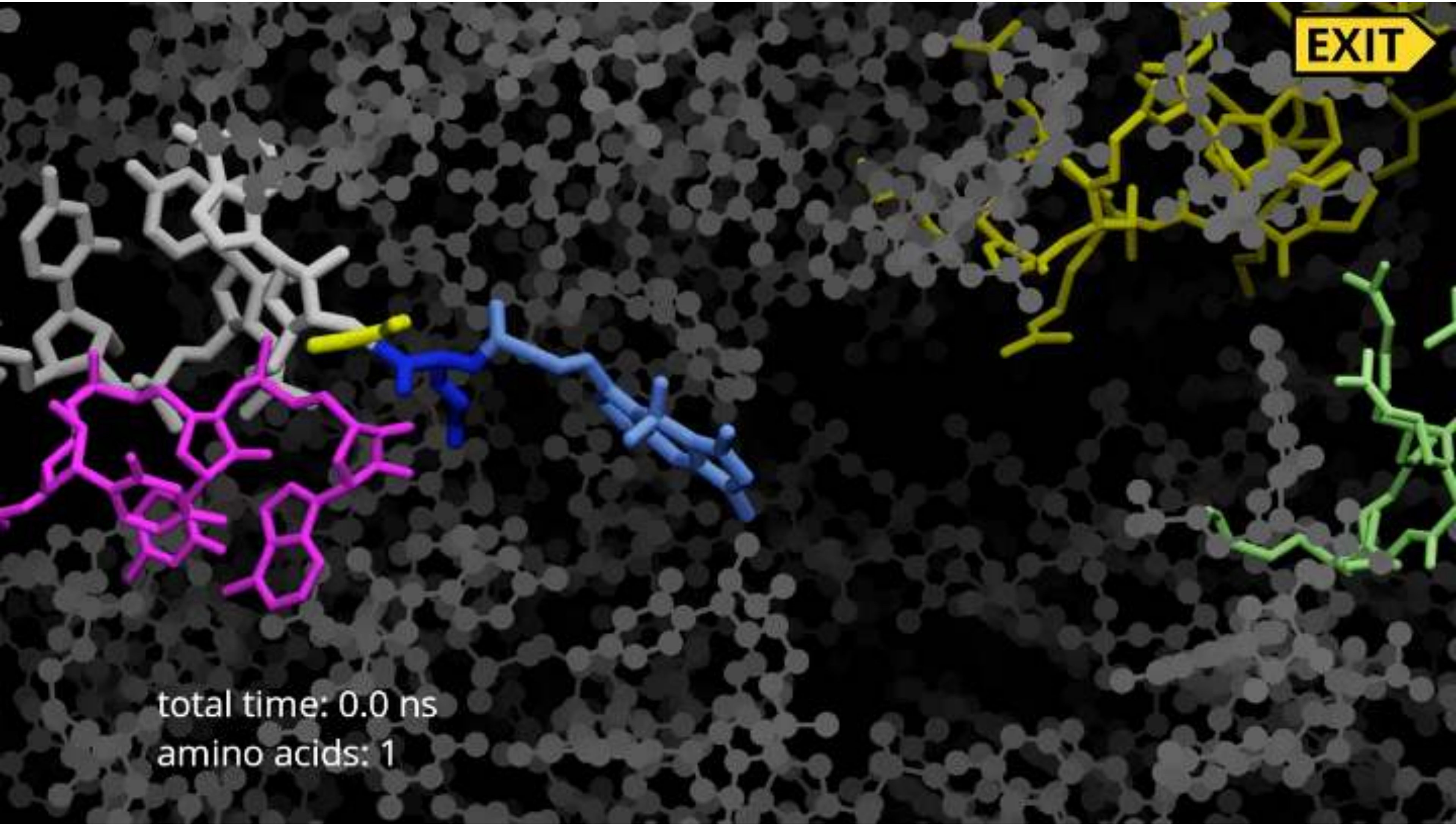

Michal Kolar, unpublished data

Erythromycin (Ery) binds in the exit tunnel

- Most peptides translated
- Stalls the ribosome during ErmBL translation
  (and others)

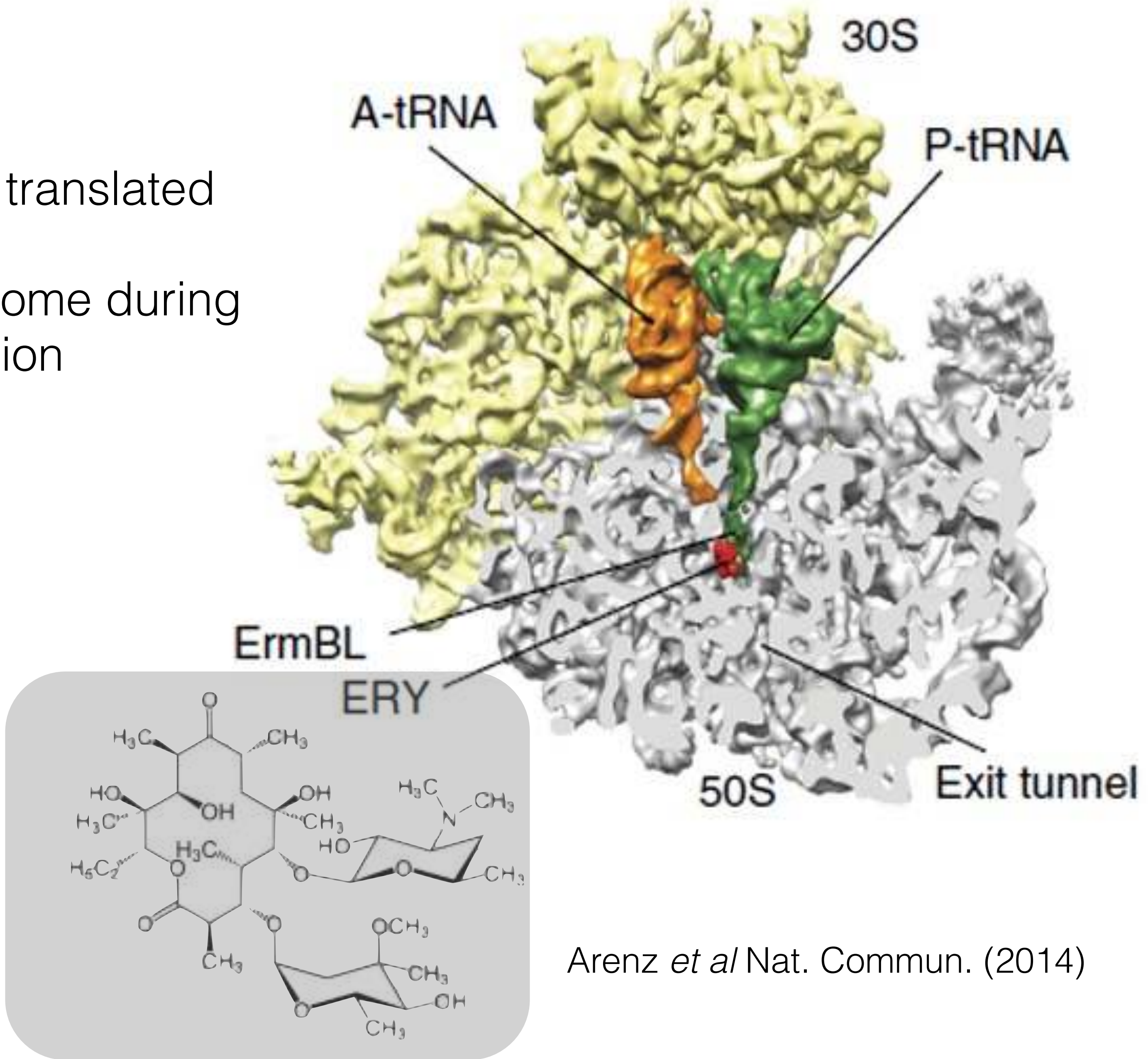

Arenz *et al* Nat. Commun. (2014)

Streptococcus sanguis

Erythromycin stalls the ribosome: Codon 10 of ErmBL

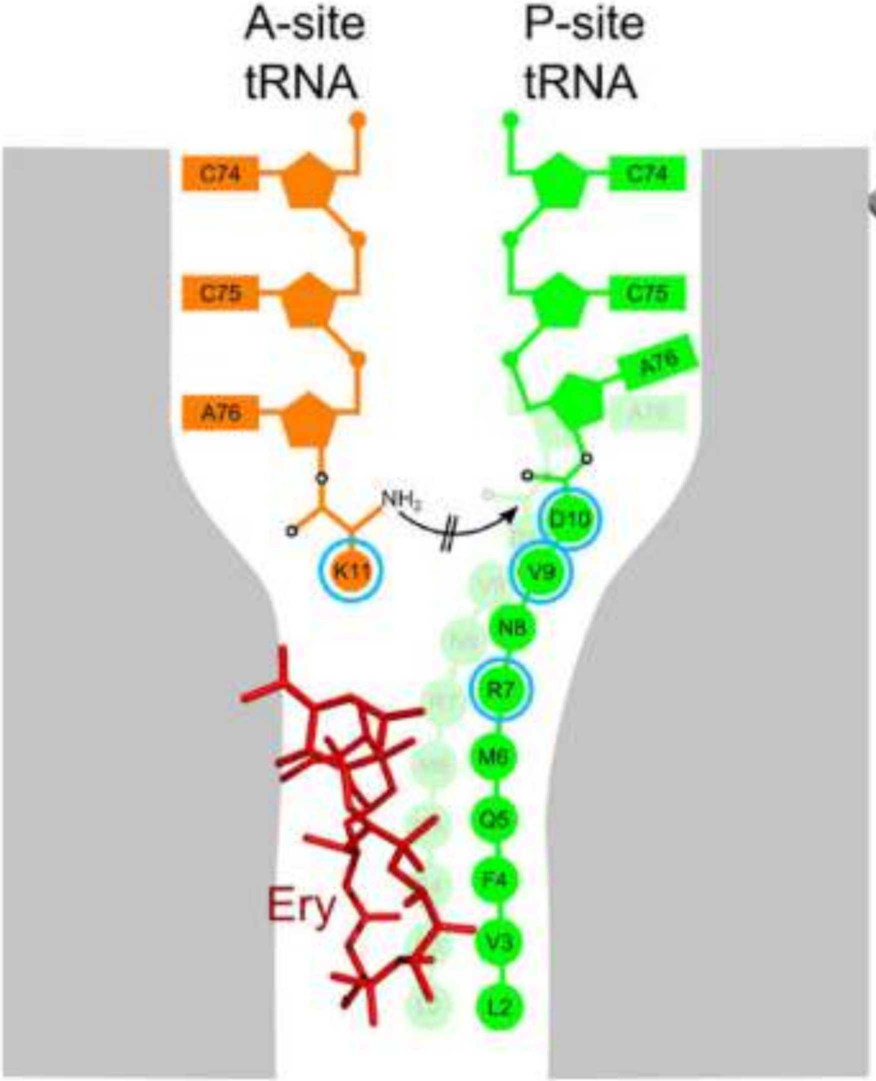

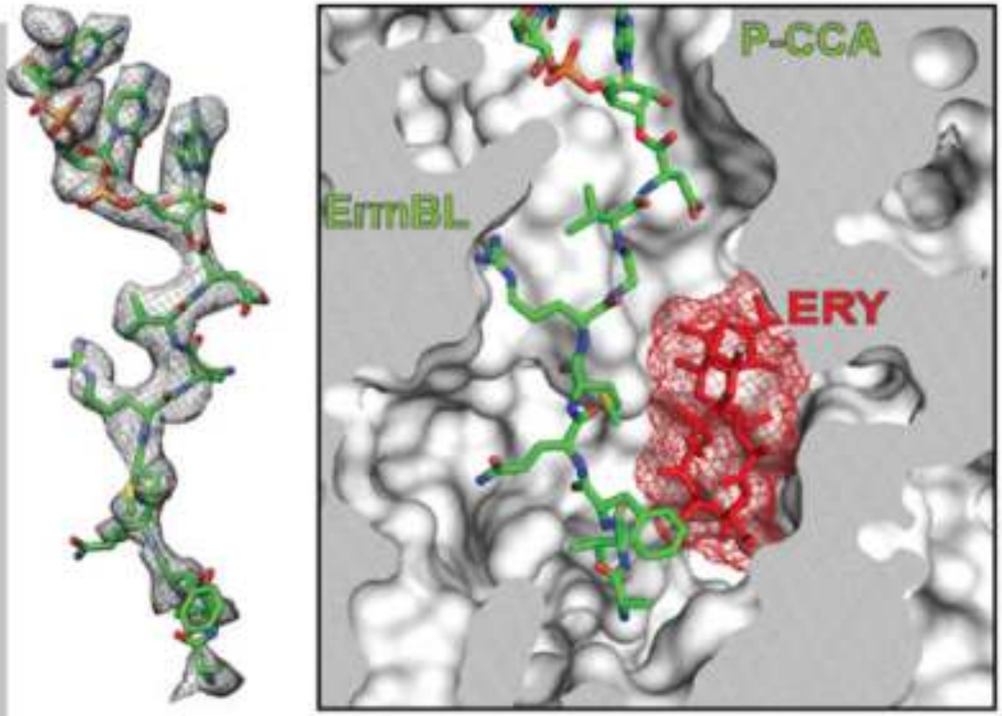

3.6 Å cryo-EM structure of ErmBL stalled complex

ErmBL with erythromycin

Gupta *et al* Nat. Chem. Biol (2016)   Arenz *et al* Nat. Commun. (2014)

Erythromycin stalls the ribosome: Codon 10 of ErmBL

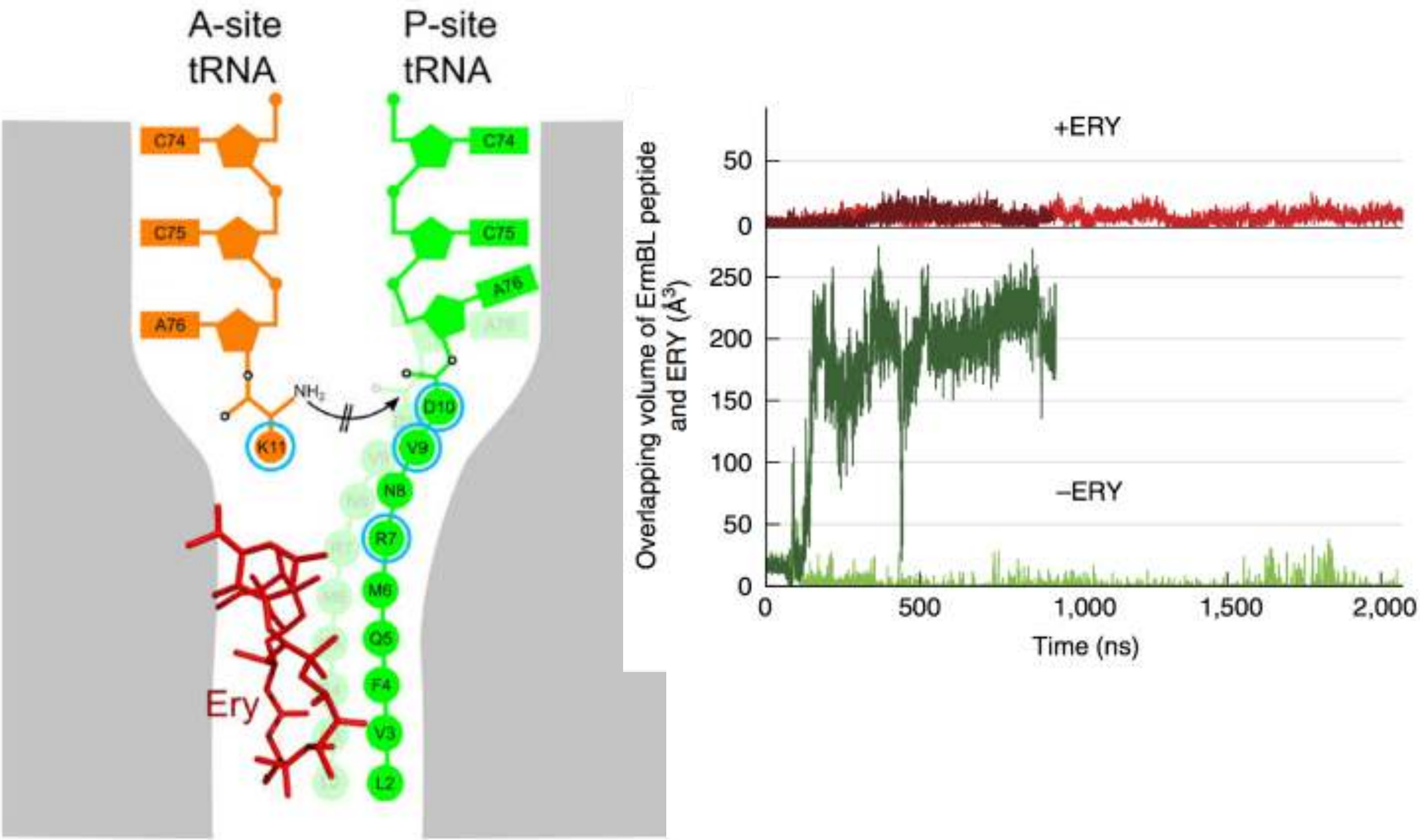

ErmBL with erythromycin

Arenz S, Bock LV, Graf M, Innis CA, Beckmann R, Grubmüller H, Vaiana AC, Wilson DN, *Nature Comm.* **7**, 12026 (2016)

Erythromycin stalls the ribosome: Codon 10 of ErmBL

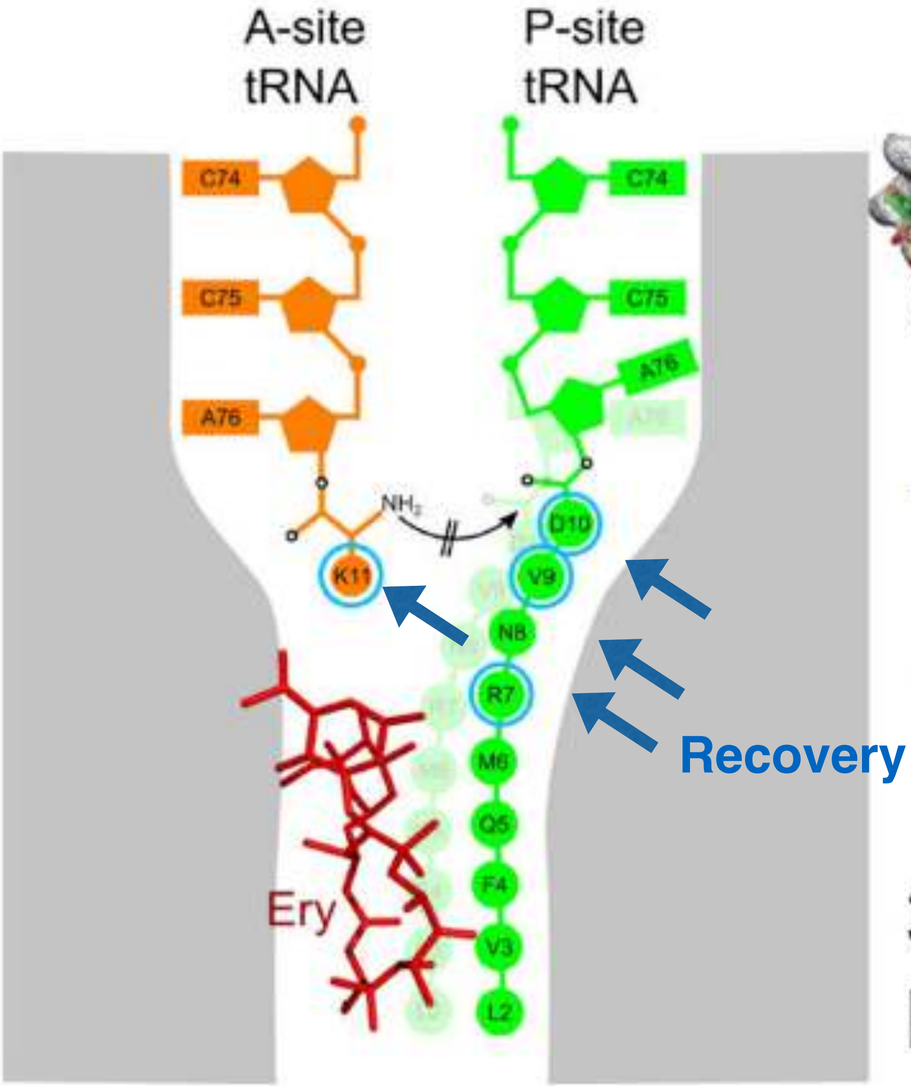

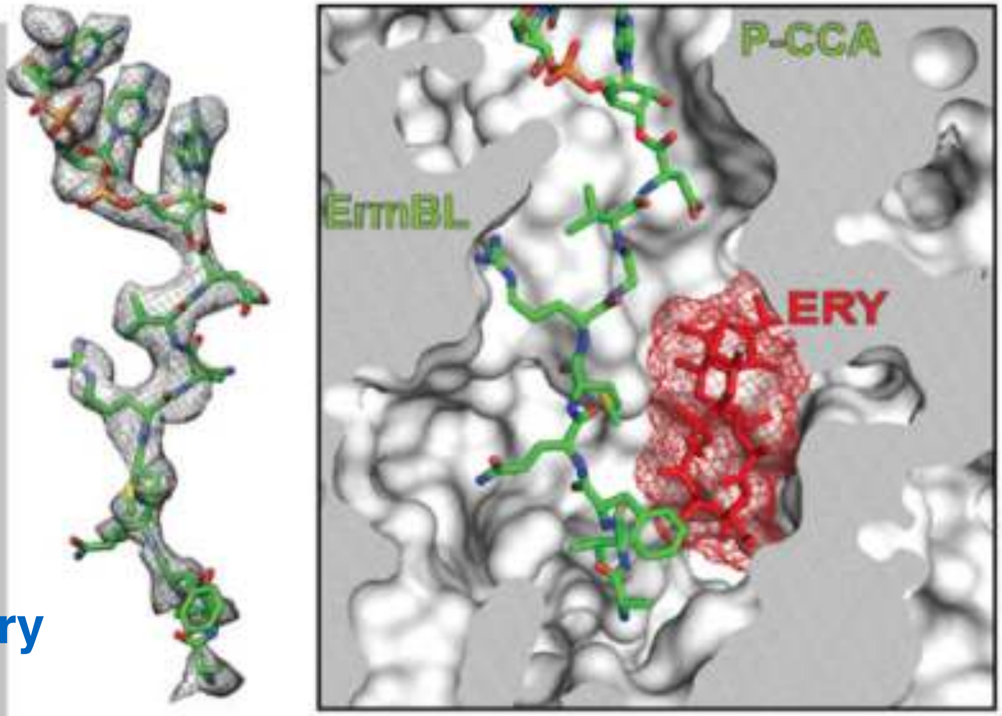

3.6 Å cryo-EM structure of ErmBL stalled complex

ErmBL with erythromycin

Gupta *et al* Nat. Chem. Biol (2016)   Arenz *et al* Nat. Commun. (2014)

MD: Backbone shift increases NH_2-C distance

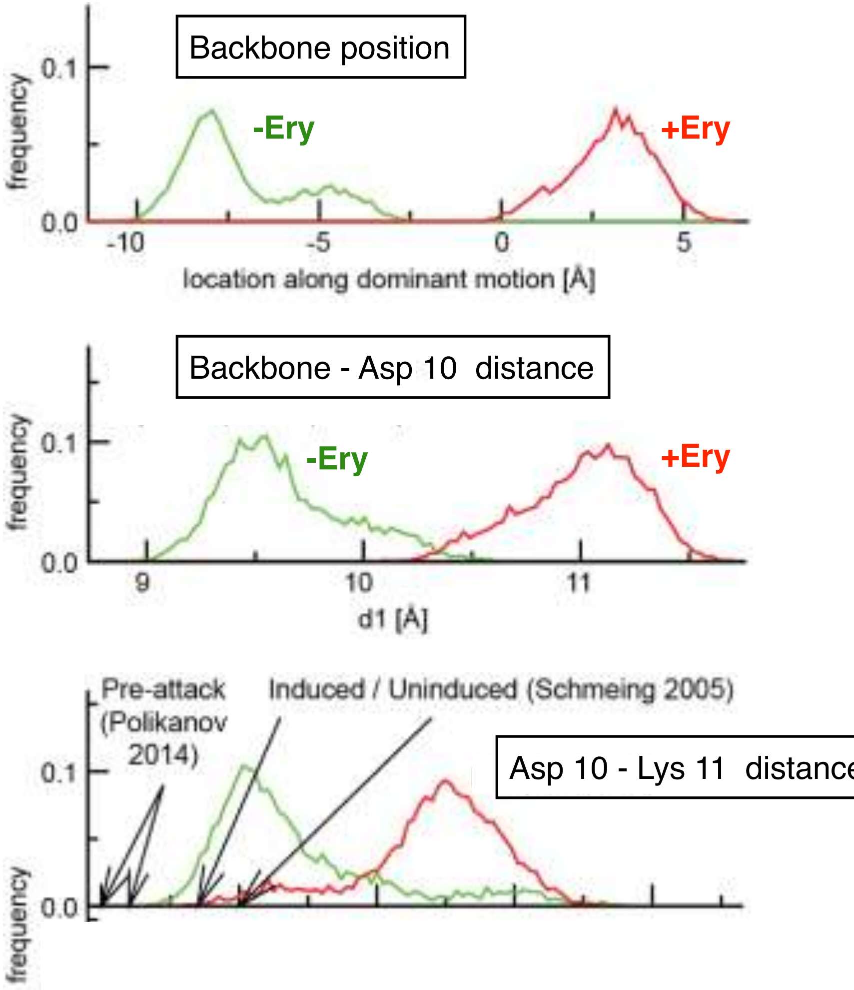

Backbone position

Backbone - Asp 10 distance

Asp 10 - Lys 11 distance

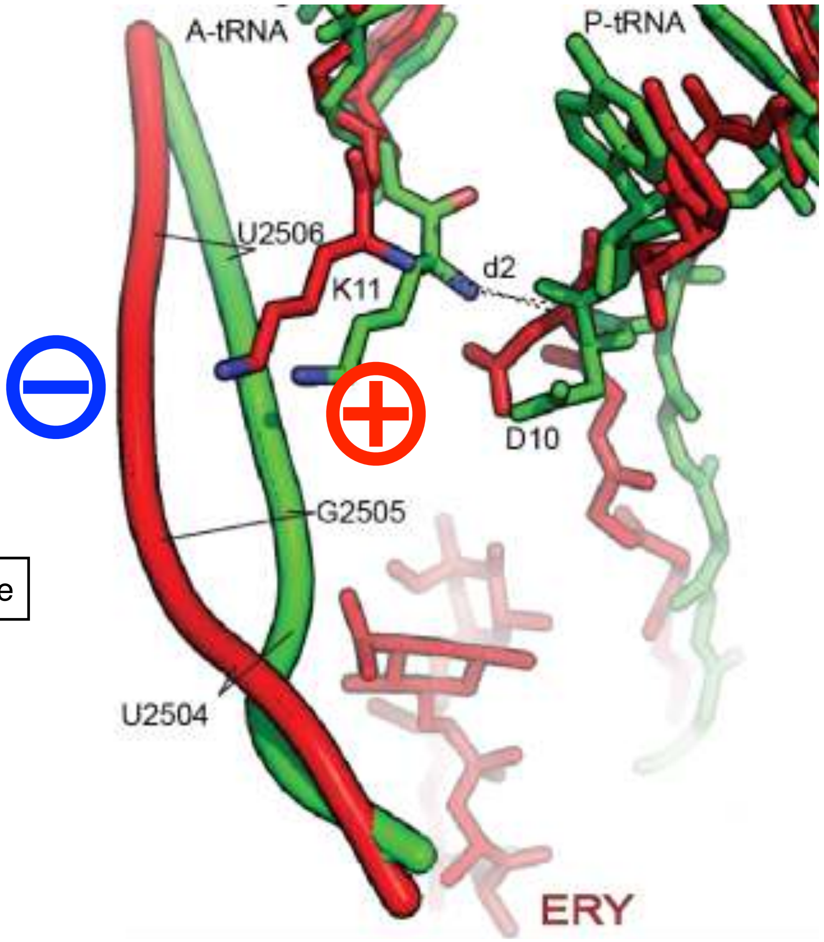

Arenz S, Bock LV, Graf M, Innis CA, Beckmann R, Grubmüller H, Vaiana AC, Wilson DN, *Nature Comm.* **7**, 12026 (2016)

MD Predicts: K11R should enhance stalling

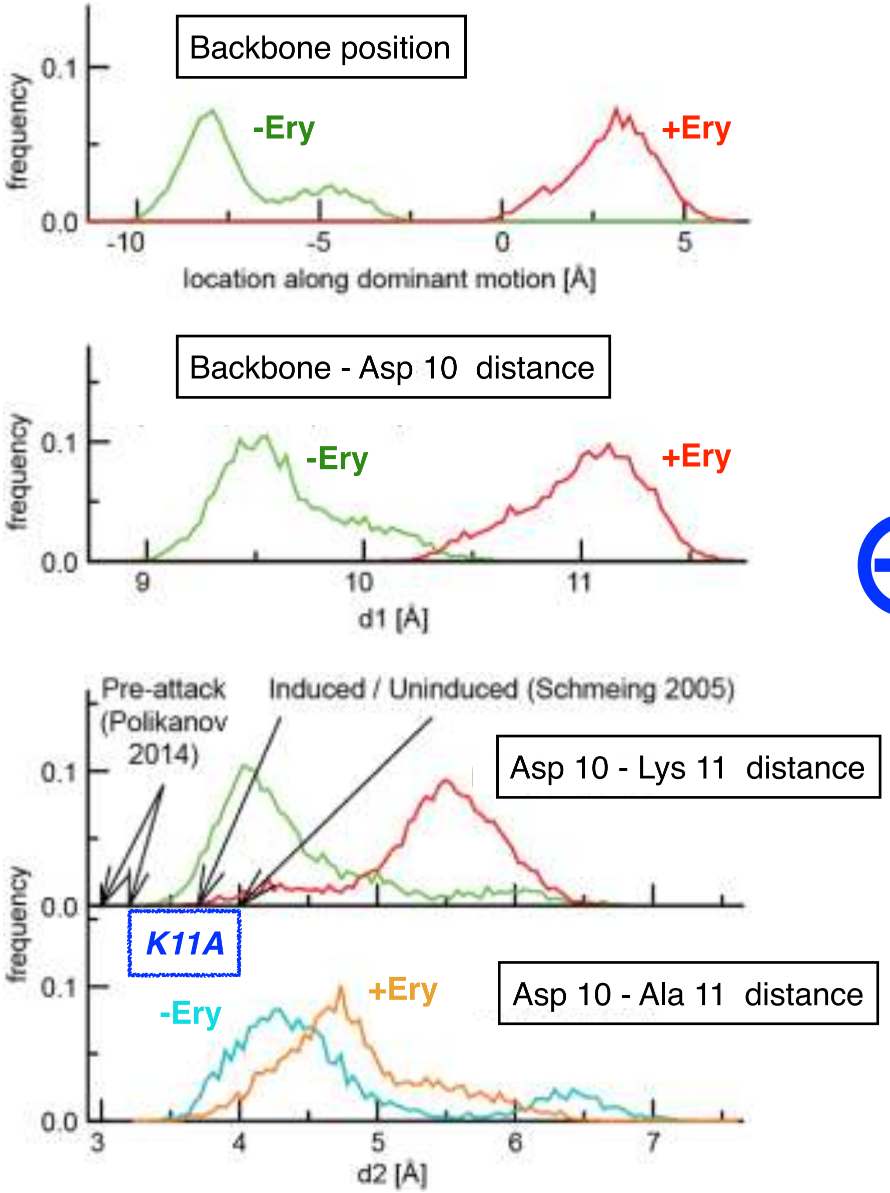

Backbone position

Backbone - Asp 10 distance

Asp 10 - Lys 11 distance

K11A

Asp 10 - Ala 11 distance

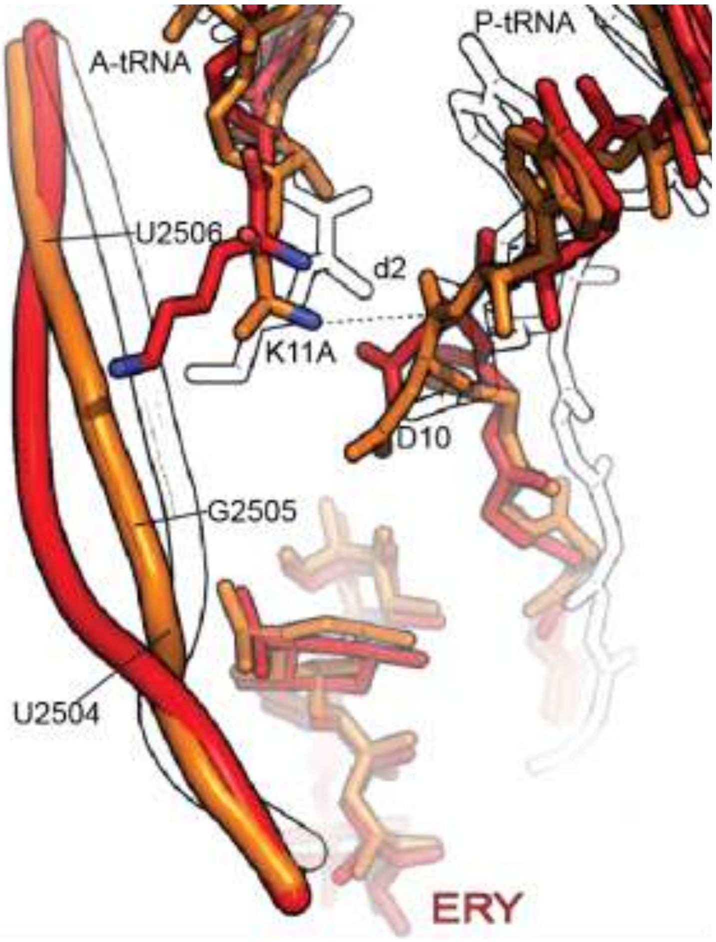

Arenz S, Bock LV, Graf M, Innis CA, Beckmann R, Grubmüller H, Vaiana AC, Wilson DN, *Nature Comm.* **7**, 12026 (2016)

MD Predicts: K11R should enhance stalling

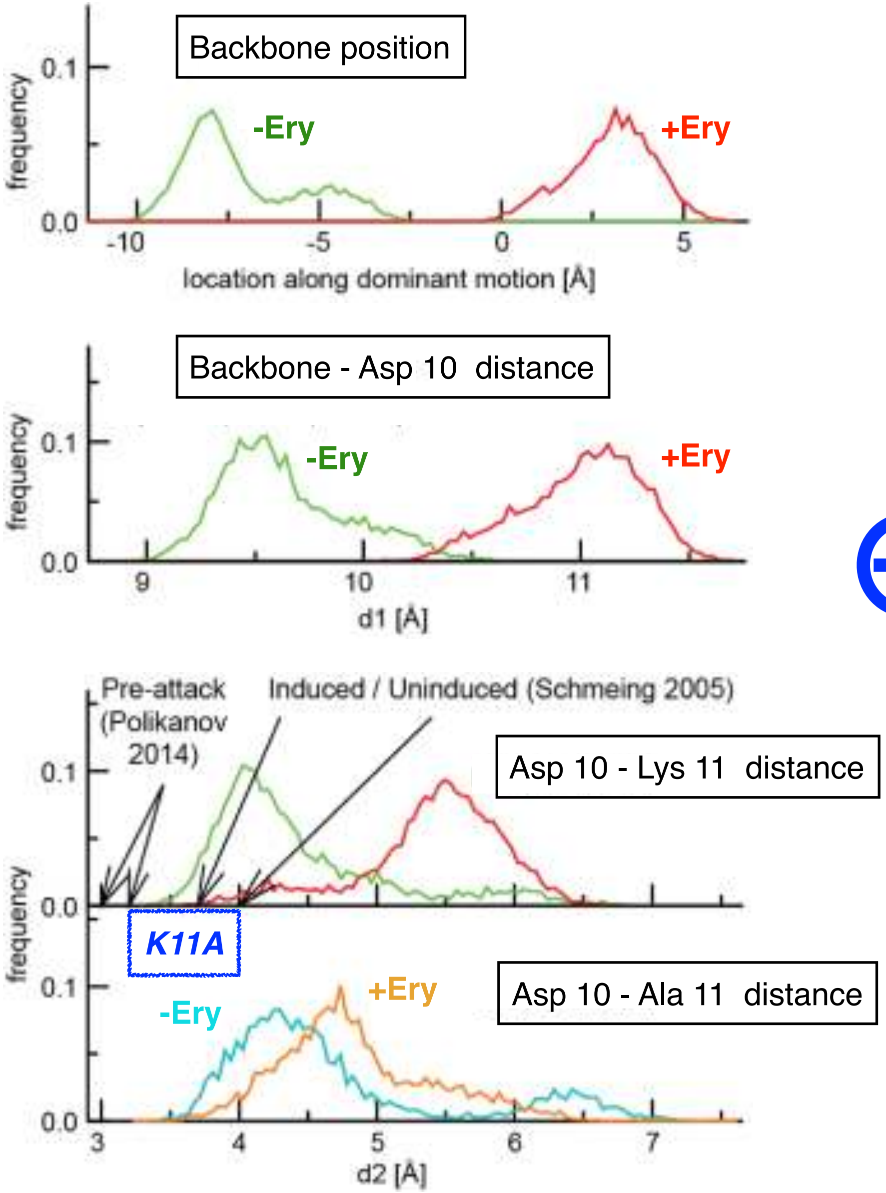

⊖

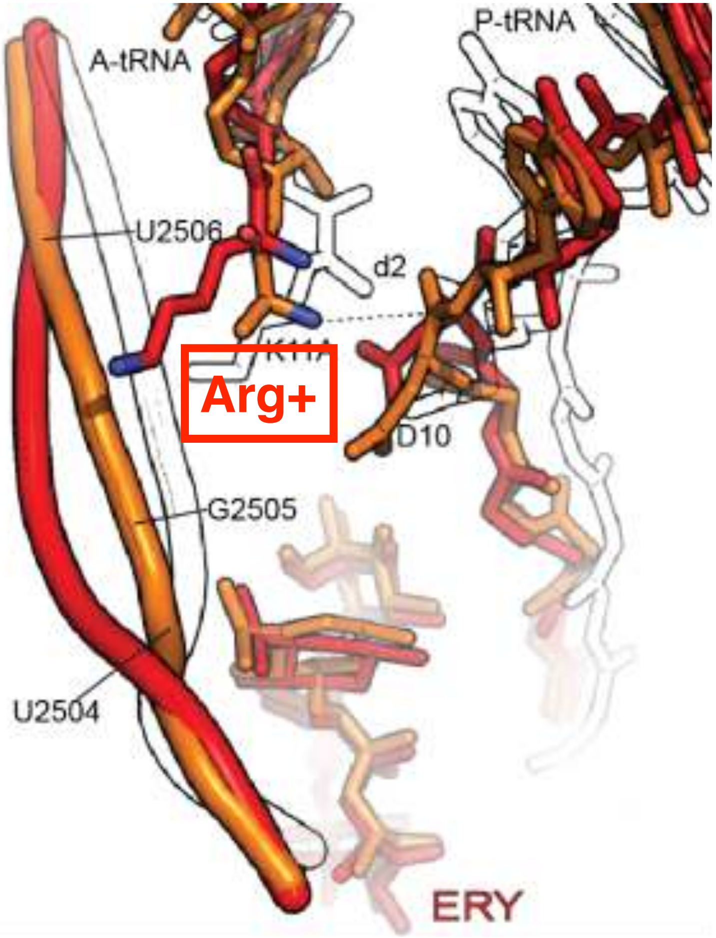

Arenz S, Bock LV, Graf M, Innis CA, Beckmann R, Grubmüller H, Vaiana AC, Wilson DN, *Nature Comm.* **7**, 12026 (2016)

Prediction confirmed

An Arg at codon 11 also stalls the ribosome

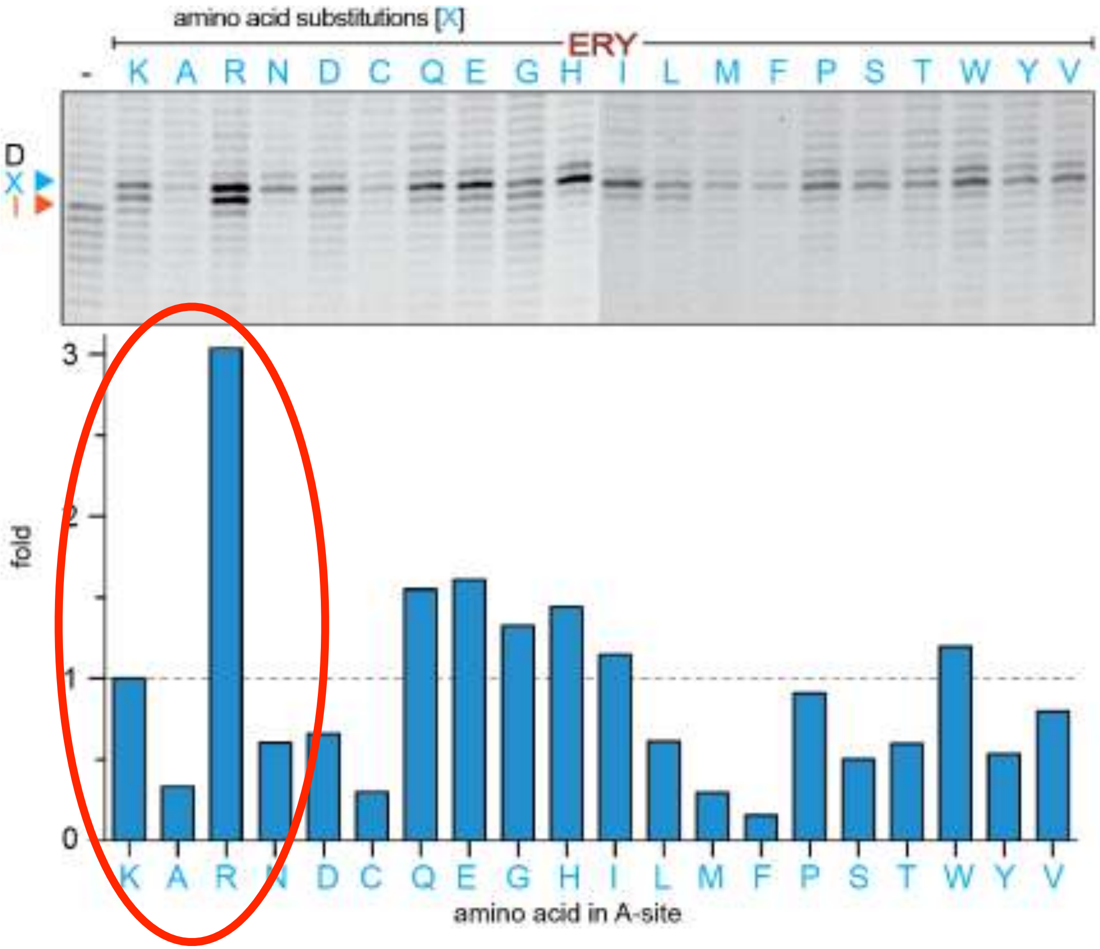

(Daniel Wilson, unpublished data)

Mechanism of stalling by erythromycin

Collaboration: Daniel Wilson (Univ. Munich)

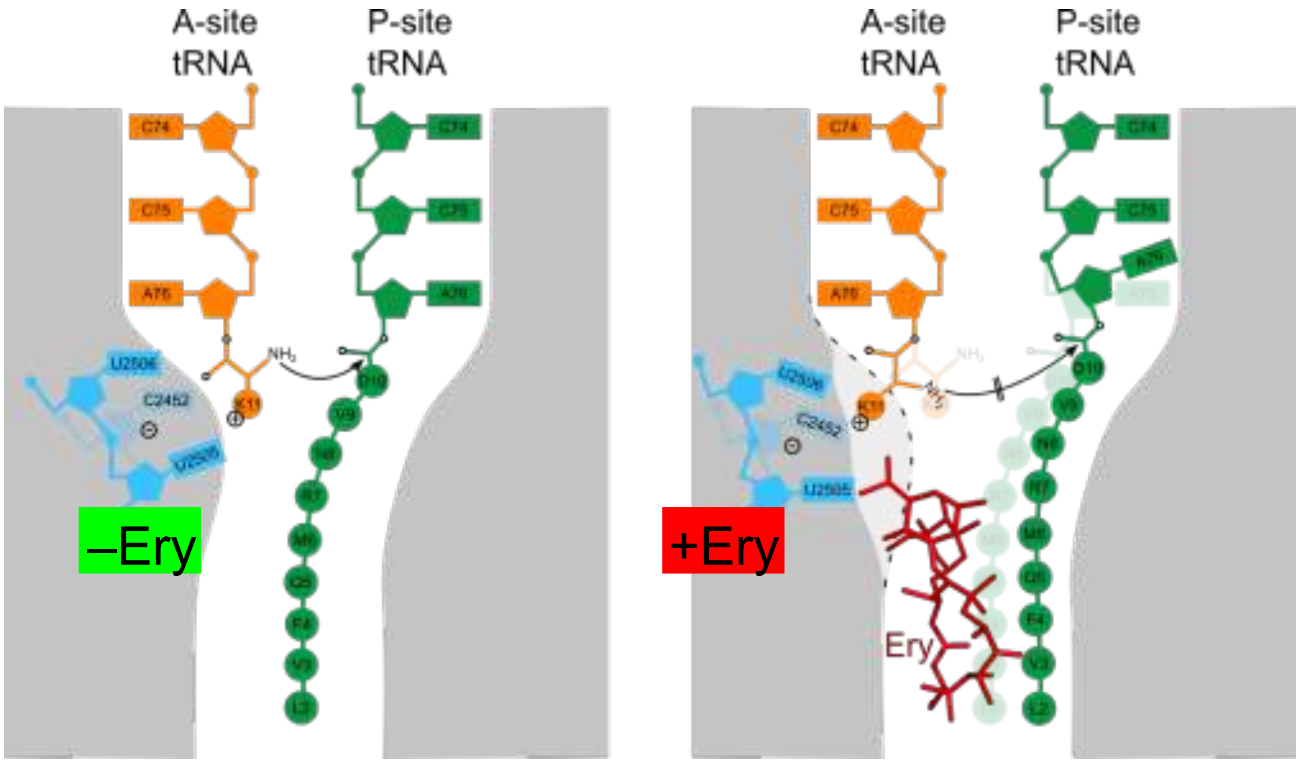

+Erythromycin:

1) peptide conformation changed → P-site tRNA

2) A-site crevice perturbed → A-site amino acid K11 shifts

Distance between attacking NH_2 and carbonyl C increased

→ Inhibition of peptide bond formation

Arenz S, Bock LV, Graf M, Innis CA, Beckmann R, Grubmüller H, Vaiana AC, Wilson DN, *Nature Comm.* **7**, 12026 (2016)

Towards a mechanistic understanding of protein function

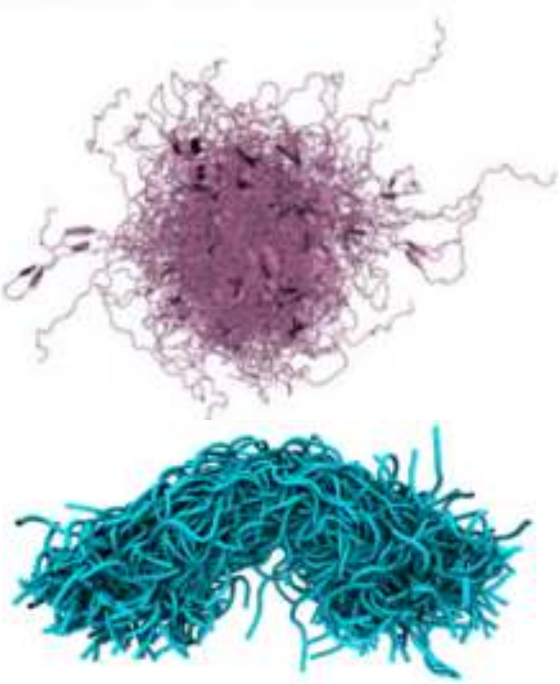

(1) Ligand unbinding revisited

(2) Ribosomal antibiotics mechanism

(3) Intrinsically Disordered Proteins

(4) The Dynasome

AFM+ X-ray + cryo EM + MD

Lars Bock, Christian Blau, Michal Kolar, Andrea Vaiana, Andreas Russek,
Sarah Rauscher, Ulf Hensen

Holger Stark, Marina Rodnina (MPI Göttingen)
Roland Beckmann, Daniel Wilson (Univ. Munich)
Simon Scheuring (Cornell Univ.)

Folded vs. disordered proteins

> ***"This came directly from a computer***
>
> ***and is neither to be doubted nor disbelieved!"***

Found in an email-signature

Folded vs. disordered proteins

> 30% of eukaryotic proteins
> 75% cancer linked proteins

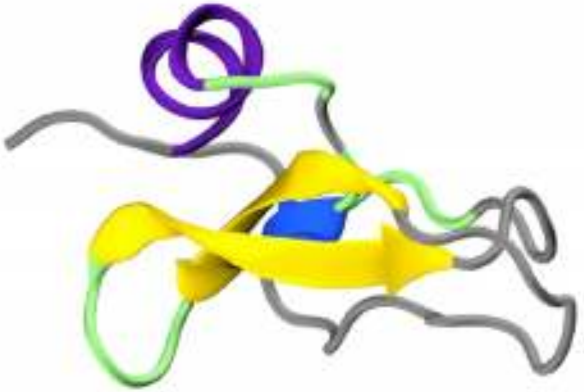

Folded

Disordered

Rauscher et al. (2015) J. Chem. Theor. Comput.

Nucleoporins are prototypic disordered proteins

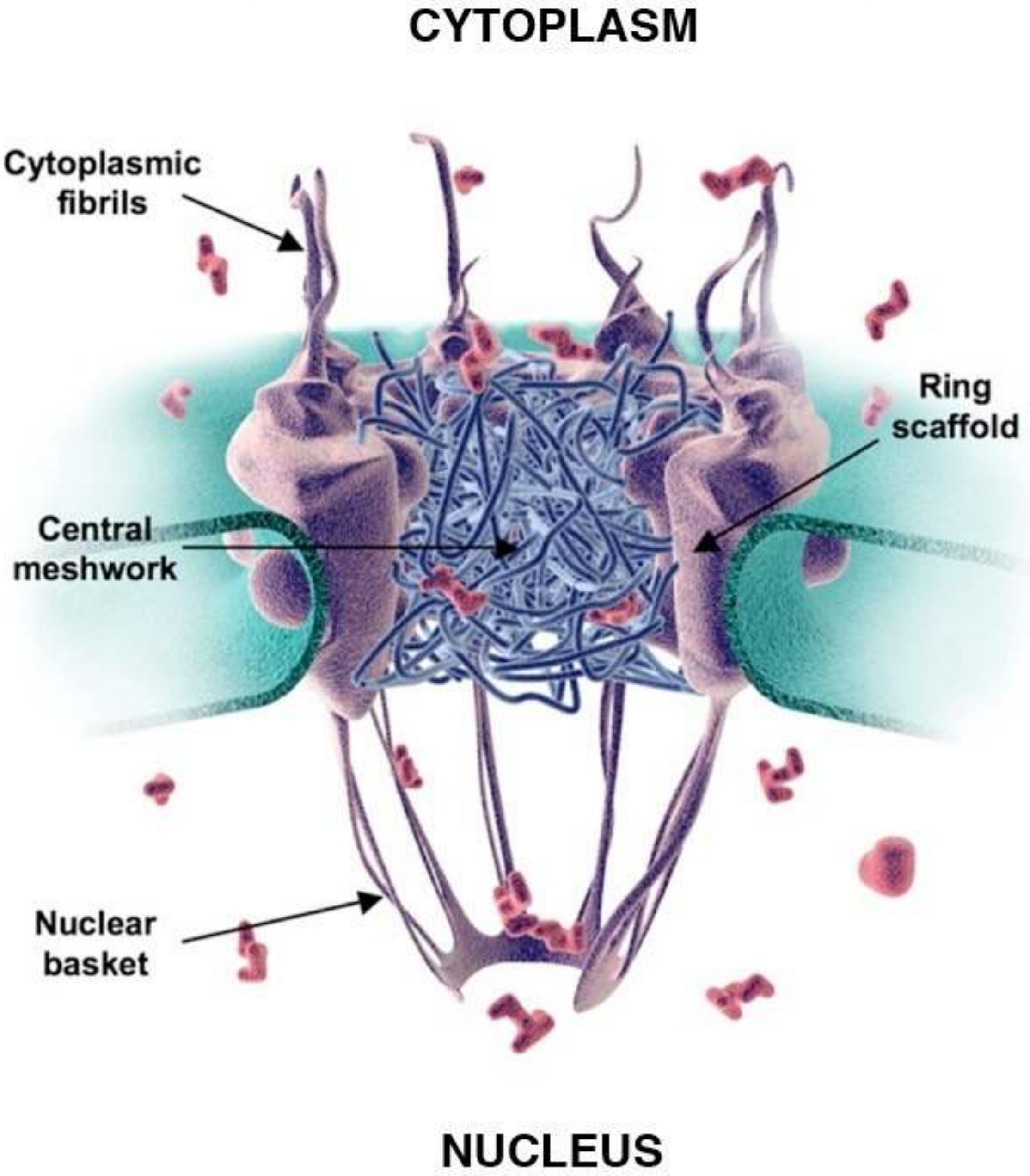

The nuclear pore complex is responsible for selective transport of macromolecules larger than 40 kDa into and out of the nucleus.

Patel, S. S. et al (2007) *Cell*, 129: 83-96.

Nucleoporins are prototypic disordered proteins

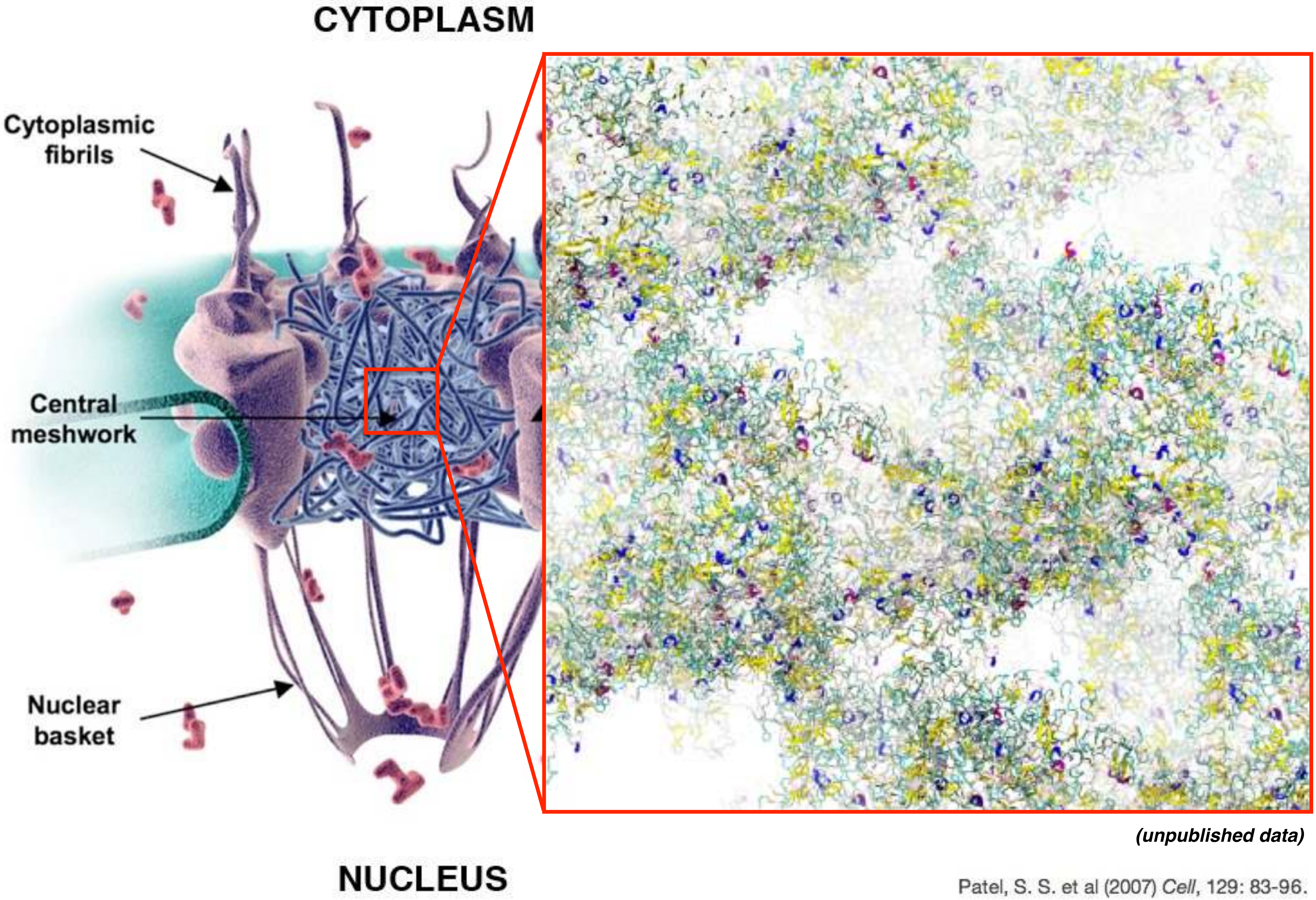

(unpublished data)

Patel, S. S. et al (2007) *Cell*, 129: 83-96.

MD Simulations of Disordered Proteins

ff99sb*-ildn

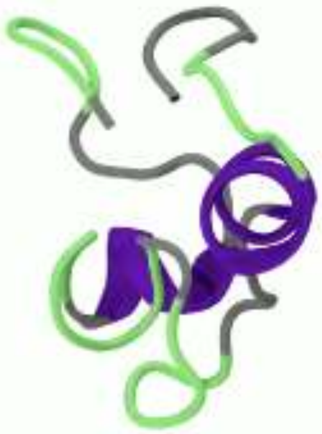

CHARMM 22*

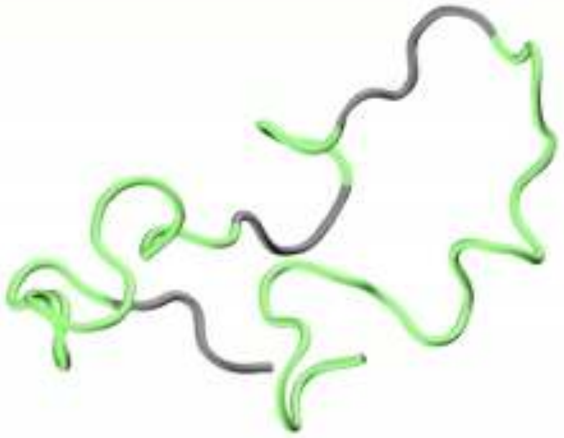

Rauscher et al. (2015) J. Chem. Theor. Comput.

Force Fields Compared for Disordered Proteins

Force Field	Peptide Force Field	Water Model	References
ff99sb*-ildn	amber ff99sb*-ildn	TIP3P	Piana, S. *et al* (2011) *Biophys. J.*, **100**: L47-L49. Jorgensen, W. L. *et al* (1983) *J. Chem. Phys.* **79**: 926–935.
ff03w	amber ff03w	TIP4P/ 2005	Best, R. B. and Mittal, J. (2010) *J. Phys. Chem. B*, **114**: 14916–14923. Abascal J. L. and Vega C. (2005) *J. Chem. Phys.* **123:** 234505.
ff03ws	amber ff03ws	TIP4P/ 2005	Best, R. B., Zheng, W. and Mittal, J. (2014) *J. Chem. Theor. Comput.,* **10**: 5113–5124. Abascal J. L. and Vega C. (2005) *J. Chem. Phys.* **123:** 234505.
CHARMM 22*	CHARMM 22*	CHARMM-modified TIP3P	Piana, S. *et al* (2011) *Biophys. J.*, **100**: L47-L49. MacKerell, A. D. *et al* (1998) *J. Phys. Chem. B* **102**: 3586–3616.
CHARMM 22*/D	CHARMM 22*	TIP4P-D	Piana, S. *et al* (2011) *Biophys. J.*, **100**: L47-L49. Piana, S. *et al* (2015) *J. Phys. Chem. B.* (online)
CHARMM 36^1	CHARMM 36	CHARMM-modified TIP3P	Best, R. B. (2012) *J. Chem. Theor. Comput.* **8**: 3257-3273. MacKerell, A. D. *et al* (1998) *J. Phys. Chem. B* **102**: 3586–3616.
CHARMM 36^2	CHARMM 36	TIP3P	Best, R. B. (2012) *J. Chem. Theor. Comput.* **8**: 3257-3273. MacKerell, A. D. *et al* (1998) *J. Phys. Chem. B* **102**: 3586–3616.
ABSINTH	OPLS-AA/L	ABSINTH (implicit water)	Vitalis A. and Pappu R. V. (2009) *J Comput Chem* **30**: 673–699.

Force Fields Differ Dramatically in Compactness

‘RS-Peptide’ GAMGPSYGRSRSRSRSRSRSRSRS

Xiang, S. Q. et al Structure , 2162–2174 (2013).

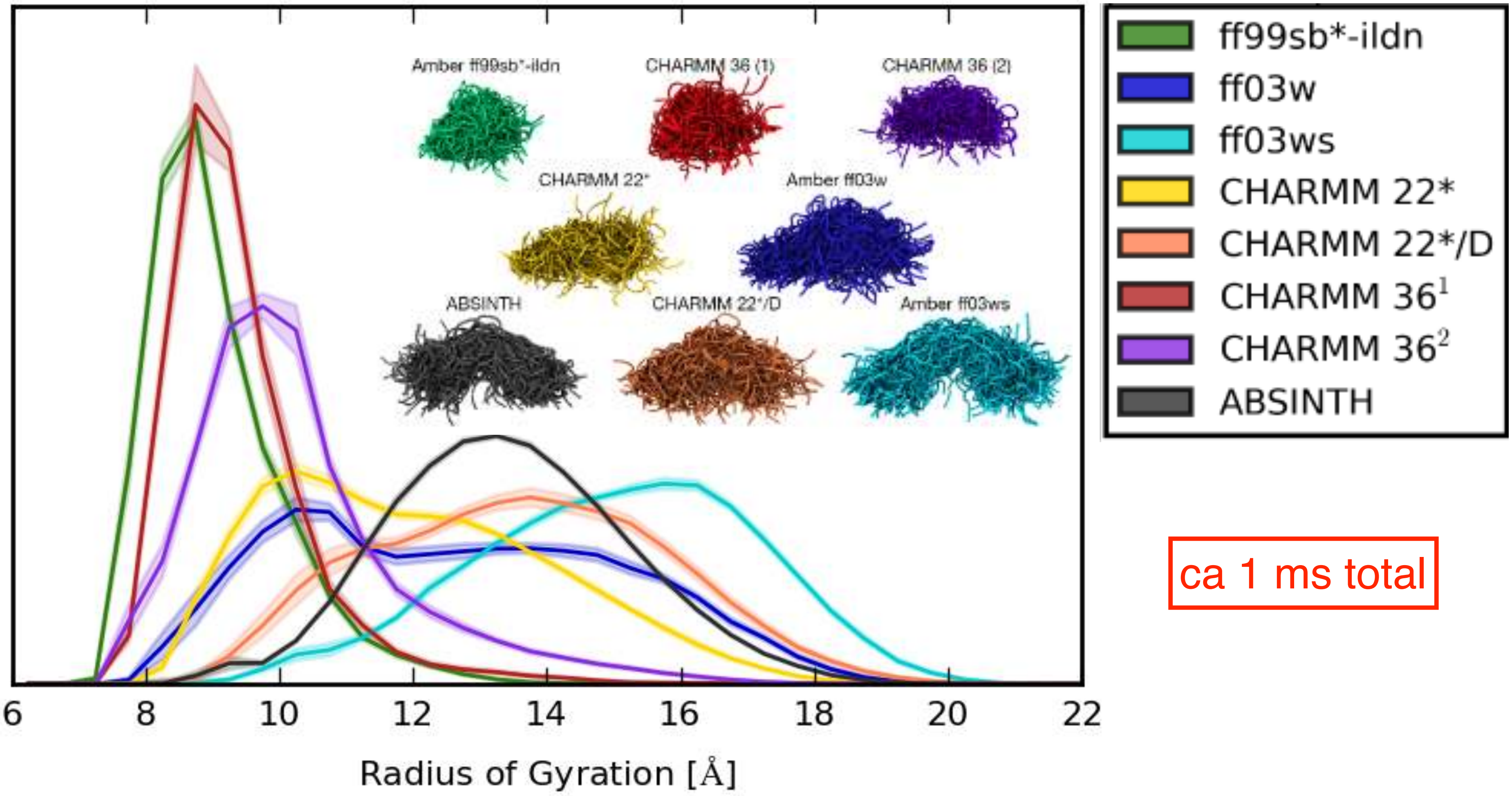

ca 1 ms total

Rauscher et al. (2015) J. Chem. Theor. Comput.

Comparison to Experiment
I. Small Angle X-Ray Scattering (Compactness)

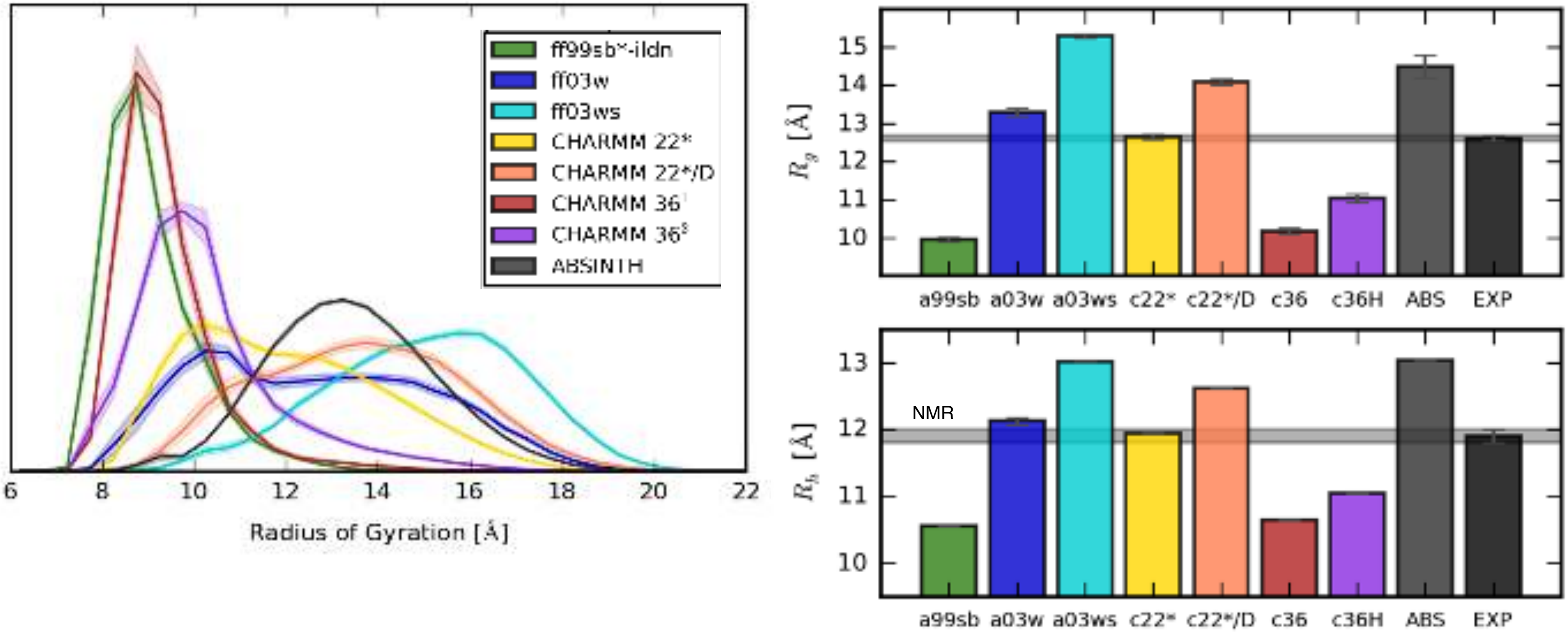

Rauscher et al. (2015) J. Chem. Theor. Comput.

Comparison to Experiment
I. Small Angle X-Ray Scattering (Compactness)

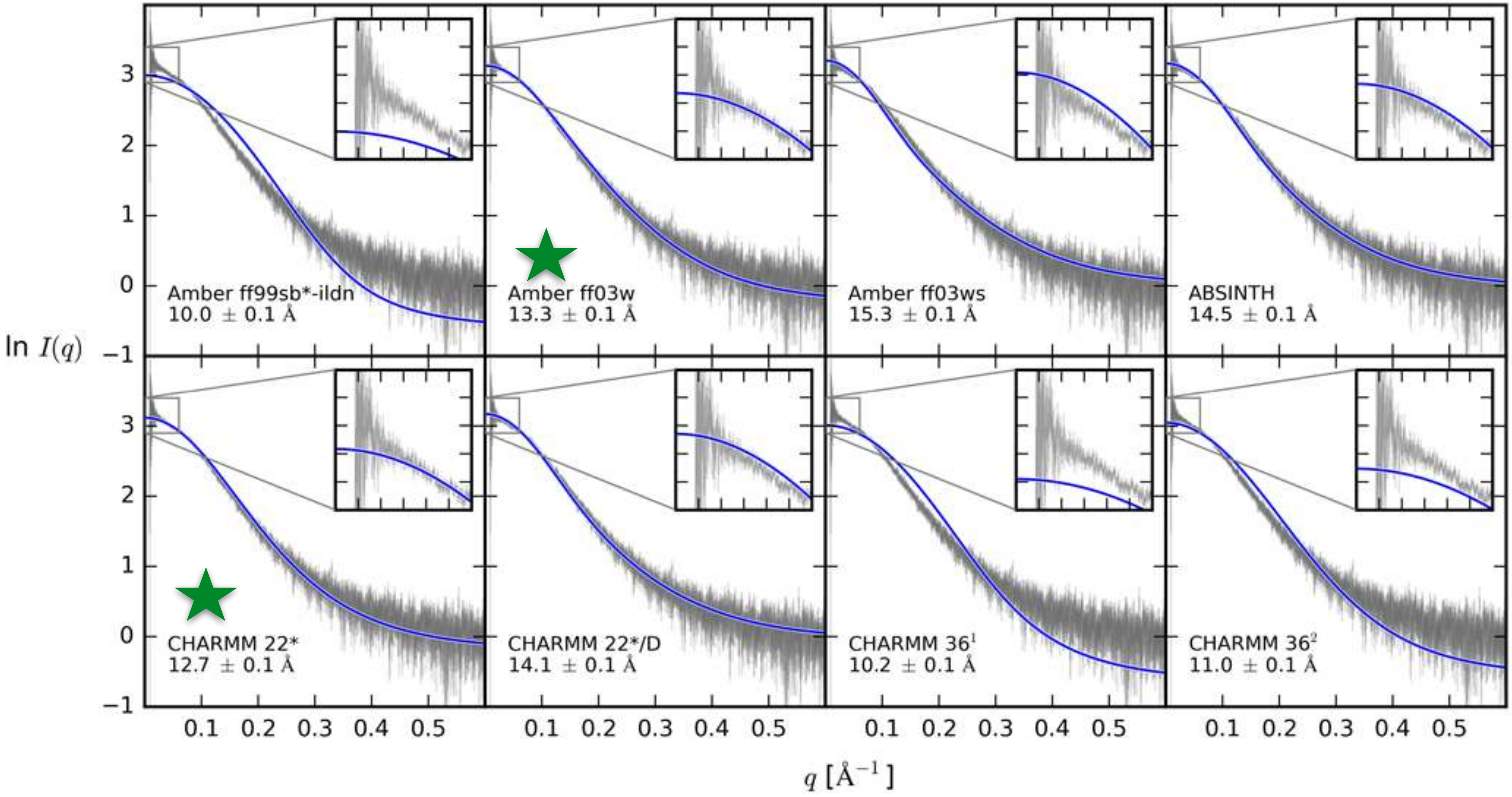

Rauscher et al. (2015) J. Chem. Theor. Comput.

Comparison to Experiment
II. NMR 3J(HNHA)-Coupling (Secondary Structure)

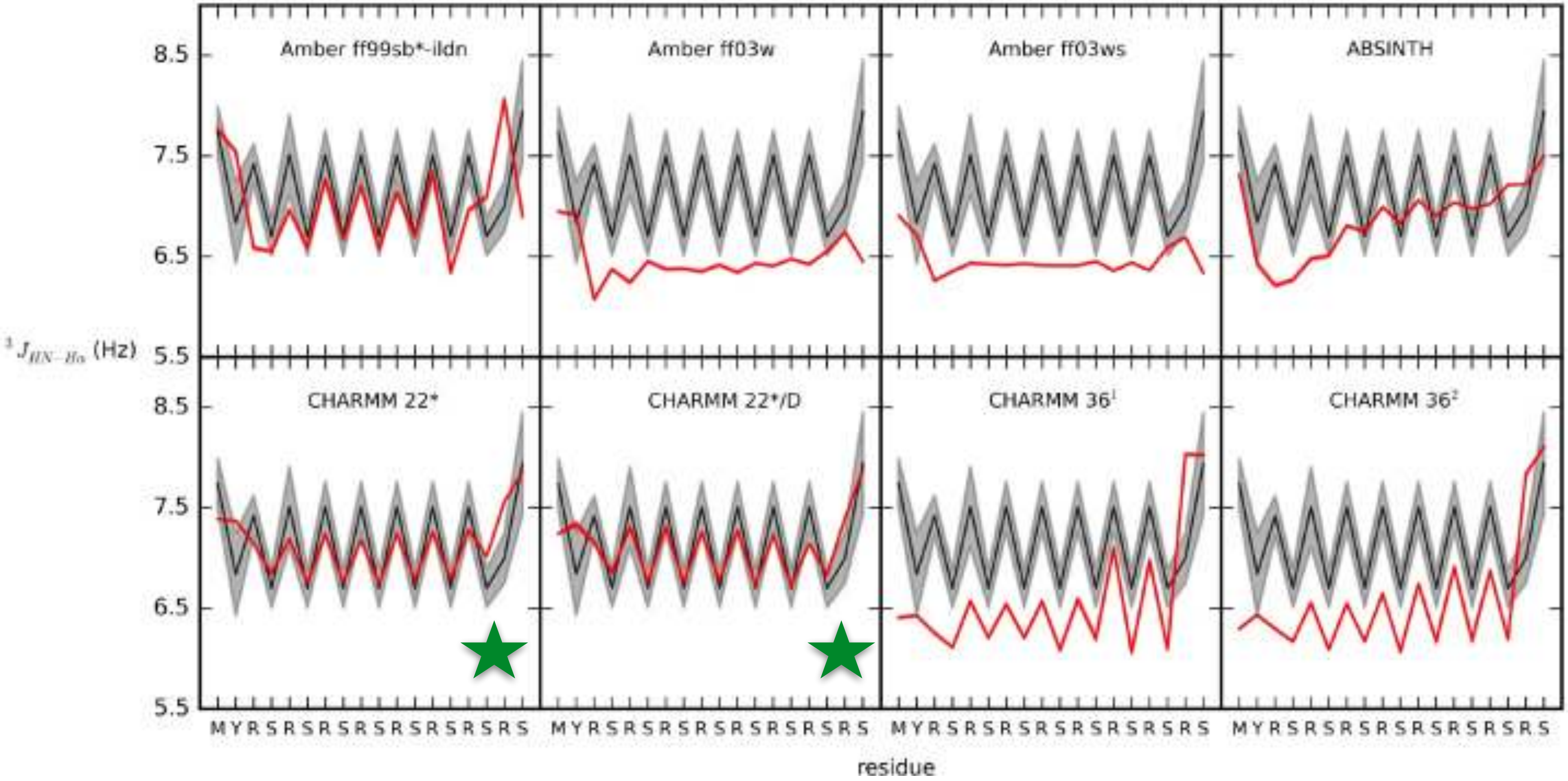

Rauscher et al. (2015) J. Chem. Theor. Comput.

Summary: Comparison to Experiment

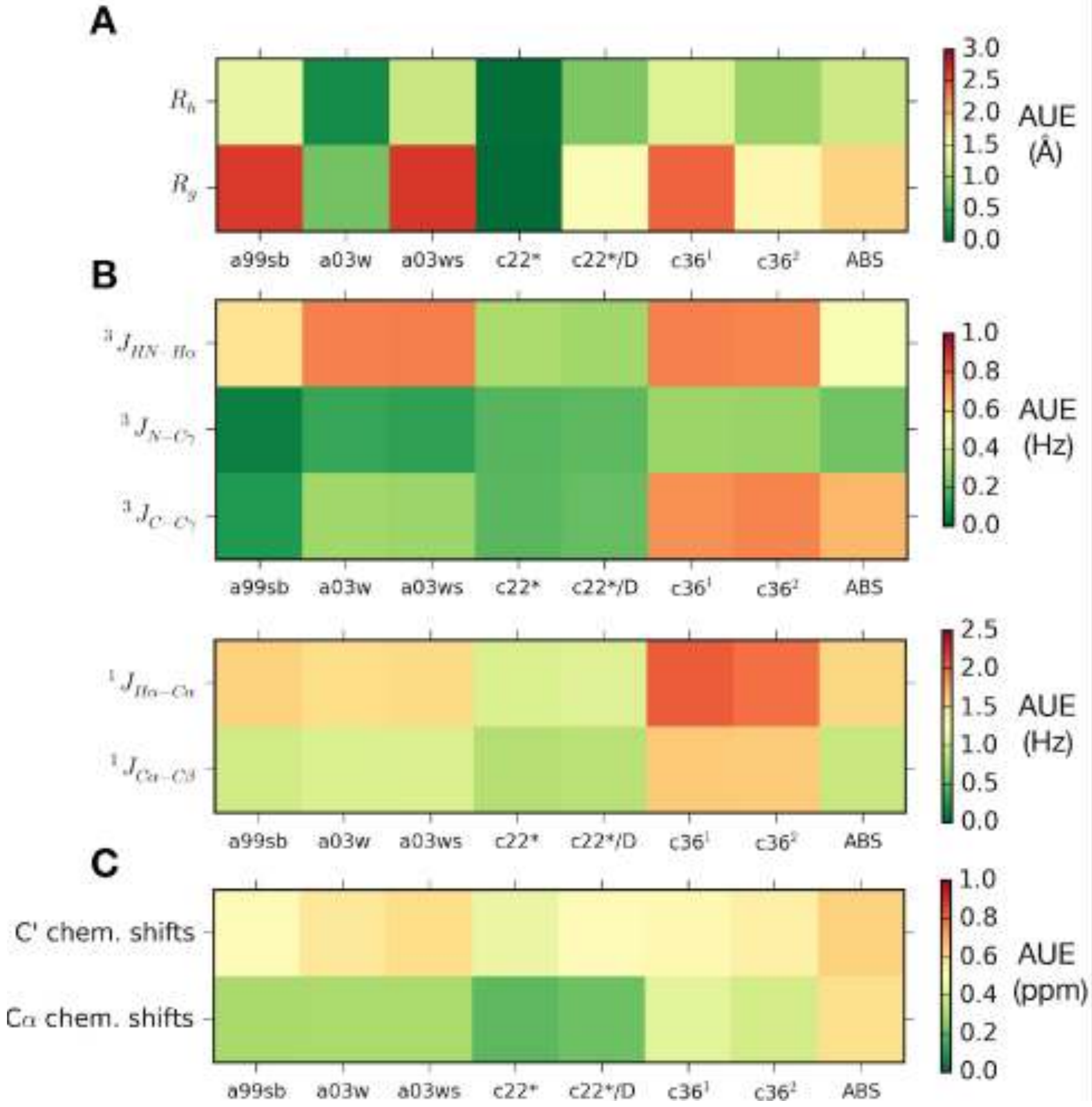

Chain Dimensions

Scalar Couplings

Chemical Shifts

Summary: Comparison to Experiment

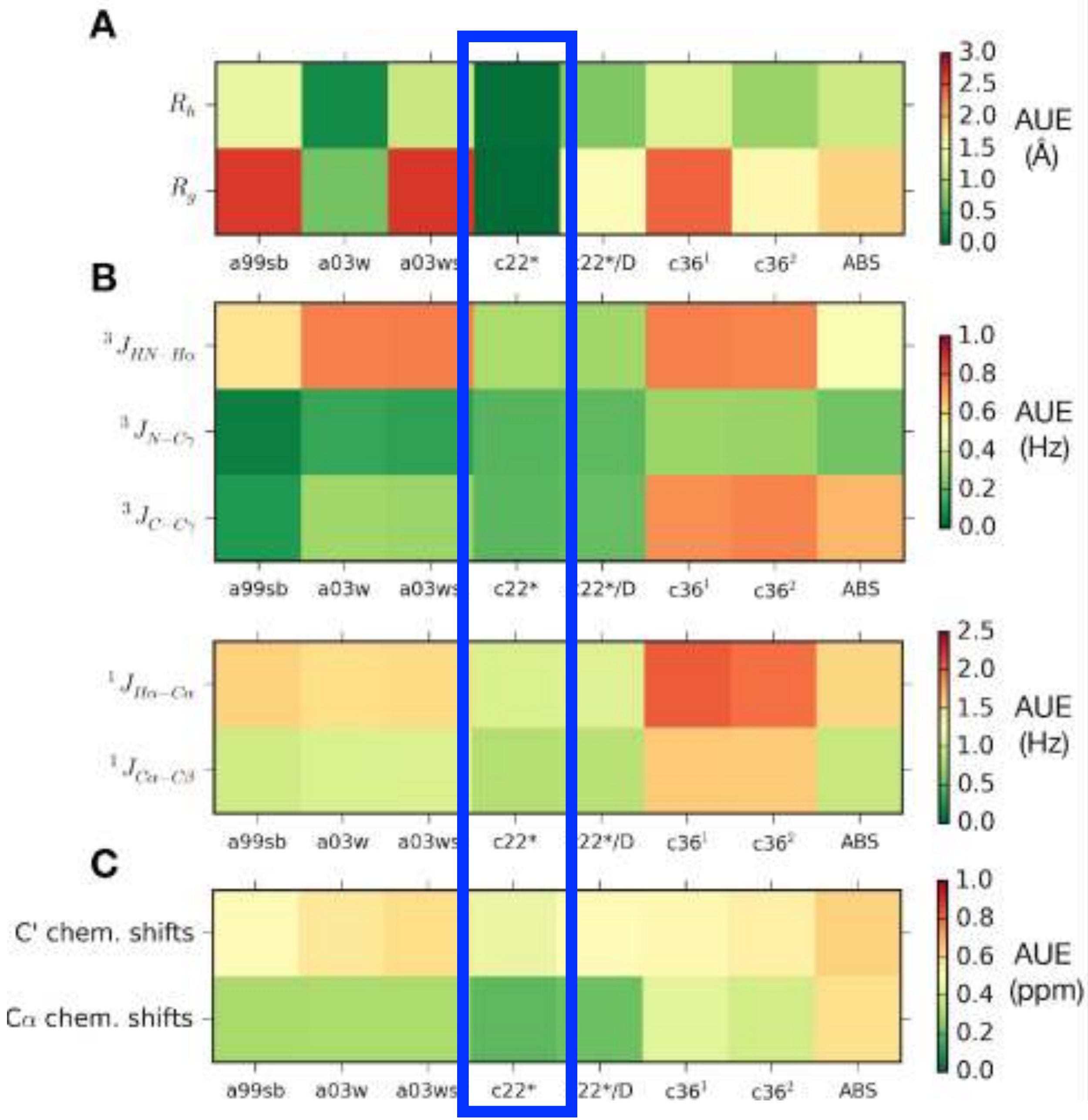

Chain Dimensions

Scalar Couplings

Chemical Shifts

Summary: Comparison to Experiment

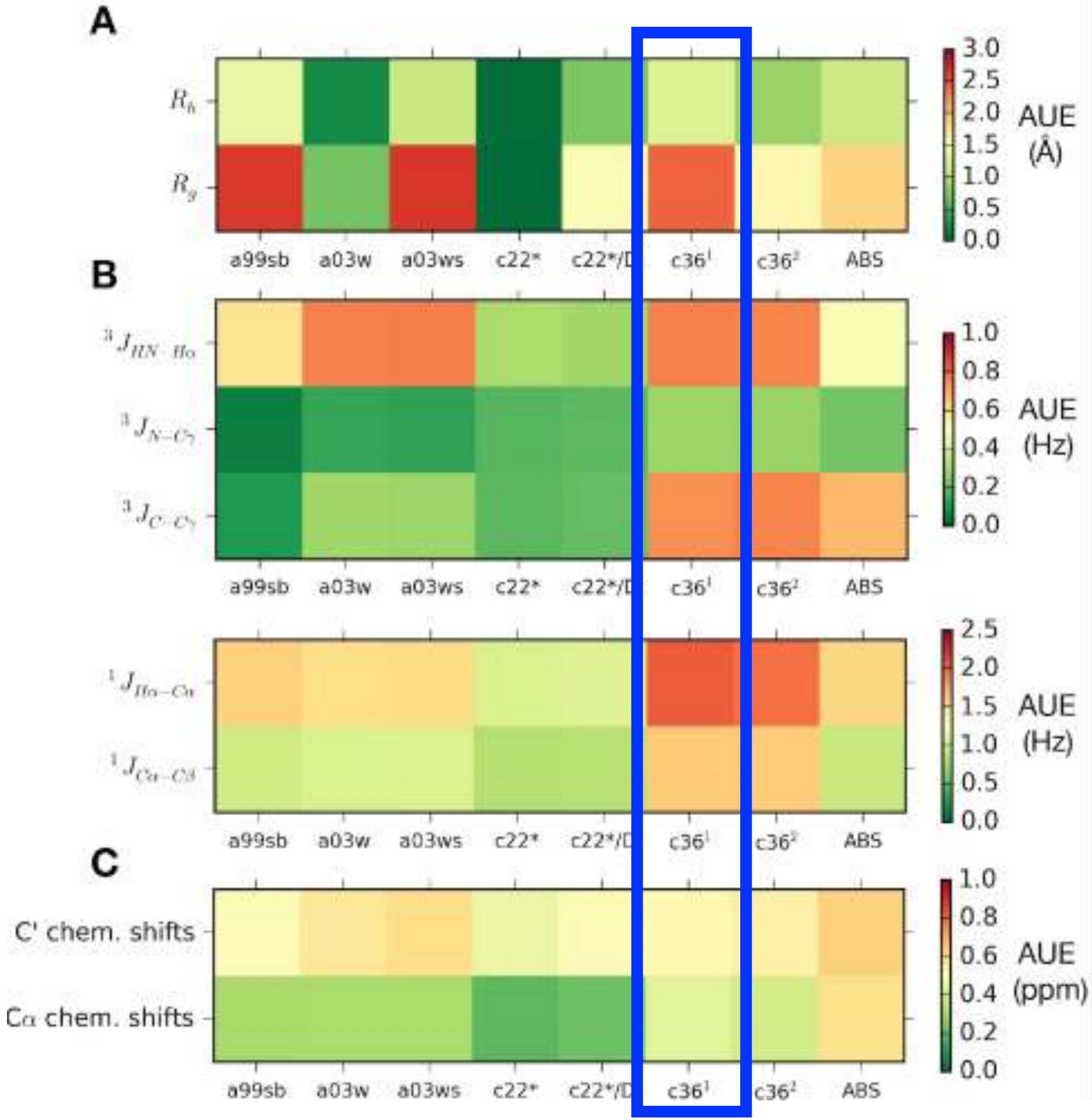

Chain Dimensions

Scalar Couplings

Chemical Shifts

New Force Field Version:

Validated against 14 peptides and 15 proteins,

cumulative simulation time of more than 500 μs

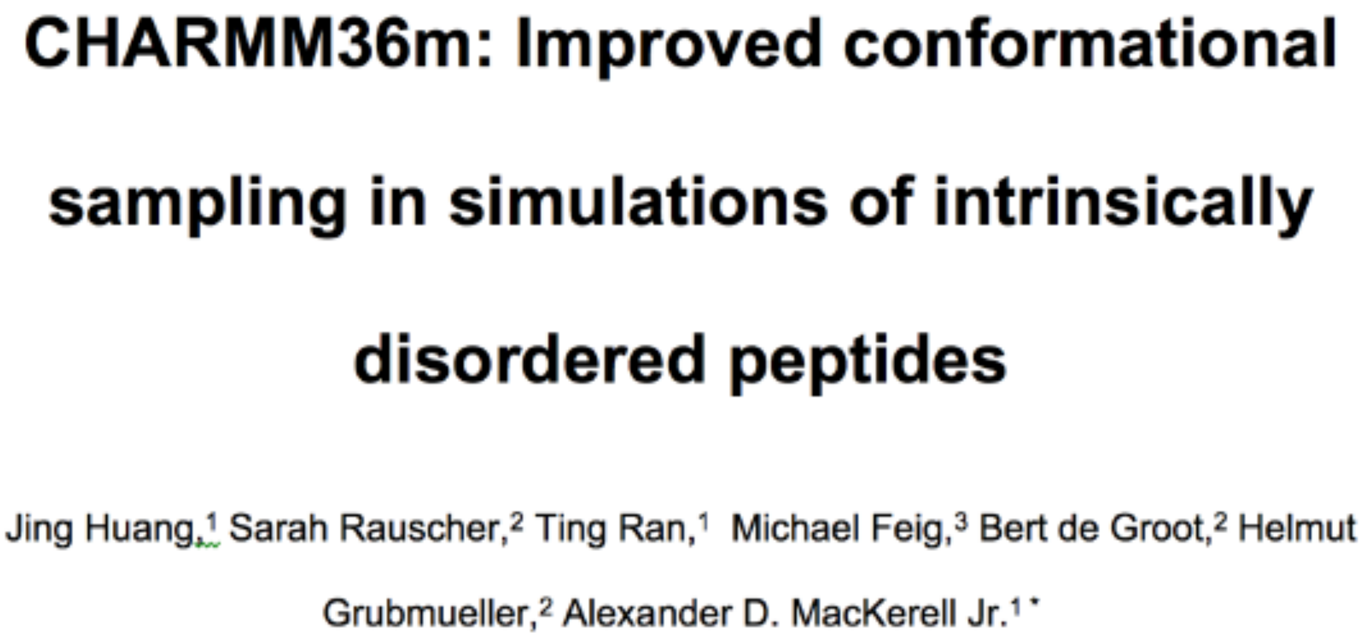

CHARMM36m: Improved conformational sampling in simulations of intrinsically disordered peptides

Jing Huang,[1] Sarah Rauscher,[2] Ting Ran,[1] Michael Feig,[3] Bert de Groot,[2] Helmut Grubmueller,[2] Alexander D. MacKerell Jr.[1*]

Nature Methods 14, 71-73 (2017)

α-synuclein (aS)

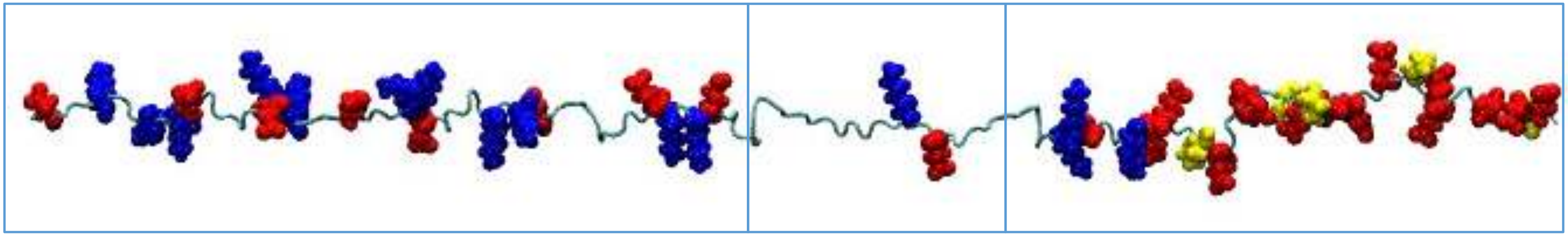

N-terminus aa::1–60, +4e NAC aa::61-95, -1e C-terminus aa::

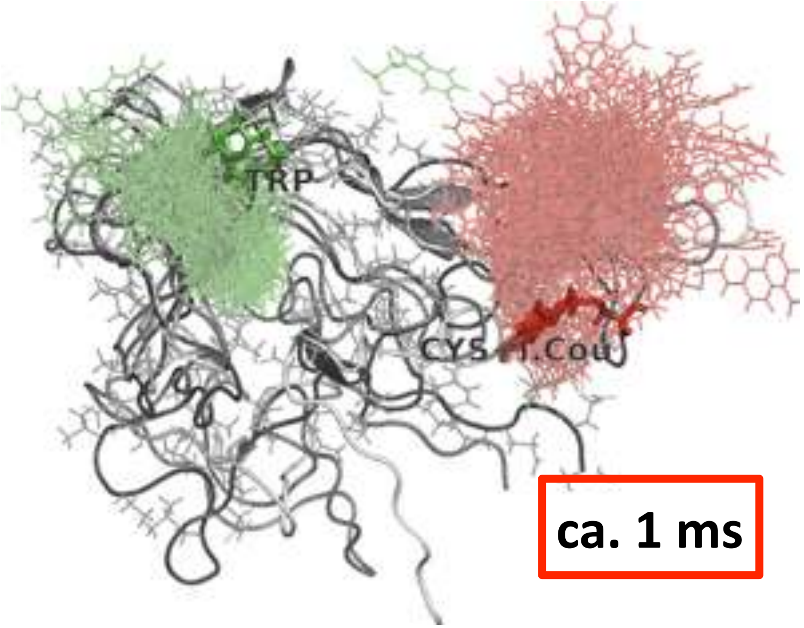

ca. 1 ms

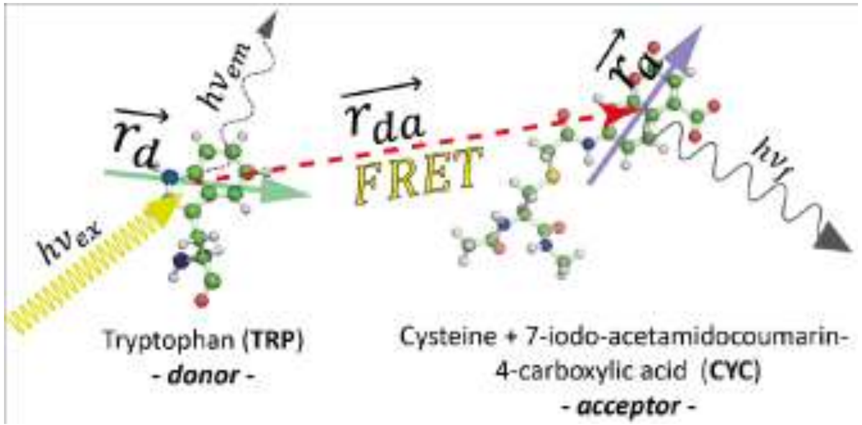

Collaborations

trFRET: Elisha Haas (Bar Illan)

NMR/SAXS: Marcus Zweckstetter (MPIbpc)

Graen et al., JCTC (2014)

Höfling et al., PloS One (2011)

Höfling et al., Comp. Phys. Comm. (2013)

Structural Dynamics of Monomeric alpha-Synuclein on the ns-µs Time Scale derived from MD Simulations

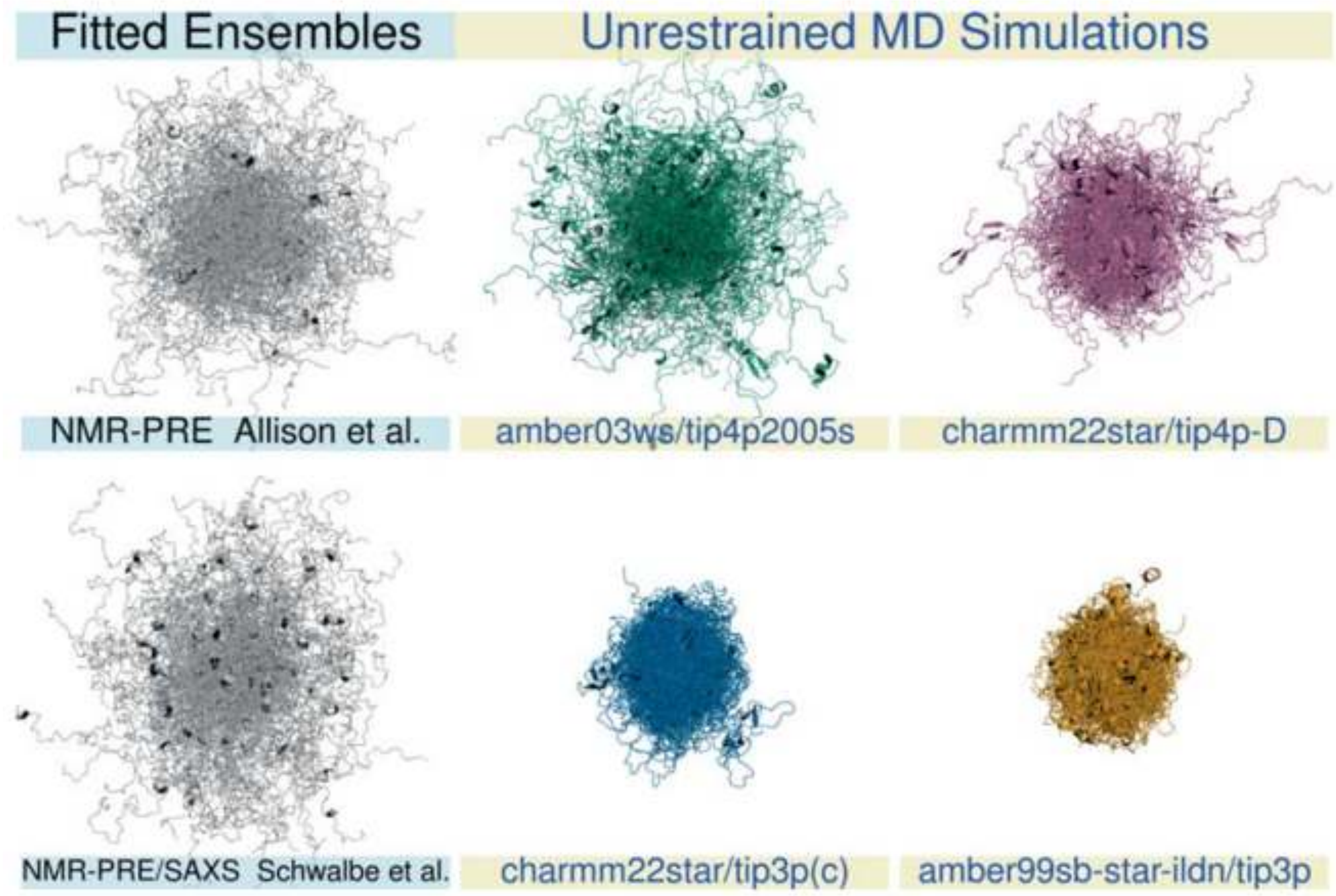

T.Graen, R.Klement, A.Grupi, E.Haas & H.Grubmüller, ChemPhysChem (2018)

free MD vs FRET

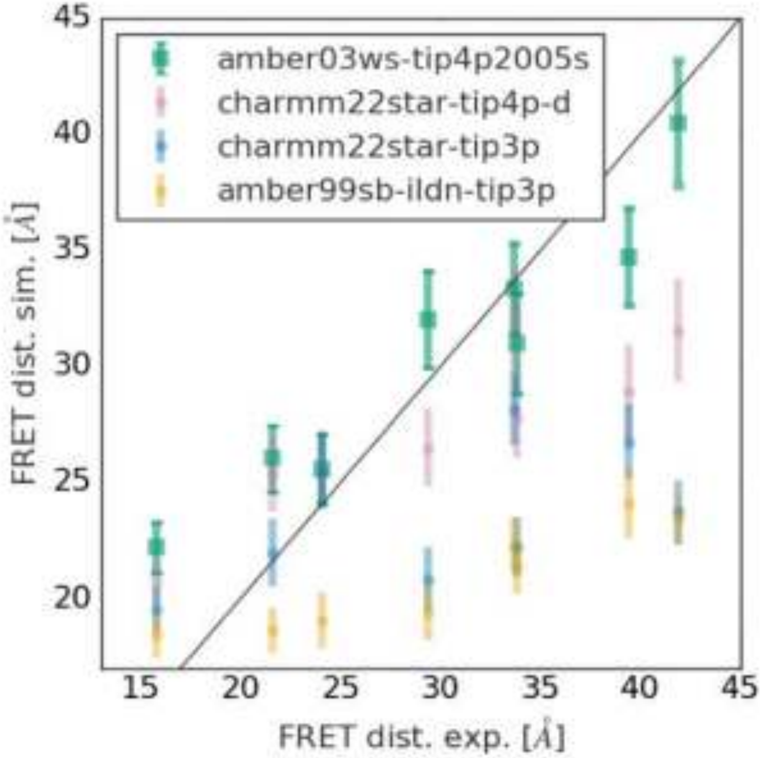

restrained NMR ensembles and free MD vs FRET

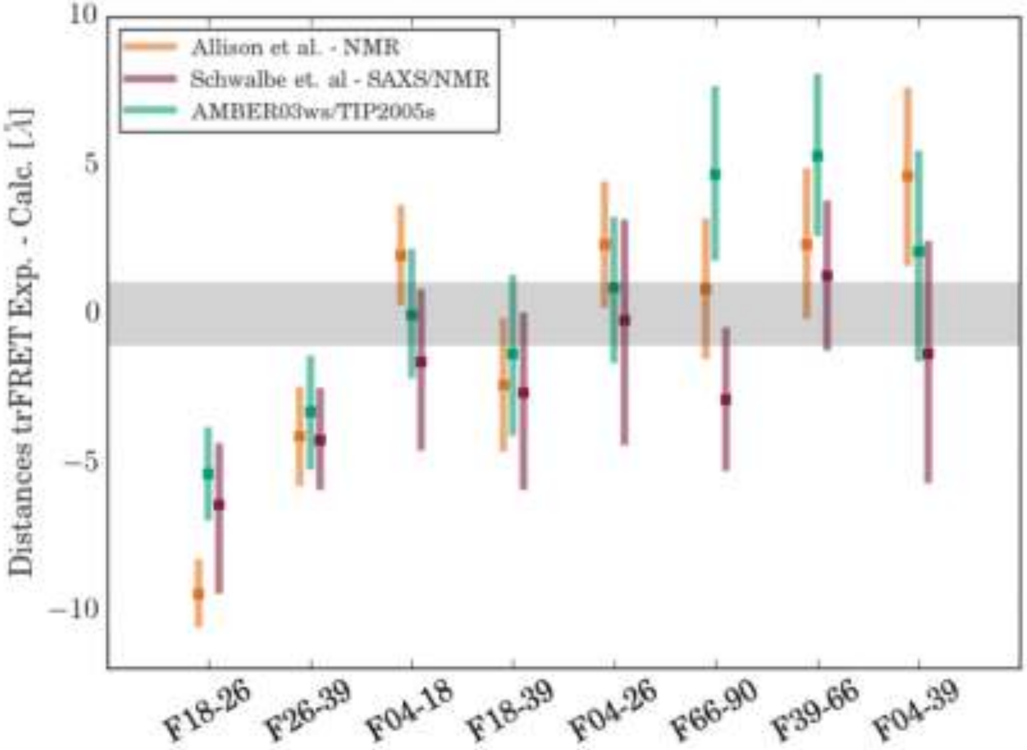

T.Graen, R.Klement, A.Grupi, E.Haas & H.Grubmüller, ChemPhysChem (2018)

Time scales, formation-, and dissociation rates

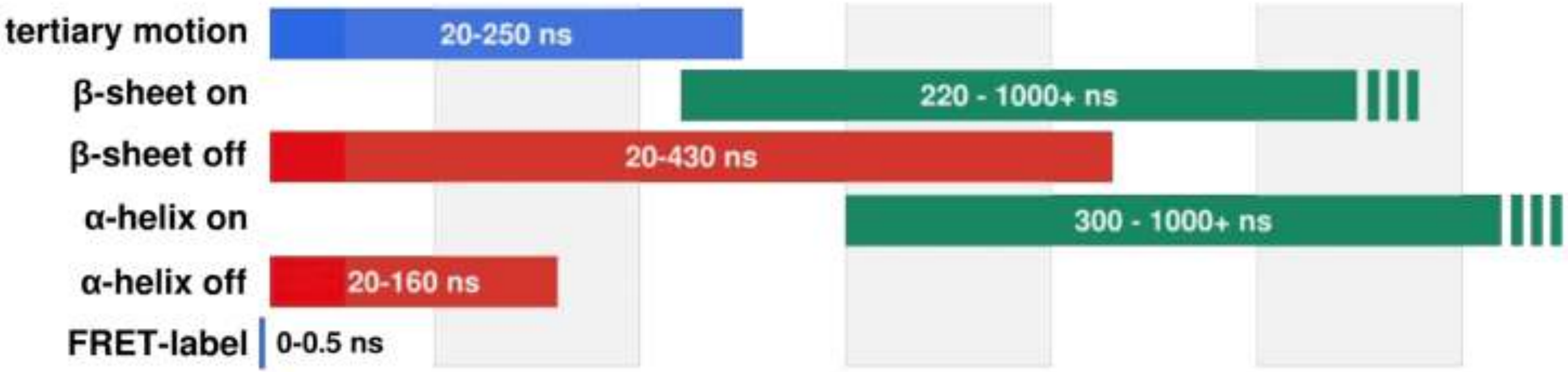

T.Graen, R.Klement, A.Grupi, E.Haas & H.Grubmüller, ChemPhysChem (2018)

Towards a mechanistic understanding of protein function

(1) Ligand unbinding revisited

(2) Ribosomal antibiotics mechanism

(3) Disordered Proteins

(4) The Dynasome

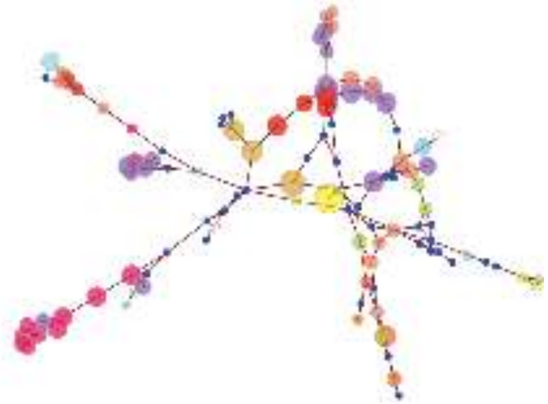

AFM+ X-ray + cryo EM + MD

Lars Bock, Christian Blau, Michal Kolar, Andrea Vaiana, Andreas Russek,
Benjamin von Ardenne

Holger Stark, Marina Rodnina (MPI Göttingen)
Roland Beckmann, Daniel Wilson (Univ. Munich)
Simon Scheuring (Cornell Univ.)

Charting the Protein Dynamics Landscape: The Dynasome

Ulf Hensen, Tim Meyer, Jürgen Haas, Rene Rex

Collab.: Gert Vriend (Nijmegen, NL)

Perspective: The ‚Dynasome'

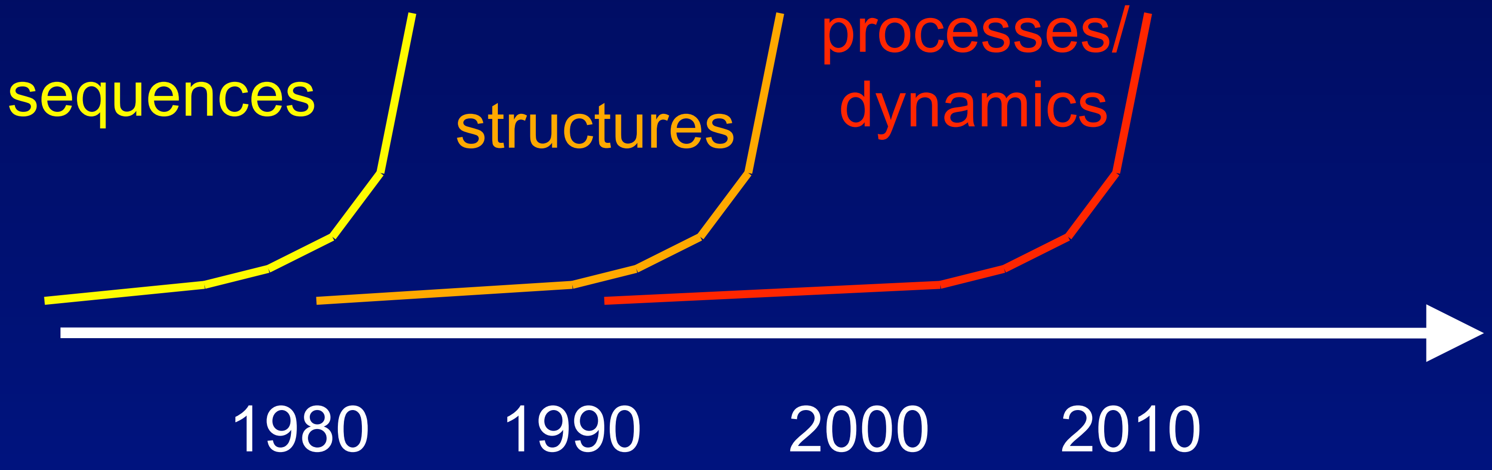

Phylogenetic trees

Protein structures fall into families

-> Can we also identify and classify <u>dynamics</u> motifs?

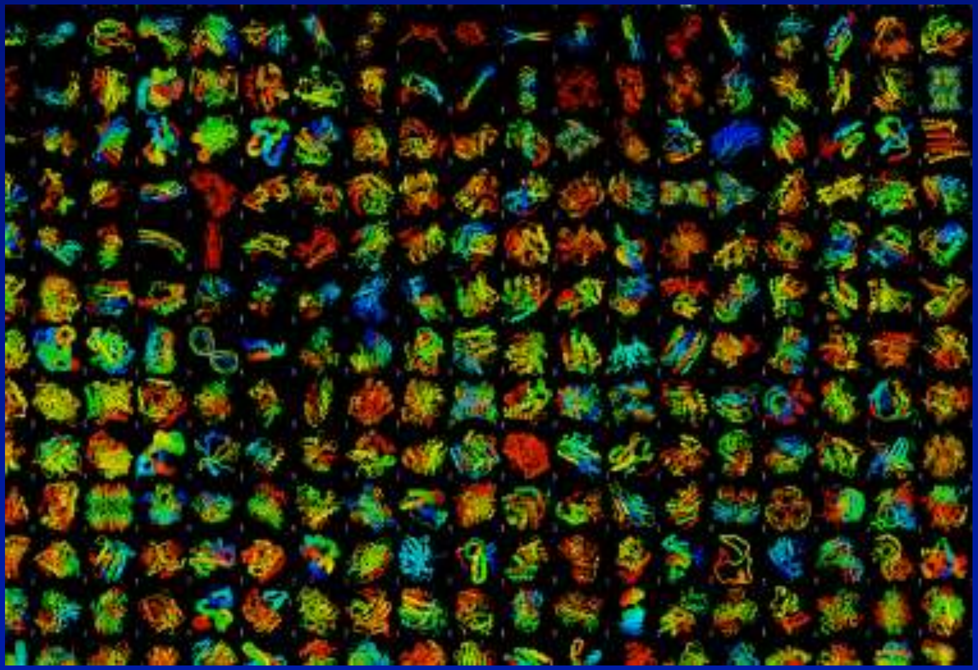

Exploring the protein dynamics space:

Structure / dynamics / function relationship

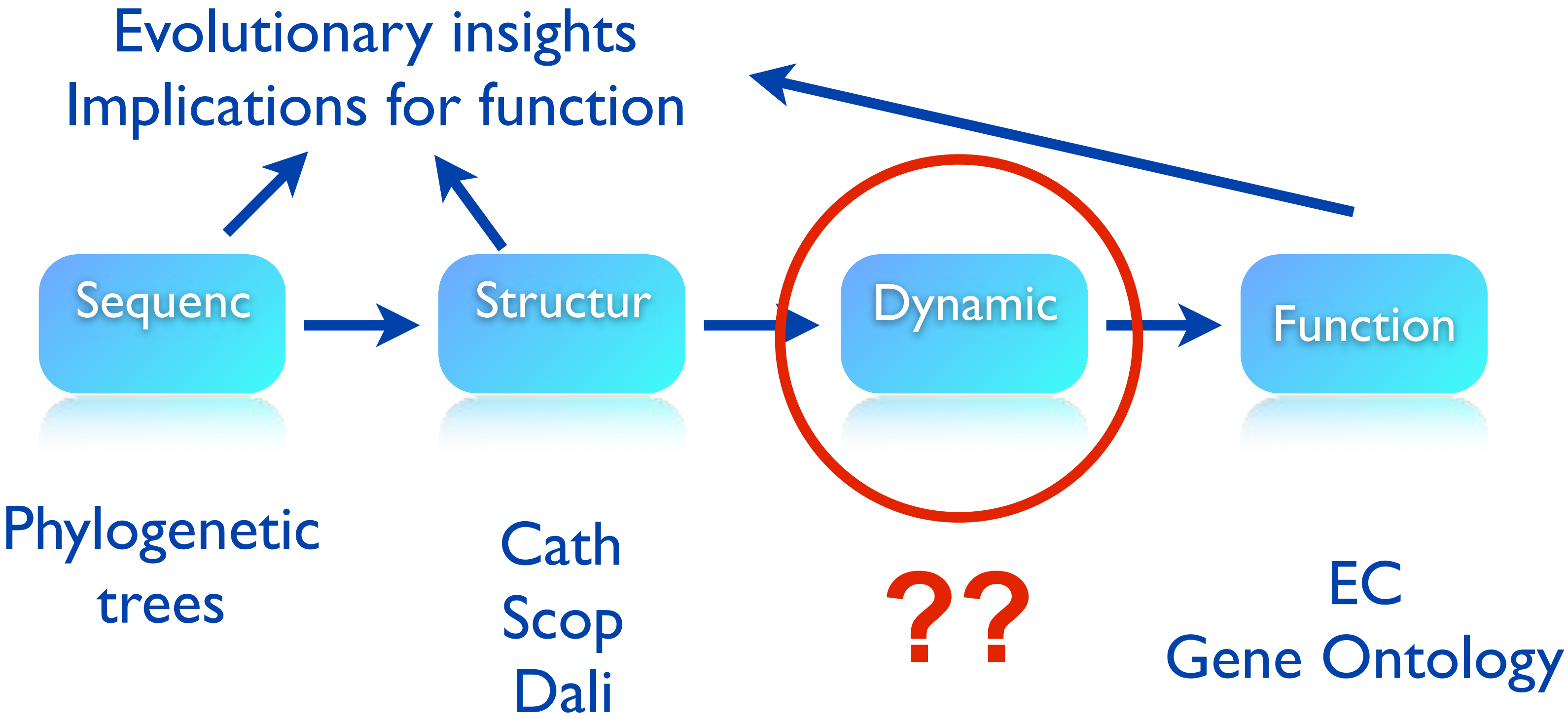

Evolutionary insights
Implications for function

Sequenc
Structur
Dynamic
Function

Phylogenetic trees

Cath
Scop
Dali

??

EC
Gene Ontology

Ulf Hensen, Tim Meyer,
Jürgen Haas, René Rex,
Collaboration: Gert Vriend

Pang A, Arinaminpathy Y, Sansom M, Biggin P (2005) Proteins 61: 809–822.
Meyer T, de la Cruz X, Orozco M (2009) Structure 17: 88–95.
Jonsson AL, Scott KA, Daggett V (2009) Biophysical Journal 97: 2958–2966.

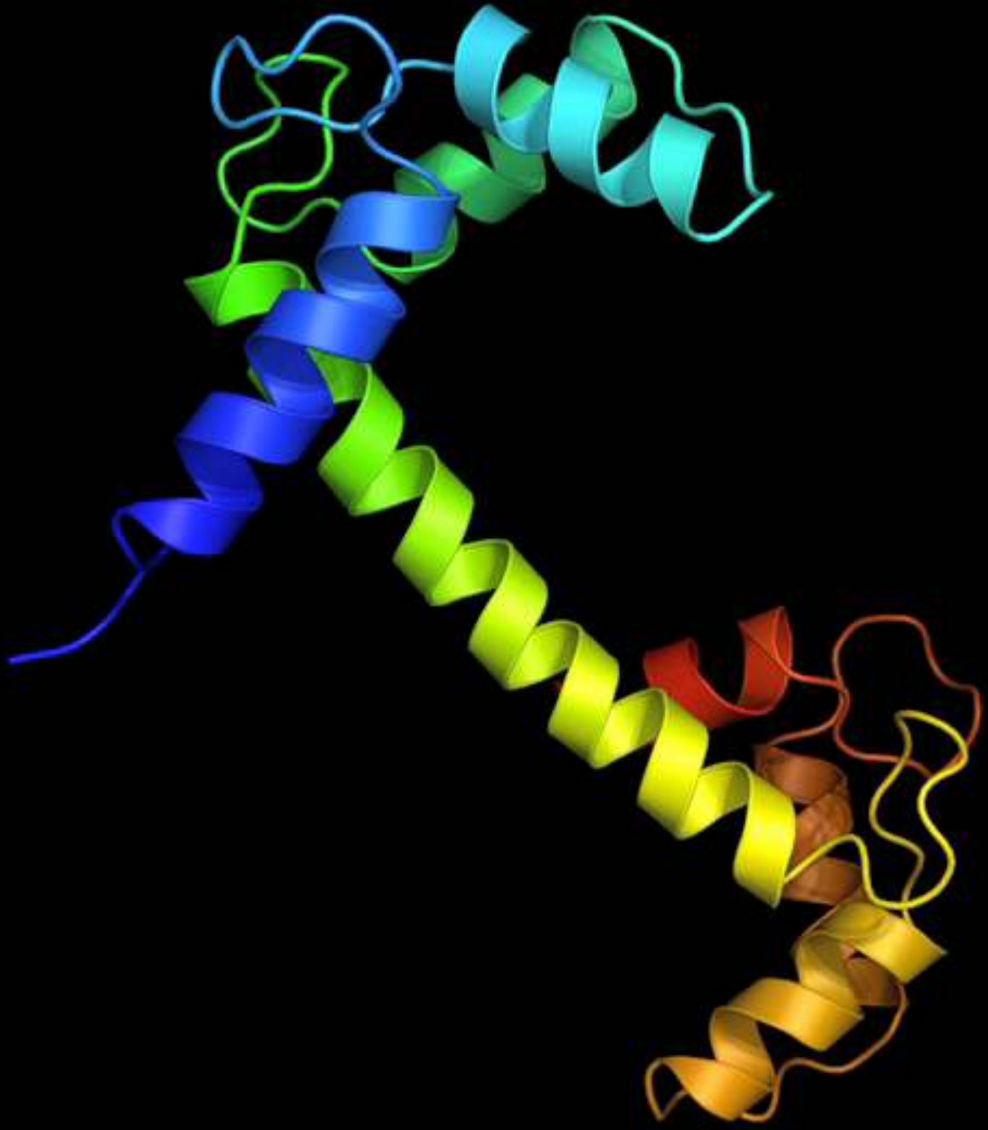

34 Dynamics observables

from 100 ns Simulations of 112 representative proteins

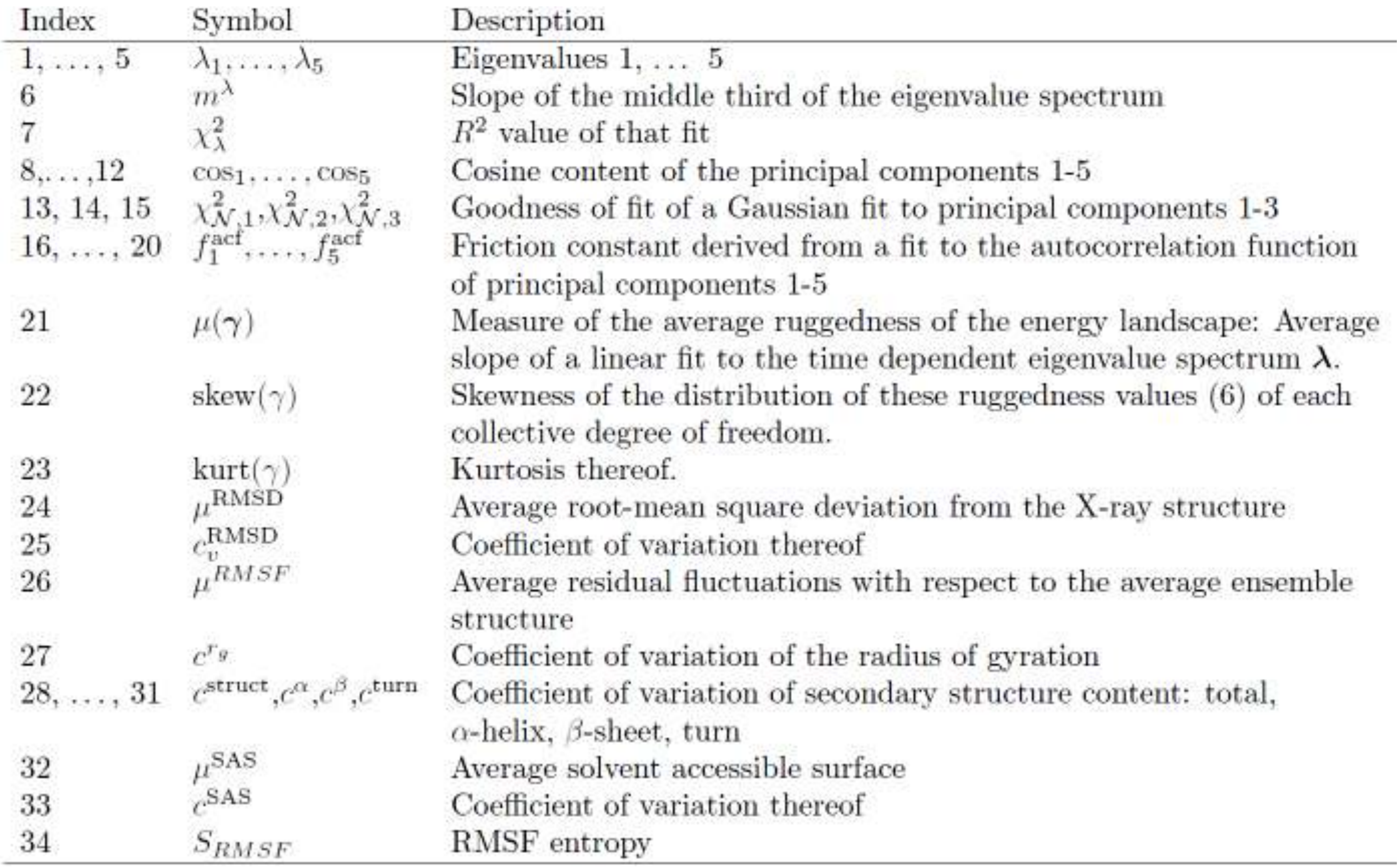

Index	Symbol	Description
1, …, 5	$\lambda_1, \ldots, \lambda_5$	Eigenvalues 1, … 5
6	m^λ	Slope of the middle third of the eigenvalue spectrum
7	χ^2_λ	R^2 value of that fit
8,…,12	$\cos_1, \ldots, \cos_5$	Cosine content of the principal components 1-5
13, 14, 15	$\chi^2_{\mathcal{N},1}, \chi^2_{\mathcal{N},2}, \chi^2_{\mathcal{N},3}$	Goodness of fit of a Gaussian fit to principal components 1-3
16, …, 20	$f_1^{\mathrm{acf}}, \ldots, f_5^{\mathrm{acf}}$	Friction constant derived from a fit to the autocorrelation function of principal components 1-5
21	$\mu(\gamma)$	Measure of the average ruggedness of the energy landscape: Average slope of a linear fit to the time dependent eigenvalue spectrum $\boldsymbol{\lambda}$.
22	$\mathrm{skew}(\gamma)$	Skewness of the distribution of these ruggedness values (6) of each collective degree of freedom.
23	$\mathrm{kurt}(\gamma)$	Kurtosis thereof.
24	μ^{RMSD}	Average root-mean square deviation from the X-ray structure
25	c_v^{RMSD}	Coefficient of variation thereof
26	μ^{RMSF}	Average residual fluctuations with respect to the average ensemble structure
27	c^{r_g}	Coefficient of variation of the radius of gyration
28, …, 31	$c^{\mathrm{struct}}, c^\alpha, c^\beta, c^{\mathrm{turn}}$	Coefficient of variation of secondary structure content: total, α-helix, β-sheet, turn
32	μ^{SAS}	Average solvent accessible surface
33	c^{SAS}	Coefficient of variation thereof
34	S_{RMSF}	RMSF entropy

Each protein -> vector in dynamics space

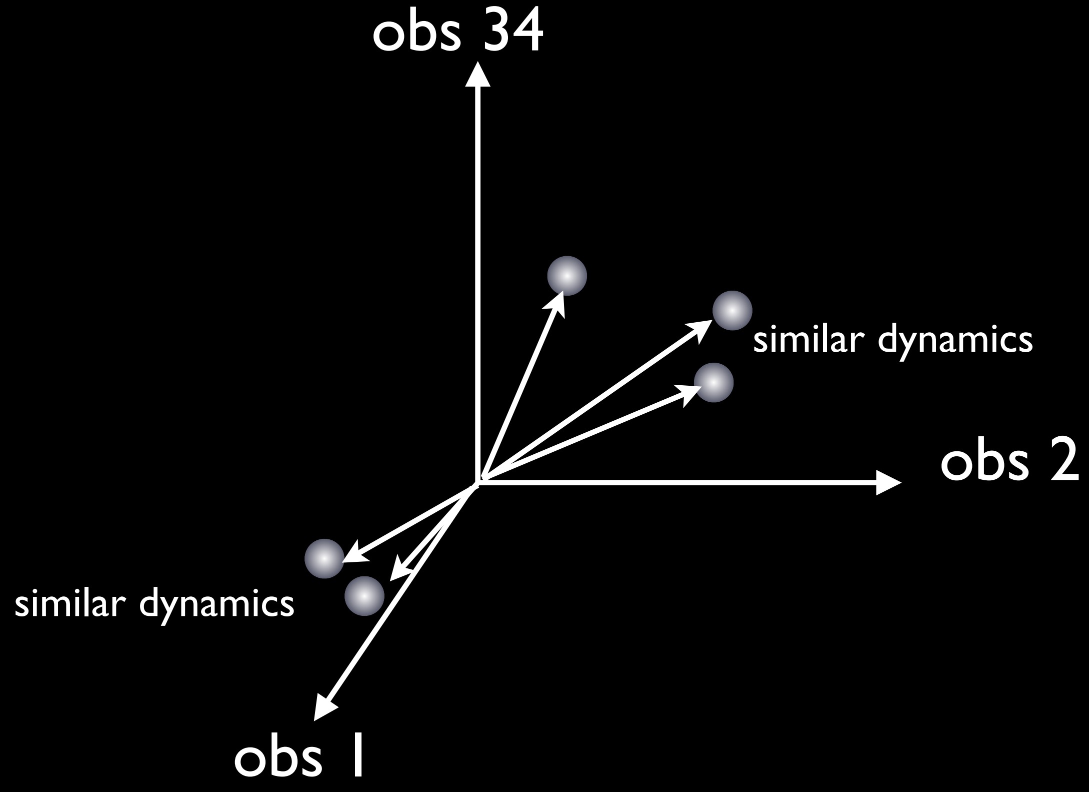

Projection into essential subspace: PCA

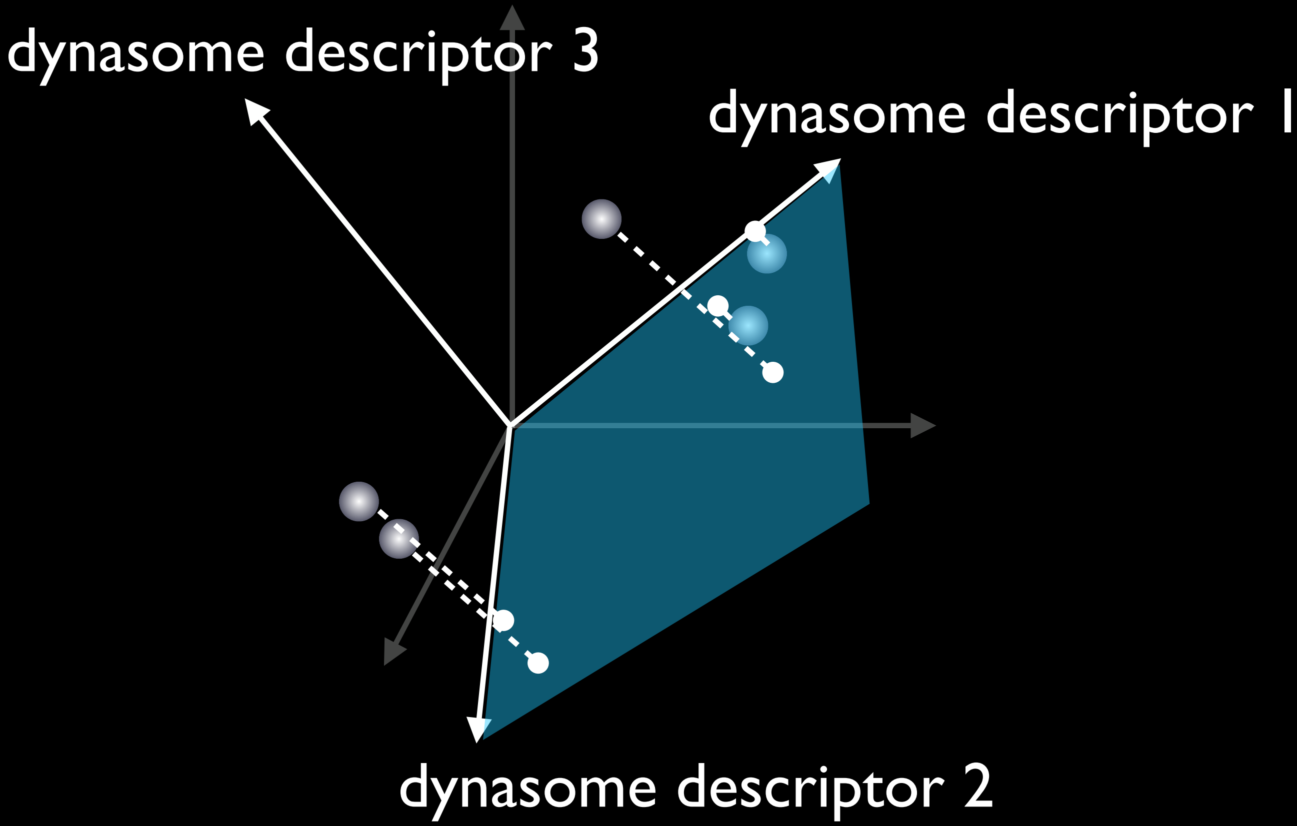

Collective descriptors: linear combinations of observables

Structure / dynamics relationship

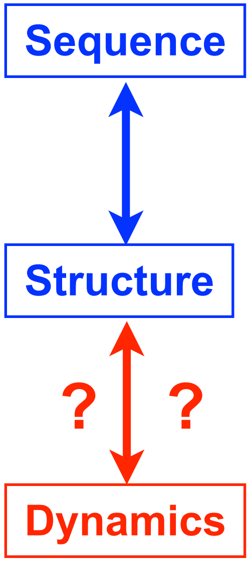

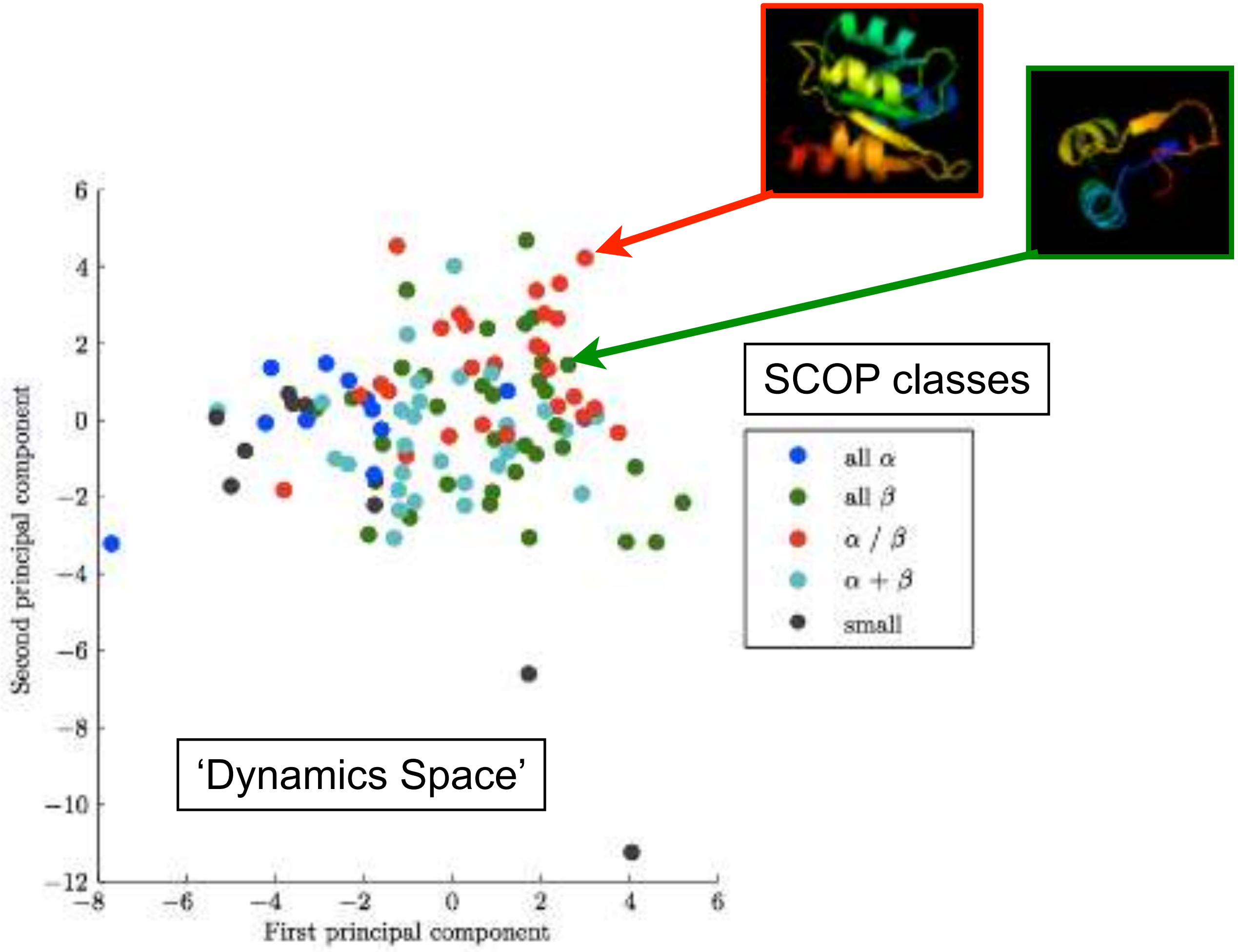

Questions:

- *What is the meaning of the principal components?*
- *Does similar structure imply similar dynamics?*
- *Does similar dynamics require similar structure?*
- *How does function correlate with dynamics?*

Collective dynamics descriptors

Descriptor 2
f_1^{acf}(-)(12 %)
f_2^{acf} (-) (8 %)
f_4^{acf} (-) (7 %)
$\chi^2_{\mathcal{N},1}$(-) (7 %)
kurt(γ)(+) (7 %)

slow

....

fast

Kinetics

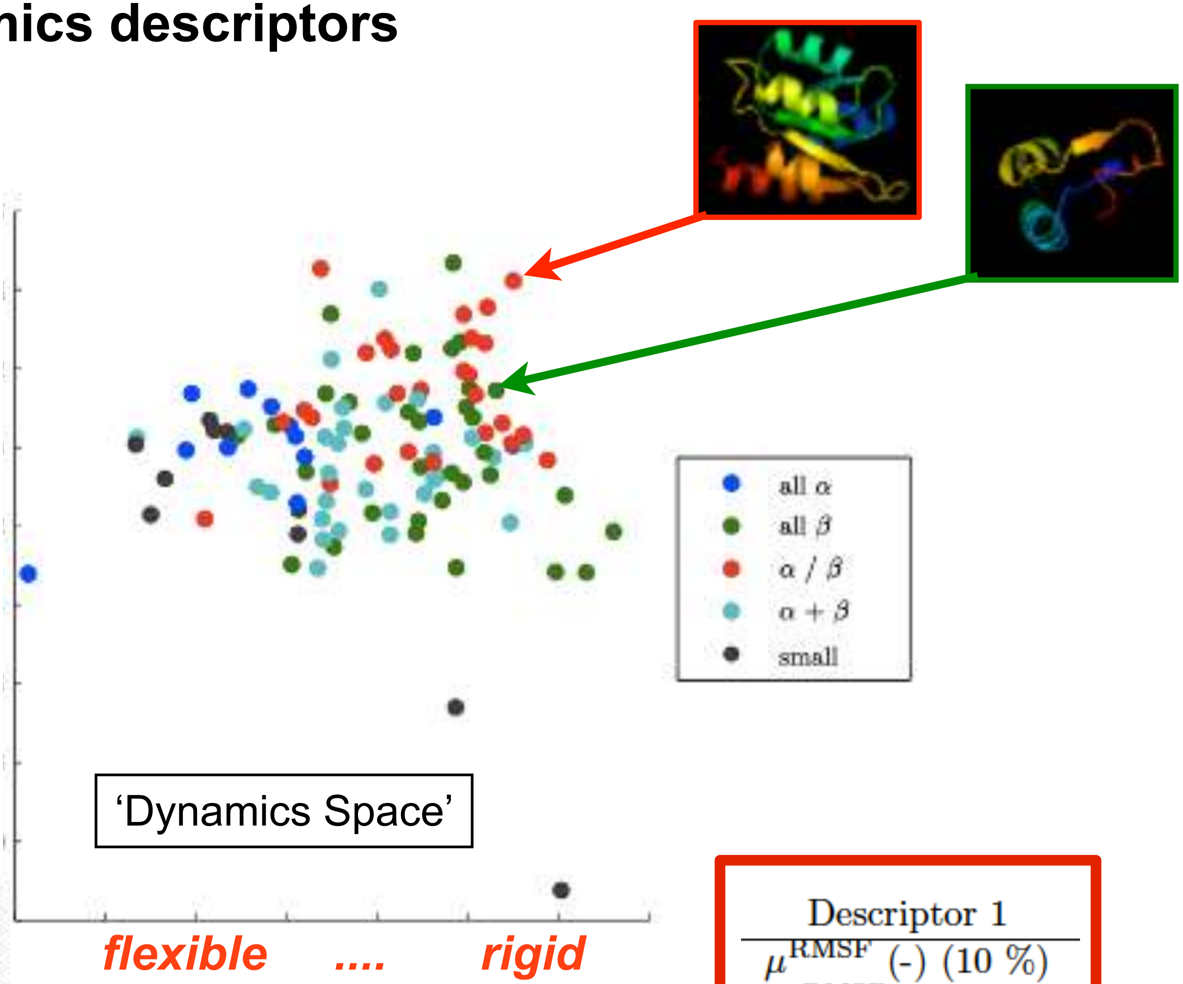

‘Dynamics Space’

flexible *....* *rigid*

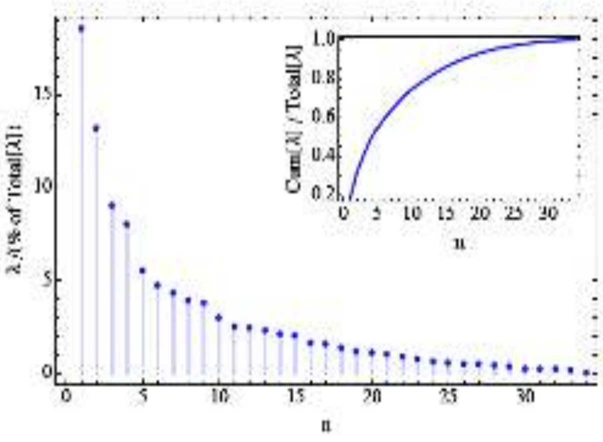

Thermodynamics

Descriptor 1
μ^{RMSF} (-) (10 %)
μ^{RMSD} (-)(9 %)
c^{r_g}(-) (9 %)
skew(γ) (+) (7 %)
$\mu(\gamma)$ (+) (7 %)

Structure / dynamics relationship

Sequence

Structure

? ?

Dynamics

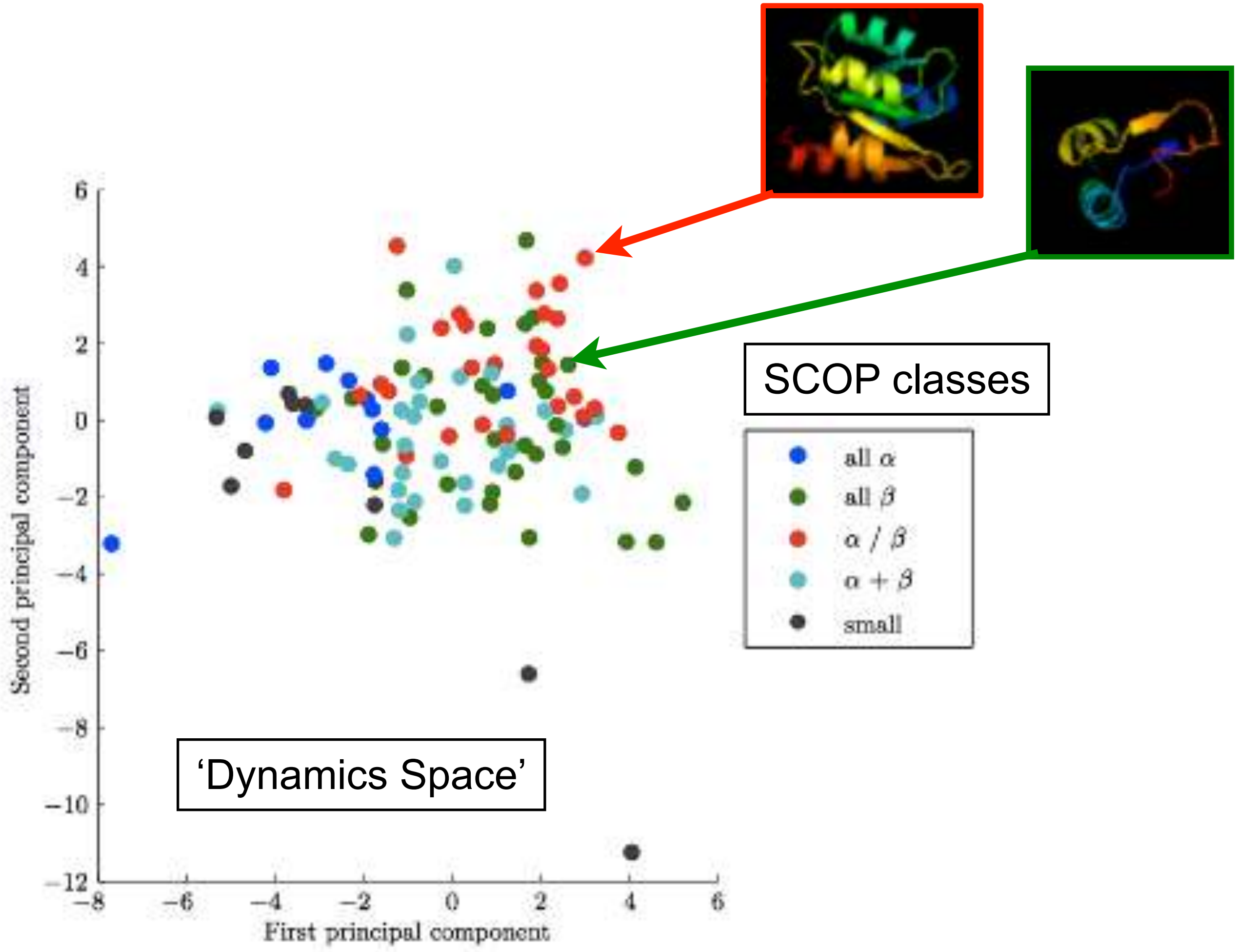

SCOP classes

'Dynamics Space'

Questions:

- *What is the meaning of the principal components?*
- *Does similar structure imply similar dynamics?*
- *Does similar dynamics require similar structure?*
- *How does function correlate with dynamics?*

Structure / dynamics relationship

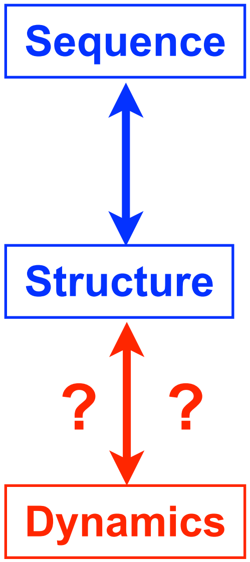

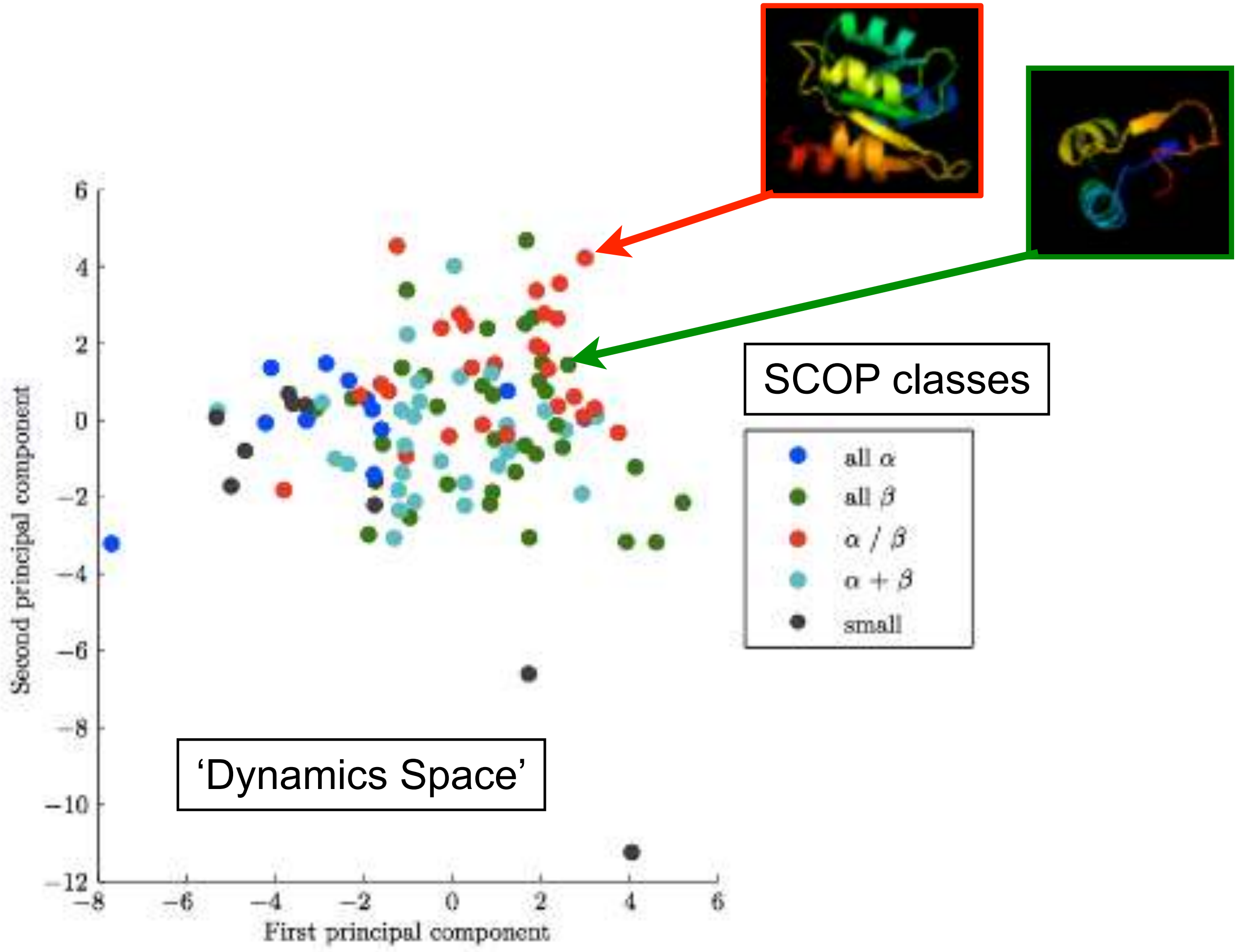

Questions:

- *What is the meaning of the principal components?*
- *Does similar structure imply similar dynamics?*
- *Does similar dynamics require similar structure?*
- *How does function correlate with dynamics?*

The fine structure or the dynasome

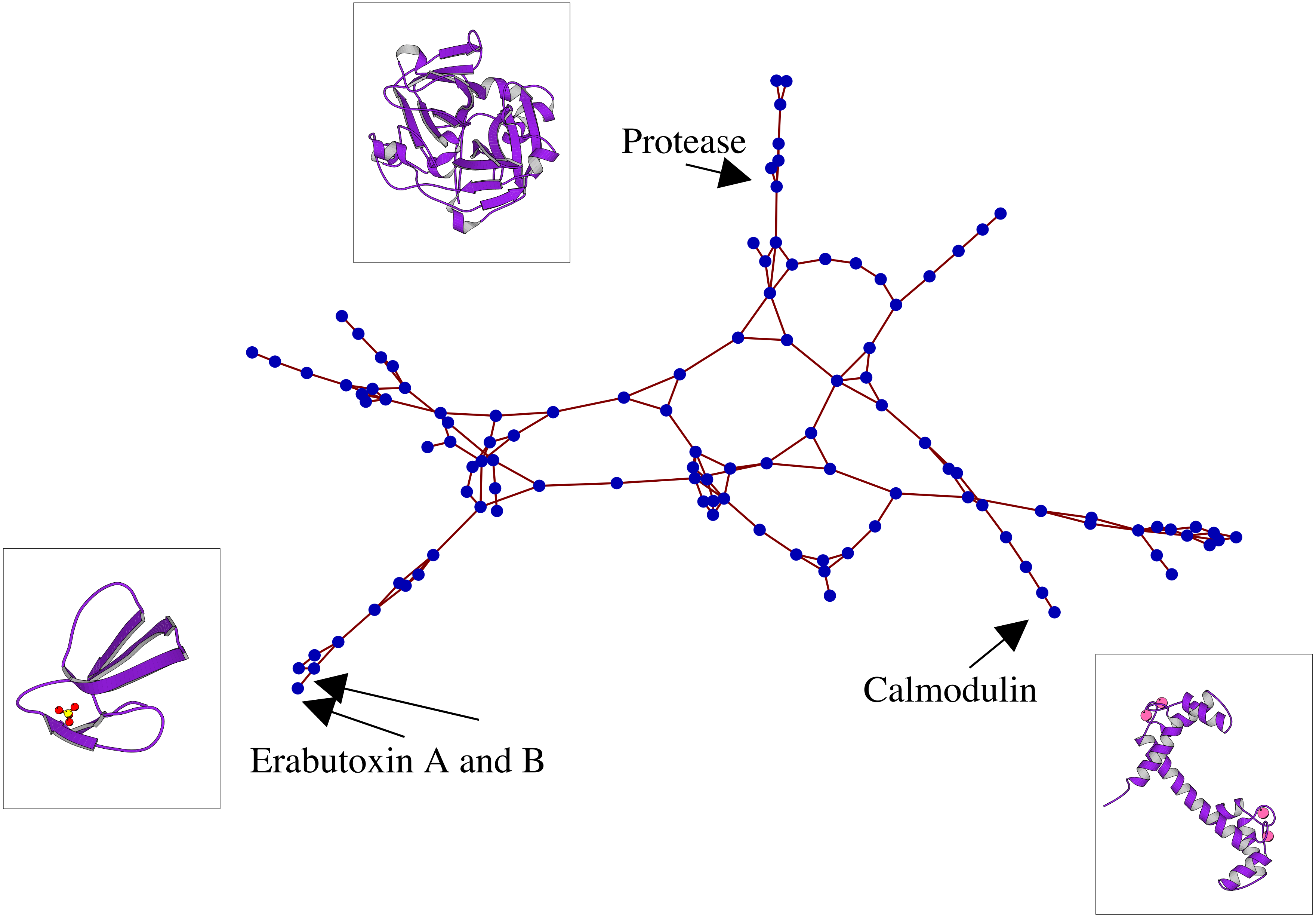

Dynamics correlates with function!

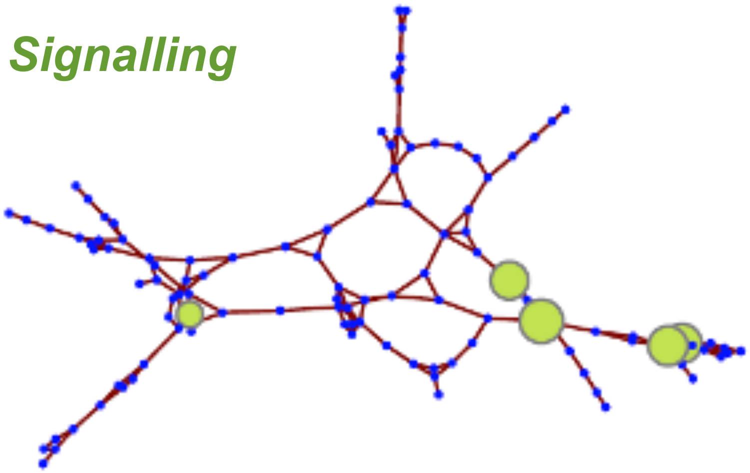
Signalling

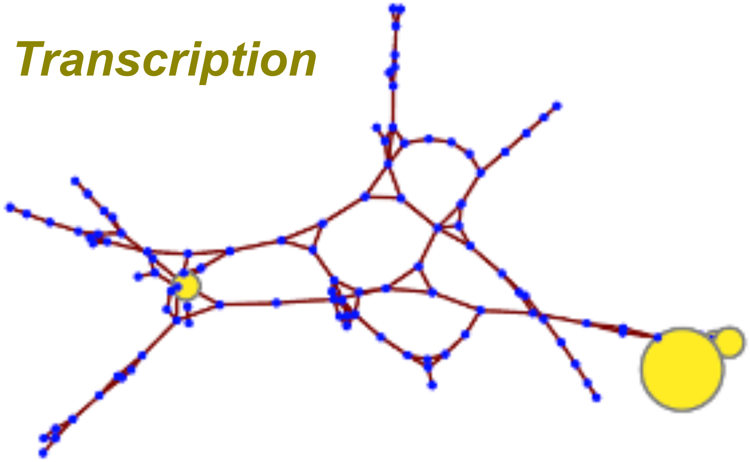
Transcription

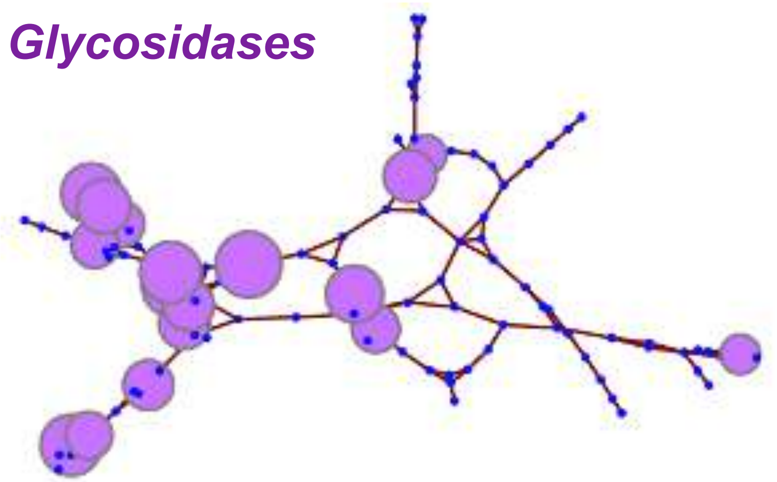
Glycosidases

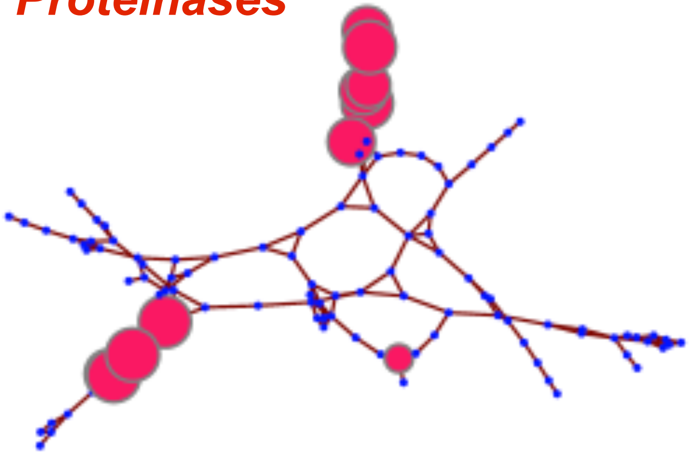
Proteinases

Protein Function Prediction

1. New protein of unknown function:
2. Based on its dynamics, determine its position in the graph.
3. function from closest cluster.

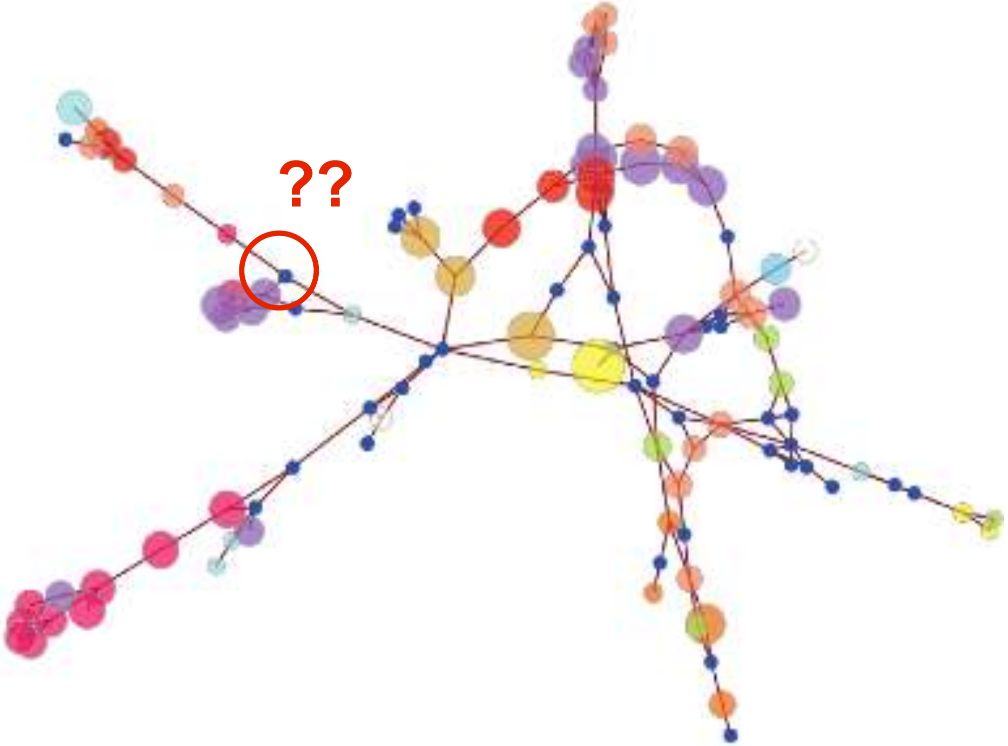

dyn	*struct*	*random*
46 %	*32 %*	*11 %*

Hensen U, Meyer T, Haas J, Rex R, Vriend G, Grubmüller H. *PLoS One* 7, e33931 (2012)

Femtoseconds XFEL single molecule diffraction

('diffract and destroy')

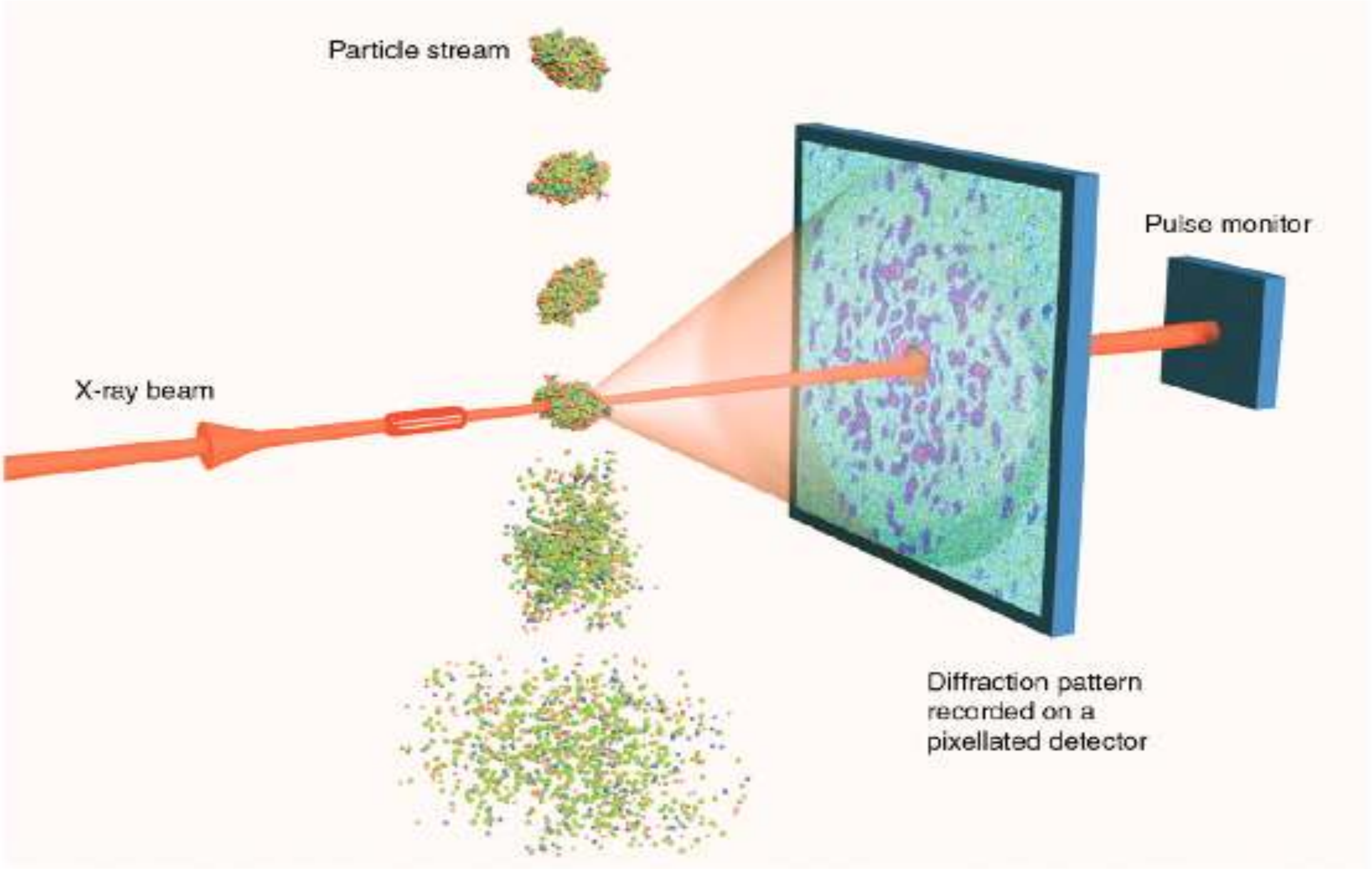

Illustration from Gaffney and Chapmann (2007), Science 316,1444

Structure determination from XFEL fs xray pulses?

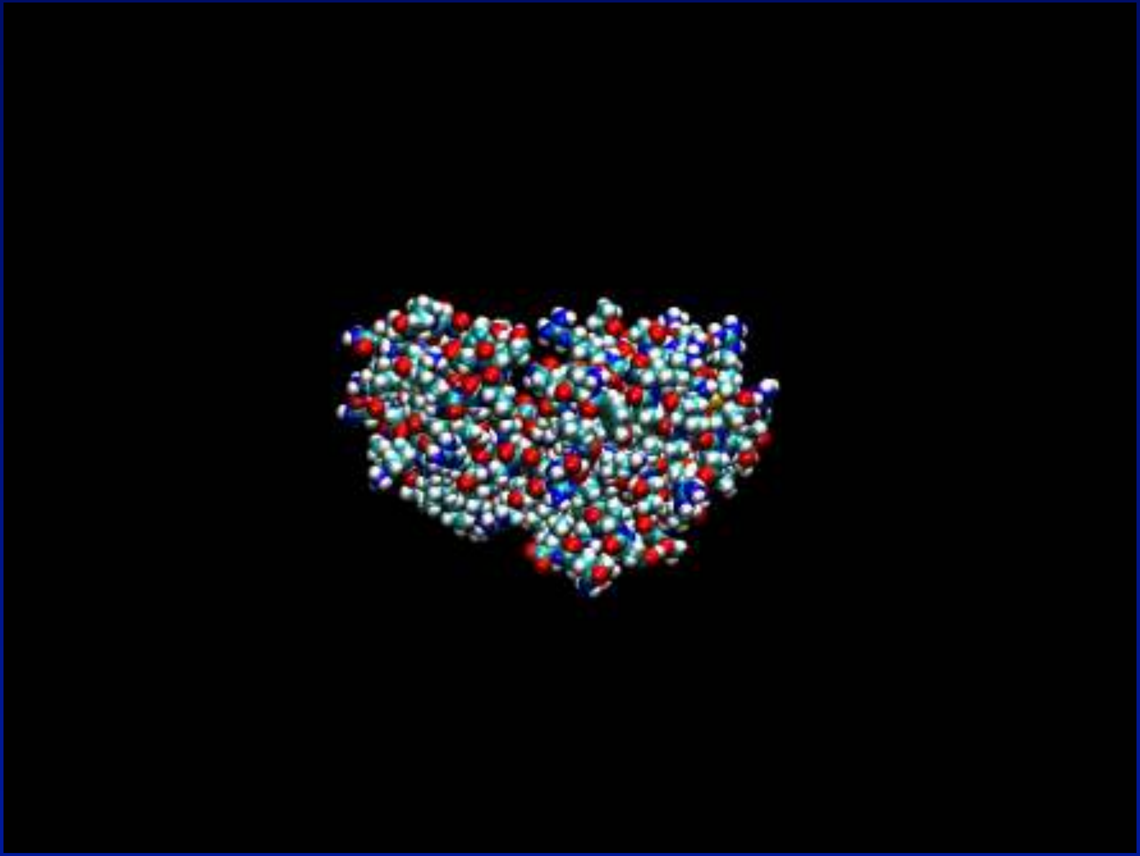

G. Groenhof & H. Grubmuller

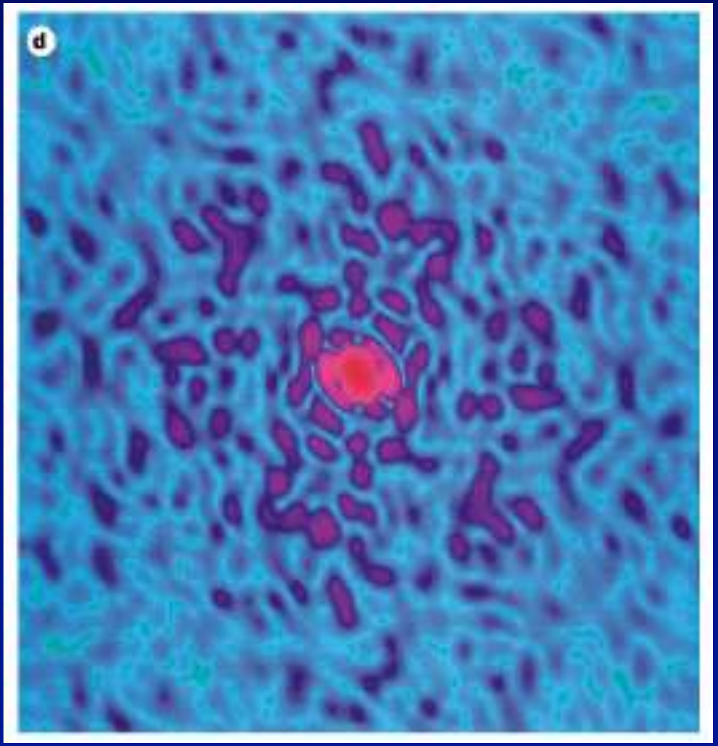

R. Neutze et al., Nature 406, 752-757

Lysozyme Coulomb explosion after XFEL xray pulse exposure

Simple Force Field!

Ideal case: continuous diffraction pattern (infinite intensity)

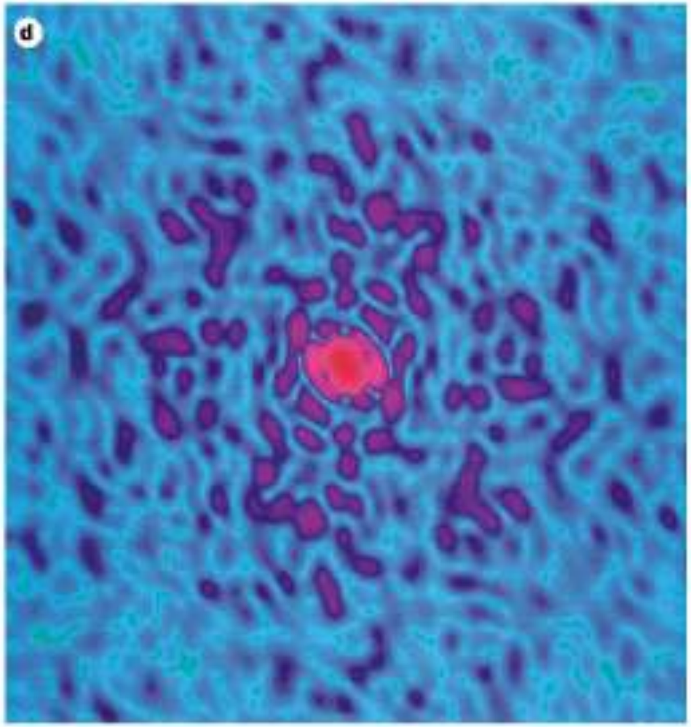

(calculated!)

Fourier Transform

no phases

<u>BUT</u>: continuous sampling
-> phase reconstruction
much easier

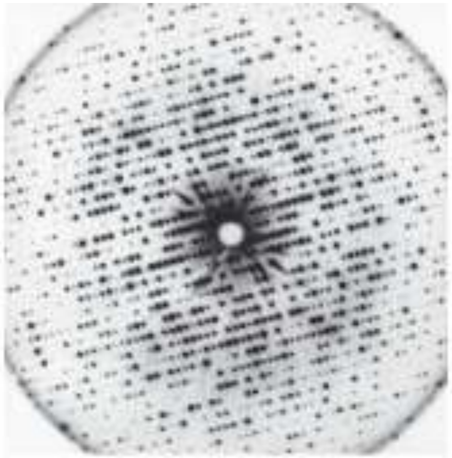

Reality: extreme low photon statistics (Poisson limit)

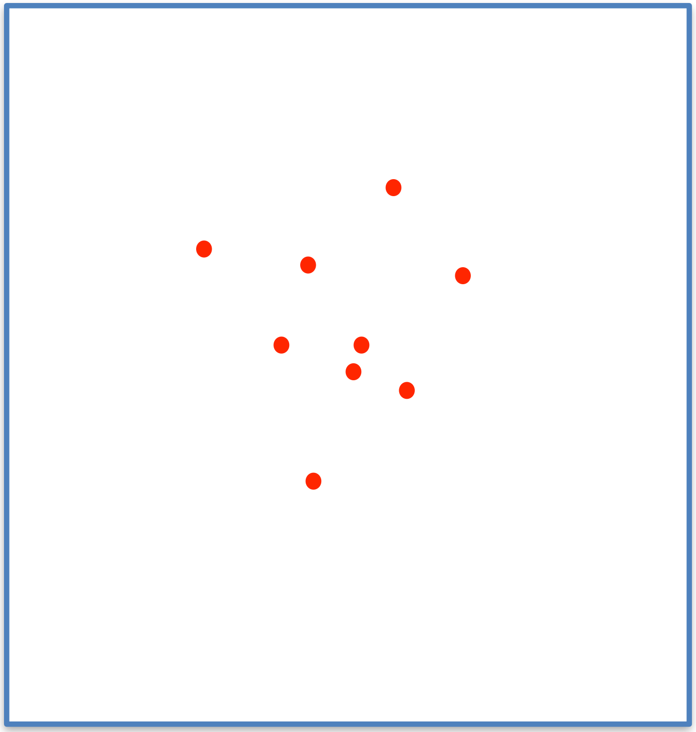

Only 10…100 photons per image!

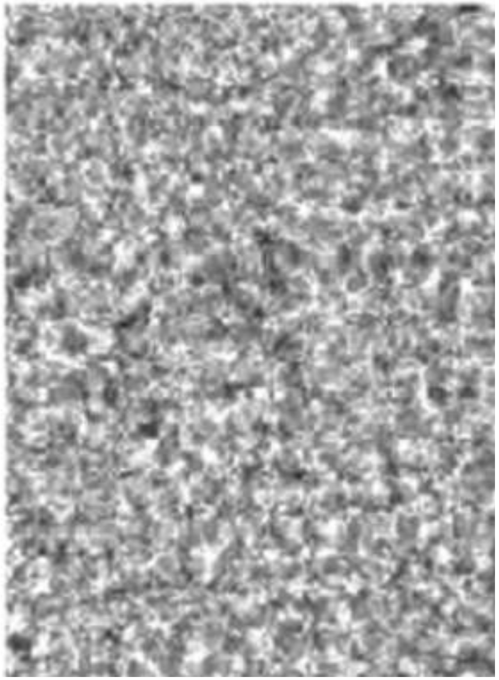

Single Molecule Cryo-EM

Wang, L., & Sigworth, F. J. (2006). Cryo-EM and single particles. Physiology, 21(1), 13–8.

Reality: extreme low photon statistics (Poisson limit)

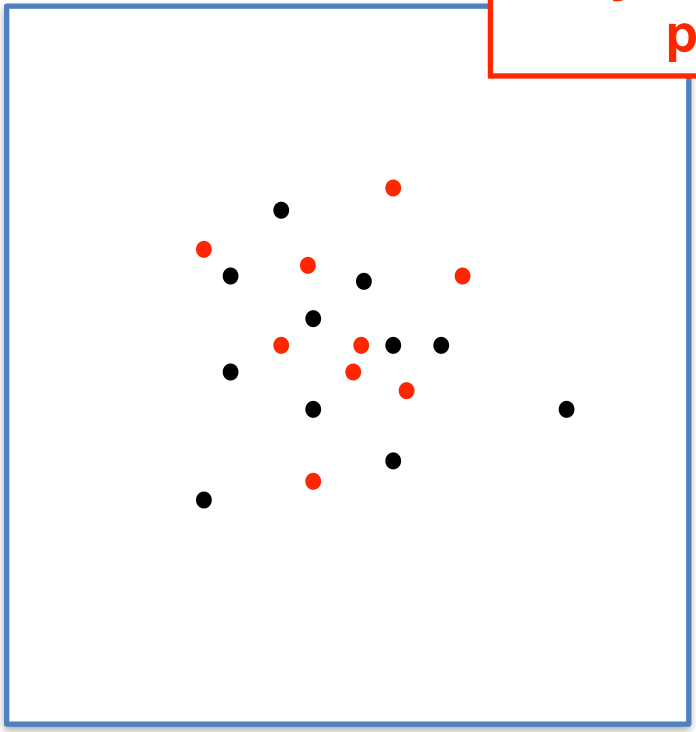

Only 10…100 photons per image!

sample orientation unknown!

> 50% noise photons

Reality: extreme low photon statistics (Poisson limit)

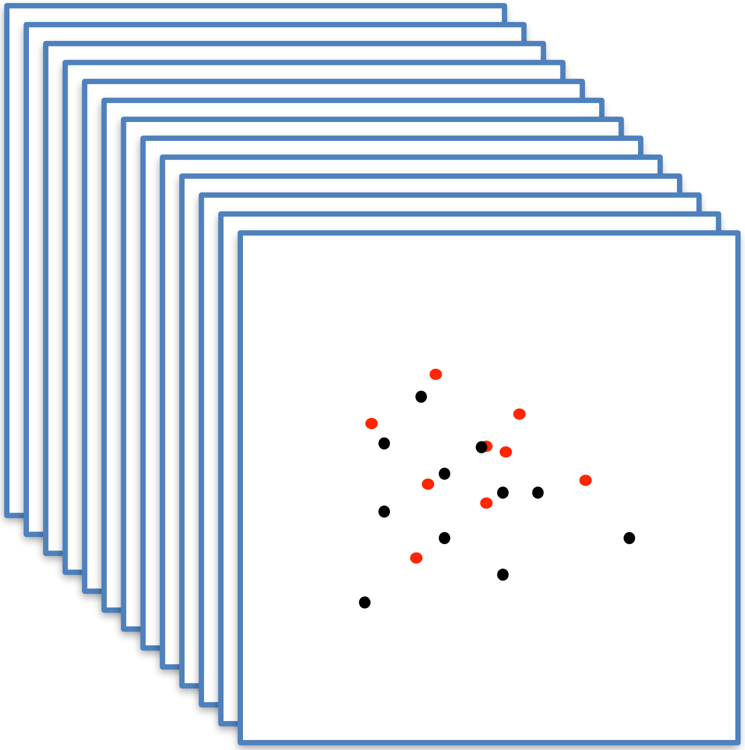

BUT: $10^6 \ldots 10^9$ images

(27000 pulses /sec)

How few photons will do?

state of the art:
>300 photons per image

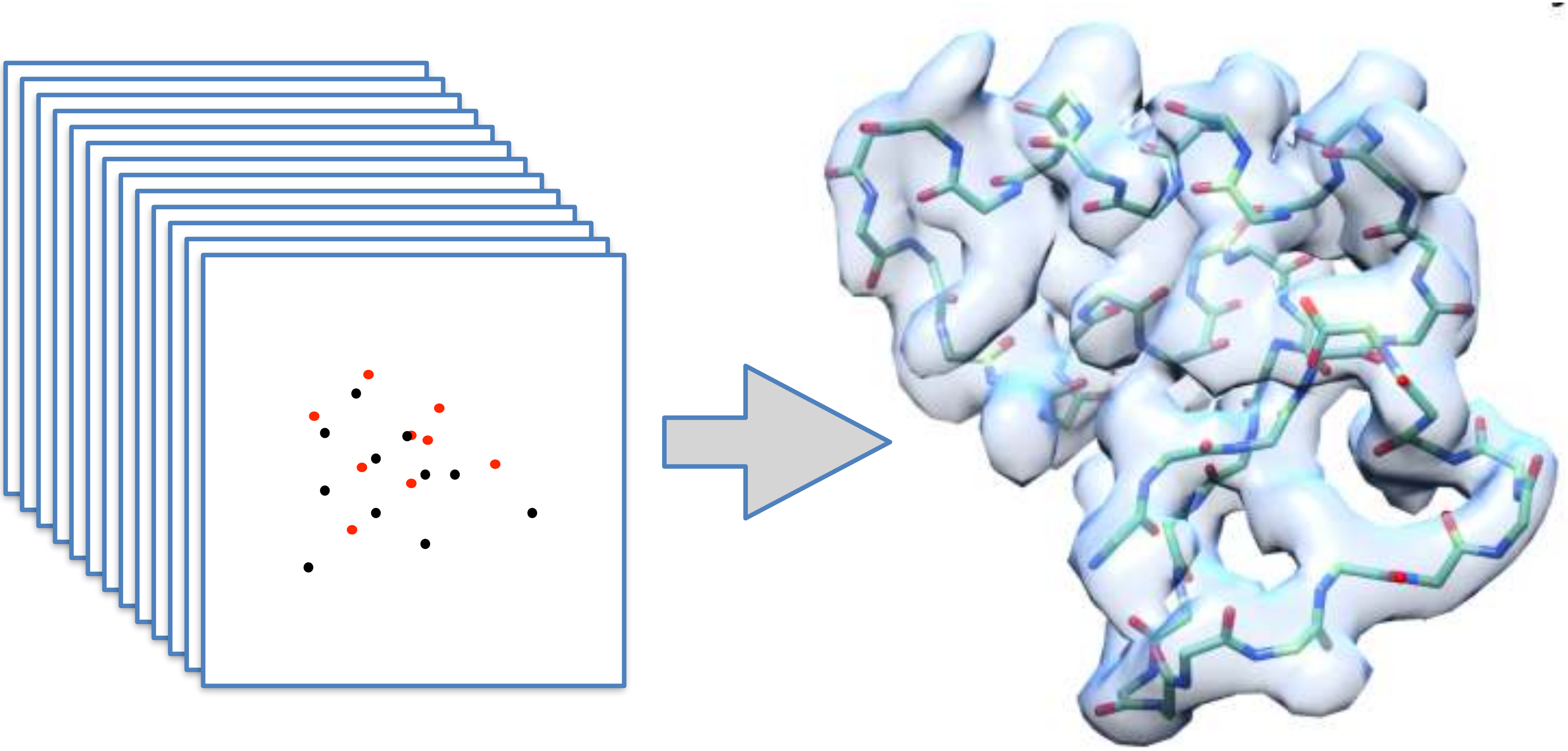

Trick #1: Maximize

Benjamin von Ardenne

Martin Mechelke

P(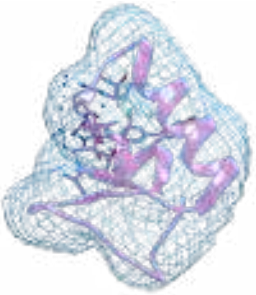 | 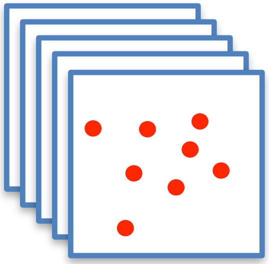)

Find the one 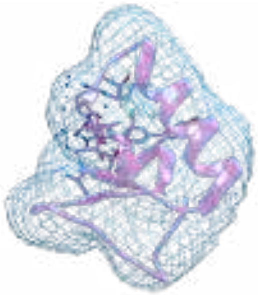 for which P(|) ist largest

Trick #1: Maximize

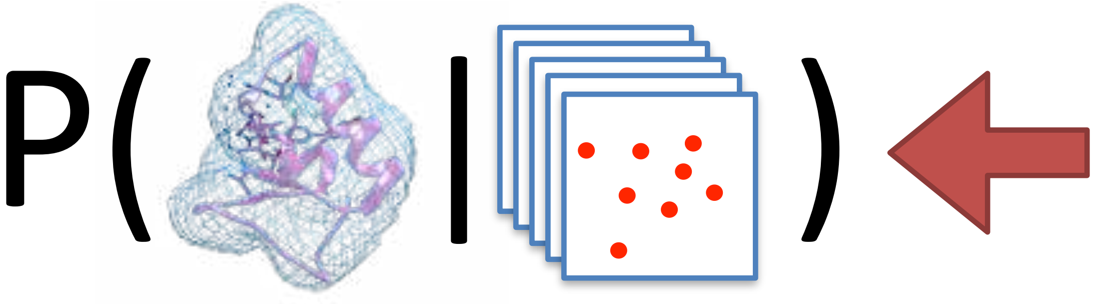

P(|)

we can NOT calculate this

Find the one

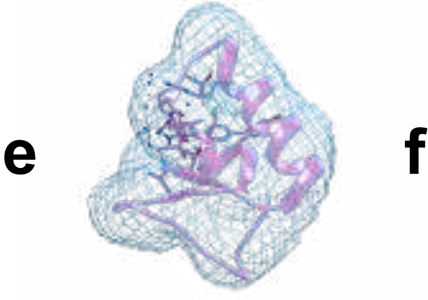

for which P(|) ist largest

Bayes’ formula

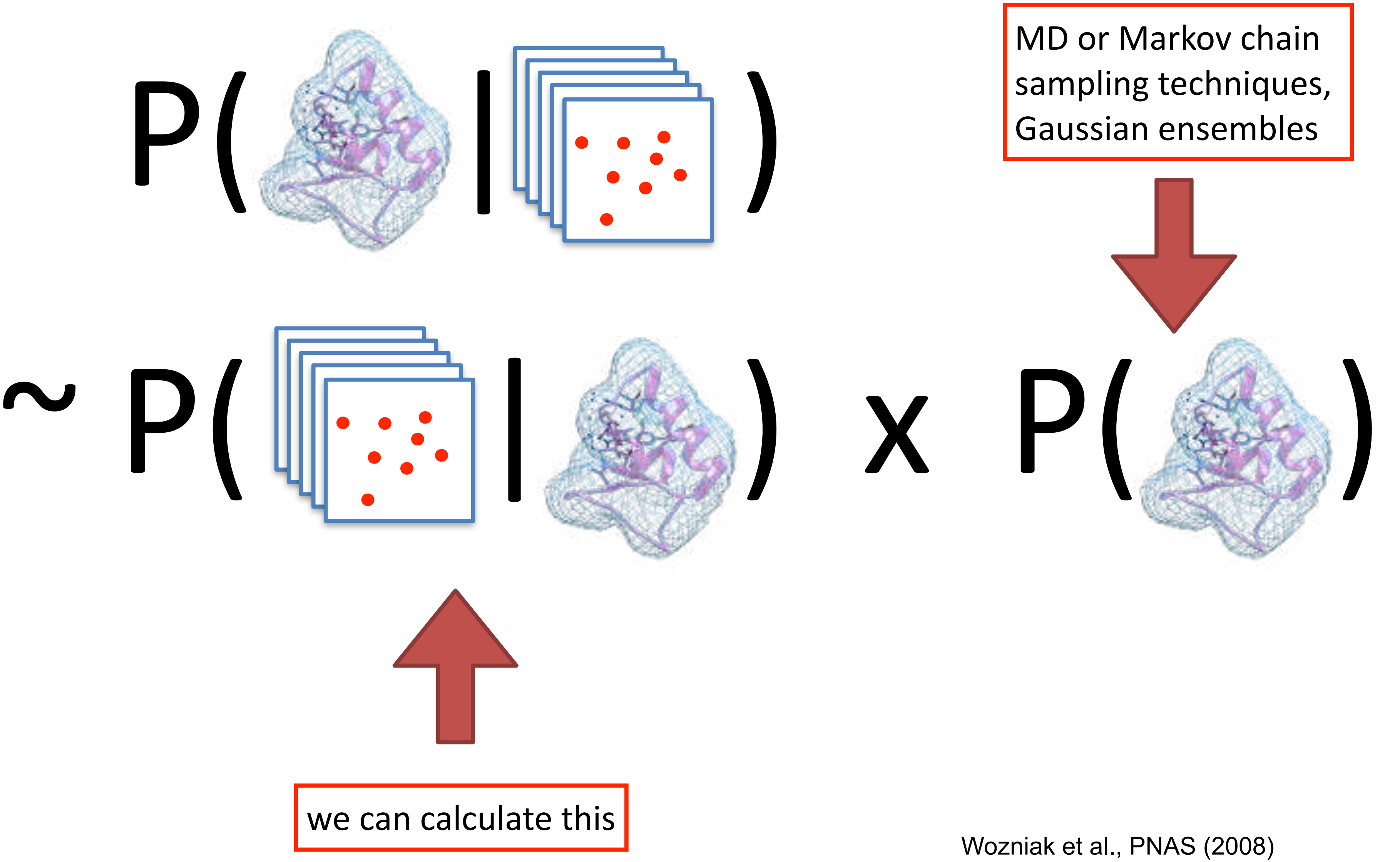

MD or Markov chain sampling techniques, Gaussian ensembles

we can calculate this

Wozniak et al., PNAS (2008)
Schröder et al., Comp. Phys. Comm (2004)
Margittai et al., PNAS (2003)
Schröder et al., J. Chem. Phys. (2003)

Trick #3: New correlation method

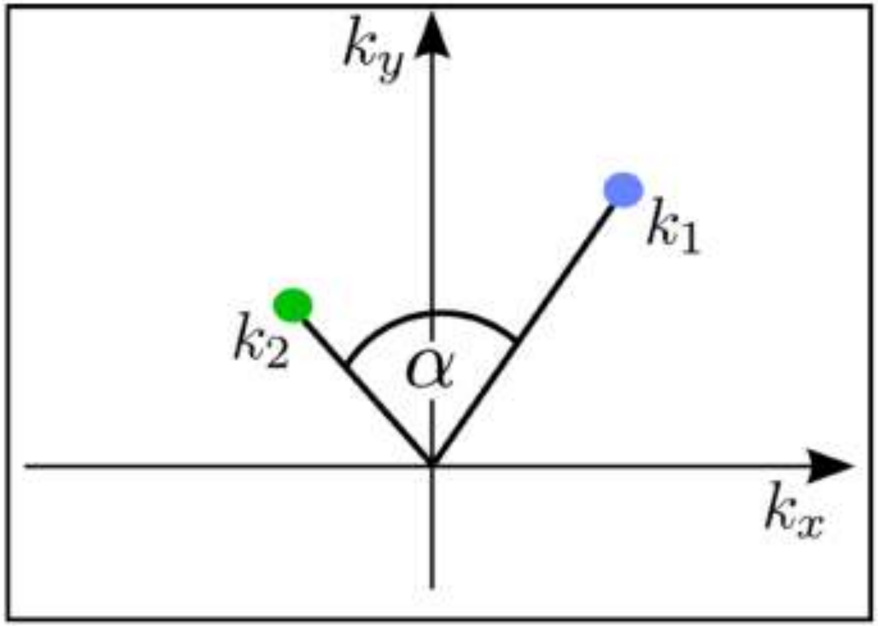

Two Photons

$$c_{k_1,k_2,\alpha} = \sum_l P_l\left(\cos\left(\alpha\right)\right) \cdot \sum_m A_{lm}\left(k_1\right)\left(\omega\right) A^*_{lm}\left(k_2\right)$$

Analytical inversion exists
BUT: underdetermined

3-photon correlations DO encode structure

Two Photons

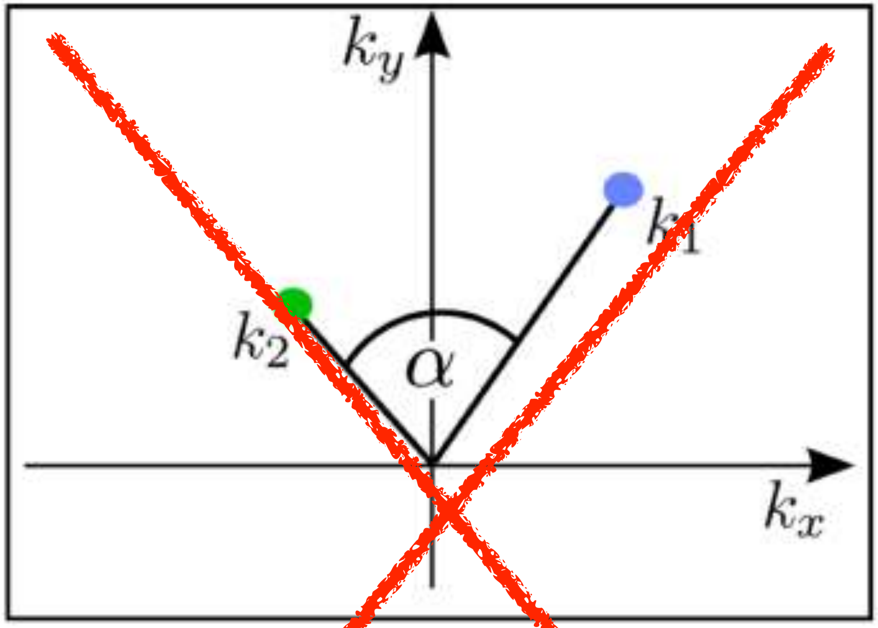

$$c_{k_1,k_2,\alpha} = \sum_l P_l(\cos(\alpha)) \cdot \sum_m A_{lm}(k_1)(\omega) A_{lm}(k_2)$$

Three Photons

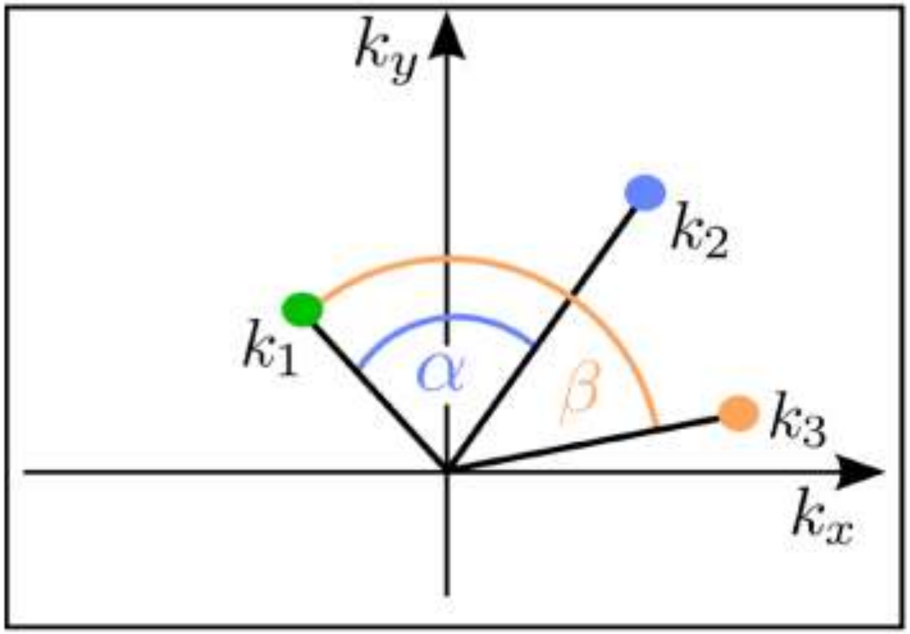

$$t_{k_1,k_2,k_3,\alpha,\beta} = \sum_{l1\,l2\,l3} \sum_{m1\,m2\,m3} A_{l1m1}(k_1) \cdot A_{l2m2}(k_2) A^*_{l3m3}(k_3) \cdot f(l_1, l_2, l_3, m_1, m_2, m_3, \alpha, \beta)$$

New: 3-photon correlation method

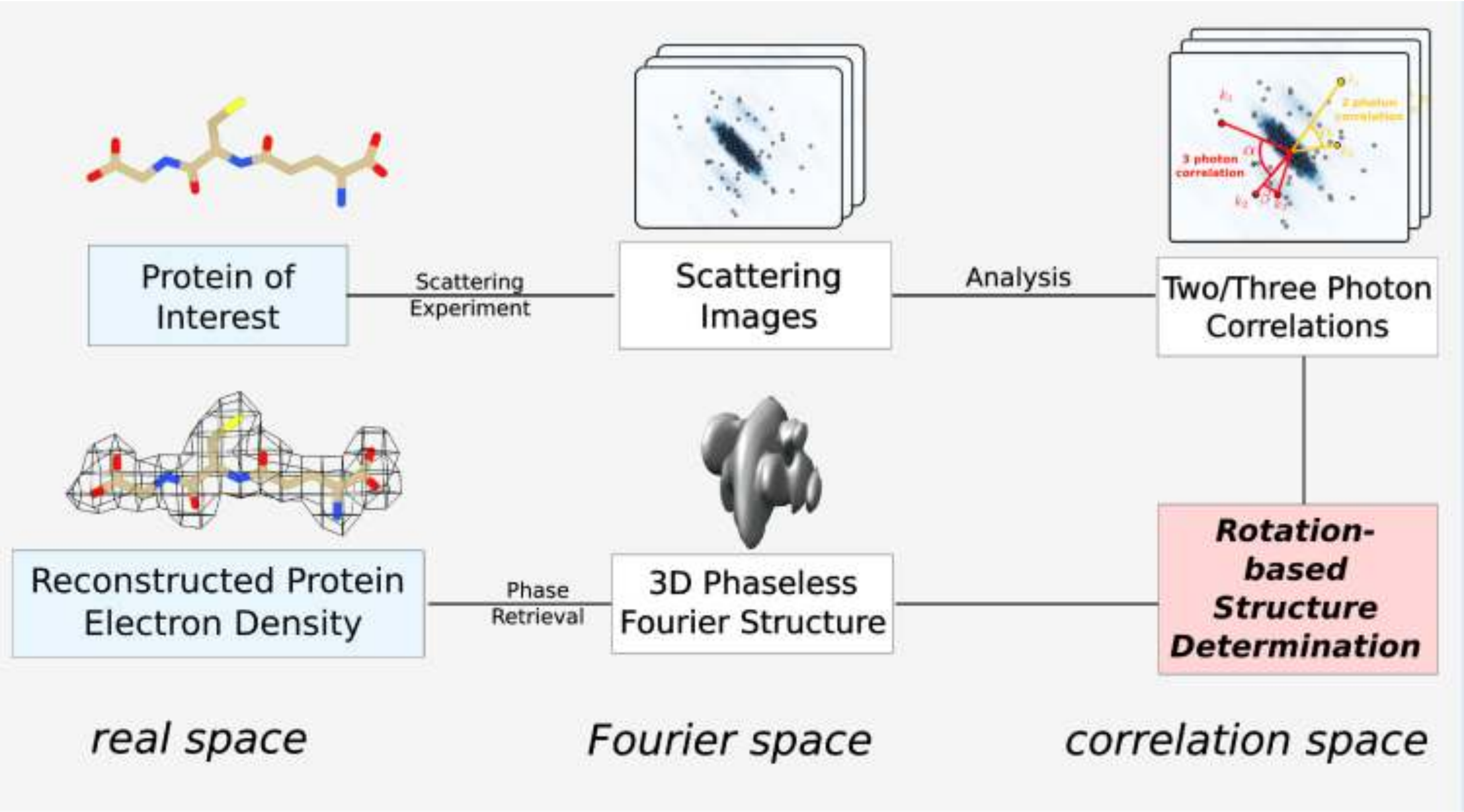

Protein of Interest

Scattering Experiment

Scattering Images

Analysis

Two/Three Photon Correlations

Reconstructed Protein Electron Density

Phase Retrieval

3D Phaseless Fourier Structure

Rotation-based Structure Determination

real space

Fourier space

correlation space

B. von Ardenne & HG, Nature Comm. 9:2375 (2018)

Fourier density derived from 3-photon correlations

$$I\left(\mathbf{k}\left(k,\varphi,\theta\right)\right)=\sum_{l=0}^{L}\sum_{m=-l}^{l}A_{lm}(k)Y_{lm}(\varphi,\theta)$$

Maximum achievable:
2.9 Å

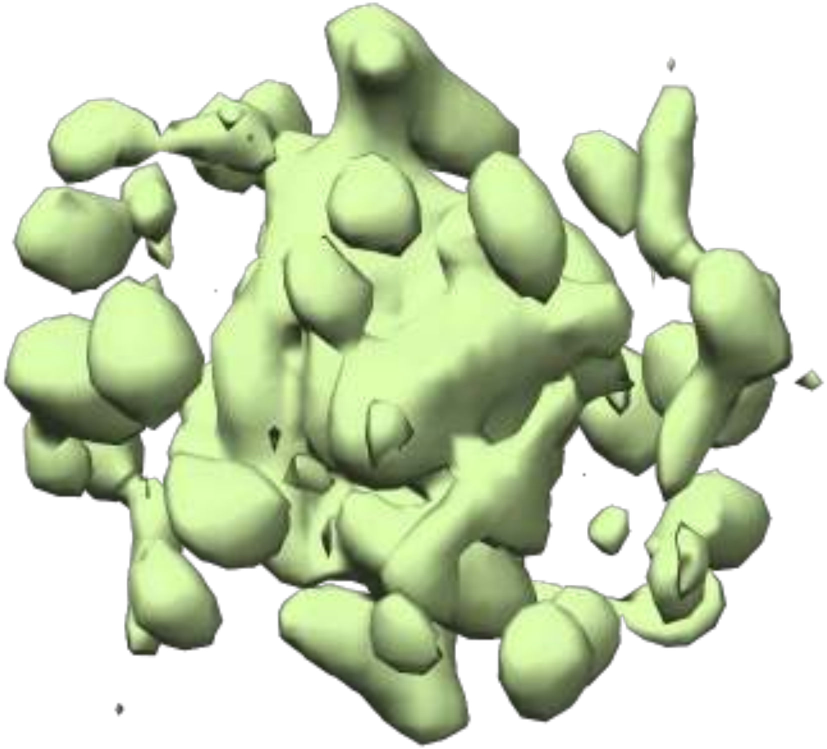

Retrieved Intensity
K=26, L=18

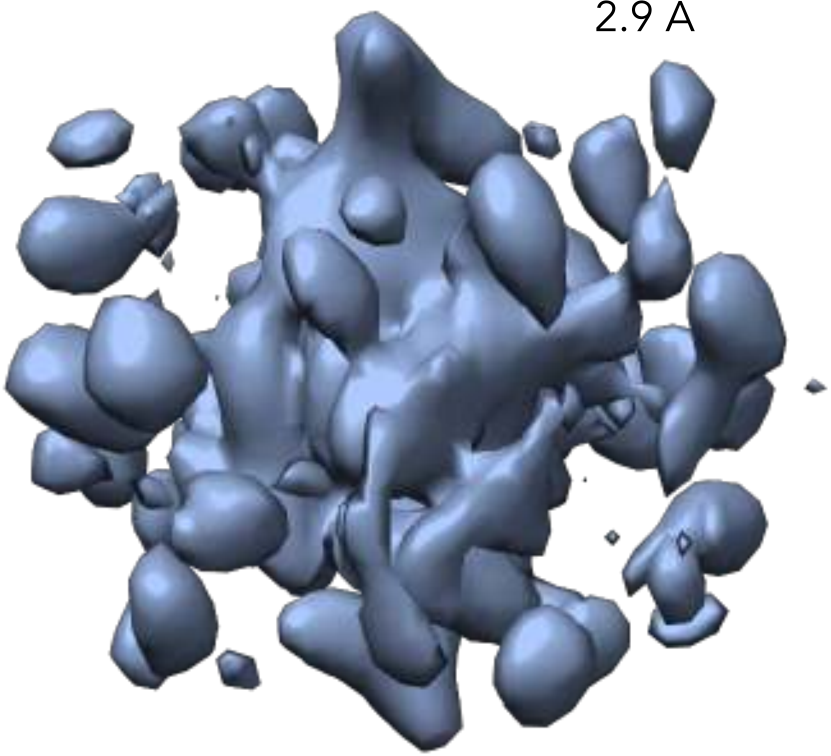

Original Intensity
K=26, L=18

Fourier density derived from 3-photon correlations

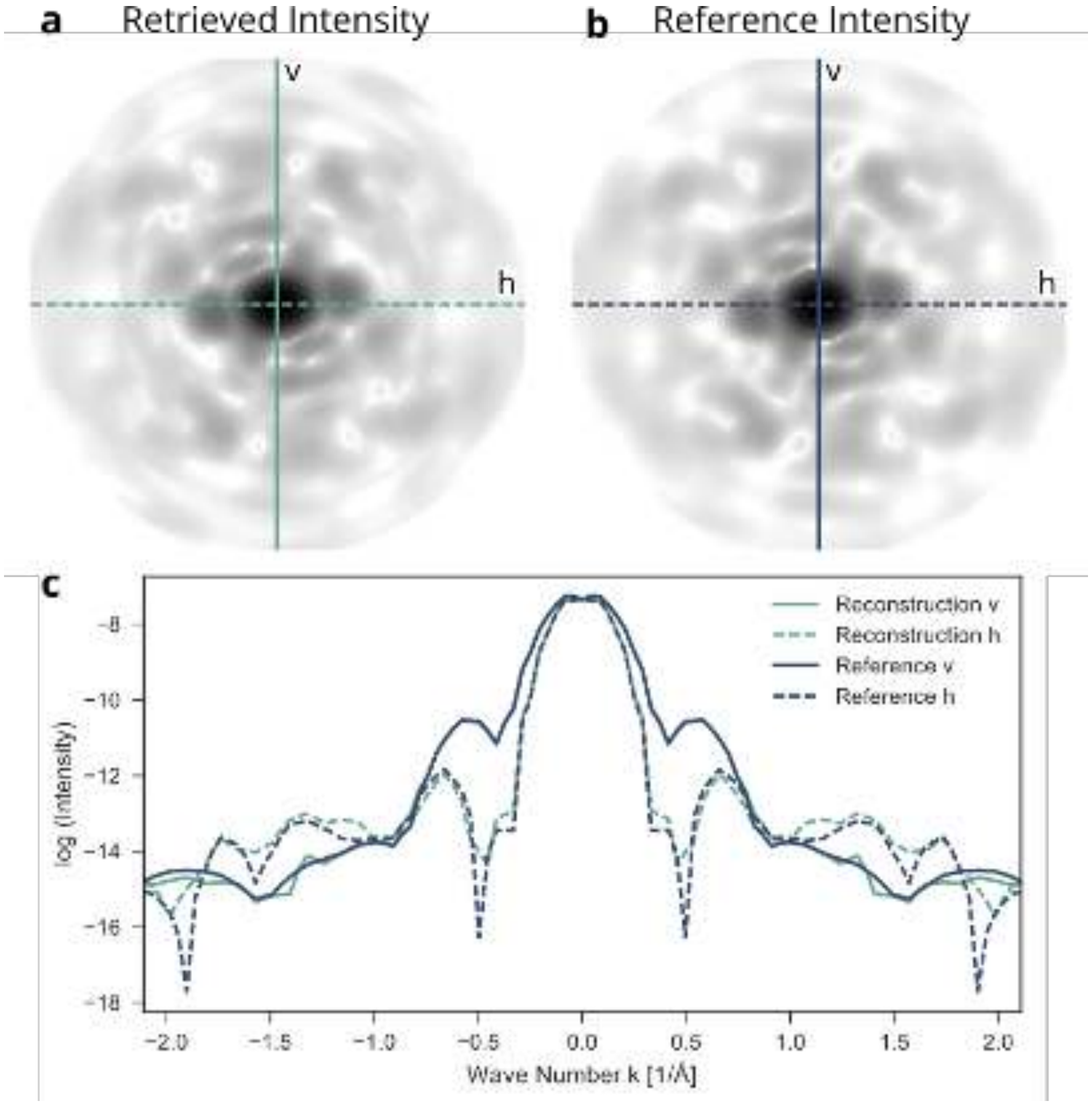

ca 10^8 photon-triples

B. von Ardenne & HG, Nature Comm. 9:2375 (2018)

New: 3-photon correlation method

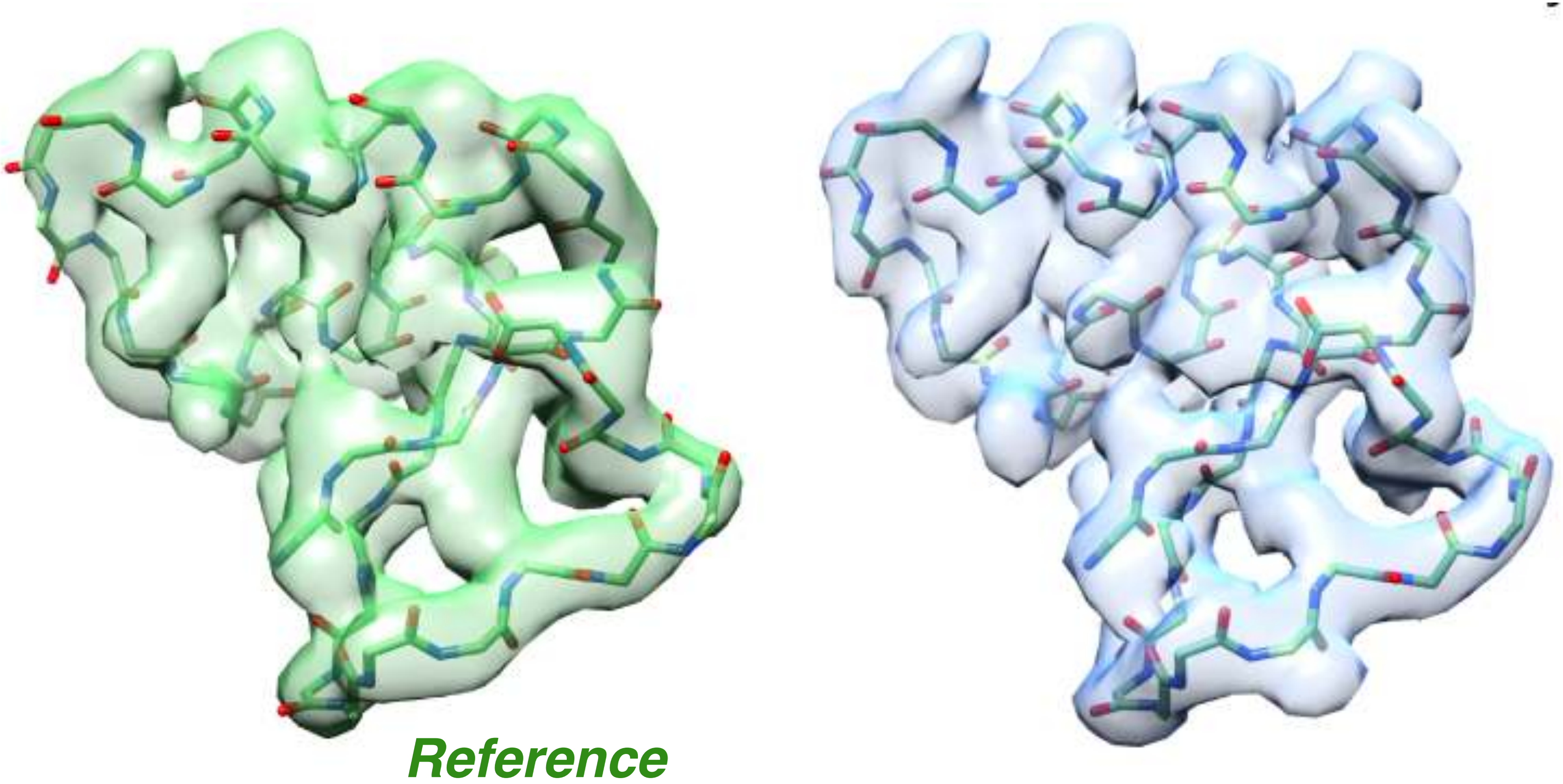

ca 4 x 10^7 pictures, 10 photons per picture

B. von Ardenne & HG, Nature Comm. 9:2375 (2018)

What resolution can be achieved?

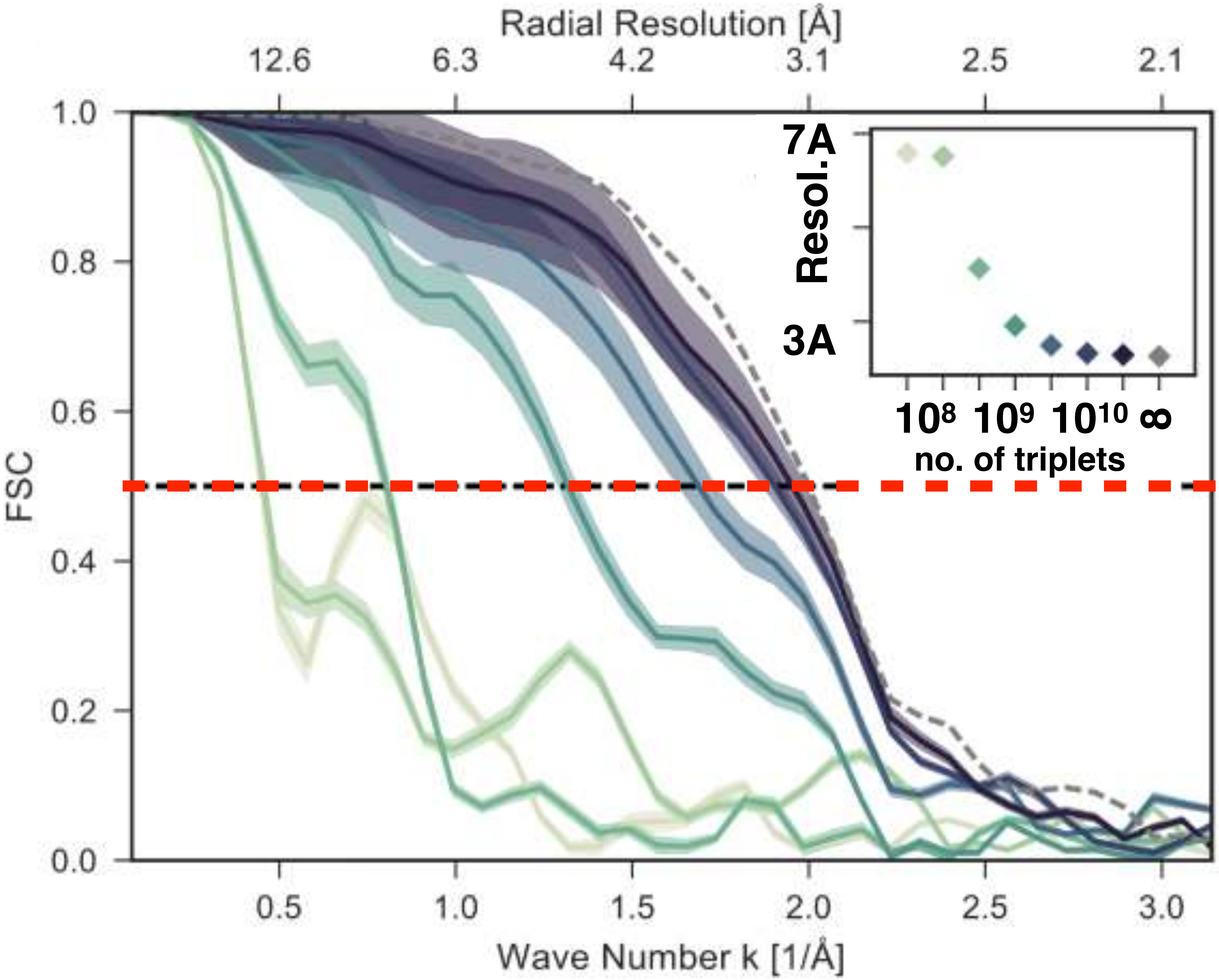

B. von Ardenne & HG, Nature Comm. 9:2375 (2018)

3 photons per picture suffice! *(for REALLY many pictures)*

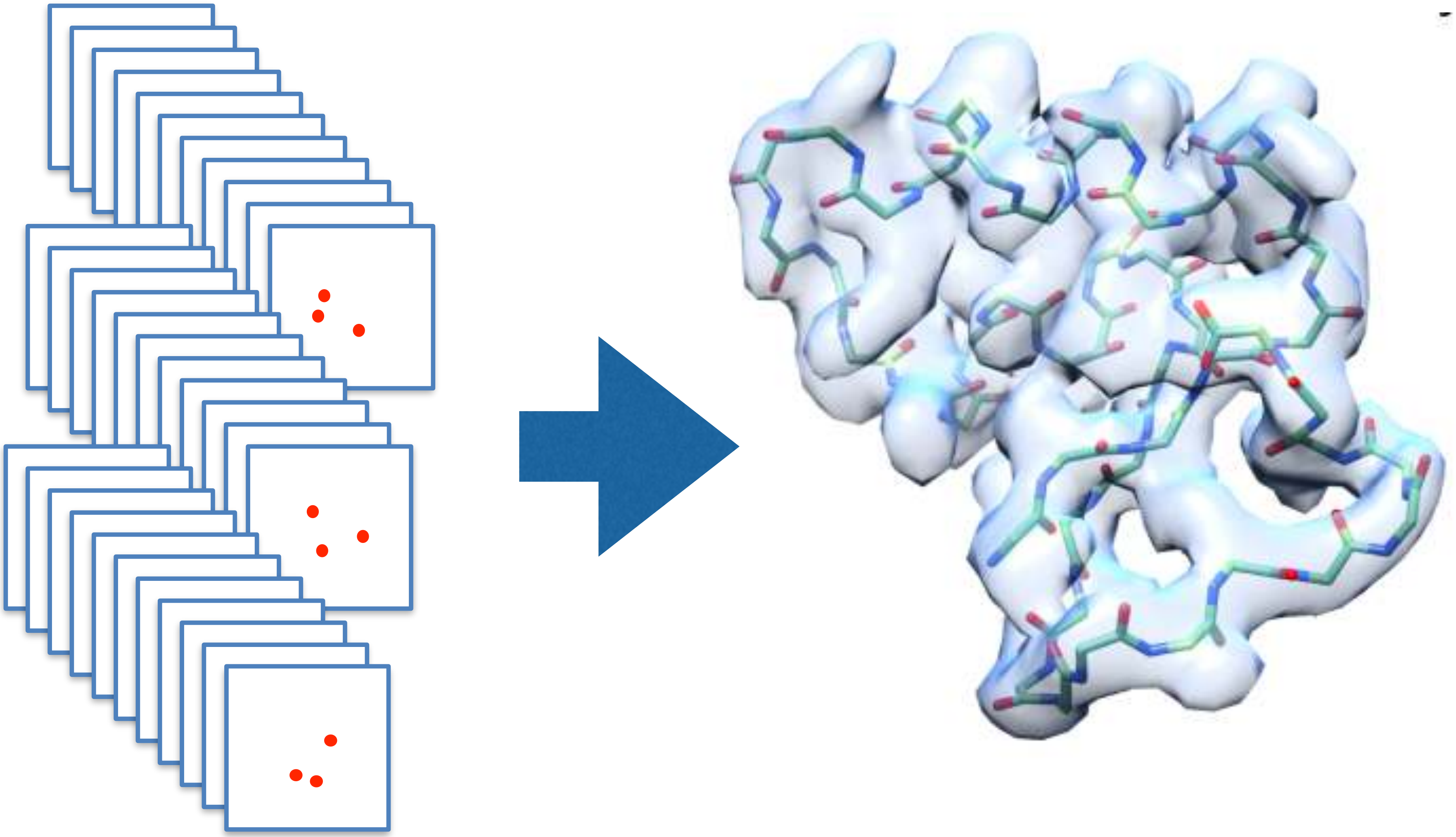

(simulated experiment)

B. von Ardenne & HG, Nature Comm. 9:2375 (2018)

Computational electrophysiology

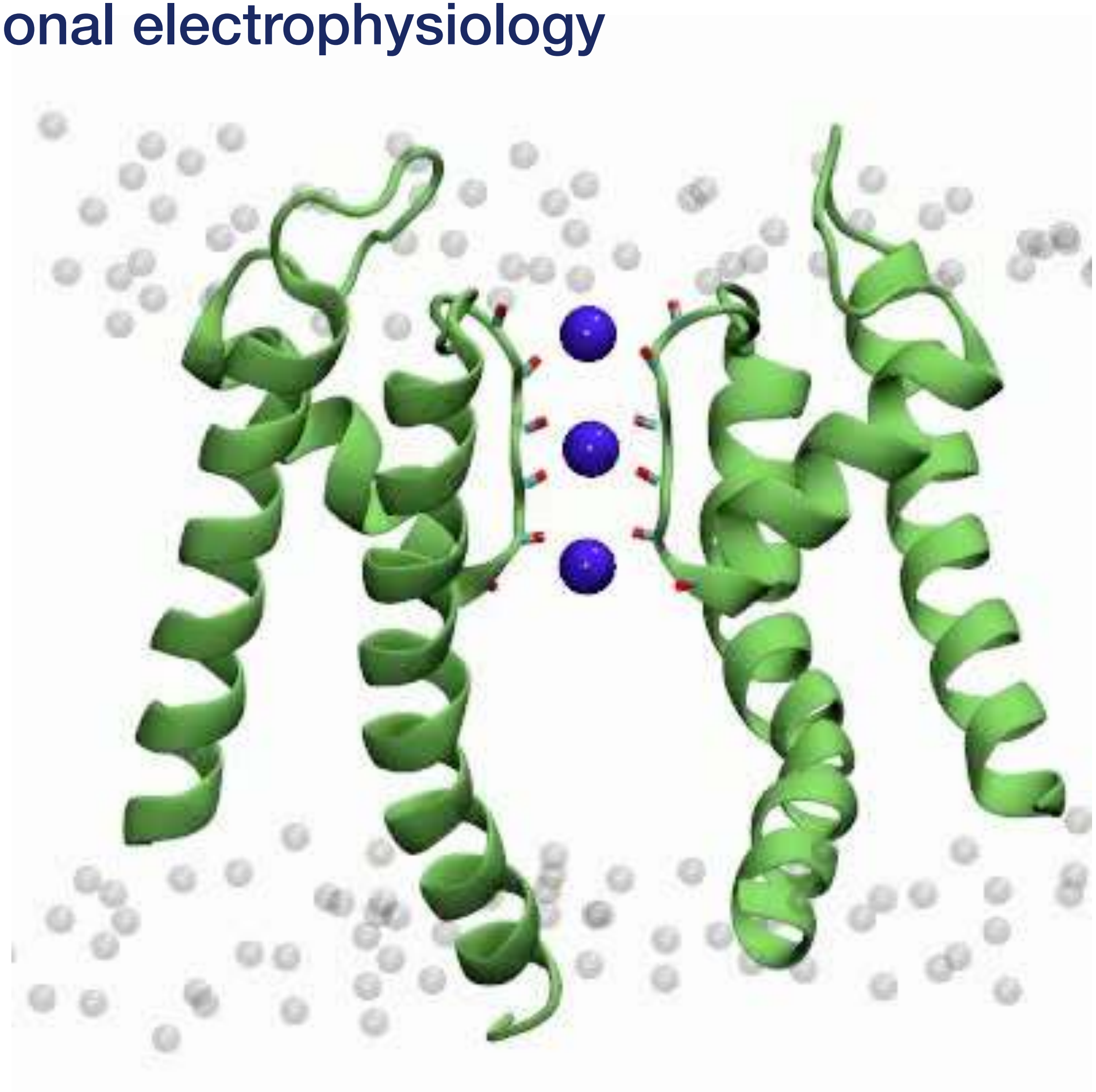

Potassium channel

Provided by: Bert L. de Groot

Computational electrophysiology

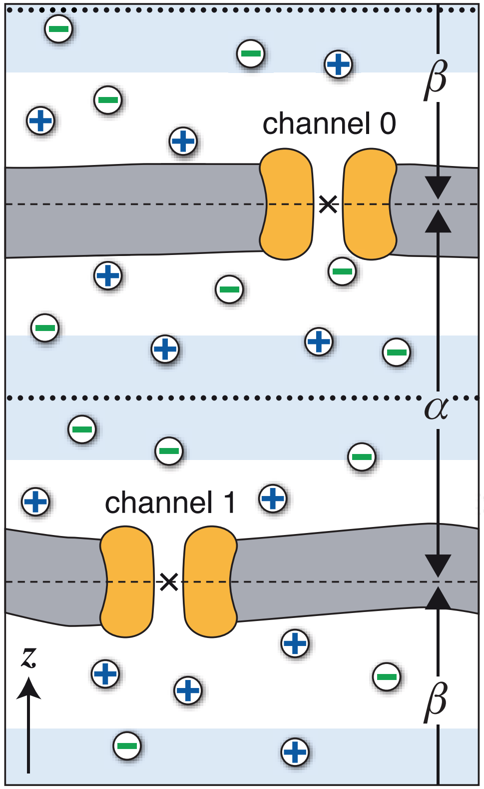

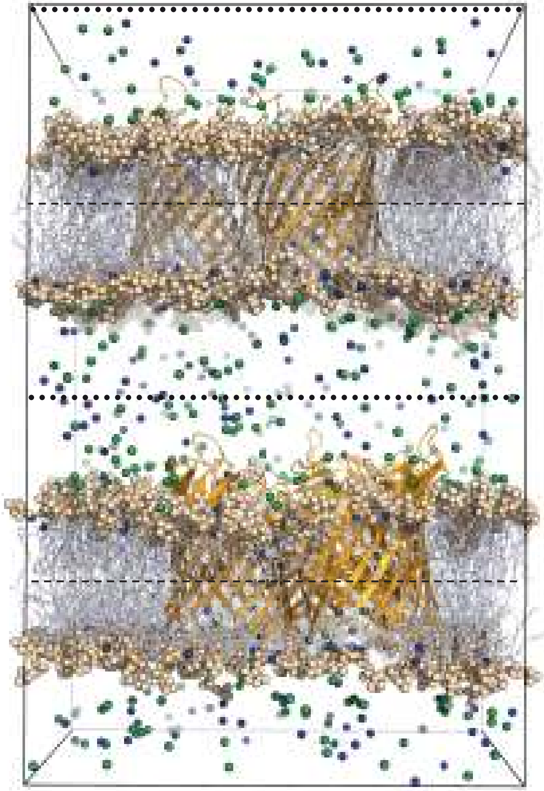

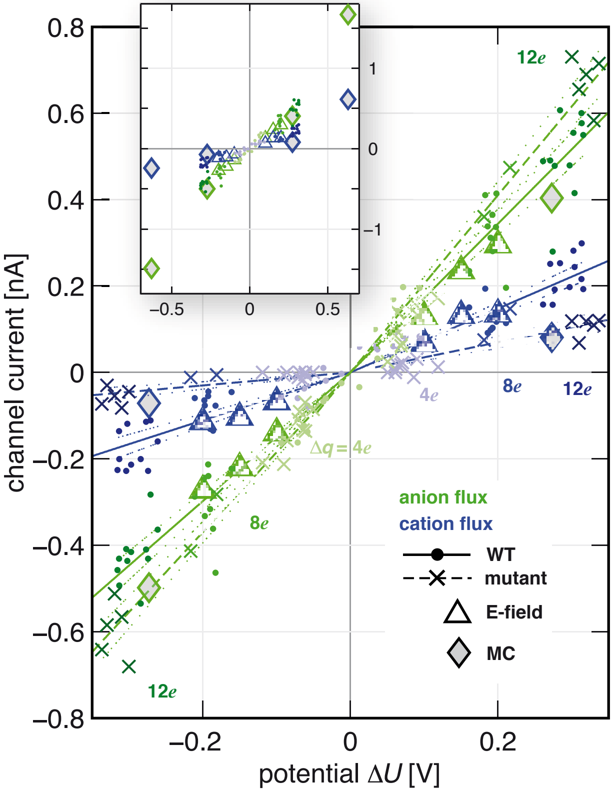

C Kutzner, H Grubmüller, BL de Groot, U Zachariae. Biophys. J. (2011)

Ulrich Zachariae

Carsten Kutzner

Bert de Groot

Synaptic fusion

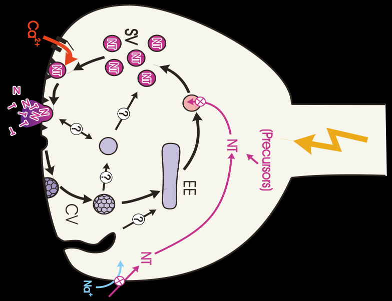

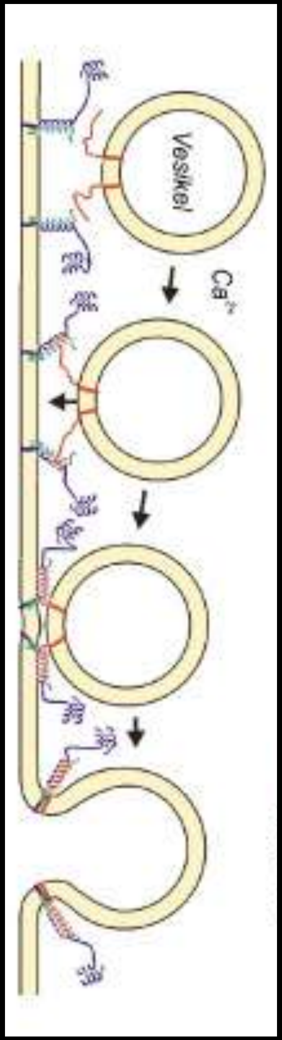

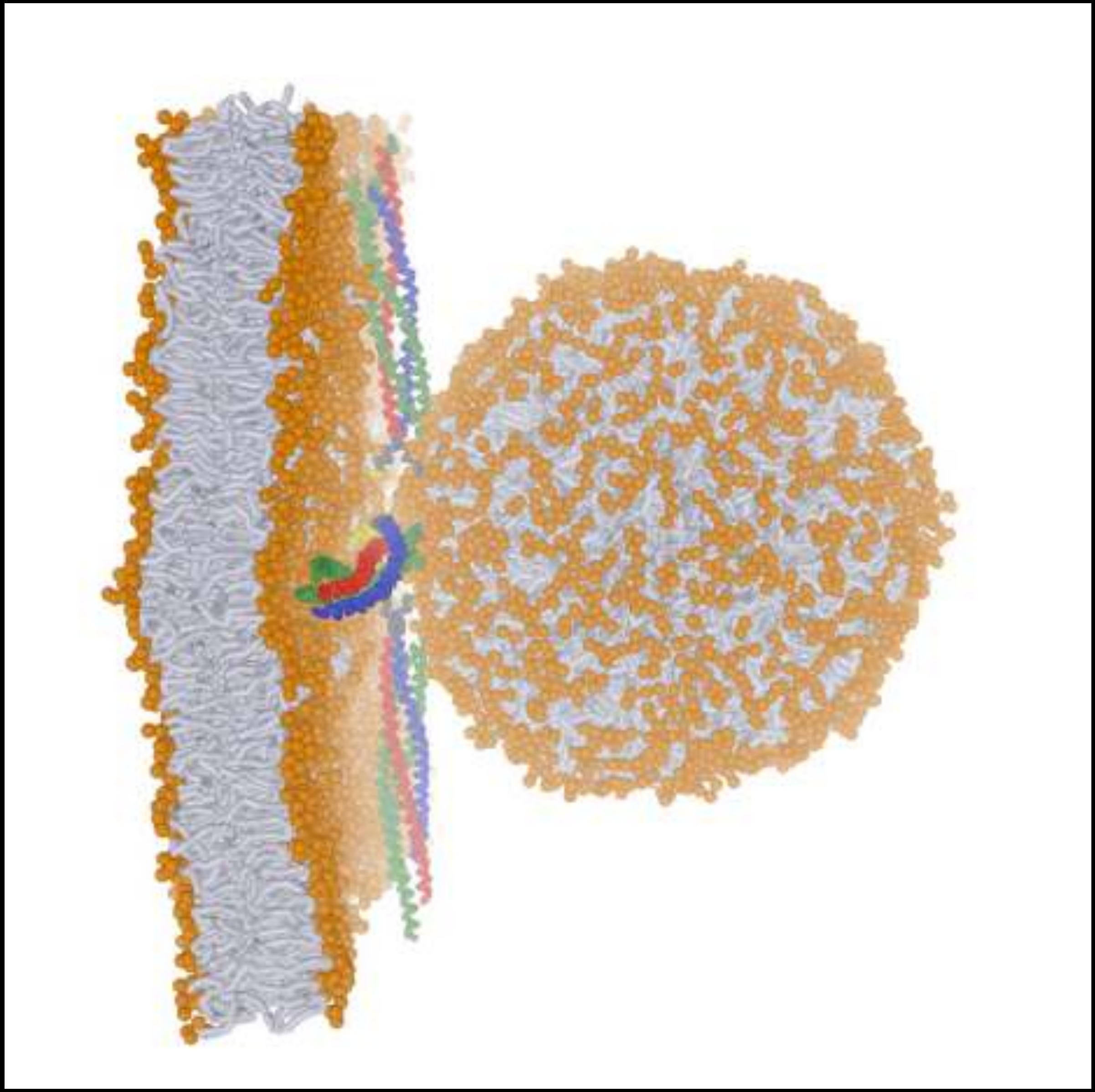

First principles docking: MloK1

Collab. Benjamin Kaupp

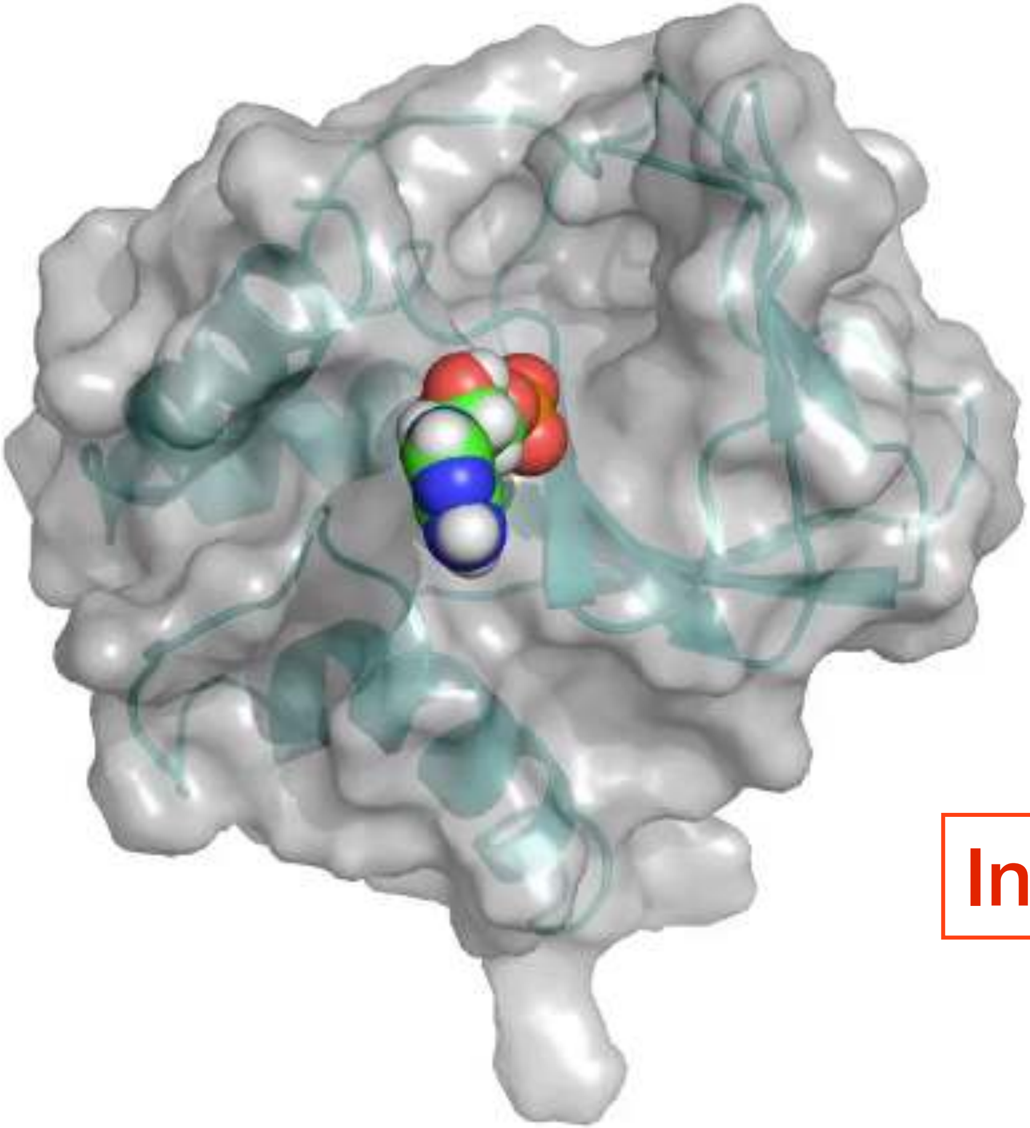

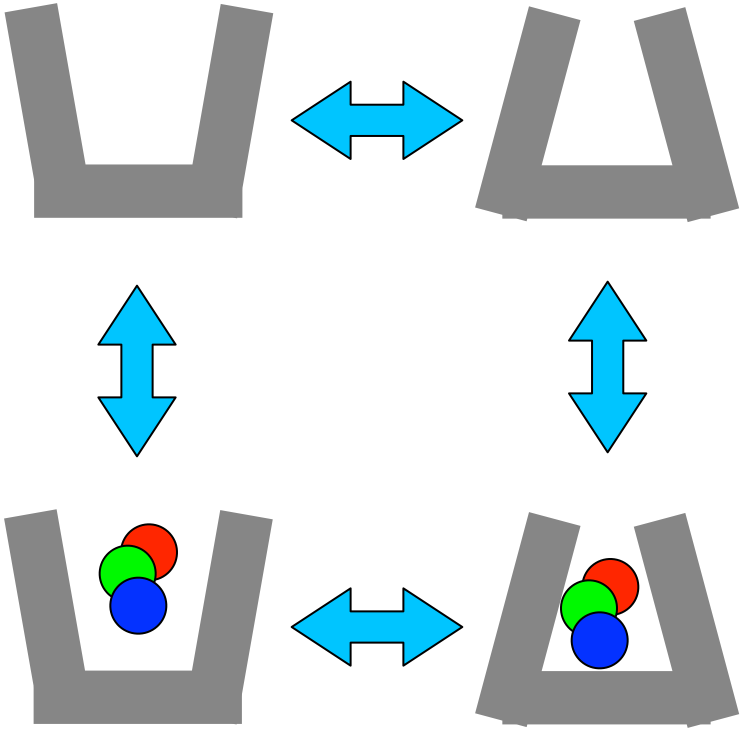

Induced Fit

Bela Voss

MloK1 – a cyclic nucleotide modulated ion channel

Southern Bean Mosaic Virus – Mechanical Properties

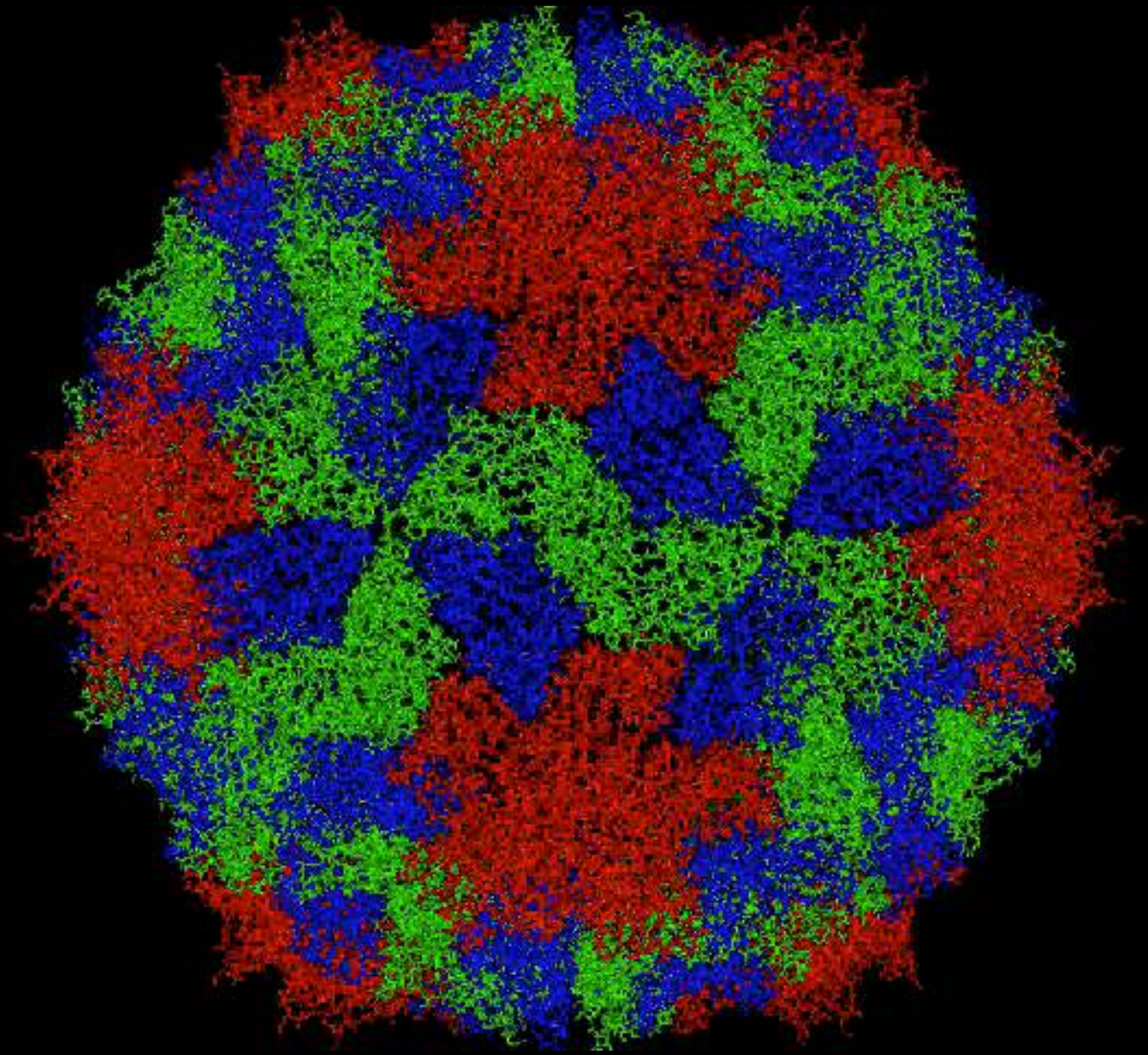

~4,500,000 particles

Anatomy of a Synaptic Vesicle

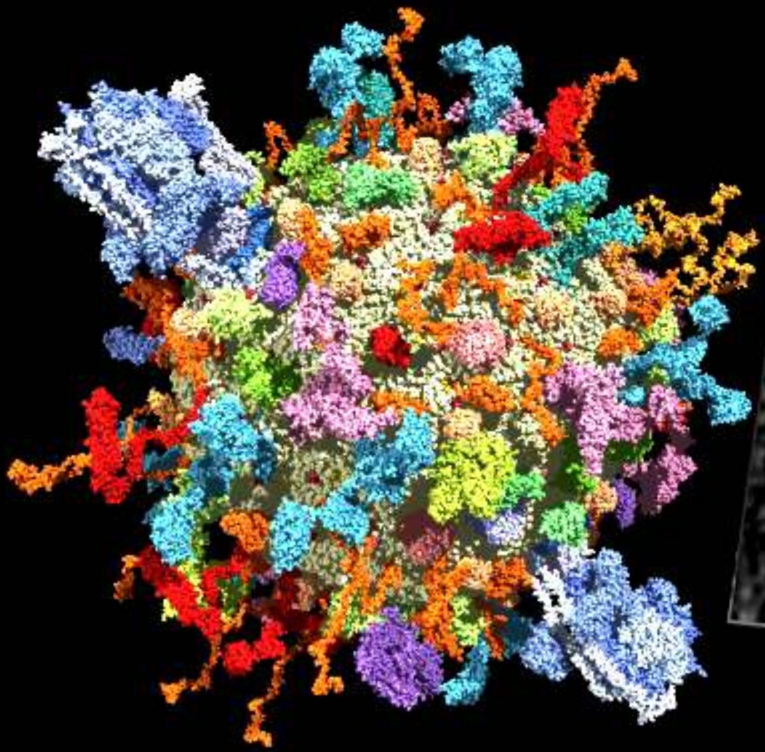

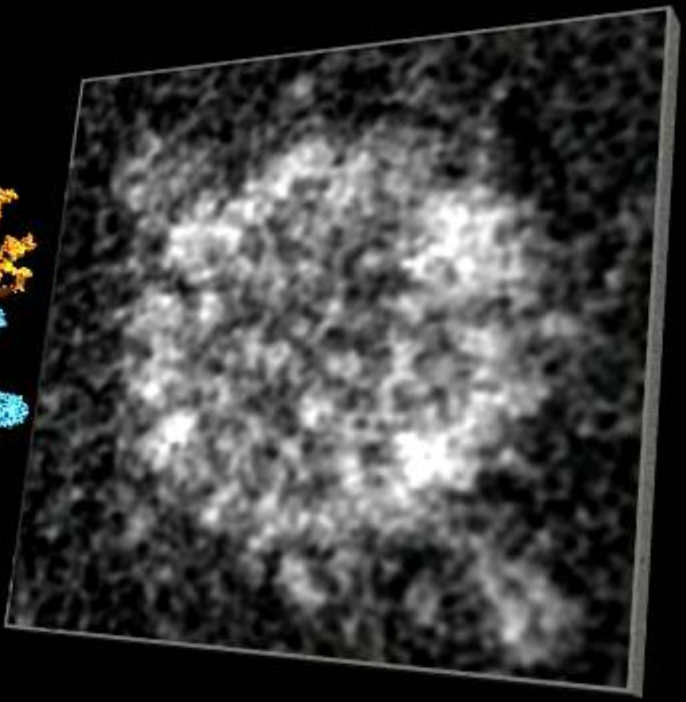

Simulated EM image

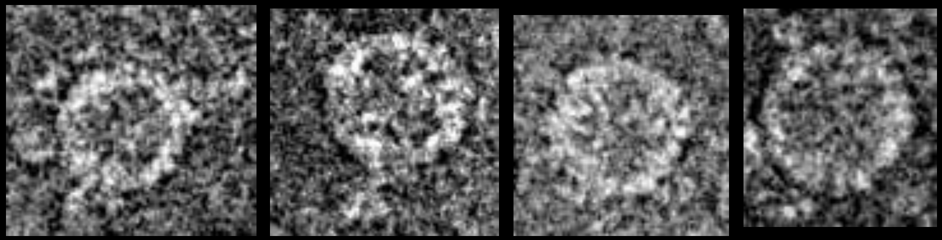

EM images by D. Riedel and R. Jahn

J. Haas, B. de Groot, H. Grubmüller, et al.
R. Jahn (Cell, 2007)

What have we learned ?

(1) AFM + force probe MD -> Overlap, 11 orders total

- *Solved puzzle of too low AFM forces*
- *Unbinding free energy landscape, 3rd barrier*
- *Loading rate dependent unbinding paths*

***(2) Combined mechanism for** erythromycin stalling:*

- *Perturbation of peptide conformation*
- *Perturbation of A-site crevice*

(3) Intrinsically disordered proteins:

- *CHARMM36m*
- *First principles alpha-Synuclein ensemble*

(4) The Dynasome:

Structure -> Dynamics -> Function

Towards a *fundamental understanding of life* processes from *first principles*

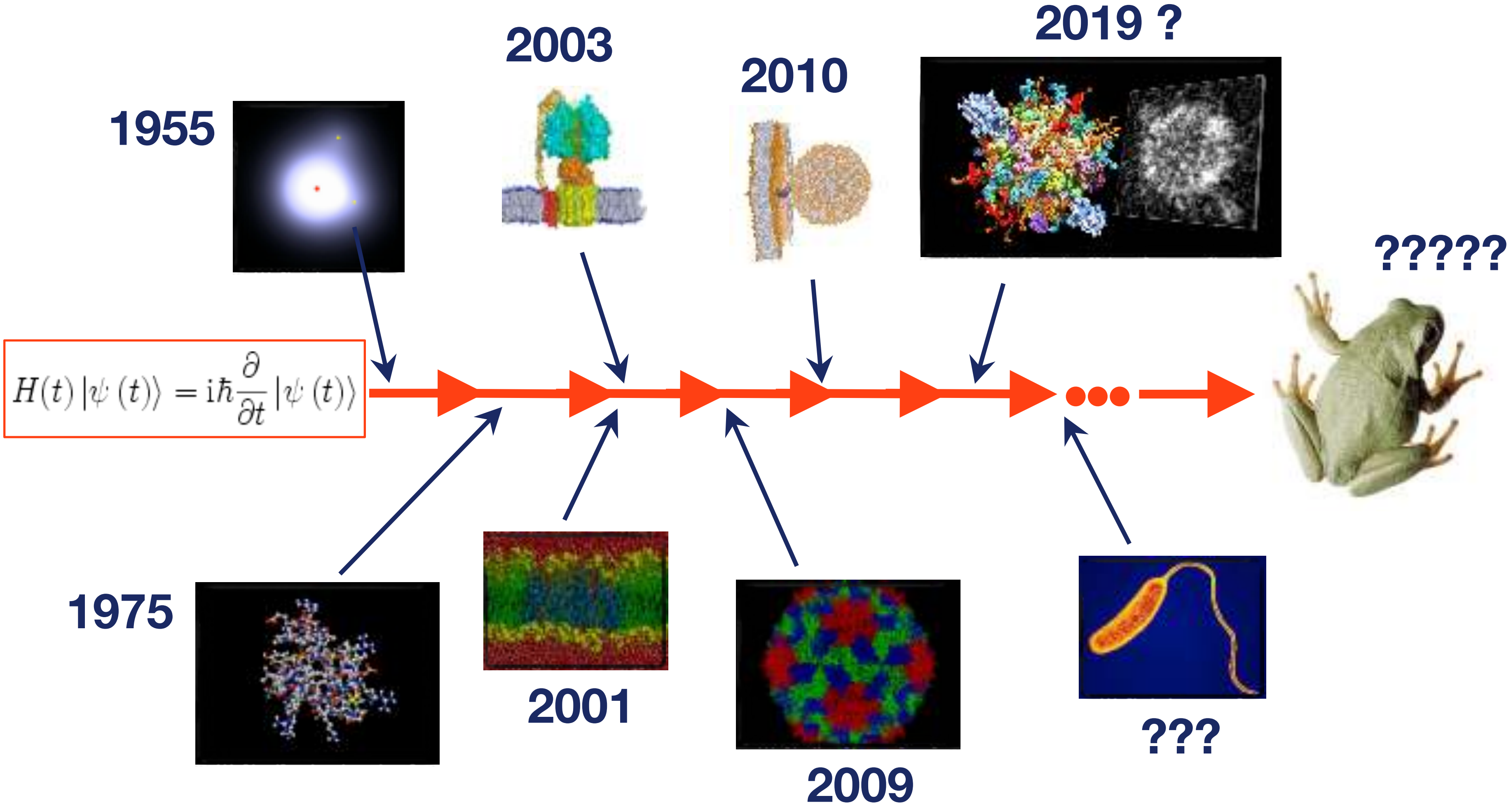

$$H(t)\,|\psi(t)\rangle = i\hbar\frac{\partial}{\partial t}|\psi(t)\rangle$$

1955

1975

2003

2001

2010

2009

2019 ?

???

?????

Positions available

ABCE1: A simpler prototypic ATPase motor domain

(collaboration: Robert Tampe, Univ. Frankfurt)

AKA: RLI, PIXIE (archaea/eukaryotes)

Translation termination:

Separation of ribosomal subunits

(Pisareva et al. EMBOJ, 2011)

Stall recovery

(Preis et al. CelRep, 2014)

Maybe translation initiation

(Heuer et al. NSMB 2017)

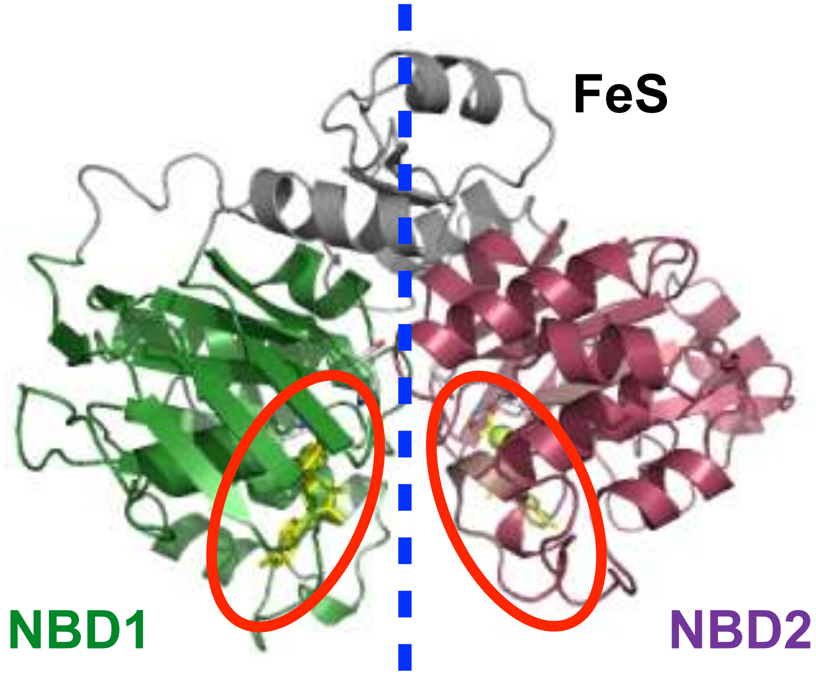

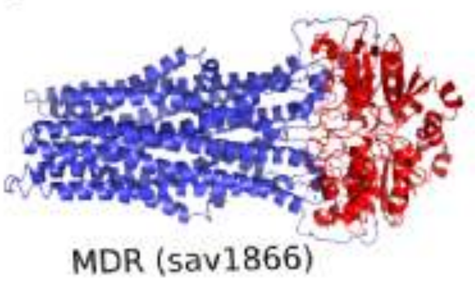
MDR (sav1866)

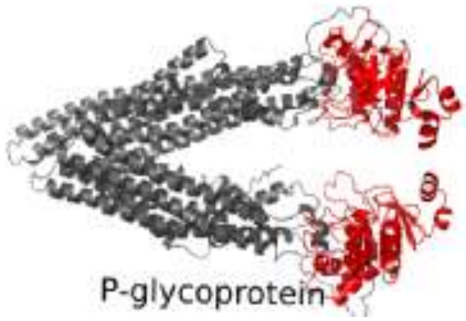
P-glycoprotein

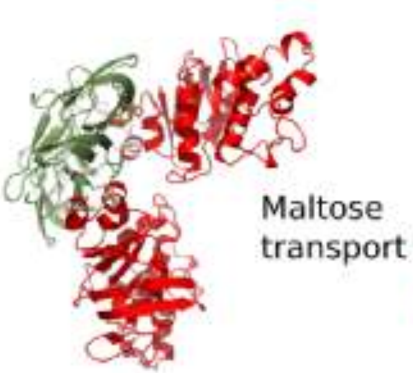
Maltose transport


Fe import

ABCE1: Two nucleotide binding sites, open/closed

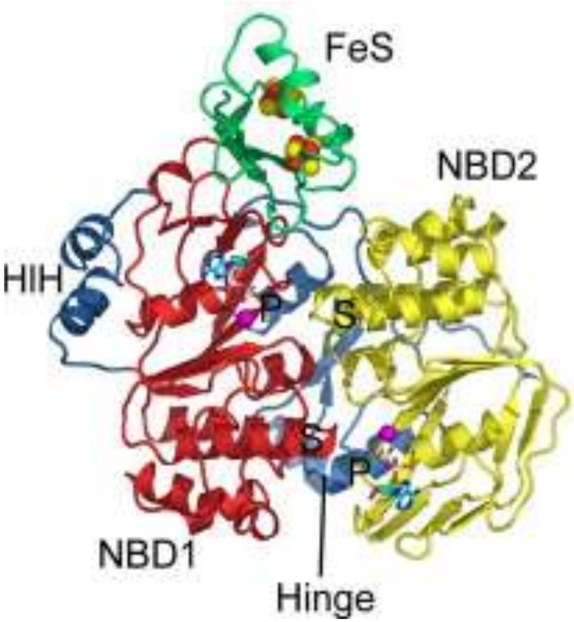

Annette Karcher et al. JBC 2008

OPEN

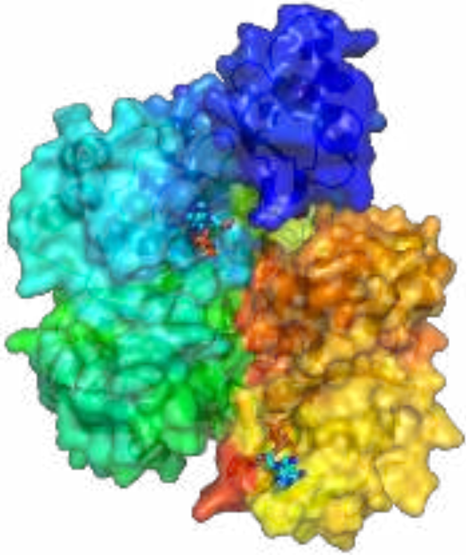

Karcher et al., J Biol Chem, 2008

CLOSED

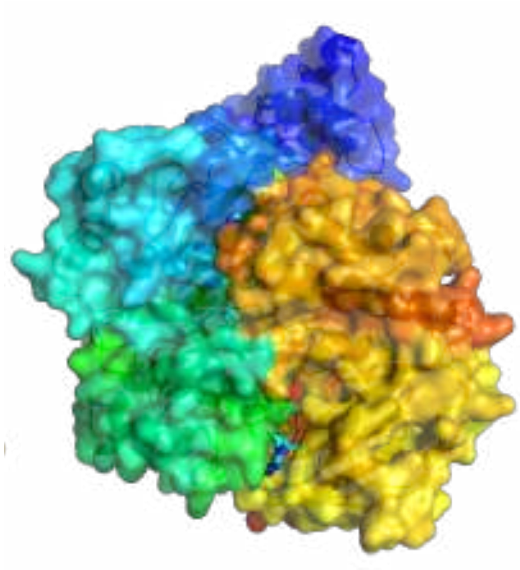

Heuer et al., Nat Struct Mol Biol, 2017

ABCE1: Both nucleotide binding sites hydrolise ATP

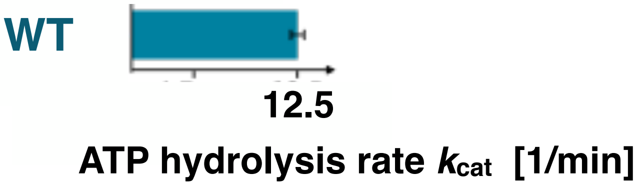

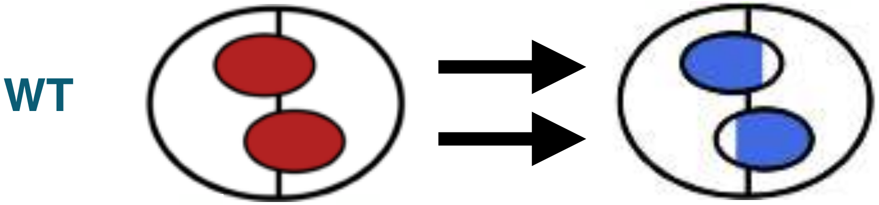

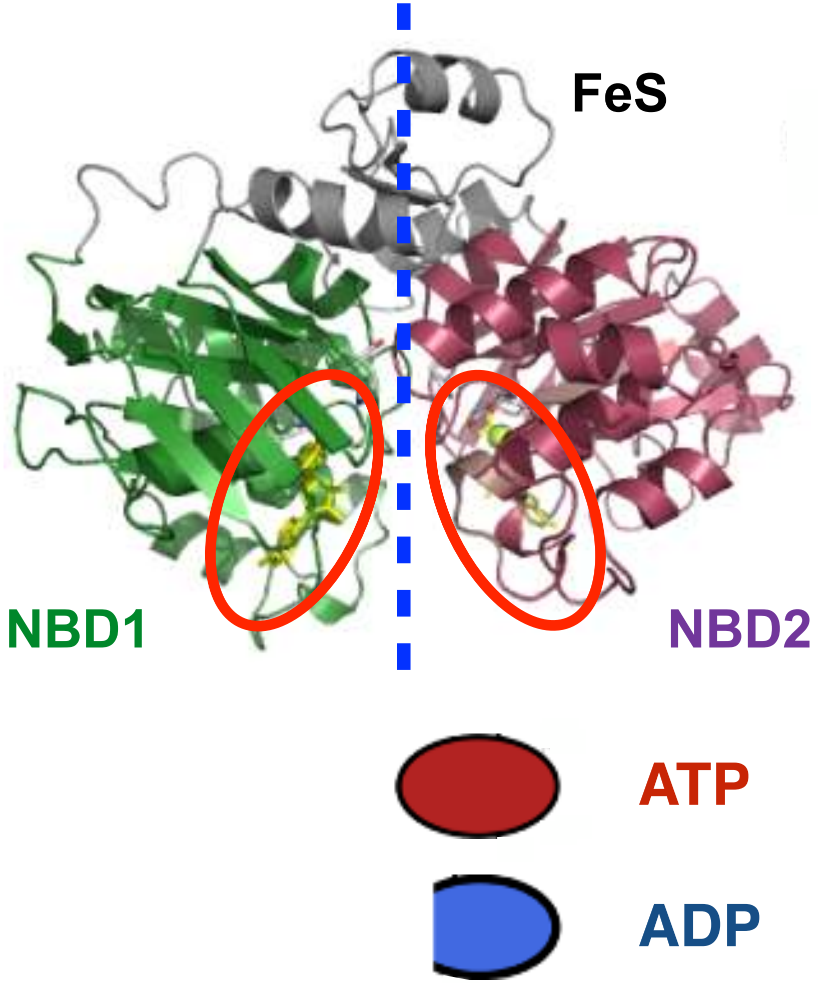

Barthelme et al., PNAS (2011)

Block binding site 1: half hydrolysis rate

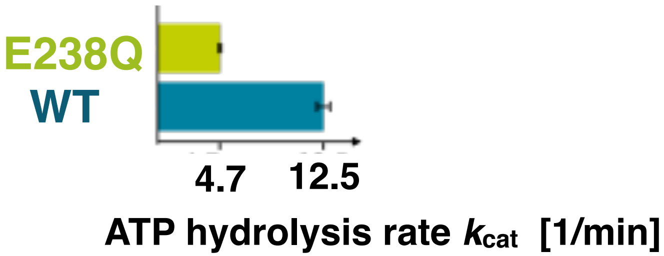

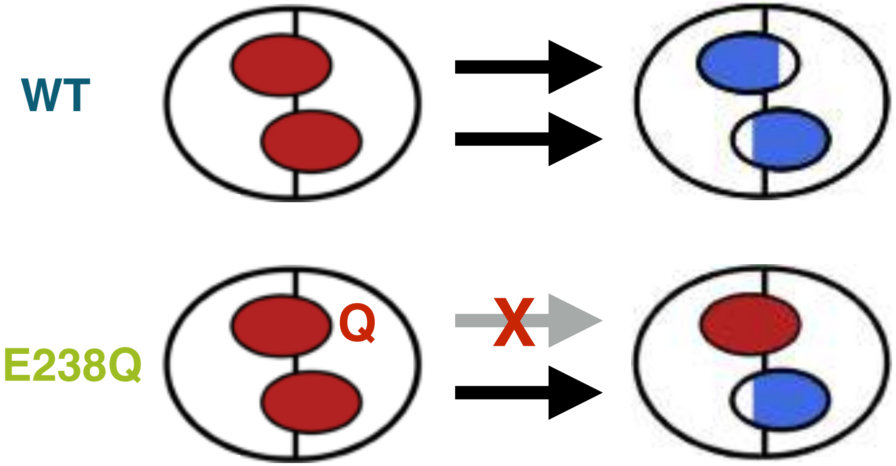

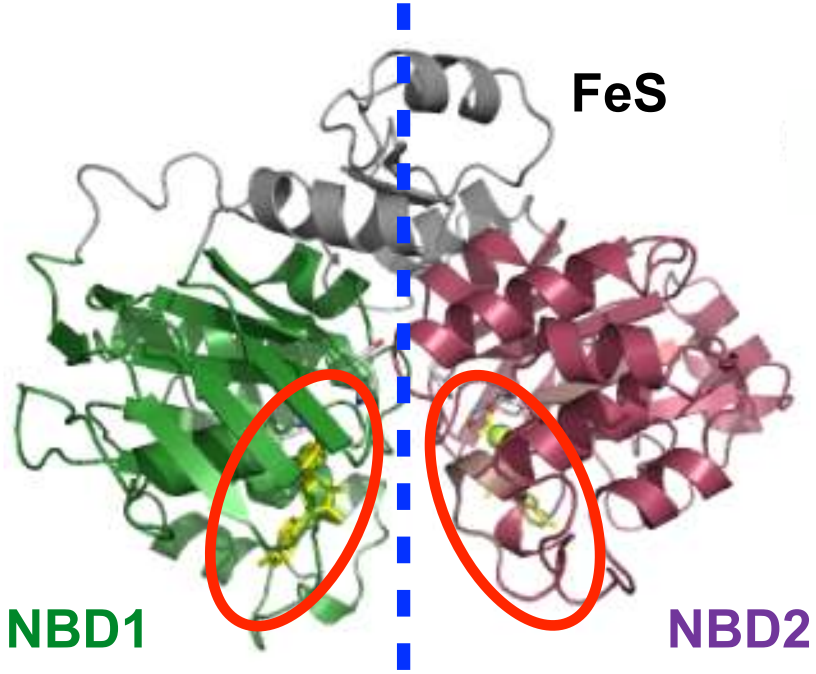

● ATP

● ADP

Barthelme et al., PNAS (2011)

Block binding site 2: 10-fold hydrolysis rate!

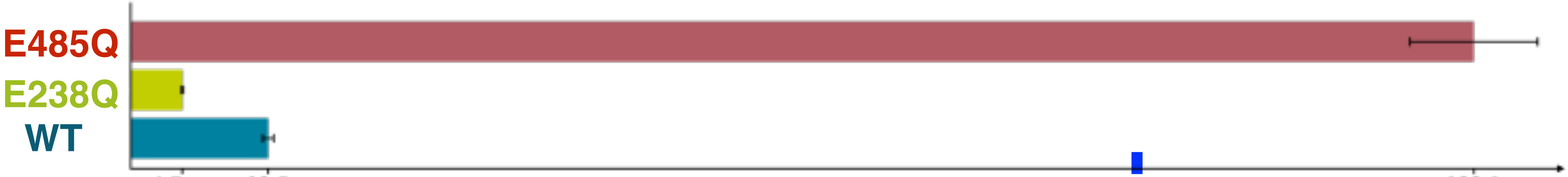

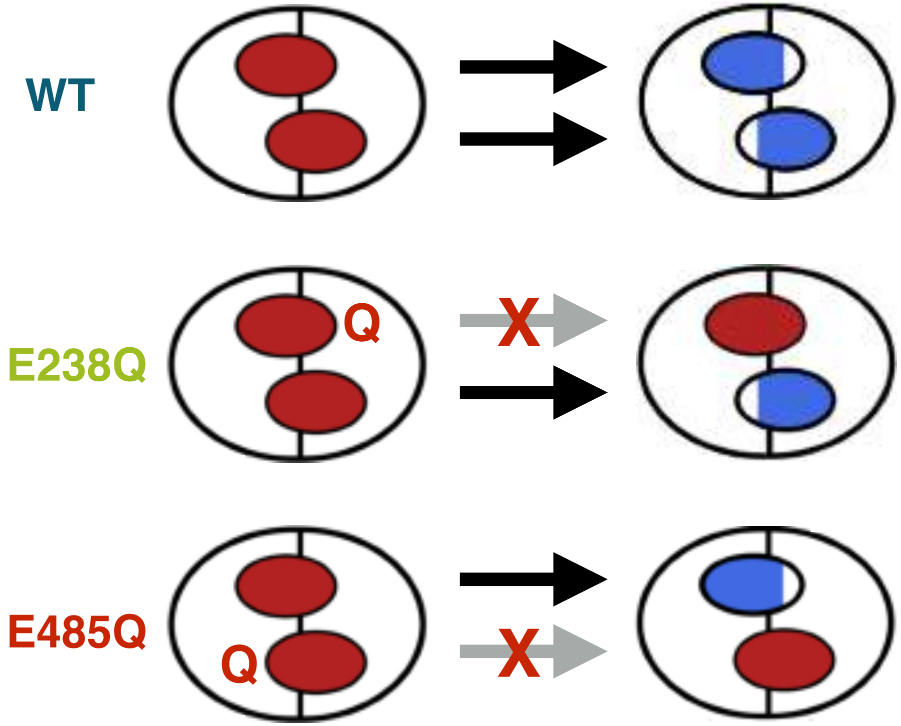

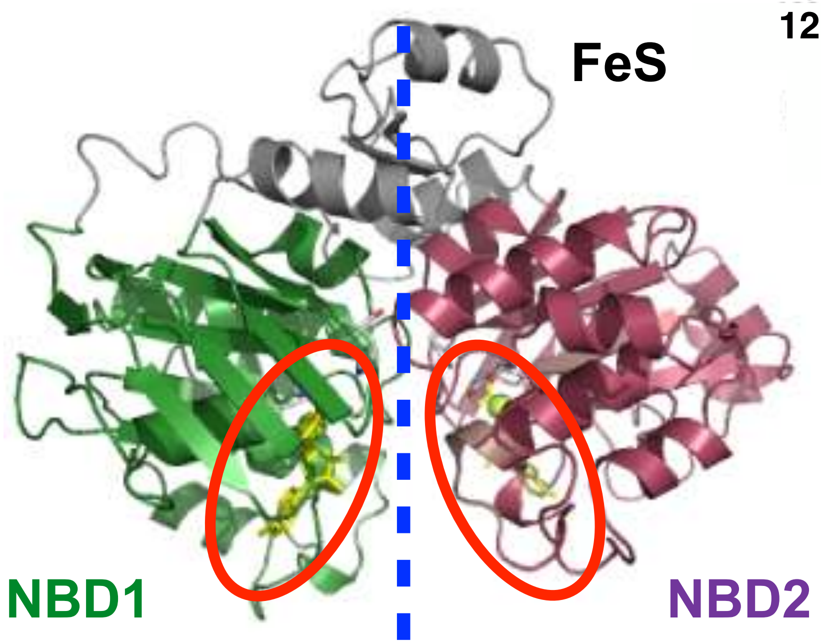

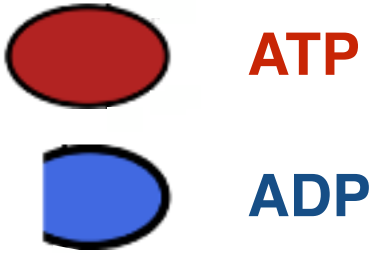

Barthelme et al., PNAS (2011)

Measured k_{cat} and K_M (WT & 2 mutants)

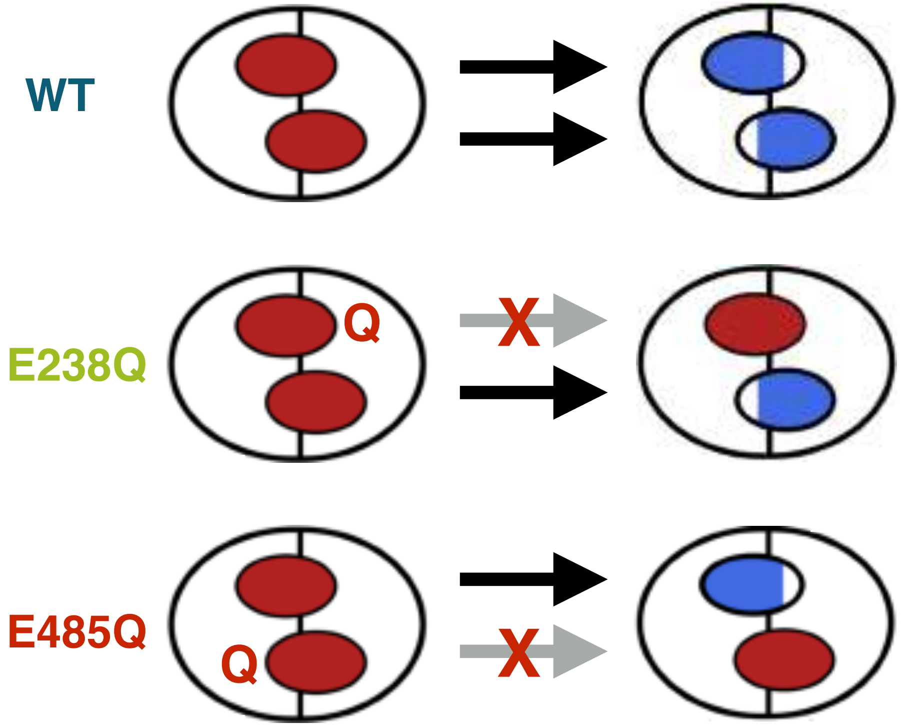

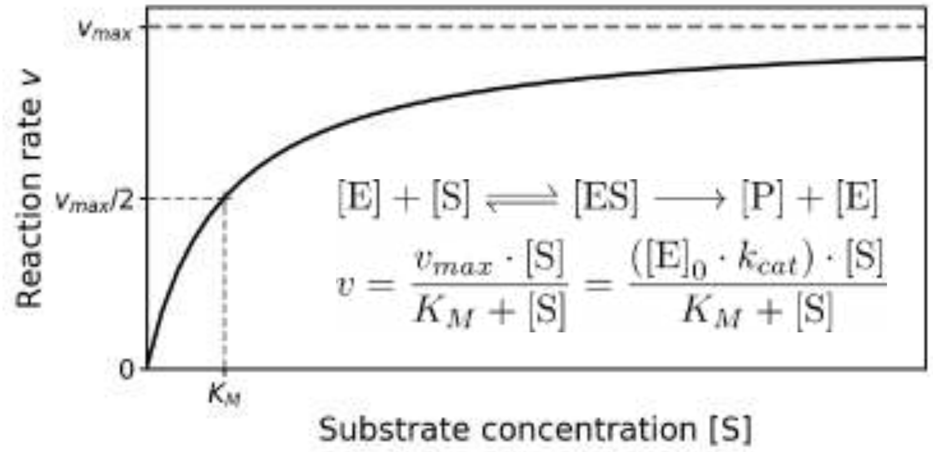

$$[E] + [S] \rightleftharpoons [ES] \longrightarrow [P] + [E]$$

$$v = \frac{v_{max} \cdot [S]}{K_M + [S]} = \frac{([E]_0 \cdot k_{cat}) \cdot [S]}{K_M + [S]}$$

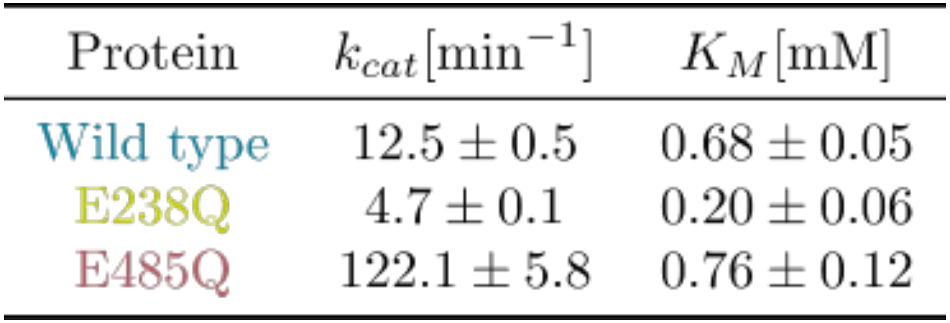

Protein	$k_{cat}\,[\mathrm{min}^{-1}]$	$K_M\,[\mathrm{mM}]$
Wild type	12.5 ± 0.5	0.68 ± 0.05
E238Q	4.7 ± 0.1	0.20 ± 0.06
E485Q	122.1 ± 5.8	0.76 ± 0.12

Barthelme et al., PNAS (2011)

ABCE1: A simple Markov State Model

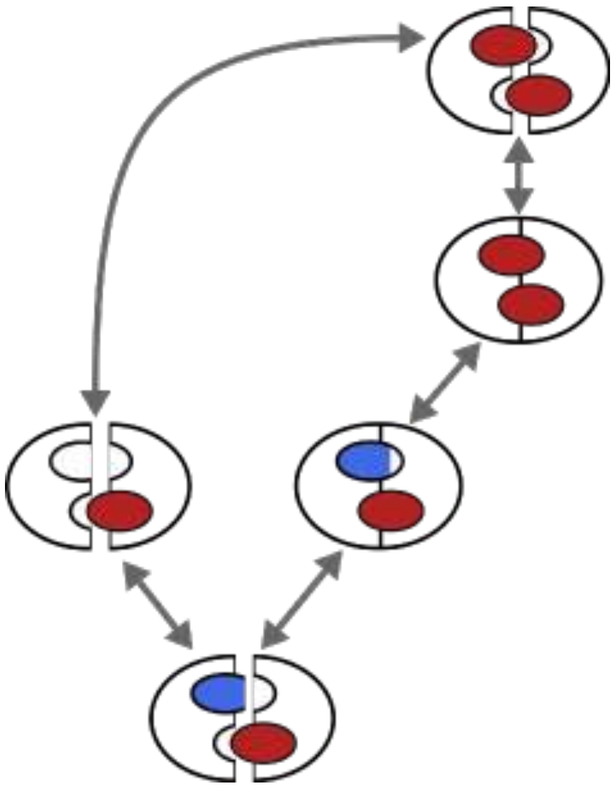

Malte Schäffner

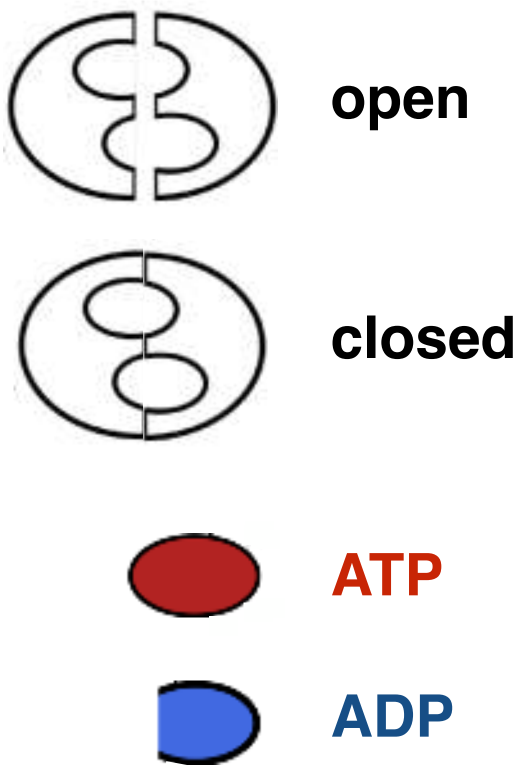

ABCE1: A simple Markov State Model

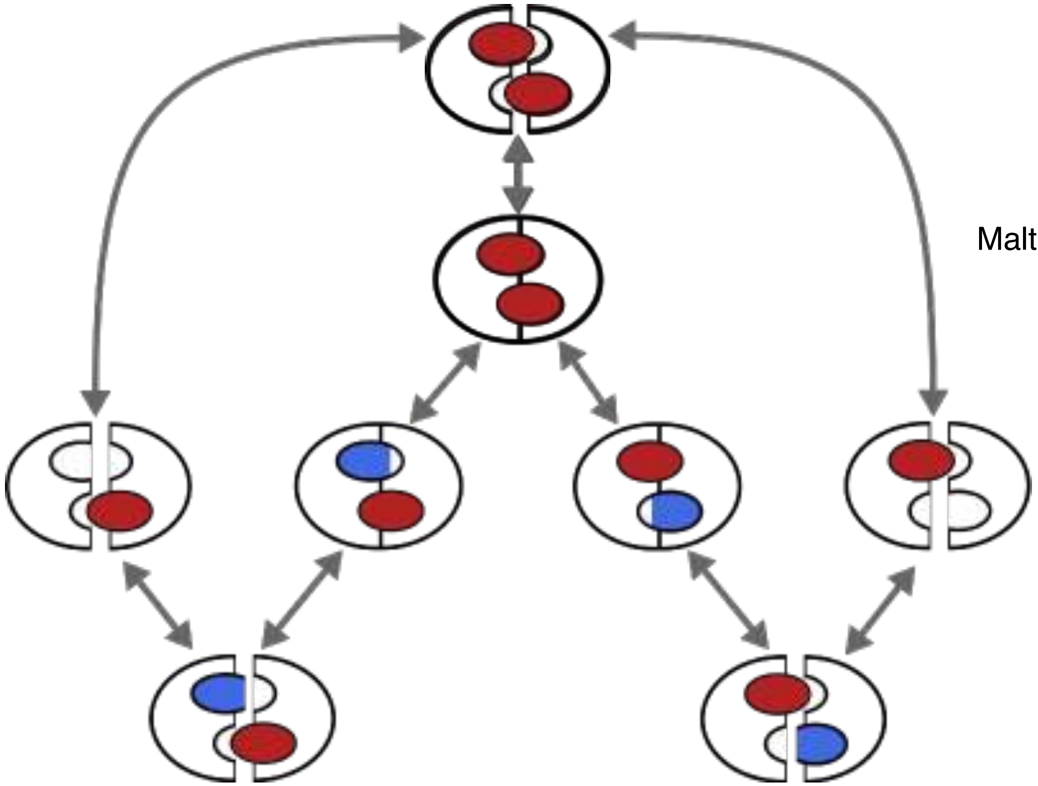

Malte Schäffner

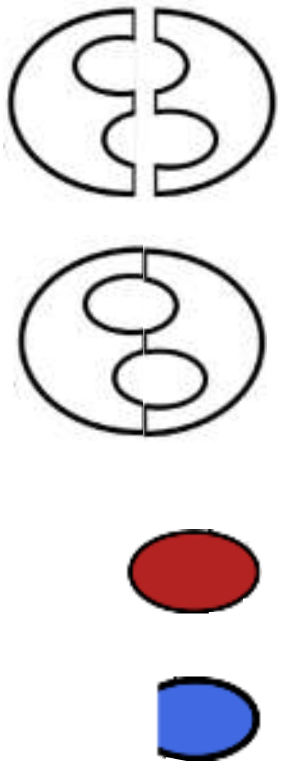

open

closed

ATP

ADP

ABCE1: A simple Markov State Model

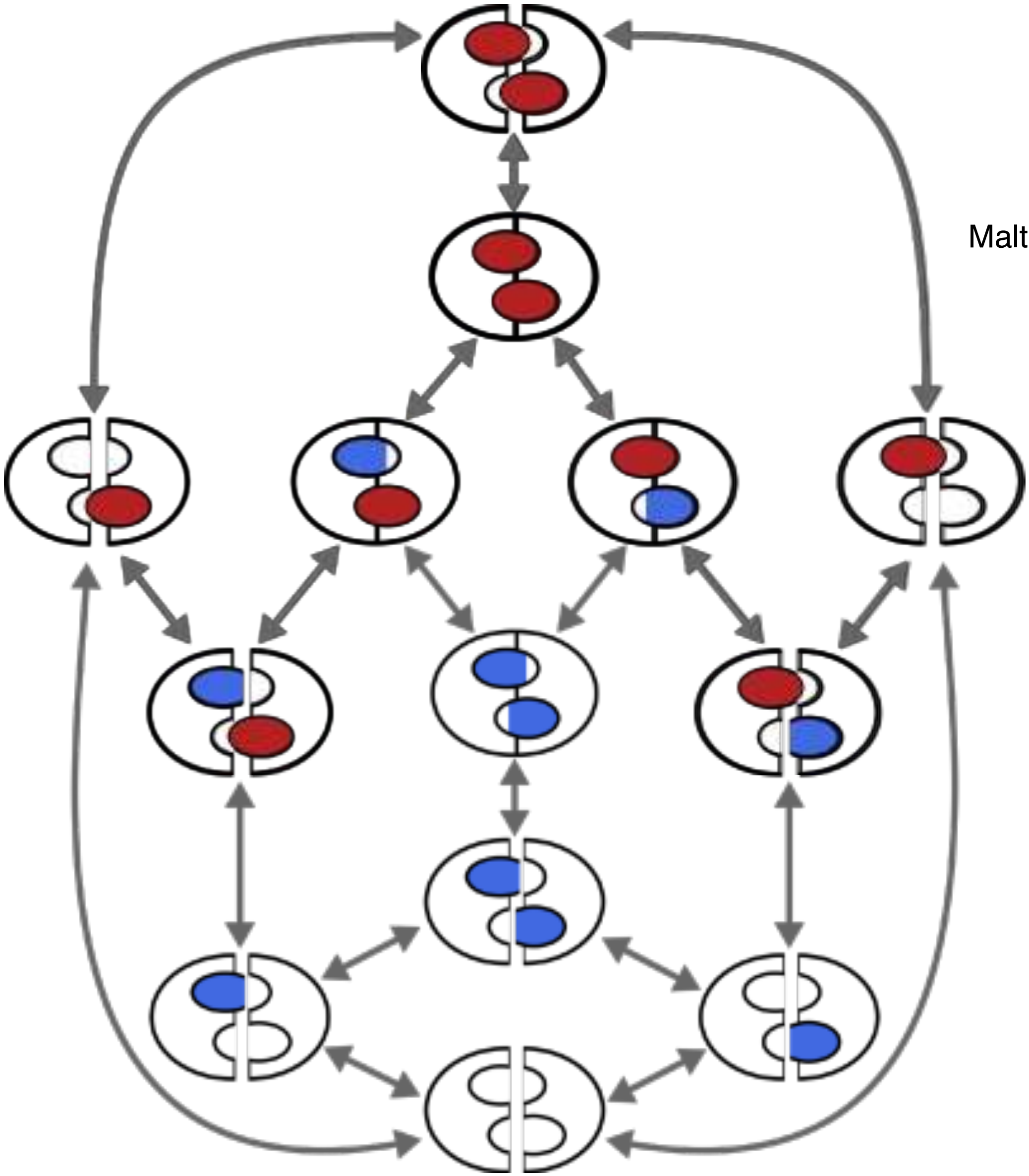

Malte Schäffner

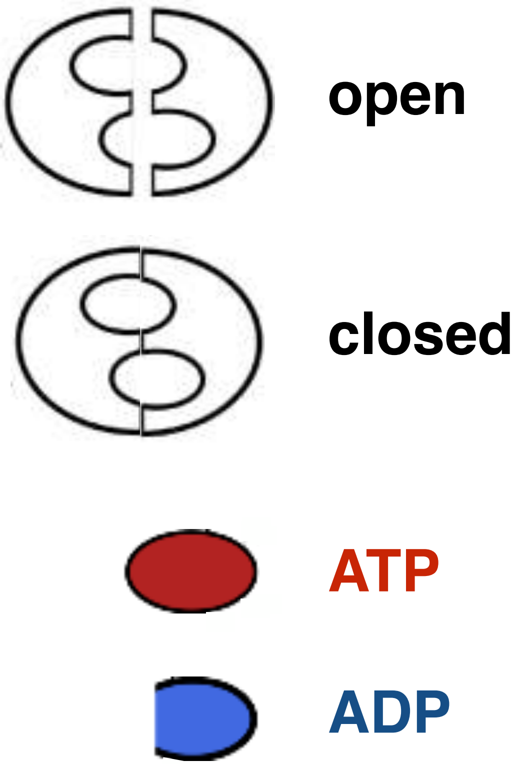

ABCE1: 13 states , 30 independent rates {*k*

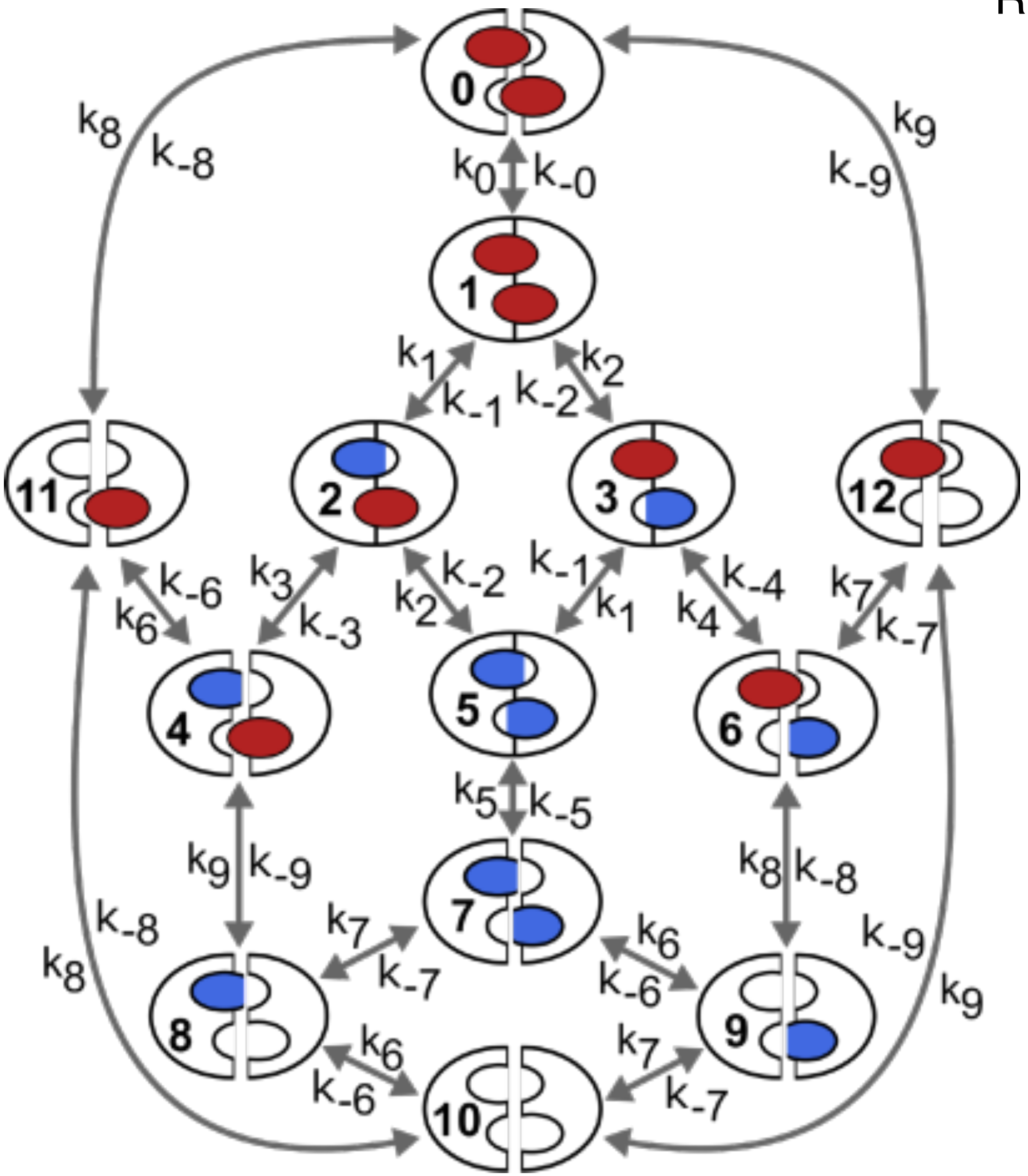

Rate coefficient Matrix $\mathbf{M}$

$$\mathbf{M_{ij}} = k_{j \to i}$$

$$\mathbf{M_{ii}} = -\sum k_{i \to j}$$

$$\mathbf{M} \cdot \mathbf{p} = \dot{\mathbf{p}}$$

Stationary state:

$$\mathbf{M} \cdot \hat{\mathbf{p}} = \mathbf{0}$$

Each set of 30 rates --> ATP hydrolysis rate

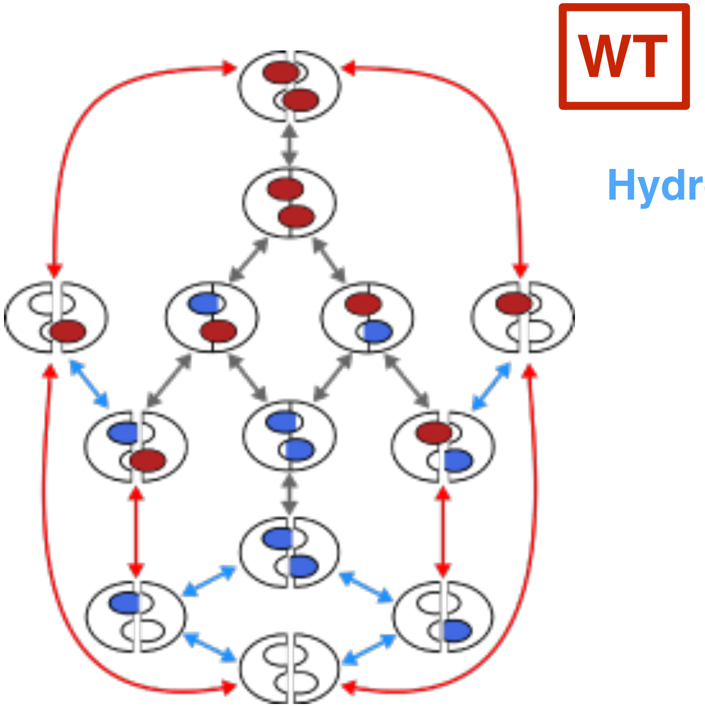

Hydrolysis rates = Σ fluxes

Rate coefficient Matrix $\mathbf{M}$

$$\mathbf{M_{ij}} = k_{j \to i}$$

$$\mathbf{M_{ii}} = -\sum k_{i \to j}$$

$$\mathbf{M} \cdot \mathbf{p} = \dot{\mathbf{p}}$$

Stationary state:

$$\mathbf{M} \cdot \hat{\mathbf{p}} = \mathbf{0}$$

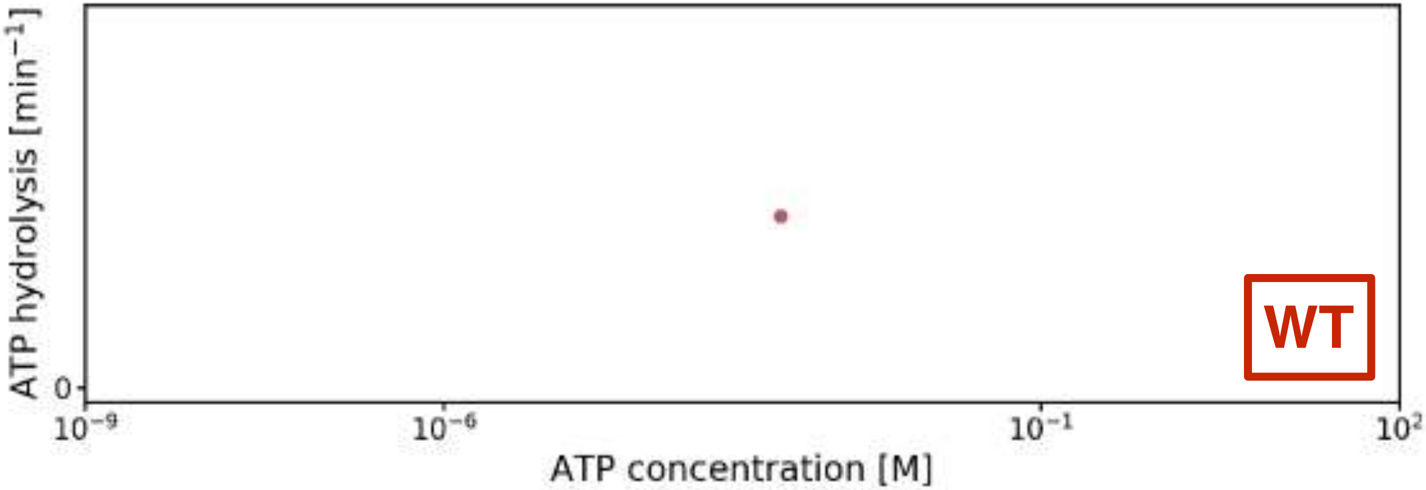

Vary ATP concentration --> k_{cat} and K_M

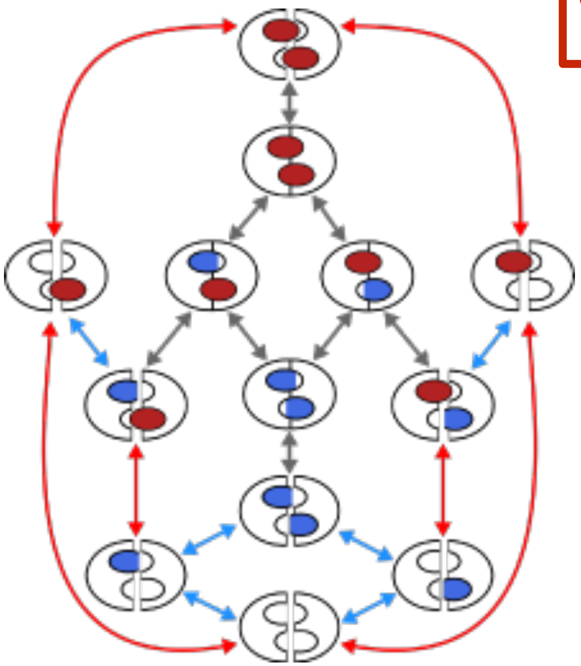

WT

Hydrolysis rates = Σ fluxes

ATP binding rates ∝ [ATP]

Rate coefficient Matrix $\mathbf{M}$

$$\mathbf{M_{ij}} = k_{j\to i}$$

$$\mathbf{M_{ii}} = -\sum k_{i\to j}$$

$$\mathbf{M}\cdot\mathbf{p} = \dot{\mathbf{p}}$$

Stationary state:

$$\mathbf{M}\cdot\hat{\mathbf{p}} = 0$$

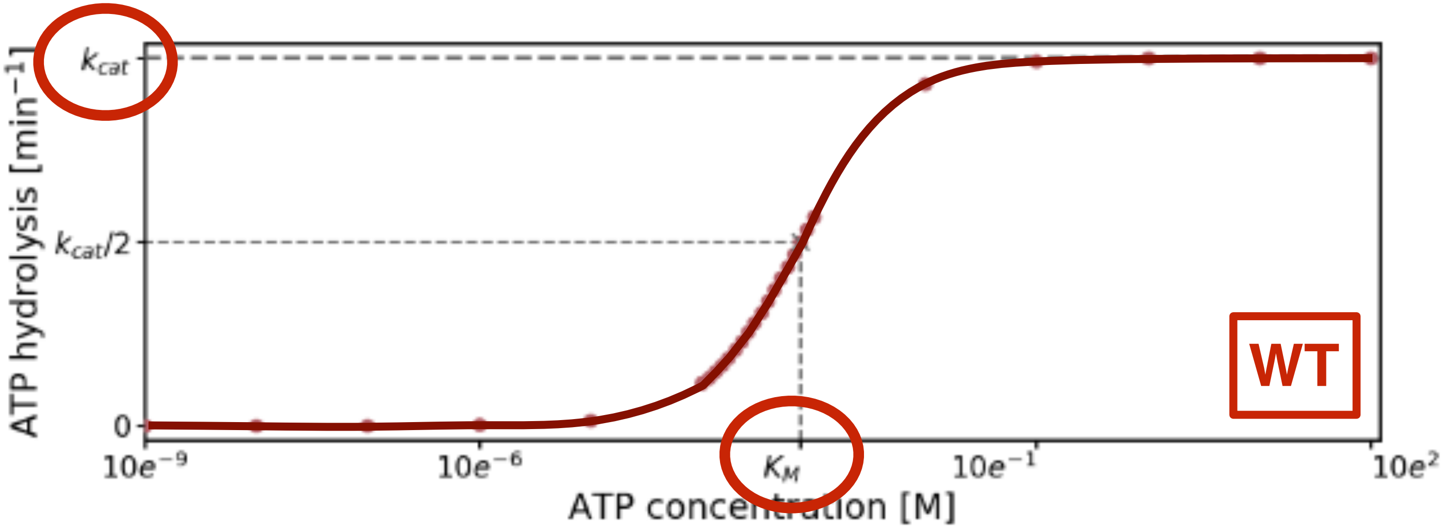

Block binding site 1 --> k_{cat} and K_M for E238Q

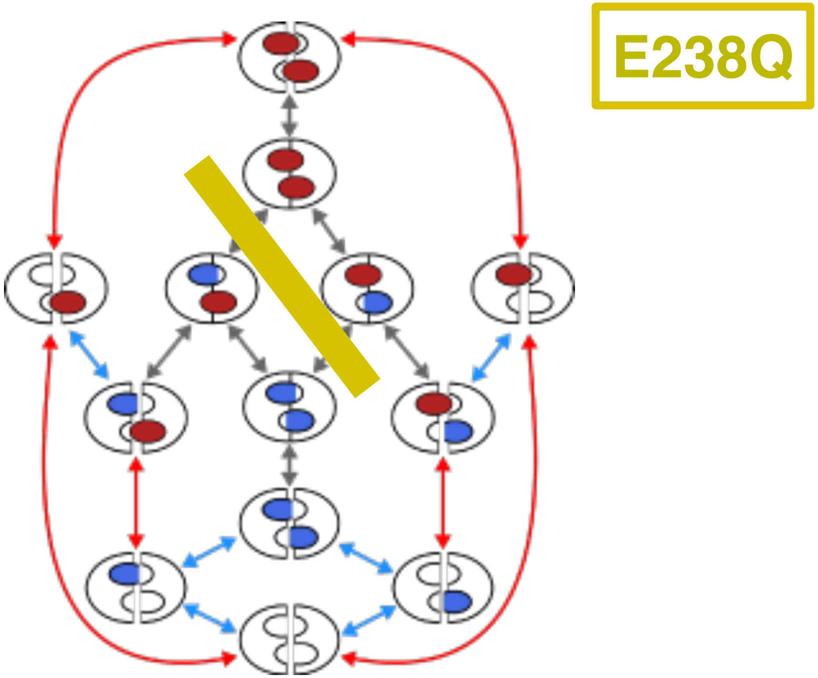

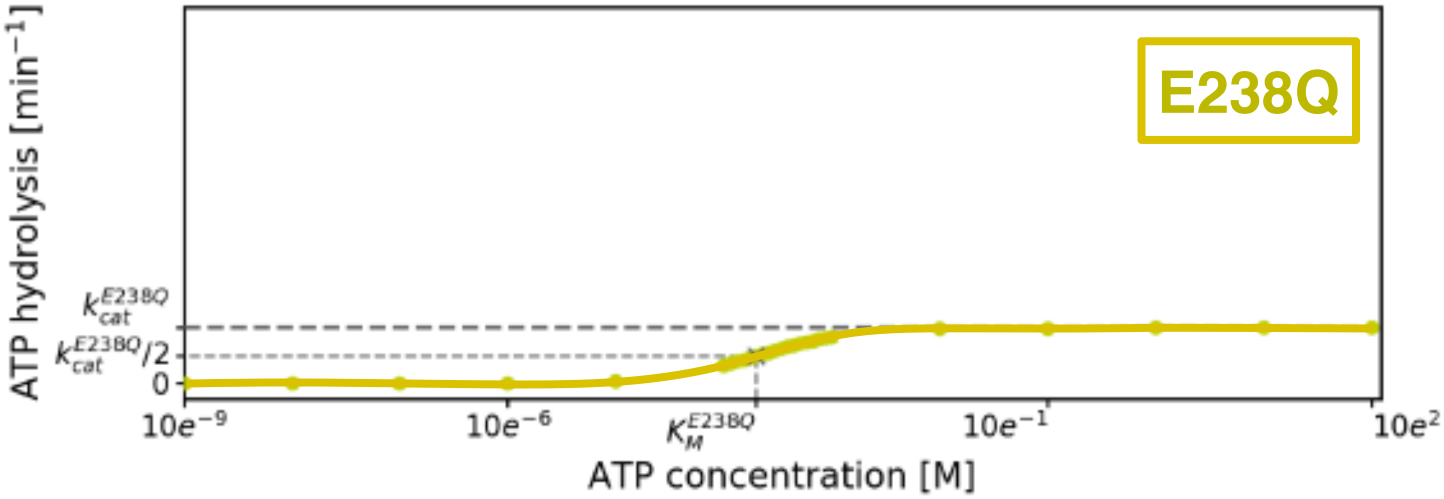

Block binding site 2 --> k_{cat} and K_M for E485Q

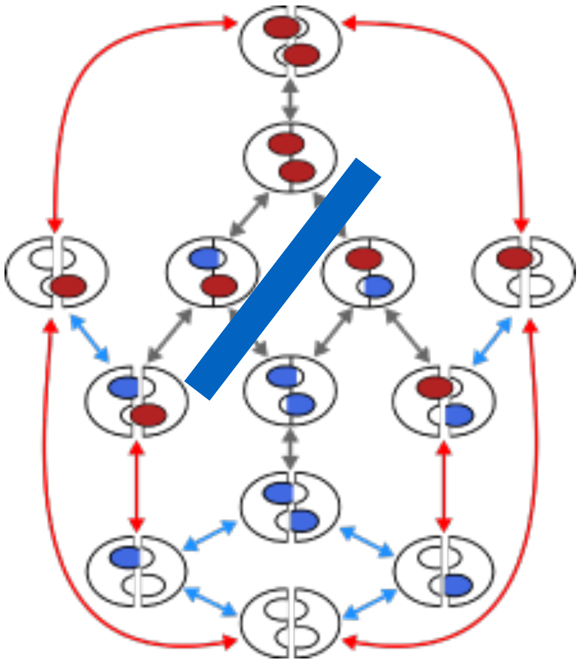

E485Q

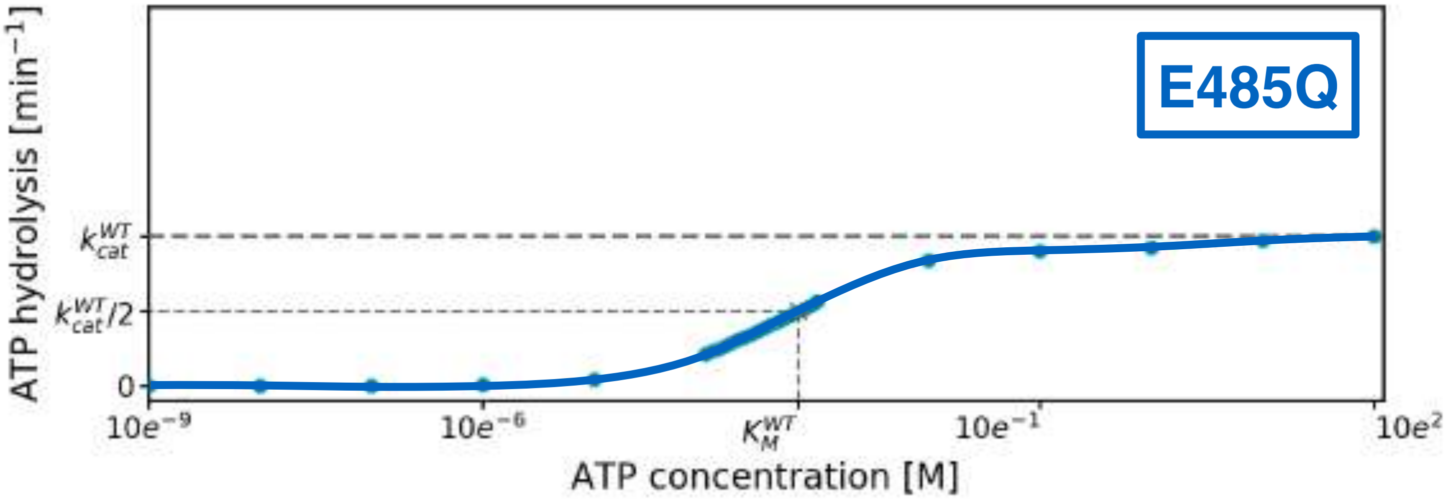

Compare 3 x k_{cat} and K_M to experiment -> $p(\{k_{ij}\} \mid \{k_{cat}, K_M\})$

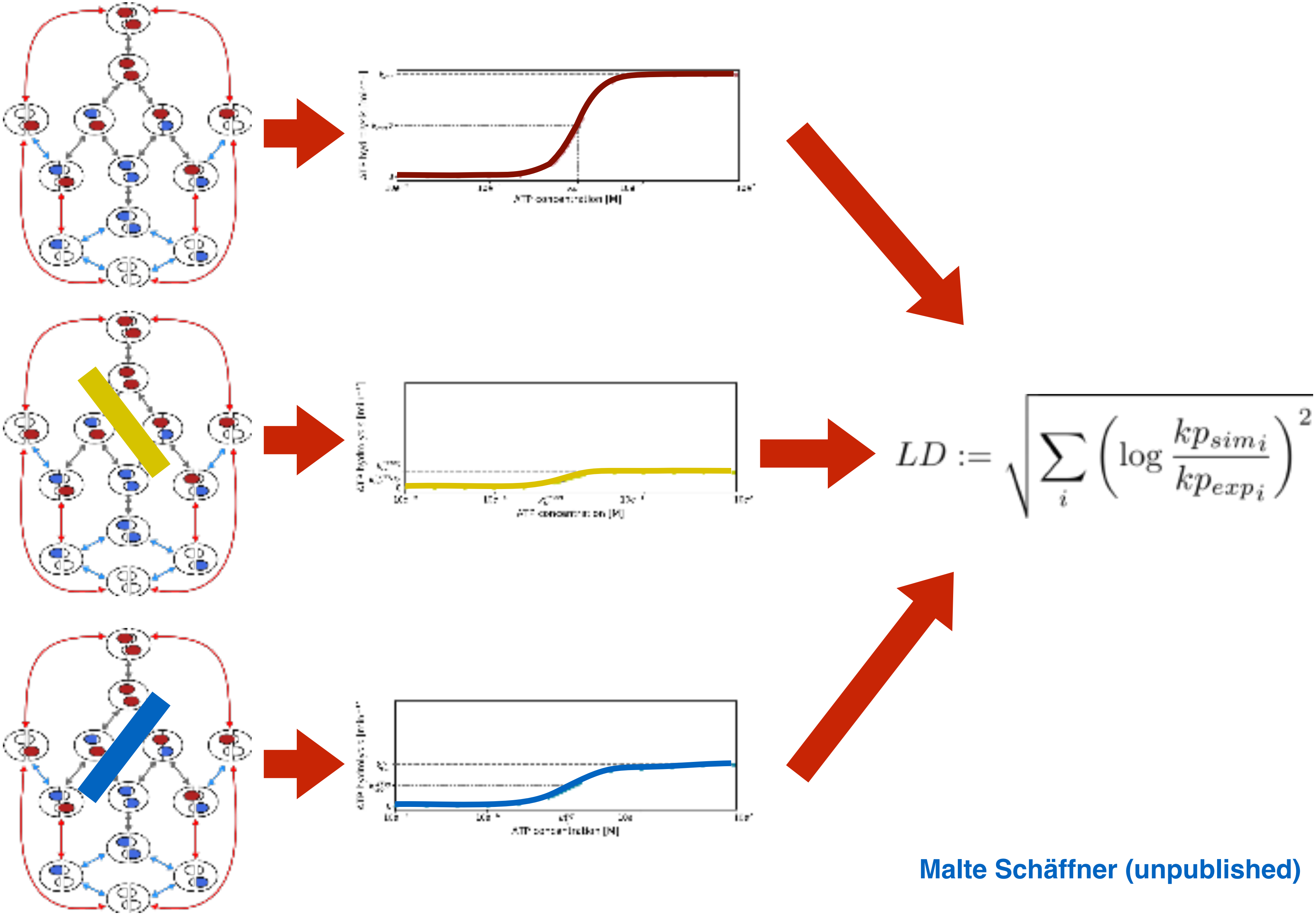

$$LD := \sqrt{\sum_i \left(\log \frac{kp_{sim_i}}{kp_{exp_i}}\right)^2}$$

Malte Schäffner (unpublished)

Exhaustive sampling of Markov models $\{k_{ij}\}$

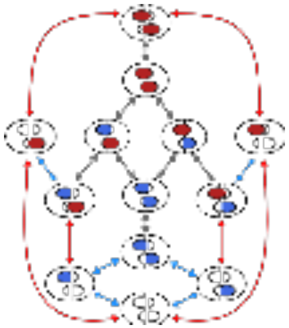

LD = 53%

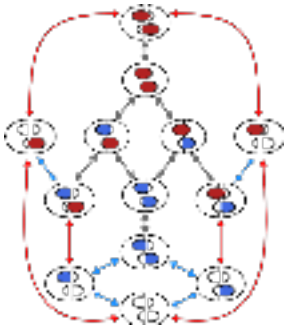

LD = 3%

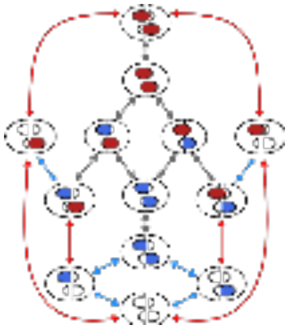

LD = 87%

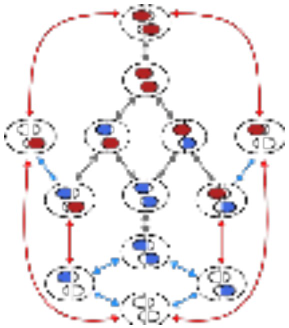

LD = 1%

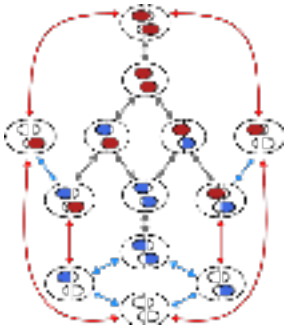

LD = 5%

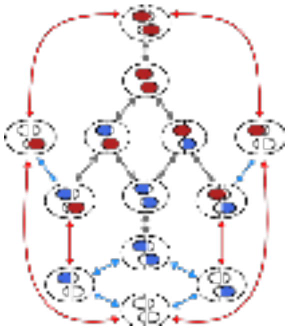

LD = 26%

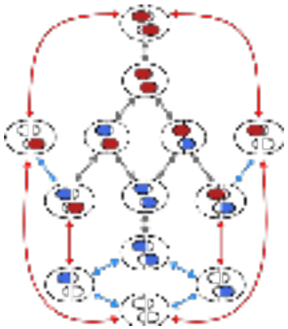

LD = 2%

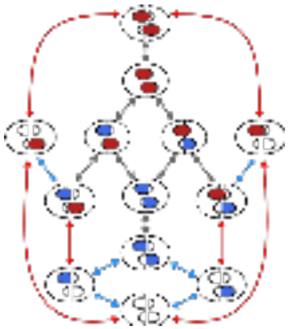

LD = 99%

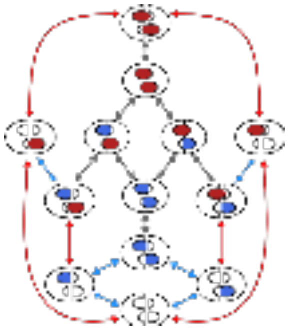

LD = 67%

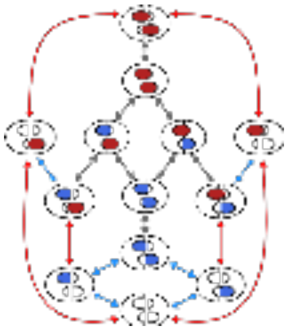

LD = 0%

--> 10,000,000 sets of rate coefficients, enhanced sampling

Malte Schäffner (unpublished)

Markov Models $\{k_{ij}\}$ that agree best with experiment

Wild type

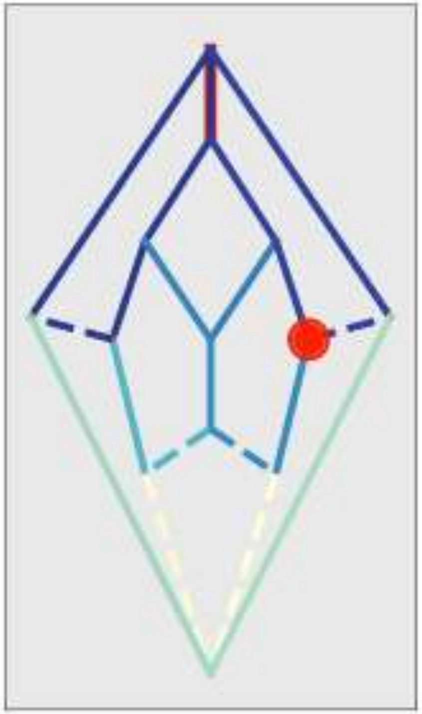

E238Q

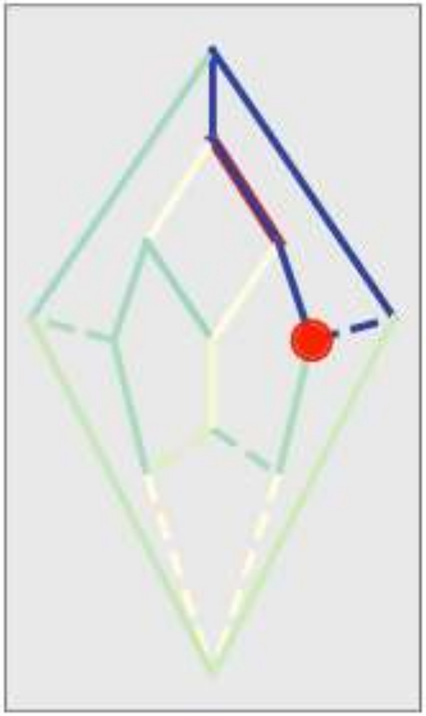

E485Q

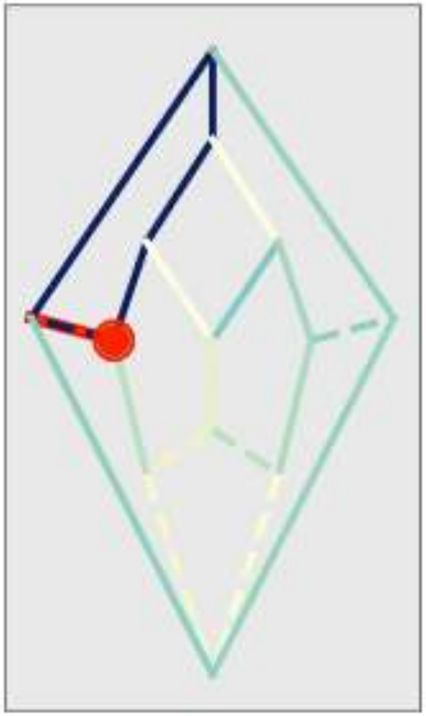

flux: low high
red: bottleneck

--> 10,000,000 sets of rate coefficients,
enhanced sampling

Malte Schäffner (unpublished)

Broad distributions of rate coefficients

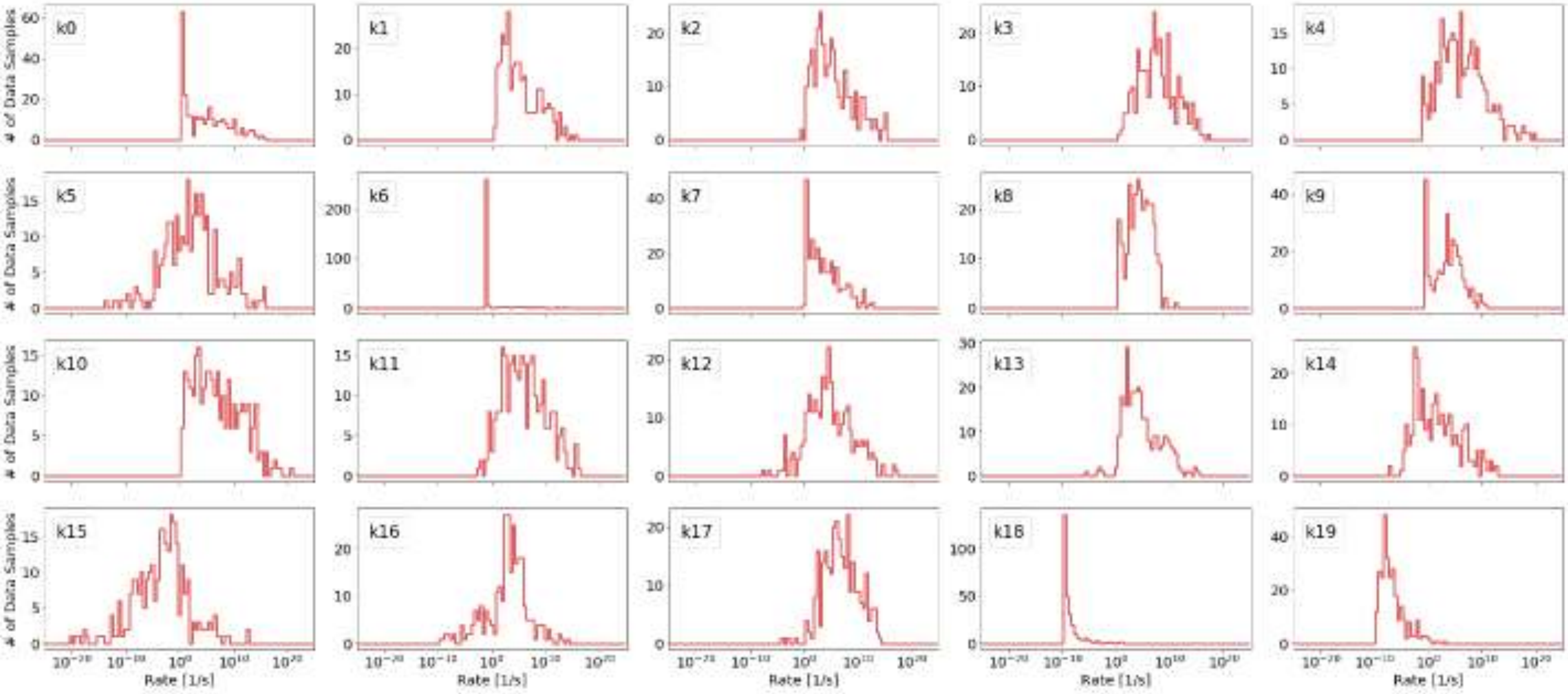

Malte Schäffner (unpublished)

Narrow distributions of fluxes

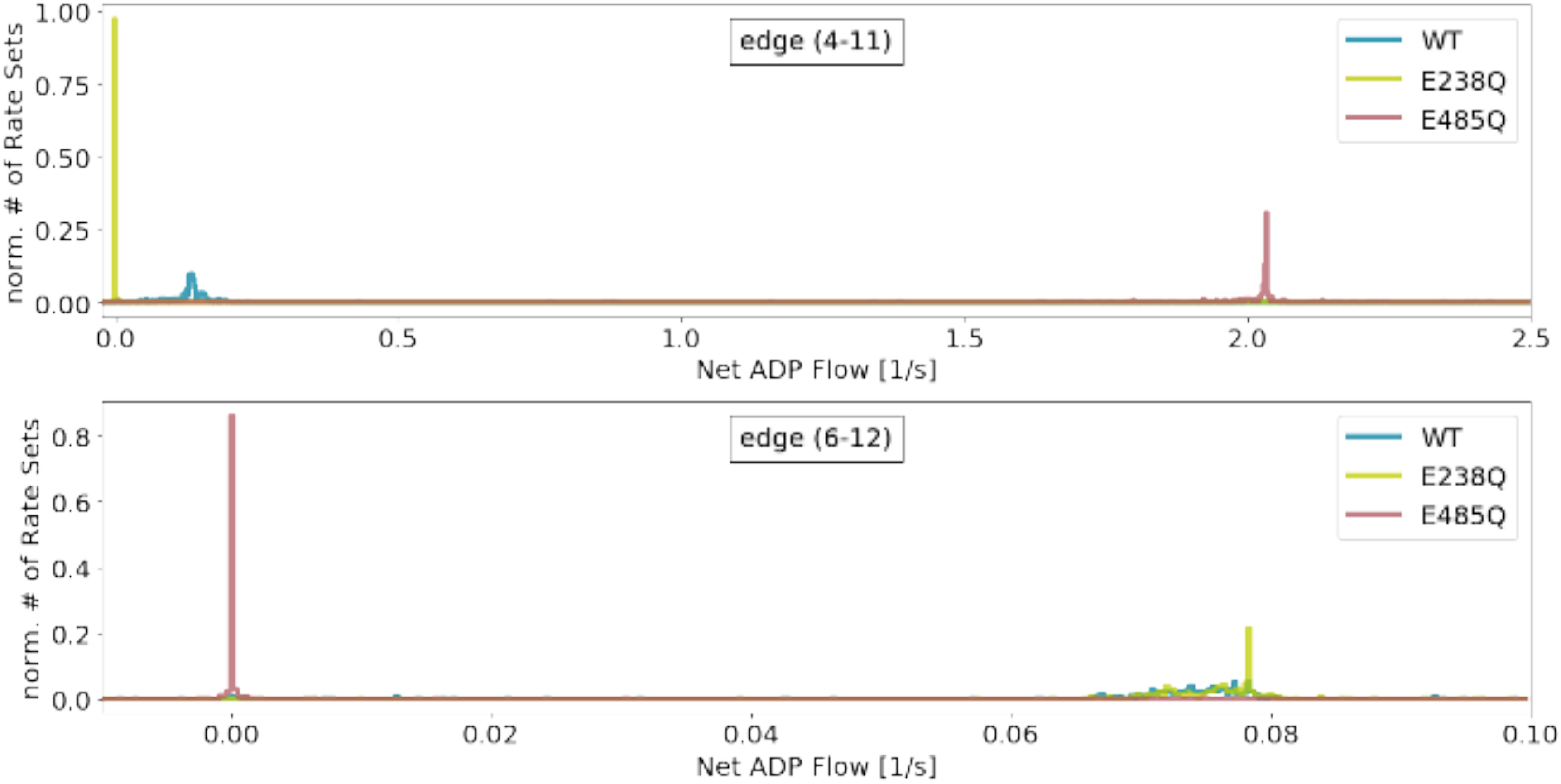

Malte Schäffner (unpublished)

ABCE1 Consensus Kinetic Model

Wild type

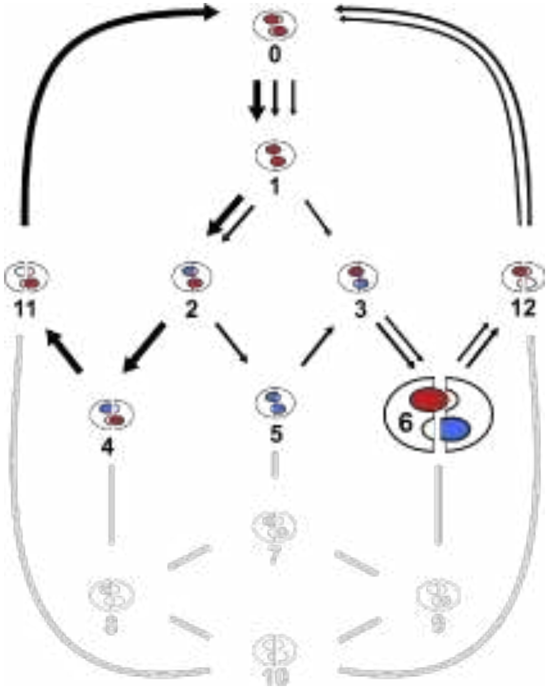

E238Q

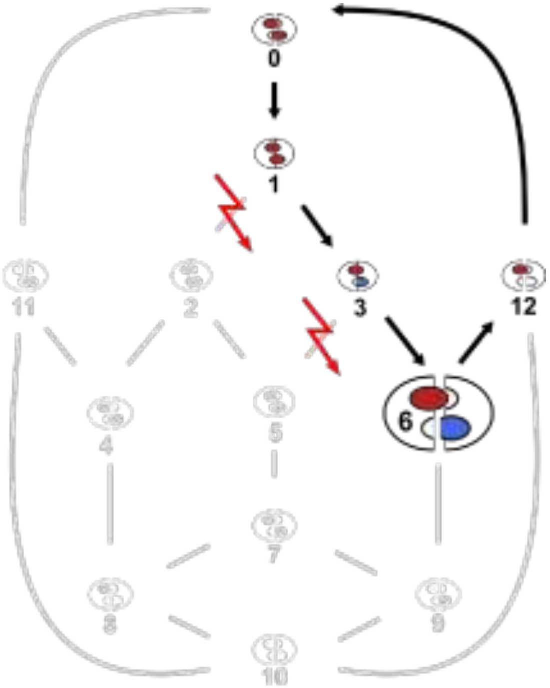

E485Q

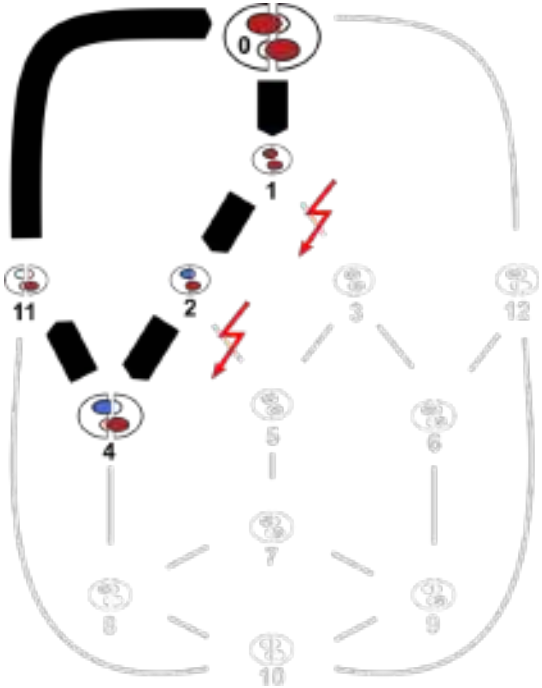

Line thickness: Flux

Symbol size: Population

Malte Schäffner (unpublished)

Prediction: Free energy difference (MD / Crooks NE-sampling)

Wild type

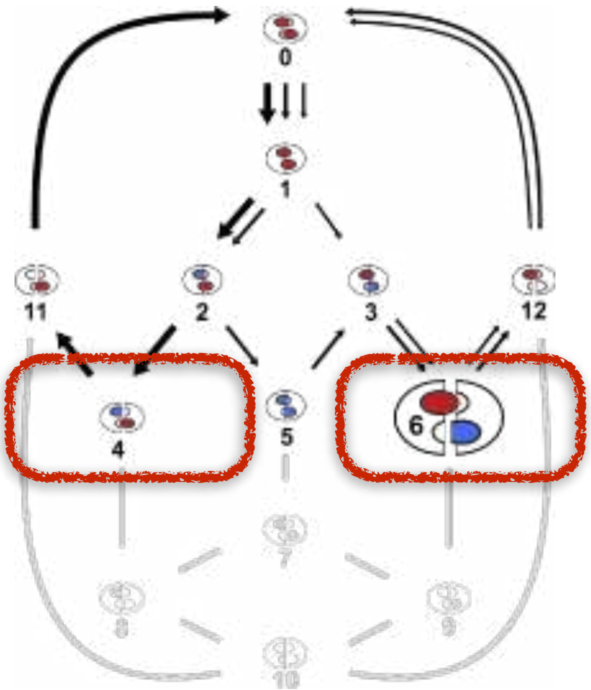

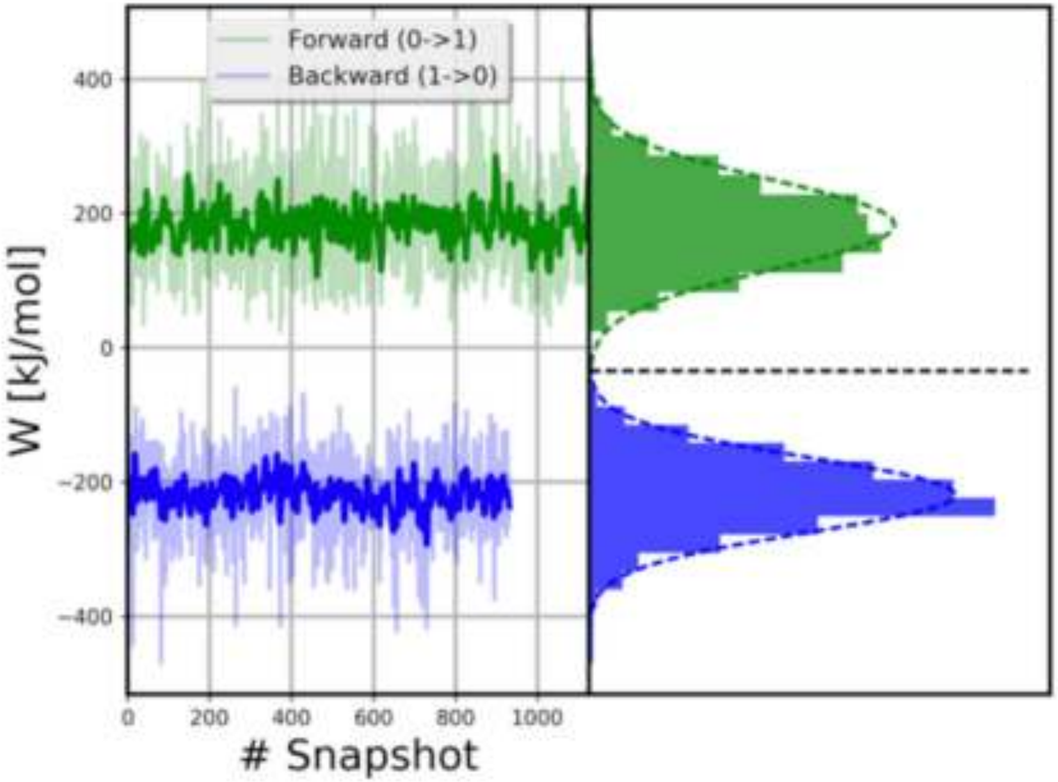

ΔG_{6-4} = - 30 kJ/mol

Nick Leioatts (unpublished)

Prediction: Free energy difference (MD / Crooks NE-sampling)

Wild type

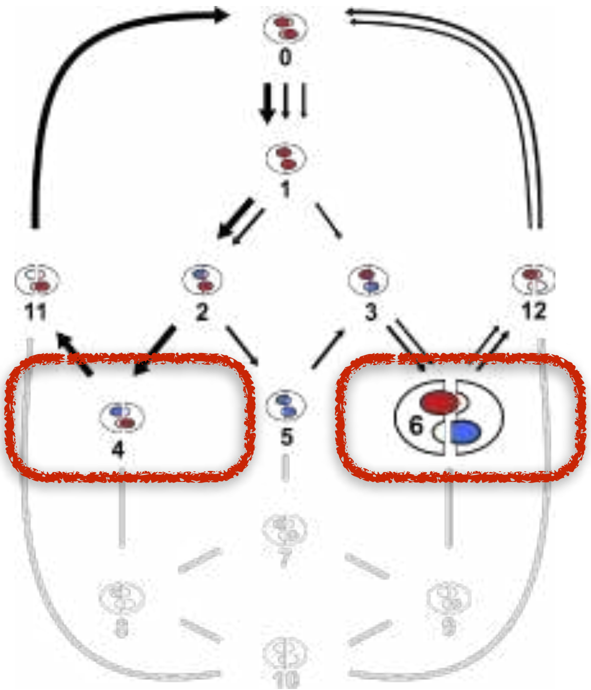

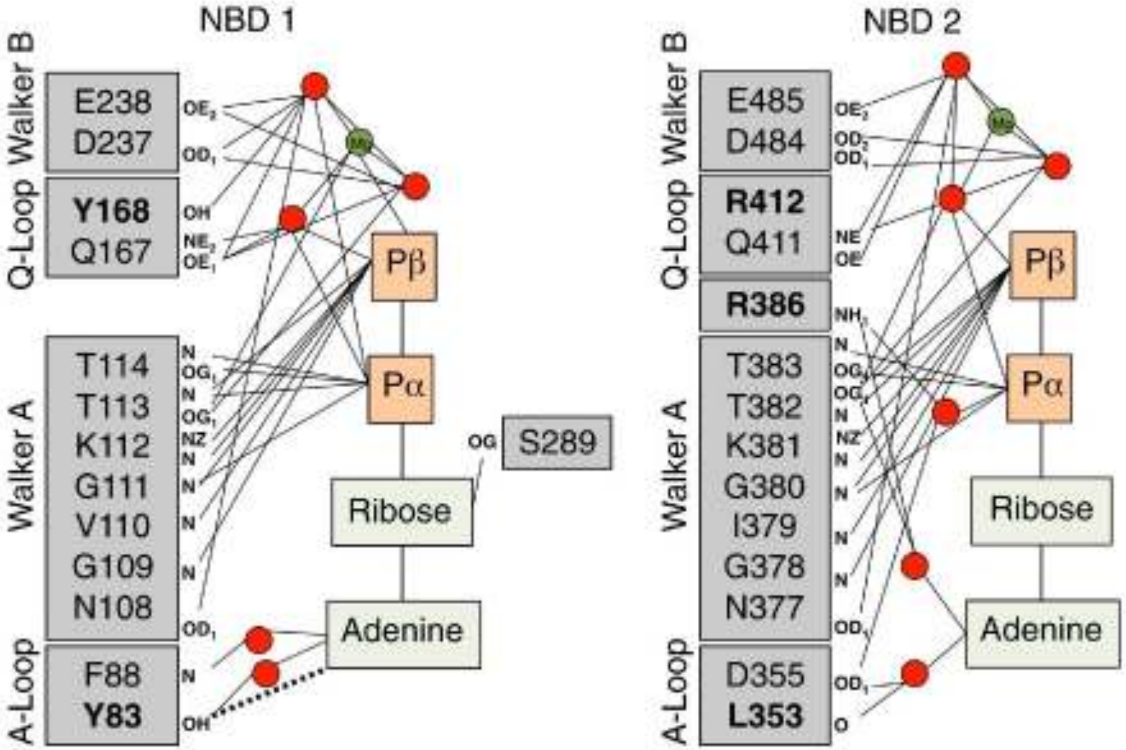

Barthelme et. al. PNAS 2011, Fig. S2

$\Delta G_{6\text{-}4}$ = - 30 kJ/mol

Theory vs. Experiment: Occupancies

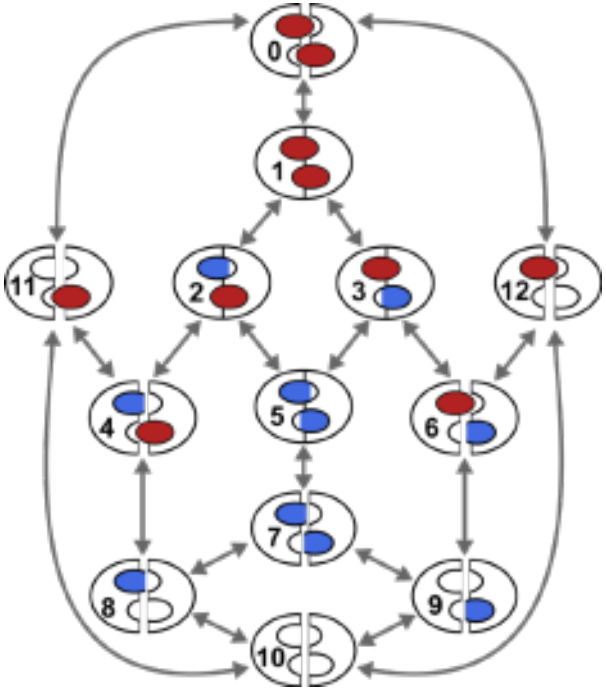

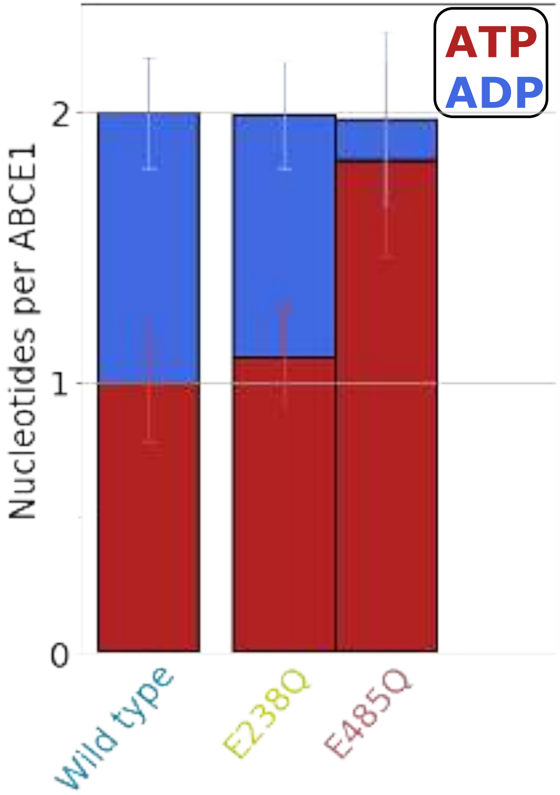

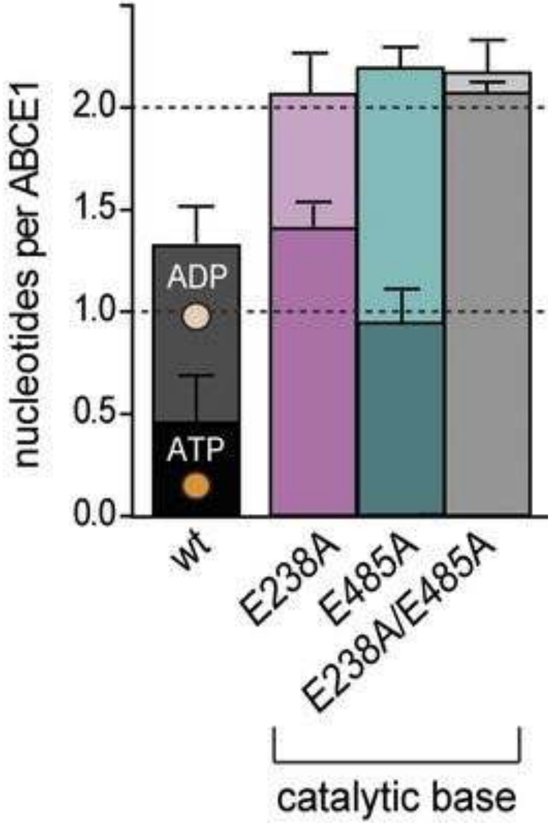

Elina Nürenberg-Goloub et al. LSA 2018